MULTI-OBJECTIVE OPTIMISATION AND ANALYSIS OF EDM OF AISI P20 TOOL STEEL

A DISSERTATION SUBMITTED TO

THE DEPARTMENT OF MECHANICAL ENGINEERING

NATIONAL INSTITUTE OF TECHNOLOGY,

ROURKELA (INDIA)

in partial fulfilment of the requirements

for the degree of

Doctor of Philosophy

By

Shailesh Kumar Dewangan

August 2014

MULTI-OBJECTIVE OPTIMISATION AND ANALYSIS OF EDM OF AISI P20 TOOL STEEL

Thesis submitted in partial fulfilment

for the Award of the degree of

Doctor of Philosophy

in

Mechanical Engineering

by

Shailesh Kumar Dewangan

under the guidance of

Dr. C. K. Biswas

Dr. S. Gangopadhyay

Department of Mechanical Engineering
National Institute of Technology,
Rourkela, India

National Institute of Technology Rourkela
Rourkela-769008, Odissa, India

Certificate

This is to certify that the thesis titled **"Multi-Objective Optimisation and Analysis of EDM of AISI P20 Tool Steel"** being submitted by Mr. Shailesh Kumar Dewangan to the National Institute of Technology, Rourkela for the award of the degree of DOCTOR OF PHILOSOPHY is a record of bonafide research carried out by him under our guidance and supervision. Mr. S. K. Dewangan has worked for about three years on the above problem and the work has reached the standard fulfilling the requirements and the regulations relating to the degree. To the best of our knowledge the work incorporated in this thesis has not been submitted to any other University or Institute for the award of any other degree or diploma.

Dr. C. K. Biswas,
Associate Professor,
Mechanical Engineering Department,
National Institute of Technology,
Rourkela (India)

Dr. S. Gangopadhyay,
Assistant Professor,
Mechanical Engineering Department,
National Institute of Technology,
Rourkela (India)

Acknowledgement

I express my deep sense of gratitude and indebtedness to my thesis supervisors, Dr. C. K. Biswas and Dr. S. Gangopadhyay for providing precious guidance, inspiring discussions and constant supervision throughout the course of this work. Their timely help, constructive criticism, and conscientious efforts made it possible to present the work contained in this thesis.

I would like to thank Prof. Sunil Kumar Sarangi, Director, NIT Rourkela, for creating a healthy working environment at NIT campus and for timely help I received from him. My sincere thank goes to Prof. K.P. Maity, Chairman of my doctoral scrutiny committee (DSC) and former head of Mechanical Engineering Department and also all members of DSC for their kind corporation and valuable suggestions during different stages of my research work. I am also thankful to Mr. Kunal Nayak and Mr. Arabinda Khuntia, technical staff members of production engineering laboratory and also to Mr. Shyamu Hembram and Mr. Subrat Pradhan (Metallurgical and Materials Science Department) for their useful suggestions and help rendered to me in carrying out this work.

I am thankful to my friends and colleagues Rahul Ganjir, Jukti Prasad Padhy, Gangadharudu Talla, Chitrasen Samantra, Bikash Ranjan Moharana and Sushant Sahoo for their inspiration, moral support and encouragement. The thesis would remain incomplete without mentioning the contributions and supports of my parents for making me what I am today.

Finally, I wish to acknowledge the financial support given by the Ministry of Human Resource Development, Government of India during my tenure of stay at National Institute of Technology, Rourkela.

Shailesh Kumar Dewangan

ABSTRACT

Electric Discharge Machining (EDM) is one of the non traditional machining processes used to produce critical shape on hard or brittle conductive materials and it can also be successfully applied on materials that are extremely difficult-to-machine using traditional machining processes. The experimental investigation of EDM process parameters is of utter importance in order to improve the productivity, surface integrity and quality characteristics. An efficient method for determining the optimum process parameters for multiple performance characteristics, through various multi-optimisation techniques from the experiment trials, is a necessity of the present industry.

The work piece material for the current research work was AISI P20 tool steel and a cylindrical copper electrode was used with lateral flushing of dielectric fluid during the first phase of the study. AISI P20 tool steel has growing range of applications like in plastic moulds, frames for plastic pressure dies, hydro forming tools, which offer difficulty in conventional machining in hardened condition. Influence of various process parameters on MRR, TWR and OC has been investigated during EDM of AISI P20 tool steel. Different multi-objective optimisation techniques such as grey-Taguchi and fuzzy logic combined with Response Surface Methodology (RSM) have been utilized in order to achieve optimal combinations of EDM parameters like discharge current, pulse-on time, work time, lift time, and inter electrode gap which would result in maximum MRR as well as minimum TWR and OC. Working time did not have any influence on performance measures of EDM, while other parameters had significant effect. Both grey relation analysis and fuzzy logic technique have been implemented to convert multiple responses in EDM into a single one and optimise the above responses. Finally, respective confirmation tests were carried out to obtain optimal process parameters.

Different surface integrity characteristics (SR, WLT, SCD) and dimensional ac-

curacy (OC) during EDM of AISI P20 tool steel have been studied based on RSM based design of experiment. Fuzzy-Technique for Order of Preference by Similarity to Ideal Solution (TOPSIS) method has been attempted with an aim to determine optimal combination of EDM parameters (pulse current, pulse-on time, tool work time and tool lift time) from five decision makers' preferences on the four responses. The optimal setting of process parameters of Ip= 1A, T_{on}=10μs, T_w=0.2s and T_{up}=1.5s has been achieved. A sensitivity analysis was further carried out to study the sensitivity of the five decision makers' preferences on optimal machining parameters. The decision makers' preferences for Surface Crack Density (SCD) were found to be most important and should be chosen first and very carefully.

Tool material in EDM plays a major role on different machining characteristics. Therefore, influence of different tool materials (brass, copper and graphite) was investigated on various aspects of surface integrity and dimensional accuracy. The result indicated that brass tool was the most suitable option, followed by copper tool when machined surface integrity was considered. Graphite tool resulted in worst surface integrity in the entire range of process parameters considered in the current study. However, minimum over cut was noted for graphite tool followed by copper and brass tools. Therefore, copper may be considered the best option in terms of surface integrity as well as dimensional accuracy together.

In EDM various discharge waveforms are generated that can be classified into different characteristic of sparking such as " open", "spark", "transient arc", "arc" and "short pulses". An experiment has been conducted with different machining conditions and wavelet transform was used to analyse the discharge waveforms. Pulse-on time significantly affected the number of "spark" and "arc" pulses while no other machining parameter significantly affected any of the three types of waveform pulses. The study indicated that pulse-on time was inversely proportional to number of "spark" pulses and directly proportional to number of "arc" pulses, thus giving an useful information about state of EDM under different machining condition.

Keywords: AISI P20 tool steel, Electric Discharge Machining, Fuzzy-Logic, Fuzzy-TOPSIS, Grey Relation Analysis, Productivity, Quality, Surface integrity, Discharge characteristics

List of Acronyms

ANFIS Neuro-Fuzzy Inference System

ANN Artificial Neural Network

ANOVA Analysis of Variance

CCD Central Composite Design

CNC Computer Numerical Control

CWT Continuous Wavelet Transforms

DF Degrees of Freedom

DOE Design of Experiments

DWT Discrete Wavelet Transforms

EDM Electric Discharge Machining

FEM Finite Element Method

GA Genetic Algorithm

GRA Grey Relational Analysis

GRC Grey Relational Coefficient

GRG Grey Relational Grade

HAZ Heat Affected Zone

MEDM Micro Electric Discharge Machining

MMC Metal Matrix Composite

MPCI Multi Performance Criteria Index

MRM Material Removal Mechanism

MRR Material Removal Rate

MS Mean of Squares

NF Neuro Fuzzy

OA Orthogonal Array

OC Radial Overcut

PCA Principal Component Analysis

PM Power Metallurgy

PMEDM Powder Mixed Electro Discharge Machining

PQLR Proportion of Quality Loss Reduction

RSM Response Surface Methodology

S/N Signal-to-Noise

SCD Surface Crack Density

SEM Scanning Electron Microscope

SEN Servo Sensitivity

Seq SS Sequential Sum of Squares

SR Surface Roughness

TOPSIS Technique for Order of Preference by Similarity to Ideal Solution

TWR Tool Wear Rate

WEDM Wire Electro Discharge Machining

WLT White Layer Thickness

WPC Weighted Principal Component

XRD X-ray diffraction

NOMENCLATURE

T_{up} Lift Time

T_w Work Time

$\triangle_i(k)$ k^{th} value in $\triangle_i$ different data series

$\triangle_{max}$ Global maximum values in the different data series

$\triangle_{min}$ Global minimum values in the different data series

γ Grey relation grade

$\overline{Y_i}$ Mean of MPCI at the optimum level of i^{th} parameter

ρ_t Density of tool

ζ Distinguishing coefficient

$d-$ distance between negative ideal value

D_{jt} Diameter of hole produced in the workpiece

D_t Diameter of tool

Fp Flushing pressure

Ip Discharge current

R_{ij} Normalise value of i^{th} attribute and j^{th} experimental run

S_{ij} Weighted normalised value of i^{th} attribute and j^{th} experimental run

S_j+ Positive ideal value

S_j- Negative ideal value

T_a Weight of tool after machining

T_b Weight of tool before machining

T_{off} Pulse-off Time

T_{on} Pulse-on Time

Tau Duty Cycle

W_a Weight of workpiece after machining

W_b Weight of workpiece before machining

$x_i(k)$ Observed data for i^{th} experiment using k^{th} response

$x_i^*(k)$ Normalised data for i^{th} experiment using k^{th} response

Y_m Mean of MPCI's of all experimental runs

ρ_w Density of workpiece

$d+$ distance between positive ideal value

$Opt\ T_{on}$ Optimum level of T_{on}

$Opt\ T_{up}$ Optimum level of T_{up}

$Opt\ T_w$ Optimum level of T_w

$Opt\ Ip$ Optimum level of Ip

R^2 Coefficient of determination

R^2_{adj} Adjusted coefficient of determination

CONTENTS

LIST OF TABLES

LIST OF FIGURES

Chapter I

Introduction

1. INTRODUCTION

There is a growing trend to use light, slim and compact mechanical components in recent years. Thus there has been an increased interest in development of new generation of advanced materials having high hardness, temperature resistance, and high strength to weight ratio to be used in mould and die making industries, aerospace component, medical appliance and automotive industries. There is a heavy demand for new manufacturing technologies to meet with productivity and accuracy requirements with these materials. The traditional processes are unable to cope up with these challenges. Electric Discharge Machining (EDM) has been a mainstay manufacturing process providing unique capabilities to machine "difficult to machine" materials with desired shape, size and required dimensional accuracy. It is the most widely and successfully applied non-traditional machining process for various workpiece materials in the said advanced industries.

1.1 Background of EDM

English scientist Joseph Priestly first observed erosive influence of electric discharge way back in 1770s. However, full advantage of this technique was not utilized until 1943 when Russian scientists learned to control the erosive effect of this phenomena to be used for machining. Material erosion was accomplished by intermittent arc discharges occurring in air between the tool electrode and workpiece connected to a DC power supply. This process was not very precise due to overheating of the machining area and is defined as 'arc machining' rather than 'spark machining' [Ho and Newman, 2003].

During 1980s, EDM made an extraordinary progress in improving the efficiency of the machining operation with the advent of Computer Numerical Control (CNC). An automatic and unattended machining, from inserting the electrodes in the tool changer to a finished polished cavity or cavities, was possible with CNC control

system. These emergent virtues of EDM have since then been intensely sought after by the manufacturing industries yielding enormous economic benefits and generating keen research interests.

EDM has been replacing drilling, milling, grinding and other traditional machining operations and is now a well established machining option in many manufacturing industries throughout the world. It is capable of machining geometrically complex or hard material components, that are precise and difficult-to-machine such as heat treated tool steels, composites, super alloys, ceramics, carbides, heat resistant steels and others, which are widely used in die and mold making industries, aerospace, aeronautics and nuclear industries. EDM has also made its presence felt in the new fields such as sports, medical and surgical, instruments, optical, including automotive research and development segment.

1.2 Categories of EDM

Basically, there are three different categories of EDM

- Die sinking EDM
- Wire cut EDM
- Electric discharge grinding

1.2.1 Die sinking EDM

Sinker EDM consists of an electrode and workpiece submerged in an insulating liquid such as hydrocarbon oil as dielectric fluid. The electrode and workpiece are connected to a pulsating power supply, which generates an electrical potential between electrode and workpiece. As the electrode approaches the workpiece, dielectric breakdown occurs in the fluid, forming a plasma channel, with occurrence of small spark. As the base metal is eroded, and the spark gap subsequently increases. The electrode is then lowered automatically by the machine so that the process can continue uninterrupted. Multiple sparks occur per second and the workpiece material gets the inverse shape of the electrode.

1.2.2 Wire cut EDM

Wire Electro Discharge Machining (WEDM) is an electro thermal machining process in which a thin single-strand metal wire is used as an electrode to cut metal by using electrical sparks. The metal wire, usually brass, is fed through the workpiece, submerged in a tank of dielectric fluid, typically deionized water. This process is typically used to cut plates up to thickness of 300mm and to make punches, tools, and dies from hard materials that are difficult-to-machine using other methods.

1.2.3 Electric discharge grinding

Electric discharge grinding is just like EDM except that it uses a rotary disk as an electrode. The electrode is designed to mimic the machining process of a surface grinder with horizontal spindles [Shih and Shu, 2008]. The workpiece is cut by the process of a stream of electric sparks between a disk (cathode) and workpiece (anode) that are immersed in a dielectric fluid.

1.3 Principle of die sinking EDM

The process of the material removal in EDM takes place by a controlled erosion through a series of the electric spark [Ghosh and Mallik, 1985]. The spark produced between the tool and work piece, generates the large amount of heat in the sparking zone, melting and vaporizing the work piece material. During the process of machining, the tool and workpiece are submerged in dielectric fluid (Kerosene/ EDM oils/deionized water/hydrocarbon/ mineral oils). A suitable gap, known as the spark gap, is maintained between the tool and workpiece surfaces with the help of servo controller.

Fig. 1.1 is shown the electric setup of the electric discharge machining. The tool is considered as cathode and work piece as anode. When sufficient voltage is generated across tool and workpiece, tool starts emitting some electrons. These electrons accelerate towards the positively charged workpiece. In this process, emitted electrons collide with dielectric molecules present in the inter electrode gap. It will result in the formation of plasma channel in inter electrode gap. This plasma channel allows current to flow between two electrodes and a spark is generated in the gap. This

produces high amount of temperature ($8000 to 12000°C$) which melts and evaporates some parts of workpiece and tool material as well.

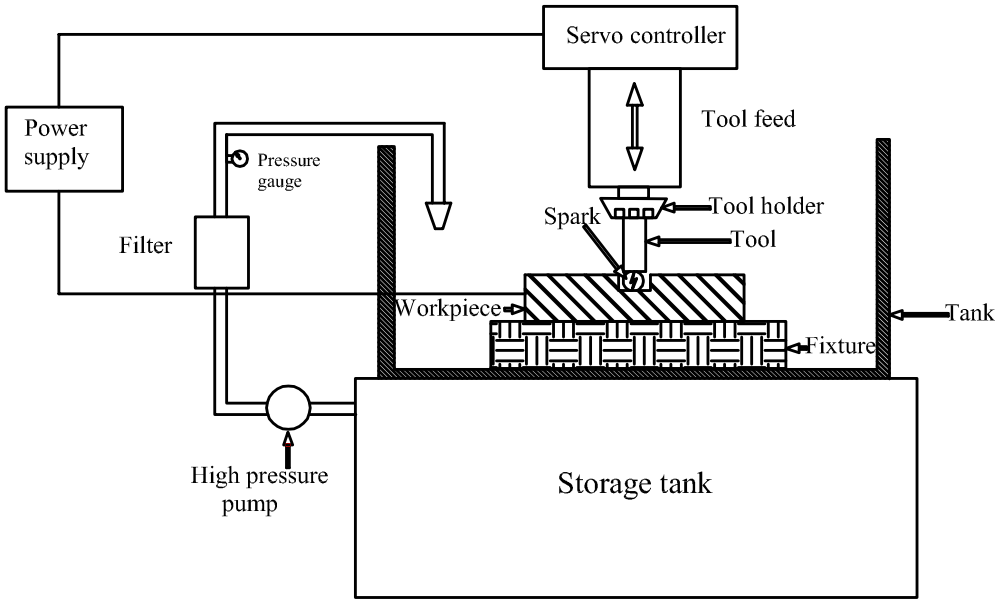

Fig. 1.1: Schematic setup of EDM

1.4 Mechanism of material removal in EDM

EDM is the most widely used non-conventional machining process. Despite the fact that the mechanism of material removal of EDM process is not yet completely understood and is still debatable, the most widely established principle is the conversion of electrical energy into thermal energy through a series of discrete electrical discharges occurring between the electrode and workpiece immersed inside a dielectric medium and separated by a small gap. Material is removed from the workpiece by localized melting and even vaporization. The sparks are created in between two electrodes in presence of dielectric liquid. A simple explanation of the erosion process due to the discharge is presented in Fig. 1.2 . There is no mechanical contact between the electrodes (held at a small distance) and a high potential difference is applied across them (Fig. 1.2(b)). As the electrode moves towards the workpiece and enhances the electric field in the gap, until the breakdown voltage of the dielectric is reached. The

spot of breakdown is normally between the closest points of the electrode and of the workpiece, but it also depends on particles or debris present in the gap. When the breakdown takes place, the voltage falls and the current rises abruptly. The flow of a current is possible at this point, because the dielectric has been ionized and a plasma channel has been created between the electrodes (Fig. 1.2(c)).

The flow of discharge current is continuous and there will be a constant attack of ions and electrons on the electrodes which will ultimately lead to strong heating of the workpiece material. The temperature rises between $8,000°C$ and $12,000°C$ [Boothroyd and Winston, 1989], resulting in formation of small molten metal pool at both the electrode surfaces. Some of the molten metal directly vaporizes due to the heating and during this discharge, the plasma channel expands and therefore, the radius of the molten metal pool increases with time (Fig 1.2(d)).

Towards the end of the discharge, voltage is shut and thus the plasma implodes under the pressure imposed by the surrounding dielectric. As a result, the molten metal pool is strongly sucked up into the dielectric, producing a tiny crater at the workpiece surface (Fig 1.2(e)). The machining process successively removes small volumes of workpiece material, molten or vaporized during discharge and is carried away from the IEG by the dielectric flow as debris. Sparking occurs where the gap between the tool and the workpiece surface is smallest. The gap increases after material removal at the point of spark, and the position of the next spark shifts to a different place, where gap is smallest on the workpiece surface. In this manner thousands of sparks occur at different locality over the whole surface of the workpiece corresponding to the workpiece-tool gap. As a consequence, a replica of the tool surface shape is produced in the workpiece.

It is well-known and elucidated by many EDM researchers that Material Removal Mechanism (MRM) is the process of migration of material from the workpiece and tool to dielectric medium in solid, liquid or gaseous state. Appreciable amount of materials is transferred between the active surfaces (form which discharges occur) and the tool resulting in alloying by means of solid, liquid or gaseous phase reactions Roethel et al., 1976; Soni and Chakraverti, 1996. Phases of sparking during MRM (breakdown, discharge and erosion) are highly influenced by the types of eroded tool

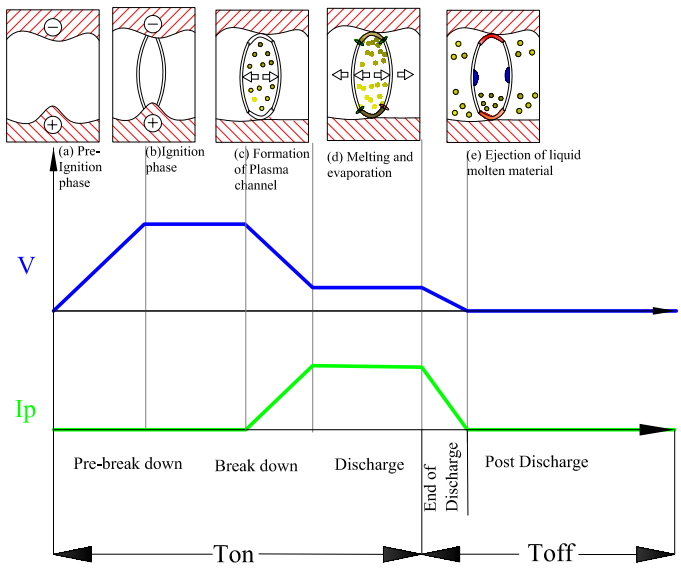

Fig. 1.2: The plasma channel

electrode and workpiece elements together with disintegrated products of dielectric fluid [Erden, 1983]. Additionally, reversing the polarity of sparking alters the material removal phenomenon with an significant amount of electrode material set down on the workpiece surface [Gangadhar et al., 1992]. The MRM has also been reported differently by many authors. Singh and Ghosh [1999] showed that the electrostatic forces and stress distribution acting on the cathode electrode were the major causes of metal removal for short pulses. Gadalla and Tsai [1989] related material removal of WC-Co composite to the melting and evaporation of disintegrated Co followed by dislodgement of WC grains which have a lower electrical conductivity Lee and Lau [1991].

EDM which is a thermal process of eroding electrically conductive materials with a series of successive electric sparks, is a complex phenomenon involving several disciplines of science and branches of engineering. The theories revolving around the formation of plasma channel between the tool and the workpiece are thermodynamics of the repetitive sparks causing melting and evaporation of the electrodes, microstructural changes and metallurgical transformations of material which are still not clearly understood. However, it is widely accepted that the mechanism of material

erosion is due to intense local heating of the workpiece causing melting and evaporation of the same.

1.5 Discharge characteristics in EDM

Usually, EDM pulses are characterised into five types such as open, spark, transient arc, arc and short pulses, based on the voltage-current (V-I) waveforms [Yu et al., 2001; Dauw et al., 1983; Pey Tee et al., 2013]. A typical waveform of the EDM pulses are shown in Fig. 1.3 depicting all pulse characteristics. Open pulse takes place when their is no discharge *i.e.* no passage of current. Spark signifies the decrease in voltage between the two electrodes with proper discharge current. This corresponds to ideal machining in EDM. Arc takes place due to sticking of debris materials to the electrodes resulting in decease in gap, so that discharge takes place even before peak voltage is attained which is evident form Fig. 1.3. Usually, spark pulses produce a better surface finish and machining stability than arc pulses. Short pulses occur if the electrodes are contaminated and are discharged owing to carbon deposited on the workpiece. In order to avoid damage to the workpiece, tool and machine, short pulses must be prevented [Yu et al., 2001]. Transient arc is characterised by extremely short ignition delay time as shown in Fig. 1.3.

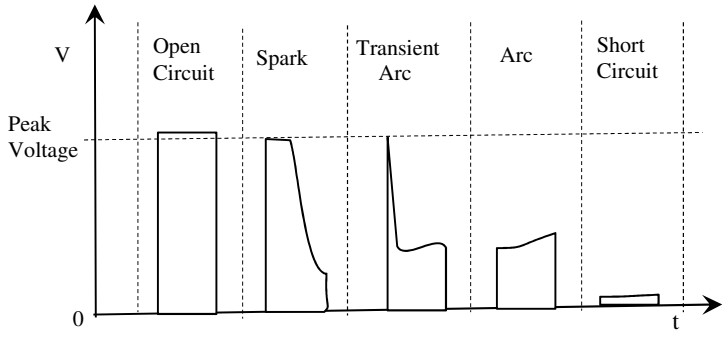

Fig. 1.3: Waveform of EDM [Jiang et al., 2012]

1.6 Important parameters of EDM operation

- Discharge current or Pulse current (Ip): It is the most significant machining parameter in EDM because it directly relates to power consumption while machining. The current increases until it reaches a specific level which is expressed as discharge current. The maximum amount of current that can be used is decided by the surface area of tool, and it is directly proportional to Material Removal Rate (MRR).

- Discharge voltage (V): It is the open circuit voltage which is applied between the electrodes. The discharge voltage de-ionizes the dielectric medium, which depends upon the electrode gap and the strength of the dielectric, prior to the flow of current. Once the current flow starts, the open circuit voltage drops and stabilizes the electrode gap. It is a vital factor that influences the spark energy, which is responsible for the higher MRR, higher Tool Wear Rate (TWR) and rough surfaces.

- Pulse-on time (T_{on}): It is the duration of time (μs) when the voltage is applied per cycle. Material removal is directly proportional to the amount of energy applied during this on-time. This energy is really controlled by the peak current and the length of the on-time.

- Pulse-off time (T_{off}): It is the duration of time (μs) between the two consecutive sparks (that is to say, on-time). During this time, the molten metal solidifies and is washed out of the spark gap. This parameter affects the speed and the stability of the cut. Thus, if the off-time is too short, it will cause sparks to be unstable.

- Duty cycle (Tau): It is a percentage of the on-time relative to the total cycle time. This parameter is calculated by dividing the on-time by the total cycle time (on- time and off-time), which is shown in Equation 1.1.

$$Tau = \frac{T_{on}}{T_{on} + T_{off}} \times 100 \tag{1.1}$$

- Polarity: Polarity refers to the potential of the workpiece with respect to tool, *i.e.* in straight or positive polarity the workpiece is positive, whereas in reverse polarity workpiece is negative. Varying the polarity can have dramatic effect, normally electrode with positive polarity wear less, whereas with negative polarity machining takes place at faster rate. On the other hand, some of the metals do not respond this way. Metal carbide, titanium and copper are generally cut with negative polarity.

- Inter electrode gap (IEG): The inter electrode gap is a vital factor for spark stability and proper flushing. The most important requirements for good performance are gap stability and the reaction speed of the system; the presence of backlash is particularly undesirable. Gap width is not measurable directly, but can be inferred from the average gap voltage. The tool servo mechanism is responsible for maintaining working gap at a set value. Mostly electro mechanical (DC or stepper motors) and electro hydraulic systems are used, and are normally designed to respond to average gap voltage.

- Dielectric fluid: Dielectric fluid serves three important purposes in EDM. The first function of the dielectric fluid is to insulate IEG and allow flow of current. after breaking down at the appropriate applied voltage. The second function is to flush away the debris from the machined area and lastly, the dielectric acts as coolant to assist during heat transfer between the electrodes. Most commonly used dielectric fluids are hydrocarbon compounds, like light transformer oil and kerosene.

- Tool work time (T_w) and Tool lift time (T_{up}): During the working time T_w multiple sparks occur with a pulse-on duration T_{on} and pulse-off time T_{off}. Then, the quill is lifted up for T_{up} duration when impulse flushing is done. The impulse flushing is an intermittent flushing through side jet and it is done through a solenoid valve that is synchronized with the lifting of tool. The dielectric is directed between the IEG to accomplish removal of the debris. The sparking cycle consist of T_w and T_{up}, which shown in Fig. 1.4.

- Flushing Pressure and Type of flushing: Flushing is an important factor in

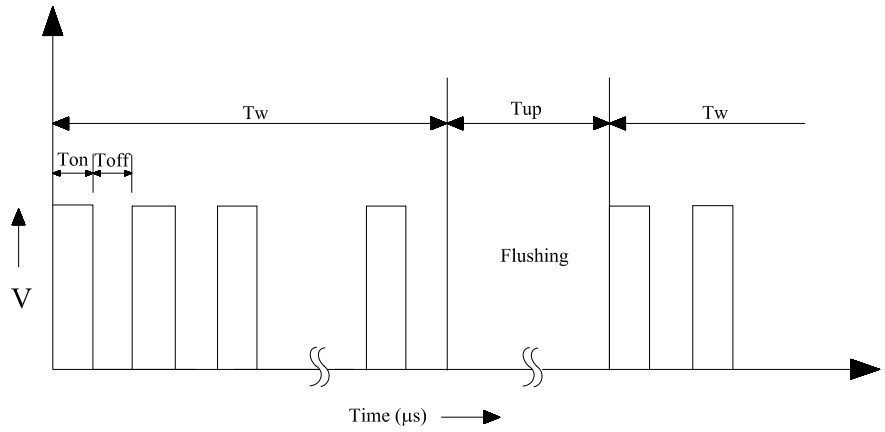

Fig. 1.4: Sparking cycle of EDM

EDM because debris must be removed for efficient cutting. Moreover, it brings fresh dielectric into the IEG. Flushing is difficult if the cavity is deeper. Inefficient flushing may initiate arcing and may create unwanted cavities which can adversely affect the quality of machined workpiece. There are several methods generally used to flush EDM gap: jet or side flushing, pressure flushing, vacuum flushing and pulse flushing. In jet flushing, hoses or fixtures are used and directed at the IEG to wash away the debris whereas in pressure and vacuum flushing dielectric flows through the drilled holes in the electrode, workpiece or fixtures. In pulse flushing the movement of electrode in up and down, orbital or rotary motion creates a pumping action to draw the fresh dielectric. The usual range of pressure lies between 0.1 to 0.4 kgf/cm^2.

1.7 Tool material

Tool material should be such that it should not undergo much tool wear when it is impinged by positive ions. Thus the localized temperature rise has to be less by tailoring or properly choosing its properties or even when temperature increases, there would be less melting. Further, the tool should be easily workable as intricate shaped geometric features are machined in EDM. Thus the basic characteristics of electrode materials are:

- High electrical conductivity, that enables to emit more cold electrons easily and there is less bulk electrical heating.
- High thermal conductivity for the same heat load: The local temperature rise would be less due to faster heat conducted to the bulk of the tool and thus less tool wear.
- Higher density for the same heat load and same tool wear by weight: There would be less volume removal or tool wear and thus less dimensional loss or inaccuracy.
- High melting point leads to less tool wear due to less tool material melting for the same heat load.
- Easy manufacturability and low cost.

The different electrode materials which are commonly used are brass, graphite, copper, aluminium alloys, copper-tungsten alloys and silver-tungsten alloys.

1.8 Applications of EDM

EDM is used in different applications which are discussed below:

- The EDM process is most widely used by the mould-making tool and die industries, but is becoming a common method of making prototype and production parts, especially in the aerospace, automobile and electronics industries in which production quantities are relatively low.
- It is used to machine extremely hard materials that are difficult-to-machine like tool steels, die steel, tungsten carbides, nickel-based super alloy etc. It is used for internal thread cutting and helical gear cutting.
- It is used for machining sharp edges and corners that cannot be machined effectively by other machining process.
- It is used for forging, extrusion, wire drawing and thread cutting dies.
- It is used for drilling of curved holes.

- Higher tolerance limits can be obtained in EDM. Hence applications that require higher surface accuracy use EDM process.
- EDM has also made its presence felt in the new fields such as sports, medical and surgical, instruments, optical, including automotive R&D segments.
- Ceramic materials that are difficult-to-machine can be machined by EDM process.
- It is a promising technique to meet increasing demands for smaller components usually highly complicated, multi-functional parts used in the field of microelectronics.

Chapter II

Literature Review

2. LITERATURE REVIEW

2.1 Major areas of research in EDM

Considerable number of papers had paid attention on approach of yielding optimal Electric Discharge Machining (EDM) performance measures of high Material Removal Rate (MRR), low Tool Wear Rate (TWR) and acceptable Radial Overcut (OC) . A vivid literature review of the development of EDM technology between 1993 and 2003 has been reported by Ho and Newman [2003]. The current research trends in EDM on ultrasonic vibration, dry EDM, EDM with powder additives, EDM in water and modelling technique in predicting EDM performances were presented by Mohd Abbas et al. [2007]. Garg et al. [2010] discussed about machining of Metal Matrix Composite (MMC) with EDM, Wire Electro Discharge Machining (WEDM) and Powder Mixed Electro Discharge Machining (PMEDM). They presented the summary of research work undertaken in these areas in the last twenty years, along with possible future trends. The general direction of study relates to machining performance evaluation for MRR, TWR and surface integrity achieved after machining. However, many investigations were also directed towards monitoring and control of the process parameters. In this section, the contribution by various researchers in the area of die sinking EDM and their development is discussed.

2.1.1 Influence of EDM parameters on various performances measure

Considerable research has been carried out on the influence of different EDM parameters on various performance measures which are discussed as follows:

Material removal rate (MRR)

Mohri et al. [2000] observed that peak current (Ip) has significant influence on MRR in EDM. Similar observation has also been reported by many researchers [Mohan et al., 2002; Kuppan et al., 2007; Kung et al., 2009] Increase in peak current leads

to enhancement of spark energy which in turn causes formation of large number of craters having higher depth. As a consequence, MRR increases.

Kung et al. [2009] reported increase in MRR with increase in pulse-on time (T_{on}). However, different observation was noted by [Mohan et al., 2002]. It was argued that long pulse duration might cause the plasma channel to expand, thus reducing energy density for the workpiece. On the contrary, Kuppan et al. [2007] did not find pulse-on time to be a significant parameter for MRR.

Wang and Yan [2000]; Mohan et al. [2002] investigated the effect of polarity on MRR. Positive (straight) polarity was found to resulting more MRR then negative (reverse) polarity. Transfer of higher energy during positive polarity was attributed.

Mohan et al. [2002] compared MRR obtained with stationary and rotatory electrode. It was observed that electrode rotation caused whirl and resulted in effective flushing of the gap. Hence, MRR for rotating electrode was more compared to that for stationary electrode. Kuppan et al. [2007] also found speed of electrode rotation to be a significant parameter. The studied indicated that rotation of speed was more significant at lower current settings compared to higher current. At lower current, MRR was low and the debris was finer. Therefore, increase in rotational speed resulted in effective flushing of debris particles from the gap. As a result, percentage increase in MRR was more compared to that for higher current settings which let to higher concentration of debris in the gap.

Kuppan et al. [2007] demonstrated increase in duty cycle caused slight increase in MRR. Since duty cycle represents that percentage of total time the spark remains on, increase in duty cycle would indicate more fraction of total time will be utilized in removing the material. This result was in complete agreement with that reported by Puertas et al. [2004].

Kunieda and Masuzawa [1988] proposed a horizontal EDM for a more productive and accurate machining than conventional vertical EDM. Experimental and analytical investigations proved the beneficial characteristics of the horizontal EDM. Eroded particles can easily flow out of the working gap as a result of buoyancy of bubbles. This effect is further significant when both the electrode and workpiece are rotated synchronously.

Tool wear rate (TWR)

The tool wear is moderately analogous to the Material Removal Mechanism (MRM) in EDM. Mohri et al. [1995] proved that tool wear is affected by the precipitation of turbostratic carbon from the hydrocarbon dielectric on the electrode surface during sparking. Also the rapid wear on the electrode edge was because of the failure of carbon to precipitate at difficult-to-reach regions of the electrode. From this easy understanding of tool wear, some useful applications exploiting both the advantages and disadvantages of electrode wear have been developed.

In addition to erosion of workpiece, EDM also results in removal of material from the tool electrode. The former corresponds to material removal rate (MRR) whereas the latter contributes to what is known as tool wear rate (TWR). Many researchers[Karthikeyan et al., 1999; Dhar et al., 2007; Kung et al., 2009; Lin et al., 2008; Tsai et al., 2003b] have found out that TWR increased with MRR. Heat and impulsive force which are generated across IEG during electrical discharge erode both workpiece and tool electrode. Their is a general agreement among researcher that increasing peak current (Ip) causes TWR to increase. However, influence of pulse-on time on TWR has been debated. Kung et al. [2009] observed quick increase of TWR with increase in T_{on}, due to increase in discharge energy associated with higher T_{on}. On the other hand, the inverse relationship has also been reported [Karthikeyan et al., 1999; Lin et al., 2008]. Dhar et al. [2007] observed intial increase followed by decrease in TWR when pulse-on duration was increased form 200 to 400 μs.

Bleys et al. [2002] devised an on-line tool wear compensation method based on the pulse analysis and controlled the tool feed movement in real time. Kunieda and Kobayashi [2004] clarified the mechanism of determining tool electrode wear ratio in EDM by spectroscopic measurement of the vapour density of the tool electrode material. Longer T_{on} results in lower TWR and deposition of a thicker carbon layer on the tool electrode surface. Conversely, the density of copper vapor evaporated from the tool electrode surface was found to be lower when the carbon layer was thicker, indicating that tool electrode wear might be prevented by the protective effects of the carbon layer. The well-known machining strategy to recompense tool wear is the orbiting of the electrode relative to the workpiece, where a planetary motion creat-

ing an effective flushing action, provided better part accuracy and process efficiency [Snoeys et al., 1986]. This technique also trimmed down the number of different electrodes necessary for initial roughing and final finishing operations [Staelens and Kruth, 1989]. Dauw and Snoeys [1986] derived the measurement of tool wear from the study of pulse characteristics based on discharge voltage fall time. Yu et al. [1998] established a uniform tool wear machining method to compensate the longitudinal tool wear by applying an overlapping backward and forward machining motion.

Overcut (OC)

The EDMed cavity produced is always larger than the tool electrode and this difference (size of the electrode and the size of the cavity) is referred to as OC. Close tolerance components are required to be produced in tools, dies and moulds for press work is of utter importance.

The dimensional accuracy of EDM is greatly influenced by the OC resulting from the discharge gap and electrode wear. Since overcut phenomenon is directly related to discharge energy, higher MRR would result in more overcut in EDM [Singh et al., 2004c; Dhar et al., 2007]. Therefore, pulse current is directly proportional to overcut [Singh et al., 2004c; Dhar et al., 2007]. The parameters such as Ip, T_{on}, voltage applied and the workpiece material significantly influence OC. It increases with the increase of Ip but up to a certain limit. Besides, it depends upon gap voltage and chip size which vary with the amperage [Singh et al., 2004c]. Copper and aluminum electrodes might be preferred option over copper-tungsten and brass electrodes for machining En-31 tool steel since the latter resulted in increase in diameteral overcut.

Surface integrity of EDMed surface

The term surface integrity is used to describe the quality and condition of the surface region of a machine component. It includes the topological, mechanical, metallurgical and chemical conditions of the surface region as well as surface and sub-surface structure. It is well established that EDMed surfaces usually experience a transformed or altered layer having different characteristics from those of the parent metal.

Rajurkar and Pandit [1988] gave a comprehensive description of surface integrity that includes the measures of Surface Roughness (SR), White Layer Thickness (WLT),

Heat Affected Zone (HAZ), micro-cracks, residual stresses, diffusion of tool material and carbon and endurance limit. It has been ascertained that the surface integrity is significantly distorted by EDM and thus efforts are being made to negate the transformations in surface integrity of machined components. The thermal changes may cause cracks in the top layer and residual stresses in the underlying base layers [Cogun and Savsar, 1990]. Although EDM has many advantages the recast layer with cracks, caused by rapid cooling results in poor surface accuracy [Kruth et al., 1995; Schumacher, 2004].

Surface texture, surface topography or surface finish are the terms, which are used to express the machined surface related to the geometric irregularities and quality of the surface. An ideal surface roughness is commonly specified by the peak to valley height or the centre line average, Ra (μm). The EDMed surfaces consist of plenty of craters formed by the discharge energy. If the energy content is high, deeper craters will be accomplished, leading to poor surface finish. The surface roughness has also been found to be inversely proportional to the frequency of discharge [Pandey and Shan, 1980]. A spark-eroded surface is a surface with a mat finish and random distribution of overlapping craters. It is often covered with a network of micro-cracks [Pandey and Jilani, 1986]. The molten metal was expelled randomly during the discharge and later solidified on the electrode surfaces. The crack formation is associated with the development of high thermal stresses of the material, as well as with plastic deformation.

Many attempts had been made for modelling of EDM process and investigation of the process performance to improve the surface quality. For the prediction of surface roughness empirical models as well as multi-regression analysis are usually applied. It has been observed that there are many process variables that affect the surface finish such as Ip, T_{on}, open circuit voltage, electrode polarity, thermal properties of the tool, work, dielectric liquid and debris concentration. Kiyak and Cakir [2007] investigated the influence of EDM parameters on Ra for machining of AISI P20 tool steel and emphasized that the choice of the machining parameters to achieve good surface quality of EDMed component should be smaller pulse current and shorter pulse time. This is because, small particle size and crater depths created by discharge.

Consequently, the smooth surface will be produced. Jaharah et al. [2008] investigated SR with copper electrode AISI H3 tool steel workpiece with the input parameters of Ip , T_{on}, and T_{off}. The optimum condition for Ra was obtained at low Ip , low T_{on}, and T_{off}. It was concluded that the Ip was the major factor affecting Ra. Keskin et al. [2006] in their experimental study obtained a regression equation and asserted that the results will help to manufacture steel parts with definite surface roughness requirements instead of trial and error. In addition, it is revealed that Ra has an increasing trend with an increase in the T_{on}, which is probably due to more discharge energy released during this time and expanding the discharge channel.

Khan et al. [2009] discussed the SR performance of EDMed mild steel for different shape configurations of the electrode. The minimum surface roughness was found for the round electrodes followed by square, triangular and diamond shaped electrodes. Tsai and Wang [2001b] reported several surface finish models by taking the effects of electrode polarity into account. They subsequently reported a semi- empirical model dependent on the thermal, physical and electrical properties of the workpiece and electrode together with relevant process parameters such as T_{on}, Ip , polarity, input power, material density, conductivity, specific heat capacity, heat conductivity, melting point and boiling point. The latter model was found to be a more trustworthy surface finish prediction for various workpiece materials (EK2 and H13) under various process conditions as reported by Tsai and Wang [2001a]. Salonitis et al. [2009] in their study developed a model for SR and stated that with the increase in process parameters, Ip , T_{on} and V, coarser workpiece surfaces were achieved. Later, it was verified experimentally and found to be in good agreement with predicted results.

The characteristics of the machined surface were explored extensively by Kanagarajan et al. [2008]. They had chosen Ip , T_{on}, electrode rotation and flushing pressure as design factors to study the EDM process performance such as SR on cemented carbide (WC-CO). The most influential parameters for minimising the SR have been identified using the RSM and experimentally verified by conducting confirmation experiments. Chiang [2008] proposed a mathematical model and investigated the influence of Ip , T_{on}, Tau, voltage and their interactions on SR. The experiments were conducted on Al_2O_3+TiC workpiece and found that Ip and T_{on} have statistical

significance on SR. It was claimed that model predicted SR very narrowly with a 95% confidence interval.

In the EDMed component, a unique structure on the surfaces of the machined parts has been observed. The microscopic observations showed that unusual phase changes occur due to high local temperature attained during the machining. The top layer is a recast layer formed by re-solidification of the molten metal and this layer is found to be heavily alloyed with the pyrolysis products of the cracked dielectric. The material surface is found to be fairly resistant to etching by conventional metallography reagents. Therefore, the recast layer on ferrous alloys is often referred to as an unmatchable 'white' layer. Micro-hardness measurements have shown that for ferrous alloys, the recast layer generally has a hardness value much higher than that of the underlying matrix and may exceed the value attainable by normal quenching techniques [Ekmekci, 2007; Mamalis et al., 1988].

HAZ lies beneath the white layer structure, which generally has a tempered micro structure and has a hardness value fairly less than that of the underlying hardened metal. An intermediate layer between the recast and the tempered layers was also observed and reported. This layer was found to exhibit a carbon gradient and contamination of materials from the tool electrode. It is possible that this layer includes part of the melted layer plus a region beyond which diffusion has occurred in solid state. The hardness of this layer is found to be comparable to or, sometimes, a little higher than that of the recast layer [Lim et al., 1991]. Under optical microscope, it generally has a darker appearance than the parent material. The bulk of the material beyond the tempered zone remains unaffected by machining.

Lee et al. [2004] studied experimentally the influence of the EDM parameters on surface integrity of AISI 1045 carbon steel and furnished that average WLT and induced residual stress tended to increase at higher values of Ip and T_{on}. However, for an extended T_{on}, it was noted that Surface Crack Density (SCD) decreased. Besides, obvious cracks are always apparent in thicker white layers. A smaller Ip (i.e. 1 A) tends to increase the SCD, while a prolonged T_{on} amplifies the opening degree of the surface crack, thereby reducing it. The effect of EDM parameters on surface crack formation for D2 and H13 tool steels was studied by Lee and Tai [2003]. High T_{on} will

increase both the WLT and the induced stress and both of them tend to support the formation of crack. Similar study of EDM parameters on thickness of white layer has also been reported by Ramasawmy et al. [2005]. Stainless martensitic chromium tool steel was used for EDM test. Relation of WLT with 3D surface texture amplitude, spatial and volume parameters were discussed and shown. Ip has comparatively more significant effect on the dimension of the crater as compared to T_{on}. It is said that the dimension characteristics of the molten metal pool define the magnitude of the surface tension, and eventually the thickness of the white layer. Bhattacharyya et al. [2007] developed mathematical models based on Response Surface Methodology (RSM) for correlating Ip and T_{on} different aspects of surface integrity of M2 Die Steel machined through EDM at the transverse section and experimentally validated them using the Scanning Electron Microscope (SEM) micrograph. The plotted graphs and revealed the correctness of the developed models. Optimal combination of parameters has been estimated, which can be used to improve surface integrity of the machined surface.

Rebelo et al. [1998] have reported quantitatively and qualitatively, the formation of plasma channel between tool (steel) and workpiece, metallurgical transformations, residual tensile stresses and surface cracking. The dimension of random overlapping surface craters increases with machining pulse energy. The cracks radiate from and circumvent the craters. The density and penetration depth of the cracks in the re-cast layer increase with the machining pulse energy. Mamalis et al. [1987] in their experimental study revealed the physico- chemical changes occurring during EDM of steel. A correlation between surface morphology and overall process parameters have been noticed. White layer and crack formation are related with the development of high thermal stresses exceeding the fracture strength of the material in addition to plastic deformation and are determined quantitatively by the use of regression equations. Their dimensional dependence on pulse energy is clearly shown.

Lim et al. [1991] provided a review on the metallurgy of EDMed surface, which is dependent on the solidification behaviour of the molten metal and subsequent phase transformation. Solidification of the molten metal takes place simultaneously from the top interface with the dielectric to the bottom interface with the underlying metal into the melt, as well as from within the melt towards both interfaces. This leads to

the formation of three distinctive sub layers within each recast layer resolidified from a given pool of molten metal. Wang et al. [2009] studied the feasibility of removing the recast layer from molds and dies using etching and mechanical grinding for Ni-based super alloy materials by means of EDM. The analysis has been carried out in three stages. The first stage is to obtain a thick recast layer by using EDM with a larger discharging energy applying the Taguchi L_{18} analytical method. Furthermore in the second stage, optimized the recast layer removal technique using Taguchi's L_9 orthogonal for the etching and mechanical grinding parameters and observed the recast layer removal quantity analysis.

Crack development can be attributed to the existence of thermal and tensile stresses within the EDMed component. Tensile stresses are generated since the melted material contracts more than the unaffected parent material. Diffusion of carbon from dielectric liquid and possibly alloying materials from tool electrode can also affect the material contraction rate. When the stress in the surface exceeds the material's ultimate tensile strength, cracks are formed [Thomson, 1989]. Results from previous studies, Lee et al. [1990, 1992] had indicated that cracking increases as the pulse energy increases. But, it was stated that maximum crack density actually occurs under the minimum Ip and maximum T_{on} [Lee and Tai, 2003].

Cracks initiate from the surface and travel down perpendicularly towards the parent material. In most of the cases, the cracks terminate within the white layer or just on the interface zone between the white layer and heat affected zone. However, under some critical machining settings, cracks can penetrate to the parent material. Grain boundary cracking is evident under such circumstance. Surface cracks that are initiated at the surface, travel down perpendicularly toward the interference zone, and terminate at this interference, are primarily produced due to an increase in non-homogeneities of metallurgical phases within the white layer as proposed by Ekmekci [2009]. Lee et al. [2004] presented EDM of H13 and D2 tool steels and introduced the concept of a Crack Critical Line (CCL) to explore the influence of electrode size, EDM parameters and material thermal conductivity on surface cracking. It is noted that cracks tend not to appear when the machining is performed with a decreased Ip and an increased T_{on}. The fatigue strength of mechanical components is dependent

on the properties of the surface and near surface regions [Abu Zeid, 1996; Zeid, 1997]. Among the surface defects, cracking was found the most significant since it leads to a reduction in the material resistance to fatigue and corrosion [Lim et al., 1991] , especially under tensile loading conditions.

Although a number of experimental efforts have been made to make better understanding of the EDM process, modelling efforts of the process are really few in comparison. There may be number of explanation for this the complex and stochastic nature of the EDM process, the understanding of the complex phenomena inside a plasma channel and the tiny duration of single discharges. Every single discharge in EDM process is accompanying with extreme thermal effect and pressure pulse effects. Besides, the pulse pressure created by discharge causes a violent erosion effect and thus a part of the molten material is get rid of, to from a crater.

Ekmekci et al. [2006] suggested a semi-empirical equation for scaling residual stresses in EDMed surfaces and reported that the stress increases from the surface and attains to a maximum value, which is approximately equals the ultimate tensile strength of the material, and then it falls gradually to zero or even to a small compressive residual stress at greater depths. Residual tensile stress increases with the increase in pulse current and pulse-on duration. Investigation of the residual stresses of EDMed components revealed their tensile nature, the extremely narrow superficial zone where they appear, their high magnitude at the surface layers, and their increase with increasing pulse energy. The formation of surface cracks has been attributed to the differentials of high contraction stresses exceeding the material's ultimate tensile stress within the white layer [Lee et al., 2004]. A qualitative relationship with the operating parameters was presented by Ekmekci et al. [2005] using AISI P20 workpiece material. Mamalis et al. [1988] experimentally investigated on low-carbon steel ST37, medium carbon steel C45 and alloyed steel 100Cr6 workpiece and found that the peak stresses are almost independent of the discharge energy and approach the ultimate tensile strength of the material. Rebelo et al. [1998] in his investigation, using XRD methodology found that the residual stress of steel workpiece increases from the bulk material to a maximum and decreases again while approaching towards the surface. The peak stresses are almost independent of the discharge energy and

the greater the discharge energy, the greater the depth at which the maximum value of residual stress occurs.

2.1.2 Optimisation of EDM Process

This section provides a study into each of the performance measures and the scheme for their enhancement. In past, significant improvement has been carried out to enhance productivity, accuracy, and the versatility of EDM process. The major issue is to pick the process parameters such as Ip , T_{on}, Tau, V, flushing pressure, dielectric fluid and polarity in such a way that MRR and accuracy increases; and concurrently overcut or gap, TWR, SR and SCD should diminish.

Single objective optimisation

There are various methods for single objective optimisation that are described in this section.

Taguchi method: Chen et al. [2013] had presented the Taguchi design to analysis the effect of responses on EDM process with A6061-T6 aluminium alloy. The control parameters are selected as pulse current, the pulse-on time, the duty cycle, and the machining time. The optimal machining parameters and the relative influence of each parameter on the SR were determined by analysing the experimental data using the Analysis of Means (ANOM) and Analysis of Variance (ANOVA) techniques. They proved that the magnitude of the SR is determined primarily by the discharge current and duty cycle. Guleryuz et al. [2013] investigated the effect of EDM parameters on the SR as an alternative method for machining of Al/SiCp metal matrix composites produced using Power Metallurgy (PM) technique. Discharge current, electrode type, pulse-on time, particle reinforcement weight ratio and voltage were used as the process parameters. These parameters were selected for L_{18} Orthogonal Array (OA) based on Taguchi design, and experimental result showed that discharge current and pulse-on time is the most influencing parameters.

Das et al. [2012] studied the effect of machining parameters on MRR in EDM of EN31 tool steel. The selected control parameters were T_{on}, T_{off}, Ip and V with L_{27} OA based on Taguchi design. They found that the optimum machining parameter combination is obtained by the analysis Signal-to-Noise (S/N) ratio and this result

showsed that discharge current has the most significant effect on MRR followed by T_{off} and V. Chen and Lee [2010] had described the optimisation of EDM parameters for machining ZrO_2 ceramic. They studied machining responses such as, MRR, TWR, and SR. Experimental study according to L_{27} OA based on the Taguchi design were adopted. ANOVA was conducted to examine the significant machining parameters affecting the machining characteristics. Experimental results indicated the peak current and pulse-on time significantly affected MRR and SR, and the adhesive conductive material was the significant parameter correlated with TWR.

Huertas Talon et al. [2010] proposed a method of manufacturing a spur tooth gear in Ti- 6Al-4V alloy (grade 5) using WEDM. Optimum value of power were chosen for cutting titanium. They found that this program simplifies the task of solving the equations originated by the mathematical model which allows the wire path. Marafona and Araujo [2009] discussed the effect of workpiece hardness and its interactions on MRR and SR. Taguchi method L_{18} OA was used and the input parameters were current intensity, voltage, pulse duration, duty factor and ram speed. They found that the EDM process is not only influenced by the thermal properties of the workpiece but also by its hardness. Lajis et al. [2009] investigated that feasibility of machining tungsten carbide ceramics by EDM with a graphite electrode by using Taguchi method. They selected the EDM parameters such as peak current, voltage, pulse duration and interval time. It was found that these parameters have a significant influence on machining characteristic such as MRR, TWR and SR. They showed the analysis of the Taguchi method. In general the peak current significantly affects the TWR and SR, while, the pulse duration mainly affects the MRR.

Lin et al. [2008] examined the effect of magnetic force on EDM characteristics. Responses such as MRR, TWR and SR were analysed using electrolytic copper as tool and SKD 61 steel as workpiece . They used L_{18} OA based on Taguchi design. Parameters namely polarity, discharge current, pulse-on time, high-voltage auxiliary current (IH), no-load voltage and servo reference voltage (Sv) were chosen. It was concluded that magnetic force-assisted EDM resulted in process with higher efficiency and stability and improved surface integrity in terms of lower SR and reduced surface cracks. Kansal et al. [2007] analysed the effect of silicon powder mixing into the di-

electric fluid of EDM on machining characteristics of AISI D2 die steel. They selected the machining parameters such as Ip , T_{on} and T_{off}, concentration of powder, gain, and nozzle flushing with Taguchi Design of Experiments (DOE). They showed that the powder concentration at a high level and gain at a low level produced optimum material removal from AISI D2 surfaces when machined by silicon PMEDM.

Response surface method: Gopalakannan et al. [2012] had conducted experiment on MMC of aluminium 7075 reinforced with 10 wt% of Al_2O_3 particles MMC was prepared by stir casting method. They used RSM along with ANOVA to investigate the influence of process parameters and their interactions viz., pulse current, gap voltage, pulse-on time and pulse-off time on MRR, TWR and SR. Rahman et al. [2010] developed a mathematical model of MRR for Ti-5Al -2.5Sn using Central Composite Design (CCD) of RSM. Peak current, pulse-on time, pulse-off time and servo voltage were considered as input parameters to correlate with MRR. Habib [2009] proposed a comprehensive mathematical model for MRR, TWR, gap size and SR in EDM using RSM approach. The analysis showed that MRR increases with an increase of pulse-on time, peak current and gap voltage. Tool wear ratio increased with an increase of both pulse-on time and peak current and decreased with increase of both SiC percentage and gap voltage. The laser texturing process has been studied using two experimental approaches: Taguchi method and RSM by Soveja et al. [2008]. They had determined a correlation between process operating factors and performance indicators, such as SR and MRR. They showed that the MRR is directly proportional to linear effects of the pulse-energy and frequency, while the SR is inversely proportional to them. Kung and Chiang [2008] proposed a mathematical models of the MRR and SR. The peak current, pulse-on time, duty factor, and wire speed, are control parameter on WEDM process of aluminium oxide based ceramic material (Al2O3 + TiC). An experimental plan of the face centred CCD-based on the RSM has been used.

Full factorial design: Kodlinge and Khire [2013] had investigated on MRR of tungsten carbide for EDM operation using Kerosene as dielectric medium. The discharge current, electrode diameter and pulse-on time are considered as control parameters. They used 2^3 factorial design and ANOVA and indicated that among

the three factors investigated current has a strongest effect on MRR. Pradhan and Jayswal [2011] described the 2^3 full factorial design that was performed to EDM machining of EN-8 alloy steel with copper and aluminium as tool electrode. It has been found that copper shows better results than aluminium in term of SR in same dielectric media. They recommended that the copper is a good electrode material for machining.

Amini et al. [2010] analysed the effect on SR on EDM process with hot work steel DIN1.2344. The DOE selected was full factorial where the control parameters were Ip, V, T_{on} and T_{off}. Statistical analysis has been done and Artificial Neural Network (ANN) has been used to choose proper machining parameters. Finally, a hybrid model has been designed to reduce the ANN errors which indicated a good performance of complex and non-linear problems. Ali and Mohammad [2008] described the effect of SR on conventional WEDM with copper substrate for micro-fabrication. Statistical models were established to predict the SR and Rt in terms of discharge current, pulse-on time and gap voltage. Using the optimised parameters, miniaturized spur gears, and plate-shaped hot embossing, micro tools were fabricated where an average surface roughness of about 1μm and dimensional accuracy of 12% were achieved. Dhar et al. [2007] estimated the effect of Ip, T_{on}, and V on MRR, TWR and Gap on EDM of Al-4Cu-6Si alloy-10 wt.% SiCP composite. Using three factors, three level full factorial designs, a second order non-linear mathematical model has been developed for establishing the relationship among machining parameters. It was revealed that the MRR, TWR and gap increase with increase in Ip and T_{on}.

Nero-fuzzy modelling : Suganthi et al. [2013] described the Neuro-Fuzzy Inference System (ANFIS) and back propagation based on ANN model of micro-EDM process. For using this method, they predicted the output responses such as MRR, TWR and SR. The feed rate, capacitance, gap voltage, and threshold values were selected as control parameters. They proved that the predicted values of the responses are in good arrangement with the experimental values. The SR and WLT responses are measured in WEDM, and these responses were predicted from ANFIS model by Caydas et al. [2009]. The pulse-on time, open circuit voltage, dielectric flushing pressure and wire feed rate are considered as control parameters. They combined

modelling function of fuzzy inference with the learning ability of artificial neural network; and a set of rules have been generated directly from the experimental data. The models predictions were compared with experimental results for verifying the approach. Gostimirovic et al. [2012] described the modelling of MRR in EDM process by using artificial intelligence tools. Their objective of this study was to design an adaptive ANFIS for prediction of MRR in EDM. The selected control parameters were discharge current and pulse-on time. They ascertained that the ANFIS modelling technique could be effectively used for the prediction of MRR in machining of manganese-vanadium tool steel.

Artificial neural network : Prajapati et al. [2013] investigated the effect of responses (MRR , SR, Kerf and Gap current) on WEDM process. The pulse-on time, pulse-off time, voltage, wire feed and wire tension are considered as input parameters. The ANN was used for prediction of output parameters of WEDM of AISI A2. Ndaliman et al. [2012] reported ANN technique to predict electrode properties with high degree of prediction accuracy and compared them to the experimental results. They used Cu-TaC compacted electrodes for before and after sinters. They showed that the sintered electrodes are not suitable for EDM, but the pre-sintered electrode is suitable for machining. Jia et al. [2011] described that high frequency and weak energy of Micro Electric Discharge Machining (MEDM) resulted in highly distorted waveforms of voltage and current. Hence fuzzy logic was used instead of commonly used EDM perceptive methods. Learning vector quantification ANN was adopted to convert this scalar to the corresponding state vector. They showed that the experimental results verify the effectiveness of this discharging pulses discriminator for MEDM. Feed forward-back propagation neural network was established for EDM by Thillaivanan et al. [2010]. The parameters *i.e.*, current and feed for a required total machining time, oversize and taper of a hole to be machined by EDM which are given as inputs. They showed that performance characteristic, total machining time, can be improved through this method. Joshi and Pande [2009] developed an intelligent model for the EDM process using Finite Element Method (FEM) and ANN. They generated the numerical data by FEM simulations for using trained and tested data for ANN, and predict the shape of crater cavity, MRR, and TWR. Esme et al. [2009]

described the two techniques, factorial design and neural network for modelling and predicting the SR. Pulse-on time, voltage, wire speed and dielectric flushing pressure were considered as control parameters of AISI 4340 steel.

Multi-objective optimisation

Multi-objective optimisation is an area of multiple performance characteristics index, that is concerned with mathematical optimisation problems including more than one objective function to be optimised simultaneously. Multi-response optimisation has been useful in various area of science, including engineering and economics where optimal decisions need to be taken in the presence of trade-offs between two or more conflicting objectives. There are several methods in related to EDM to reduce multiple quality characteristics to a single quality parameter, which can be optimised easily [Aslan, 2008; Gaitonde et al., 2006]. Multi-attribute optimisation is a highly demanded research area of recent trend in EDM process also for other machining process.

Grey relation analysis : The Grey Relational Analysis (GRA) is the one of most important method for multi-objective optimisation in EDM process. Murugesan and Balamurugan [2012] described the optimisation of EDM process with multiple quality characteristics by using this method. They selected machining parameter like electrode polarity, discharge current, pulse-on time, pulse- off time and dielectric pressure and optimised the multiple responses like machining time, TWR and SR, simultaneously. The Taguchi method was adopted and found the relations between machining parameters and responses. Natarajan and Arunachalam [2011] used GRA to optimise multi-performance characteristics of Micro-EDM. They optimised the process parameters for higher MRR, lower TWR and lower OC and verified through a confirmatory experiment. An improvement of 12.88, 14.57 and 6.1% were observed for MRR, TWR and OC respectively.

GRA theory has been used to optimize the multiple quality characteristics in EDM process [Jung and Kwon, 2010]. In the analysis they found the optimal machining conditions under which the micro-hole can be formed to a minimum diameter and a maximum aspect ratio. The Taguchi method was adopted to determine the relations

between machining variable and their responses. Applying this method, they found that the optimal machining parameters, among which the input voltage and the capacitance were found to be the most significant factors. Panda [2010a] had analysed characterize spark-eroded craters formed on both anode and cathode surfaces. This experiment was based on L_9 OA. GRA has been implemented to find out the significant process parameters. Due to the stochastic nature of machining, the observations of crater morphology fail to provide complete information regarding the parametric effects. Finally, confirmatory experiments have been done to recognize the nature of the relative erosion of anode and cathode with respect to EDM process parameters.

Beri et al. [2011a] presented the multi-response optimisation using GRA and proved that the copper tungsten PM electrode provides better multi-objective performance than conventional copper electrode. In this experiment, AISI D2 tool steel as a workpiece material with copper CuW (25% Cu and 75% W) electrode was used. Taguchi L_{18} OA was used. The control parameters selected were electrode material, duty cycle, flushing pressure and discharge current. The responses measured were of MRR, SR and surface hardness. Beri et al. [2011b] described the multi-response parametric optimisation of EDM process by Taguchi method integrated with GRA. They used L_{18} OA with the effect of process parameters (polarity, electrode type, peak current, pulse-on time, duty cycle, gap voltage, retract distance and flushing pressure) on the responses of MRR , TWR and SR. In this analysis, they observed that the optimal machining parameter combination gives significant improvement of the Grey Relational Grade (GRG) . Pradhan [2012] proposed a new combination of RSM, GRA and Principal Component Analysis (PCA) modelling and optimisation method for the determination of the optimum process parameters that maximises MRR without compromising the surface quality in AISI D2 tool steel. Based on optimisation results, using the RSM, the interactive effects of the machining parameters on the responses were evaluated. It is found that the GRG was dominantly influenced by Ip and their interactions with the other parameters. The assessment outcome provides a scientific reference to obtain useful information about how to control the modelling parameter to ensure high productivity without compromising the quality of the EDM surfaces.

The optimisation of the EDM process with multiple optimisation process based on the OA with the GRA has been carried out by Dhanabalan et al. [2012]. They optimised the MRR, TWR and SR with two different Titanium grades using brass electrodes. Singh et al. [2004a] presented multi-response optimization using GRA for EDM process. The response parameters were MRR, TWR, taper, radial OC and SR. EDM was performed on $Al - 10\%SiC_P$ cast metal matrix composites using OA. Finally, confirmatory experiments were conducted.

Grey-fuzzy logic : Prabhu and Vinayagam [2013] used the multiple quality characteristics optimisation of process parameters like SR and MRR of EDM of carbon nano tube (CNT) mixed dielectric fluid. They used GRA integrated with fuzzy logic system to examine precision and accuracy of EDM process parameters and comparing each parameter influencing the machining, with and without using CNT mixed dielectric fluid. Lin and Lin [2005] had presented the optimisation of multiple process responses viz., MRR, TWR and SR. They applied the grey-fuzzy logics method for multi-optimisation. The selected machining parameters are pulse-on time, duty factor and discharge current with the SKD11 alloy steel as a workpiece material.

Fuzzy logic : Tzeng and Chen [2007] described the optimisation of multiple responses like machining precision and accuracy using fuzzy logic techniques in high speed EDM. The optimum design condition reported were voltage (120 V), pulse-on time ($12\mu s$), duty cycle (66%), Ip (12A), powder concentration (0.5 cm^3/l), regular distance for electrode lift (12mm) , time interval for electrode lift (0.6s), powder size ($40\mu m$). Additionally, the authors verified the results with confirmatory experiments. Puri and Deshpande [2004] used Taguchi method coupled with fuzzy logics system for the optimisation of wire-cut EDM process for multiple performance characteristics, such as SR and MRR. They suggested that both the responses can be improved through this approach. They acertained that in roughing machining poor surface finish were obtained, but in finish machining better surface finish can be achieved in the high-chromium -high-carbon die steel material. Lin et al. [2000] presented the optimisation of multiple responses for MRR and TWR using Taguchi method coupled fuzzy logic on EDM and found the best optimum conditions with a confirmatory test. They selected the control parameters such as polarity, pulse-on time, duty cycle,

voltage, discharge current and dielectric fluid on the SKD11 as workpiece material. In this experiment, they proved that MRR and TWR were greatly improved through this study.

Zhang et al. [2012] presented the micro-EDM for high noise. In this process, type-2 fuzzy logic sets are presented which is able to handle these uncertainties effectively. Based on interval type-2 fuzzy sets theory, a two- stage servo feed controller is designed. Identifying the discharge state for a single sample point in the first stage controller and the second stage is used to obtain the servo feed speed. They proposed interval type-2 fuzzy logic based two-stage servo feed controller is an effective way to enhance the efficiency and stability of micro-EDM. Reddy et al. [2010] proposed the modelling and analysis of the responses (such as MRR and SR) in WEDM. The experimental results of WEDM process is modelled using fuzzy logic for predicting the cutting velocity for given input parameters. Experiments were planned by Taguchi method and the results showed that the discharge current is the most significant parameter influencing the surface finish and cutting velocity.

Fuzzy TOPSIS : Sivapirakasam et al. [2011] presented the effect of the parameters like peak current, pulse duration, dielectric level and flushing pressure on the responses such as process time, relative electrode tool wear rate, process energy, concentration of aerosol and dielectric consumption. They used mixed Taguchi and fuzzy TOPSIS methods to solve multi- objective optimisation problems in EDM.

Loss function : Dave et al. [2012] presented the multi-response optimisation using Taguchi's loss function for EDM process with Inconel 718 as workpiece material. The selected control parameters were discharge current, voltage, pulse-on time and duty cycle at five levels each. L_{25} OA based on Taguchi method was used.

Desirability function : El-Taweel [2008] optimised multiple responses (MRR and TWR) of EDM process on workpiece CK-45 tool steel and electrode as Al-Cu-Si-Tic P/M composite material using desirability function. In this experiment, titanium carbide percent (TiC%), peak current, dielectric flushing pressure, and pulse-on-time were considered as input process parameters. Finally, the experimental results were found in good agreement with observed value based on RSM model. The error between experimental and predicted values at the optimal combination of parameter

settings for MRR and TWR lie within 7.2% and 4.74%, respectively. Assarzadeh and Ghoreishi [2013] proposed a multi-optimisation technique for the responses, MRR and TWR of PMEDM with aluminium oxide fine abrasive powders. The CK45 heat-treated die steel was selected as workpiece material and copper was used as tool electrode material. RSM had been used as DOE technique. The pulse-on time, discharge current and voltage were considered as control parameters in this experiment and they optimised the desirability functions with the machining regime of finishing, semi finishing and roughing range. EDM was engaged to machine the metal matrix nano-composite with copper electrode by implementing RSM by Gopalakannan and Senthilvelan [2013]. It has been detected that pulse current was found to be the most important factor effecting all the three output responses such as MRR, TWR and SR. Finally, the parameters were optimized for maximum MRR, minimum TWR and SR using desirability function approach.

Kanlayasiri and Jattakul [2013] investigate the optimal cutting condition of dimensional accuracy and SR for finishing cut of WEDM K460 tool steel. The selected control parameters were cutting speed, peak current, and offset distance. Box-Behnken design was used as the experimental approach, and multiple response optimization on responses was completed using the desirability function approach. They proved that both peak current and offset distance have a significant effect on the dimension of the specimen while peak current alone affects the surface roughness. Sivasankar et al. [2012] described the maintainability of ZrB2 using EDM with different tool materials such as graphite, aluminium, tantalum, niobium, copper, brass, silver, tungsten and titanium. SR, MRR, TWR, taper angle and WLT were measured. Desirability function analysis was employed to rate the performances of tools. They proved that the graphite is the best tool and WLT of the machined surfaces are indirectly proportional to the product of melting point and thermal conductivity of tool.

Utility theory : Chakravorty et al. [2012a] described the PCA- based utility theory approach and proposes the necessary modifications. Two sets of past experimental data on EDM processes were analysed using the modified procedure. The results show that the modified PCA-based utility method leads to better optimisation performance than that obtained by the earlier researchers. This proved that the mod-

ified PCA- based utility approach is very useful technique for optimising the EDM processes. Chakravorty et al. [2013] comparatively studied EDM processes and investigated using four different methods. They imitated the utility theory and weighted S/N ratio. It gave the better performance compared to GRA and other method. They used two sets of past experimental data and their relative performance for comparison.

Principal component analysis : Chakravorty et al. [2012b] presented four PCA-based optimization methods to simplify multi-response problems and using L_{18} orthogonal array and two sets of past experimental data on EDM processes, found that among the four PCA- based approaches, PCA- based Proportion of Quality Loss Reduction (PQLR) method results in the best optimization performance on machining characteristics, MRR, TWR and SR. Gauri and Chakraborty [2009a] described some modifications in the PCA- based approach and two sets of experimental data published by the past researchers was analysed using this modified procedure. It was observed that the PCA-based optimisation can give better results than the constrained optimisation and Multi-Response S/N ratio based methods, which can be attributed to the fact that the possible correlation among the multiple responses is taken care in the PCA-based approach. Gauri and Chakraborty [2009b] described a model for the WEDM process using the Weighted Principal Component (WPC) method. This method used to optimise the multiple responses of WEDM process. The results show that the WPC method offers significantly better overall quality than the other approaches. Pradhan [2013] presented the effect of process parameters on MRR, TWR and OC of EDM with AISI D2 tool steel. The control parameters selected were discharge current, pulse-on time, duty cycle and discharge voltage. Thirty experiments were conducted based on a face-centred CCD. The experimental results obtained were used with GRA, and the weights of the responses were determined by the PCA and further evaluated using RSM. The results indicate that the GRG was significantly effected by the machining parameters considered and some of their interactions.

Genetic algorithm : Non-sorted Genetic Algorithm (GA) has been implemented to optimise the responses of EDM technology using a powder-mixed dielectric by Padhee et al. [2012]. They used mathematical models for prediction of MRR and SR

through the knowledge of four process variables such as discharge current, concentration of powder (silicon) in the dielectric fluid, pulse-on time and duty cycle with EN-31 tool steel as a workpiece material. RSM was adopted to study the effect of control variable on responses and developed the predictive models.

Kuruvila and Ravindra [2011] investigated the multi-objective optimization using single GA in which the objective function is defined as composite function of the responses OC, SR and MRR *i.e.*, objective = OC+SR-MRR. The objective function was minimized by executing the GA. They used L_{16} OA based on Taguchi design with the control parameters are pulse-on time, discharge current, pulse -off time, bed-speed and flushing rate. Mukherjee and Chakraborty [2012] had used the composite function for multi-objective optimization of three responses (SR, WLT and SCD) using single objective GA. The composite function they had used is Min (Z1) = W1 *Yu (SR)/ SRmin+W2 *Yu (WLT)/WLTmin +W3*Yu (SCD)/SCDmin. Experiment models were developed for SR and MRR with machining parameters like pulse-on time, pulse-off time, and discharge current [Baraskar et al., 2013]. They used multi-optimisation method for non-dominating sorting GA-II to obtain the Pareto-optimal set of solutions. The RSM has been applied for evolving the models using the technique of DOE and multi linear regression analysis. Golshan et al. [2012] presented the effect of EDM on SR and MRR in metal matrix composite Al/SiC composite was examined. They studied the correlation between four input variables such as pulse-on time, pulse peak current, average gap voltage and percent volume fraction of SiC and process outputs. Finally, they found optimal conditions for outputs extracted from non-dominated sorting GA-II.

Other multi-objective optimisation techniques: A new hybrid approach of Neuro-Grey Modelling (NGM) technique of multi-objective optimisation process on EDM had been recommended by Panda [2010b]. They defined that simulate through ANN for description of multiple process attributes coupled with GRA method, and proved that the NGM technique is better and easy to implement.

2.1.3 Tool materials and design

According to Droza [1998], any material to be used as tool electrode is required to be electrically conductive. In fact, there is a wide range of materials used to manufacture electrodes, for instance, brass, tungsten carbides, electrolytic copper, copper-tungsten alloys, silver-tungsten alloy, tellurium-copper alloys, copper-graphite alloys, graphite etc. Amorima and Weingaertner [2007] suggested that graphite has a much lower density than copper, which makes it the best material for large electrodes. They reported that negative polarity of graphite electrode is better than copper electrode in the measurement of MRR. And best SR was obtained for copper electrodes under negative polarity. Janmanee et al. [2012] reported that the positive polarity of electrode give the higher micro crack density comparable to negative electrode while machining tungsten carbide. Reza et al. [2010] described that the positive polarity (tool -, workpiece +) gave the better result for MRR, TWR and SR when machining tool steel work piece using EDM.

Kumar and Singh [2007] described that copper-chromium alloy tool gives better results compared to copper and brass electrode in terms of MRR, OC and SR in two dielectric mediums (kerosene and distilled water). And also gave the information about when used of distilled water is used as a dielectric medium, MRR is less and TWR is higher as compared to kerosene for all the three electrode materials. Graphite tool is more advantageous than the copper tool for the measurement of MRR and TWR in steel work piece [Kumar et al., 2012]. Pradhan and Jayswal [2011] recommended that copper is better tool material in EDM process as compared to aluminium in the terms of SR.

2.1.4 Workpiece Material

AISI P20 tool steel

Amorima and Weingaertner [2005] performed experiments on AISI P20 material of both positive and negative polarity and investigated the MRR, TWR and SR. They had concluded that positive tool electrode with Ip=8A, T_{on}= 50 μs give the maximum MRR, and negative tool electrode with Ip=3A, T_{on}= 12.8μs give the minimum surface roughness. Amorima and Weingaertner [2007] presented comparative study

of both tool materials, graphite and copper with positive and negative polarity. It has been concluded that the maximum MRR is obtained by negative polarity with graphite tool and minimum TWR obtained by graphite and copper at positive polarity and best surface roughness was obtained for copper electrodes under negative polarity. Curodeau et al. [2005] discussed hybrid EDM process using finishing and polishing operations in deionized water and two processes described replica and successive imprints of surface roughness. Both methods use an adapted compression moulding process to fabricate efficiently, multiple composite electrodes. Responses were MRR, TWR and surface roughness. Kiyak and Cakir [2007] presented the effect on SR of P20 work piece and concluded that electrode was influenced by, high pulsed current and pulse time provide low surface finish quality. However, this combination would increase MRR and reduce machining cost.

Joshi and Pande [2011] did extensive experiments with AISI P20 tool steel material and studied MRR, TWR and crater size. These results were used to model EDM quality characteristics using ANN and GA. They concluded that the intelligent process modelling and optimization approach developed in this work will provide a very effective tool to a process engineer to choose optimum process parameters for enhancing the productivity and finishing capability of the EDM process. The papers related to AISI P20 tool steel material is summarised in Table 2.1.

Table 2.1: EDM literature review on AISI P20 tool steel

Author with Year	Machining variables ranges						Response variable	Remark
	Ip (A)	$T_{on}(\mu s)$	$T_{off}(\mu s)$	Tau (%)	V	Other variable		
Joshi and Pande [2011]	5-40	200-700		50 -80	30-50		Crater Size, MRR and TWR	Integrated FEM, ANN, GA for multi-optimisation of MRR,TWR and crater size.
Reza et al. [2010]	0.8-1.8	2-56	1-55		60-100	Polarity	MRR, TWR and SR	The +ve polarity was used to find optimum MRR, TWR and SR.
Joshi and Pande [2010]	5-40	25-700		50-80	30-50		MRR, crater cavity	Developed the thermo-physical model of EDM process using the FEM for the shape of crater cavity and the MRR.
Kiyak and Cakir [2007]	6-24	2-100	2 and 3				SR	Low current and pulse time with high pulse off time produce better SR. SR increases as tool wears out.

Continued on next page

Table 2.1: *EDM literature review on AISI P20 tool steel*

Author with Year	Machining variables ranges						Response variable	Remark
	Ip (A)	$T_{on}(\mu s)$	$T_{off}(\mu s)$	Tau (%)	V	Other variable		
Amorima and Weingaertner [2007]	3-8	6.4 -100			160	Polarity	MRR, TWR, SR	Comparative experimental study of Graphite and copper as tool material with +ve and -ve polarity. Higher MRR was obtained with -ve graphite electrodes. Graphite and copper tools yielded similar MRR for +ve polarity. For graphite and copper tools the lowest TWR was with +ve polarity. The best SR was obtained for copper electrodes under -ve polarity.

Continued on next page

Table 2.1: *EDM literature review on AISI P20 tool steel*

Author with Year	Machining variables ranges						Response variable	Remark
	Ip (A)	$T_{on}(\mu s)$	$T_{off}(\mu s)$	Tau (%)	V	Other variable		
Curodeau et al. [2005]	5-10	50-100			100-150		MRR, TWR and SR	Hybrid EDM process with a polymer-carbon electrode in deionised water. A better surface finish was achieved for smaller T_{on} and Ip. TWR was minimised with low V, +ve polarity and low flushing pressure.
Amorima and Weingaertner [2005]	3-8	6.4-200			160-200	Polarity	MRR, TWR, SR	Experiments were performed to determine MRR, TWR and SR for AISI P20 material using both positive and negative polarity.
Curodeau et al. [2004]	1-1.5	60-90	120-180		150		SR	Thermoplastic composite electrode and air as dielectric were used in EDM for automated polishing of tool steel cavity.

Other tool steels

Wang and Tsai [2001] presented semi-empirical models of MRR for various workpiece (EK2, D2 and H13) and tool electrode combinations (Copper, graphite and silver-tungsten alloy). The research done by Pradhan and Biswas [2010] studied the effect discharge current, pulse duration, duty cycle, and voltage on AISI D2 tool steel with copper electrode. They compared two Neuro Fuzzy (NF) models and a ANN model for predictions of MRR, TWR, and radial OC in die sinking EDM process. Further, Izquierdo et al. [2009] discussed EDM operation with multiple discharges phenomena and the model generated EDM surfaces by calculating temperature fields inside the work piece (AISI D2 tool steel) using a finite difference-based approach. Prabhu and Vinayagam [2009] investigated the surface finish of AISI D2 steel when cut with and without multi wall carbon nanotube in dielectric. The surface morphology, surface roughness and micro-crack of AISI D2 tool steel EDMed component were analysed by the atomic force microscopy technique by Guu [2005], and establish experimentally that the discharge energy determines the surface texture of the EDMed surface. They also ascertained that surface roughness and cracks are proportional to the power input during the process. Guu and Hocheng [2001]; Guu et al. [2003] reported their works on EDM Turning of the same tool steel. They also reported an AFM study of D2 with die sinking EDM. The optimisation procedure was reported by Marafona and Wykes [2000]. They used the effect of carbon which has migrated from the dielectric to tungsten-copper electrodes on D2 tool steel. A two-stage EDM machining process was suggested where different EDM settings are used for the two stages of the process giving a significantly improved MRR for a given TWR. Prabhu and Vinayagam [2009] investigated the SR of AISI D2 steel when cut with and without multi wall carbon nano-tube in dielectric. They examined that good surface finish can be found using multi walled carbon nano- tubes in the dielectric with graphite tool.

Singh et al. [2004b] reported an experimental investigation to study the effects of machining parameters such as pulsed current on MRR, diameteral OC, TWR, and SR in EDM of En-31 tool steel. The electrodes with copper, copper tungsten, brass and aluminium electrodes by varying the pulsed current at reverse polarity. Investigations indicate that the output parameters of EDM increase with the increase in

pulsed current and the best machining rates are achieved with copper and aluminium electrodes. Kanagarajan et al. [2008] used electrode rotation, T_{on}, Ip, and FP to study MRR on Tungsten carbide/cobalt cemented carbide and shown experimentally that $Ip$and T_{on} are the most significant factors. Puertas et al. [2004] analysed the impact of EDM parameters on MRR and electrode wear in cobalt-bonded tungsten carbide workpiece. A quadratic model was developed for each of the responses, and it was reported that for MRR, the current intensity factor was the most influential, followed by Tau, T_{on} and the interaction effect of the first two. The value of MRR increased, when current intensity and Tau were increased, and decreased with T_{on}. The paper published by Mahdavinejad and Mahdavinejad [2005] elaborated the experimental results of MRR and TWR of tungsten carbide cobalt work piece material with DOE techniques. Lin et al. [2008] in their paper investigated EDM of cemented tungsten carbides grade K10 and P10. They studied the effect on MRR, TWR and SR. The effects of the electrical discharge energy on heat-affected layers, surface cracks and machining debris were also determined.

Kung et al. [2009] have used RSM design to machine cobalt-bonded tungsten carbide (WC-Co) using power mixed dielectric. They evaluated MRR and TWR. MRR increases with an increase of aluminium powder concentration and TWR value tends to decrease with the aluminium powder concentration down to a minimum value after which it tends to increase.

Jaharah et al. [2008] investigated MRR, TWR on AISI H13 tool steel. Ip was found to be the major factor which influences MRR. Higher MRR was obtained with high Ip, medium T_{on}, and low T_{off}. However, smaller TWR was obtained at high Ip, high T_{on}, and lower value of T_{off}. Simao et al. [2003] have investigated the electrode wear, workpiece surface hardness of AISI H13 hot work tool steel using partially sintered WC/Co electrodes. Experiments were conducted by Lin et al. [2006] on SKH 57 high speed tool steel work material using Taguchi method (L_{18} OA) and found the S/N ratios associated with the observed values in the experiments.

El-Taweel [2008] investigated the correlation of process parameters in EDM of CK45 steel with Al-Cu-Si-TiC composite produced using powder metallurgy technique and evaluated MRR and TWR. It is found that such electrodes are more

sensitive to Ip and T_{on} than conventional electrodes. To achieve maximum MRR and minimum TWR, the process parameters are optimised and on experimental verification the results are found to be in good agreement. Experiments were performed by Keskin et al. [2006] to determine parameters effecting surface roughness on steel. A profound equation was obtained for the surface roughness using power, pulse time, and spark time parameters. Bhattacharyya et al. [2007] developed mathematical models for SR, WLT and SCD based on RSM for M2-die steel material.

Composite

Curodeau et al. [2005] discussed hybrid EDM process for finishing and polishing operations in deionized water. And two processes described replica and successive imprints of surface roughness. Both methods used an adapted compression moulding process to fabricate efficiently, multiple composite electrodes. Responses were MRR, TWR and surface roughness. Chiang [2008] explained the influences of Ip, T_{on}, Tau and voltage on the responses; MRR and electrodes wear ratio. The experiments were planned according to a CCD on Al_2O_3+TiC workpiece and the influence of parameters and their interactions were investigated using ANOVA. A mathematical model was developed and claimed to fit and predict MRR accurately with a 95% confidence. The main two significant factors affecting the response were Ip and Tau. Dvivedi et al. [2008] identified the machining performance in terms of MRR and TWR by obtaining an optimal setting of process parameters (T_{on}, T_{off}, Ip, and FP) during EDM of Al 6063 SiCp metal matrix composite. It was revealed that $Ip$is predominant on MRR than other significant parameters. MRR increases with increasing Ip and T_{on} up to an optimal point and then dropped. Habib [2009] presented the mathematical model for correlating the interactive and higher order influences of various EDM parameters for Al- SiC composites material as a workpiece through RSM. Wang [2009] investigated the feasibility of EDM of W/Cu composites using L_{18} OA. They used both positive and negative polarity of machining along with discharge current, pulse duration, duty factor, electrode rotation and gap voltage as input parameters. They studied MRR, TWR and SR with surface integrity in particular.

Other Workpiece Materials

Puertas and Luis [2004] discussed the mathematical models devised using design of experimental techniques and optimized machining parameters for EDM of Boron carbide, a conductive ceramic material. It is these conditions that determine such important characteristics as SR, TWR and MRR. Tsai et al. [2003a] in their paper used Cu-Cr composite electrode and optimized the responses like MRR, TWR, SR and thickness of the recast layer. Copper powders contained resin with chromium powders to form tool electrodes for EDM. Khan et al. [2009] discussed the performance (MRR and TWR) of EDMed mild steel due to the shape configuration of the electrode. The maximum MRR was found for round electrodes followed by square, triangular and diamond shaped electrodes. However, the highest TWR was found for the diamond shaped electrodes. It is also considered as an off-line process planning technique as the simulation algorithm is largely based on MRR, TWR and spark gap. However, the simulation of discharge location and spark gap, which are dependent on the distribution of debris concentration, was reported to yield a more realistic representation of the sparking phenomenon. Subsequently, Khan [2008] reported overall performance comparison of copper and brass electrodes and observed that the highest MRR was observed during machining of aluminium using brass electrodes. Comparatively low thermal conductivity of brass as an electrode material does not allow the absorption of much heat energy, and most of the heat is utilized in the removal of material from aluminium workpiece at a low melting point.

Salah and Ghanem [2006] presented numerical results relating to the temperature distribution in EDM process and from these thermal results, MRR and roughness are inferred and compared with experimental explanation. They revealed that temperature variation of conductivity is of vital significance and provides the better correlations with experimental data. Subsequently, they analysed numerical results concerning the temperature distribution, the thermal and residual stresses of EDMed stainless steel AISI 316L workpiece with experimental data, which was in good agreement [Salah et al., 2008]. Kuppan et al. [2007] derived mathematical model for MRR for deep hole drilling of Inconel 718. The experiments were planned using CCD and RSM was used to model the same. It revealed that MRR is more influenced by peak current and duty factor. The parameters were optimised for maximum MRR with

the desired Ra value using desirability function approach.

Caydas and Hascalik [2007] made an attempt to analyse the electrode wear in EDM of Ti alloy using statistical analysis technique. ANOVA and regression analysis were done, the proposed mathematical models obtained can adequately describe the performances within the limits of factors being studied. The experimental and predicted values were in a good agreement. Khanra et al. [2006] reported X-ray diffraction (XRD) analysis of machined surface of sintered FeAl and showed the formation of Fe_3C phase during the EDM process. The debris analysis was used to identify the material removal mechanism occurring during the EDM of sintered FeAl. Wu et al. [2005] had discussed the effect of roughness and surface status of the workpiece after EDM of SKD steel when Al powders was added in the dielectric. It is observed that best distribution effect is found when the concentrations of the Al powder and surfactant in the dielectric are 0.1 and 0.25 g/L, respectively.

2.1.5 Discharge characteristics in EDM

Discharge characteristics in EDM include various types of pulses as discussed in the previous chapter.

Dauw et al. [1983] developed an EDM pulse discriminator (EDM-PD) for EDM process analysis and an on-line control. Pulse train detection was made by analysing EDM-PD data. Yu et al. [2001] analysed various waveforms (*i.e.* voltage current characteristics) of EDM using wavelet transform. The result indicates that after the transformation, the original data can easily identify the different machining condition, thus, providing clear and useful information for the on-line control of EDM. Jiang et al. [2012] utilised wavelet transform techniques for analysis of EDM pulse characteristics. A data acquisition and processing system based on digital signal processing was developed for high- speed wavelet transforms and related calculations. Pey Tee et al. [2013]presented the method for discrimination of different type of discharge waveform during EDM for using rotating electrode. Advantage of this method was its correctness for discrimination of the narrow width pulses that were usually created with targeted types of EDM equipment.

2.2 Motivation and objective of research work

From the available literature, it can be seen that though some work has been reported on influence of EDM parameters on surface integrity of the machined surface, no attempt has so far been made to systematically optimise the process variables with a view to obtain favourable surface integrity. Moreover, surface integrity can not be characterised as a single response since it typically includes surface roughness and formation of white layer and surface cracks. Therefore, there should be research endeavour to apply multi-objective optimisation techniques in order to achieve reasonably low value of SR, WLT and SCD.

Moreover, some study has been reviewed in the preceding section, on EDM of AISI P20 grade tool steel which primary dealt with optimisation of EDM parameters for favourable MRR, SR, TWR and OC. Hence, the important aspect of surface integrity of AISI P20 tool steel which is one of the vital materials in mould making industries, has not been reported so far. Existing works primarily focussed on machining parameters such as Ip, T_{on}, V and duty cycle, while parameters like tool work time (T_w) and tool lift time (T_{up}) were rarely incorporated.

It is also observed from the literature that various methodologies were adopted to analyses different discharge characteristics in EDM. However, no attempt has been made to correlate the EDM process parameters with generation of different pulses in EDM.

Considering the above mentioned gaps or incompleteness in the reviewed literature, the first major objective of the current research work is to investigate the influence of various machining parameters (using various ranges corresponding to different machining conditions like roughing, semi finishing and finishing operations) on major performance measures in EDM during machining of AISI P20 grade tool steel. Since, there are multiple number of input parameters and output response are involved, single objective optimisation techniques would fail to recommend the optimal settings of EDM process variables. Considering the fact, the second objective of the present work includes simultaneous optimisation of multiple responses using different methodologies.

The detailed objectives specific to the different sections of chapter 4 (results and

discussion) are formulated as follows:

1. To study the influence of EDM parameters (with range chosen for rough machining) on MRR and TWR followed by simultaneous optimisation of the responses using grey relational analysis (GRA) methodology in order to recommend optimal parameter settings.

2. To study the effect of EDM parameters (with range chosen for semi finishing), arranged using RSM-based design of experiment, on MRR, TWR and OC and optimise them using fuzzy logic technique.

3. To investigate the influence of different process variables (with same range as before) on various aspects of surface integrity such as WLT, SCD, SR and dimensional accuracy (OC) and adopt fuzzy-based TOPSIS methodology combined with sensitivity analysis for multi-objective optimisation.

4. To carry out the comparative evaluation on influence of different tool electrode materials (copper, brass and graphite) on EDMed surface integrity and dimensional accuracy.

5. To study the influence of EDM process parameters (Ip,T_{on} and T_{au}) on the formation of different pulses by analysing voltage-current (V-I) waveforms using wavelet transform as a pulse discrimination methodology.

Chapter III

Experimental Details and Analytical Techniques

3. EXPERIMENTAL DETAILS AND ANALYTICAL TECHNIQUES

3.1 Experimental setup

All experiments were conducted on Electronica Electraplus PS 50ZNC die sinking machine. The enlarge view of experimental set-up with tool and workpiece are shown in Fig. 3.1. Full view of machine setup for die shinking Electric Discharge Machining (EDM) is shown in Fig. 3.2. The workpiece material selected for this experiment was AISI P20 tool steel having semi-circular shape (100 mm diameter and 10 mm thickness). The workpiece was heated to the temperature range of $843 - 898°C$ in a controlled furnace and held for half an hour. Then it was oil quenched and later tempered for better toughness.

Fig. 3.1: Enlarge viewed of experimental set-up with tool and workpiece

Fig. 3.2: Experimental setup for die sinking EDM

Commercial grade EDM oil (specific gravity = 0.763, flash point = 94°C) was used as dielectric fluid under The impulse flushing and side flushing modes.

3.2 Selection of workpiece

In this experiment AISI P20 tool steel was used as a workpiece material which is shown in Fig.3.3. It is also known as "General Mold Steel Grade" Tool Steel. This tool steel has growing range of applications like plastic moulds, frames for plastic pressure dies, hydro forming tools. But often difficult to machine by conventional machining in its hardened condition.

The composition of AISI P20 tool steel with physical and mechanical properties is listed in Table 3.1 to 3.3.

Fig. 3.3: AISI P20 Tool Steel material

Table 3.1: Composition of AISI P-20 tool steel material

Elements	Weight limit %	Actual weight %
C	0.28-0.40	0.4
Mn	0.60-1.00	1
Si	0.20-0.80	0.4
Cr	1.40-2.00	1.2
Mo	0.30-0.55	0.35
Cu	0.25	0.25
P	0.03	0.03
S	0.03	0.03

Table 3.2: AISI P20 tool steel categories

Category	Steel
Class	Tool steel
Type	General mold steel
Designations	Germany : DIN 1.2330
	United States : ASTM A681 , UNS T51620

Table 3.3: Mechanical properties of P20 steel

Properties		Unit	Conditions T(°C)
Density	7.85x1000	kg/m^3	25
Poisson's Ratio	0.27-0.30		25
Elastic Modulus	190-210	Gpa	25

3.2.1 Description of tool electrodes

According to Droza [1998], tool electrode material should be electrically conductive. In fact, there are a wide range of materials that can be used to manufacture electrodes, for instance, brass, tungsten carbides, electrolytic copper, copper-tungsten alloys, silver-tungsten alloy, tellurium-copper alloys, copper-graphite alloys, graphite etc.

Current study used cylindrical copper tool electrode with diameter of 30mm and 12mm while brass and graphite tool electrodes of 12mm diameter were used. The detailed description of selection of tool electrodes along with dimension has been provided in the chapter 4.

3.3 EDM parameters

During the current research work, the influence of various parameters on different performance measure in EDM were studied. The machining parameters which were investigated include,

- Discharge current (Ip)
- Pulse-on time (T_{on})
- Work time (T_w)
- Lift time (T_{up})
- Inter electrode gap (IEG)
- Duty cycle (T_{au})
- Polarity (P)

Some parameters are fixed for all experiments design such as flushing pressure, discharge voltage, dielectric fluid. The details description of machining parameters has been presented in section 1.6.

3.4 Performance measures in EDM

The different performance measures (or output response) that were studied during the current study are discussed below along with the methodology of measurement.

3.4.1 Material removal rate

Material removal in EDM takes place due to local melting and vaporisation of workpiece material due to high energy spark generated between tool electrode and workpiece. Each spark produces a tiny crater. Crater forms in the material along the cutting path by melting and vaporization, thus eroding the workpiece to the shape of the tool.

3.4.2 Tool wear rate

Tool wear is an important factor because if affects dimensional accuracy and the shape produced. Tool wear is related to the melting point of the tool material. Tool wear is affected by the precipitation of carbon from the hydrocarbon dielectric on the electrode surface during sparking [Mohri et al., 2000].

Evaluation of MRR and TWR

Material Removal Rate (MRR) and Tool Wear Rate (TWR) was calculated by weight loss method using precision electronic balance weight machine with an accuracy of 1 mg. MRR and TWR was calculated by measuring the weight loss of workpiece (Equation 3.1) and tool (Equation 3.2), respectively.

$$MRR = \frac{W_b - W_a}{t\rho_w} \tag{3.1}$$

$$TWR = \frac{T_b - T_a}{t\rho_t} \tag{3.2}$$

Where W_b and W_a are the weights of workpiece before and after machining respectively. T_b and T_a are the weights of tool before and after machining respectively. Where t is the machining time. The density of AISI P20 tool steel material is ρ_w = 7.85x10^{-3} g/mm^3 and density of copper electrode is ρ_t = 8.92 x10^{-3} g/mm^3.

3.4.3 Surface roughness measurement

The measurement of Surface Roughness (SR) (Ra value) was made with portable style type profilometer, Talysurf (Model: Taylor Hobson, Surtronic 3+) , with parameters cut-off length, L_n = 4 mm, sample length, L_c = 0.8mm and filter = 2CR ISO.

3.4.4 Overcut measurement

It is the dimension by which the machined hole in the work piece exceeds the electrode size, mainly depending upon initiating voltage and the discharge energy. During the process of machining EDMed cavity produced are always larger than the electrode this difference (size of electrode and cavity) is called Radial Overcut (OC). It becomes important when close tolerance components are required to be produced for space application and also in tools, dies and moulds for press work [Singh et al., 2004b].

The tool maker microscope with a least count of 1 μm was used for measurement of OC and was calculated as per Equation 3.3.

$$OC = \frac{D_{jt} - D_t}{2} \tag{3.3}$$

Where, D_{jt} is the diameter of hole produced in the workpiece and D_t is the diameter of tool.

3.4.5 White layer thickness

During the process of machining, the discharge energy develops very high temperature at the sparking point on workpiece surface. In this process some material melts and vaporises. Part of this molten metal in flushed away and rest of molten material get quenched by dielectric and later re-solidifies to form recast layer. This material was heated upto molten state but is not removed. This re-solidified/ recast layer is called white layer [Bhattacharyya et al., 2007]. This layer has fine grain and is hard, and may be alloyed with carbon with cracks and other surface irregularities [Ramasawmy et al., 2005].

Evaluation of WLT

After machining, each specimen was sectioned vertically. This was followed by polishing of the specimens with different grades of polishing papers with deceasing grit size. The polished surface was then etched with Nital solution to reveal micro-structure along with recast layer or white layer. Images were then captured on three different locations of each specimen using optical microscope (with model: SCD313 BPD and make: Radical Instrument) with a magnification of 400X. The measurement of WLT

was carried out with an optical microscope with 400X magnification. Recast area was measured using a software (PDF X- change viewer) and then the area was divided by total length of optical microscopic images, to get the average hight of recast layer (*i.e.* WLT).

3.4.6 Surface crack density

In the process of EDM the high temperature generated in the sparking zone causes the workpiece metal to melt during pulse-on time. During pulse-off time part of the molten metal re-solidified and quenched due to rapid cooling. This rapid heating and cooling cycle results in formation of surface crack on the recast layer [Rao et al., 2008].

Evaluation of SCD

For each sample, Scanning Electron Microscope (SEM) images were taken three different locations in order to obtain average value of Surface Crack Density (SCD). From the trial experiment, it was observed more number of location did not resulting significant change in the value of SCD.

In order to measure SCD, the top surface morphology of the EDMed surface was studied using SEM at a magnification of 1000X. Randomly three sample areas were selected on each specimen and the length of cracks was measured using same software. The average crack length on each specimen is divided by area of each micrograph to measure the SCD. The similar measurement of SCD has been reported else where [Bhattacharyya et al., 2007; Rajendran et al., 2013].

3.5 Design of experiment

In order to study the effect of various EDM process variable on performance measures, different Design of Experiments (DOE) techniques were adopted in the current investigation. Depending on number of parameters and level considered, these include Taguchi, Response Surface Methodology (RSM) and full factorial design. The flow chart of the all experiment design are shown in Fig. 3.4.

The detailed description of the methodology has been provided in the appendix section B.

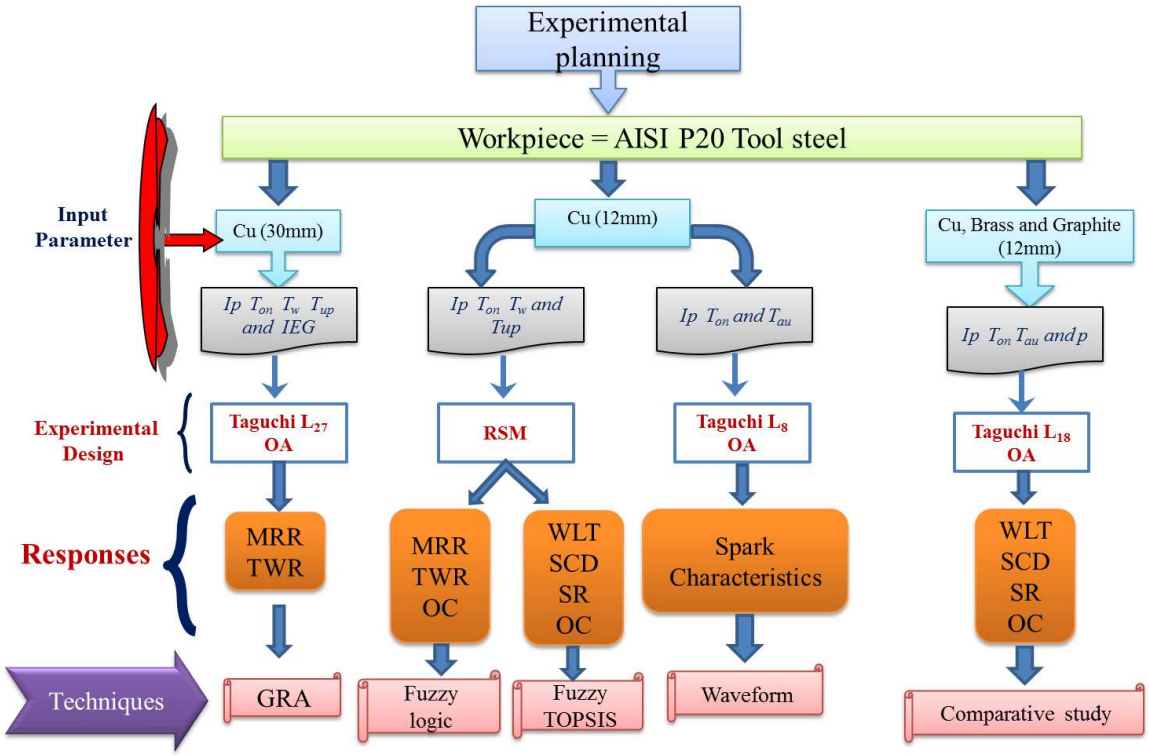

Fig. 3.4: Flowchart of experiments

3.6 Multi-objective optimisation techniques

Multi-objective optimisation is an area of multiple performance characteristics index, that is concerned with mathematical optimisation problems including more than one objective function to be optimised simultaneously. EDM is characterized by multiple performance measures such as MRR, TWR, OC, SR, WLT, SCD etc. Therefore, with an aim to optimise EDM parameters for obtaining favourable output responses, number of multi-objective optimisation techniques were applied in the present research work. These methodologies have been briefly discussed as follow:

3.6.1 Grey relation analysis

Grey Relational Analysis (GRA) is an impacting measurement method in grey system theory that analyses uncertain and insufficient information between one main factor and all the other factors in a given system [Lin and Wang, 2010]. In this section, the use of orthogonal array with the grey relational analysis and methodology for multi-response optimisation is discussed [Singh et al., 2004a]. The optimisation of the process was performed in the following steps:

1. Normalising the experimental results of MRR and TWR for all experimental run.

2. Calculating the Grey Relational Coefficient (GRC).

3. Calculating theGrey Relational Grade (GRG) by averaging the GRCs.

4. Performing statistical Analysis of Variance (ANOVA) for the input parameters with the GRG and to find the parameters significantly effecting the process.

5. Selecting the optimal levels of process parameters.

Calculation of GRG

The indication of the better performances in EDM process for MRR is "higher the better" where as it is "lower the better" for TWR. In the analysis of grey relation for "higher is better" response normalising was done by Equation 3.4 and when the response is " lower is better", normalising was done by Equation 3.5.

$$x_i^*(k) = \frac{x_i(k) - \min x_i(k)}{\max x_i(k) - \min x_i(k)} \tag{3.4}$$

$$x_i^*(k) = \frac{\max x_i(k) - x_i(k)}{\max x_i(k) - \min x_i(k)} \tag{3.5}$$

Where $x_i^*(k)$ and $x_i(k)$ the normalised data and observed data, respectively, for i^{th} experiment using k^{th} response. The smallest and largest value of $x_i(k)$ for the the k^{th} response are $\min x_i(k)$ and $\max x_i(k)$, respectively. After pre-processing the data, the grey relation coefficient $\zeta_i(k)$ for the k^{th} response characteristics in the i^{th} experiment can be expressed as following:

$$\zeta_i(k) = \frac{\triangle_{min} + \zeta\triangle_{max}}{\triangle_i(k) + \zeta\triangle_{max}} \tag{3.6}$$

Where $\triangle_i(k)$ is the k^{th} value in $\triangle_i$ different data series. $\triangle_{max}$ and $\triangle_{min}$ are the global maximum and global minimum values in the different data series, respectively. The distinguishing coefficient ζ lies between 0 and 1, which is to expand or compress the range of GRC. It is selected by decision makers by their own judgement, and its different values usually provide different results in GRG. The mean of the range

of $\zeta = 0.5$, is chosen without any prejudice of the decision maker judgement. After calculating the GRCs, for n number of responses, the GRG γ can be calculated using Equation 3.7.

$$\gamma = \frac{1}{n}\sum_{i=1}^{n}\zeta_i(k) \tag{3.7}$$

The magnitude of γ reflects the overall degree of standardised deviation of the i^{th} original data series from the reference data series. In general, a scale item with a high value of γ indicates that the respondents, as a whole, have a high degree of favourable consensus on the particular item.

3.6.2 Fuzzy-logic method

Fuzzy logic is a mathematical theory of inexact reasoning that allows modelling of the reasoning process of human in linguistic terms. The fuzzy logic control allows the existence of uncertainty in handling parameter values [Pandey and Dubey, 2012; Kao et al., 2007]. Fuzzy logic system (Mamdani type) mainly consists of fuzzifier, knowledge based, inference engine, and defuzzifier [Tzeng and Chen, 2007], as shown in Fig 3.5. The fuzzifier uses membership functions to fuzzify Signal-to-Noise (S/N) ratios of each performance characteristic. Then, the inference engine (Mamdani fuzzy inference system) performs fuzzy reasoning on fuzzy rules to generate a fuzzy value. Finally, the defuzzifier converts fuzzy predicted value into Multi Performance Criteria Index (MPCI) . This process was repeated for all the runs of experiment and respective MPCI value was found out.

3.6.3 Fuzzy-TOPSIS method

Technique for Order of Preference by Similarity to Ideal Solution (TOPSIS) method is used for multiple responses optimisation of responses. This method was used in fuzzy environments [Uysal and Tosun, 2012], which fits human thinking under actual environment. The detailed description of fuzzy-TOPSIS method has been provided in section 4.3.5

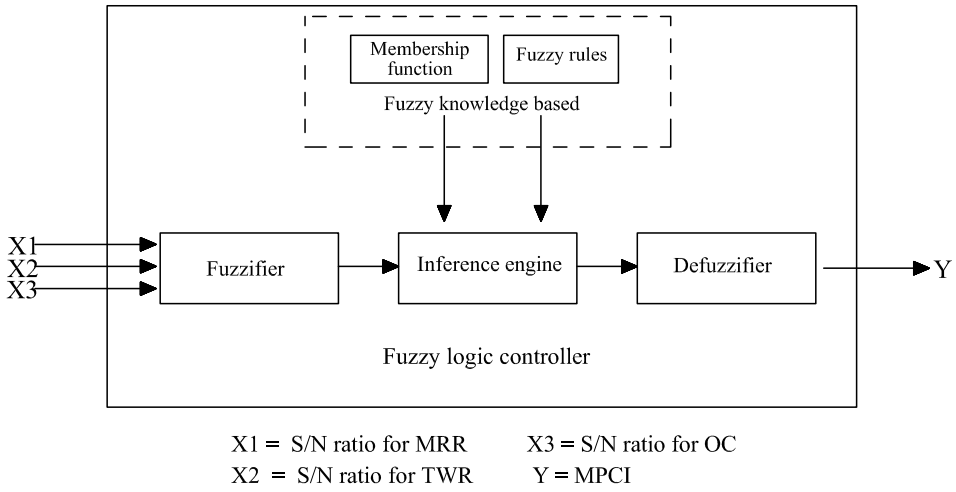

Fig. 3.5: Three-input-one-output fuzzy logic unit

Chapter IV

Results and Discussion

4. RESULTS AND DISCUSSION

4.1 Multi- objective optimisation of machining parameters using grey relation analysis in EDM

AISI P20 tool steel has application of mould making industries which offer difficulty in conventional machining in hardened condition. An efficient method for determining optimum process parameters for multiple performance characteristics, through integrating the grey relation theory with Taguchi method is discussed. The objective of the present work is to investigate main effect on MRR and TWR on EDM of AISI P20 tool steel and to optimise these performance characteristics with maximum MRR and minimum TWR, simultaneously, because these responses are linked with productivity.

4.1.1 Design of Experiment

In this study, Taguchi design using L_{27} Orthogonal Array (OA) is used for multi-response optimisation of EDM process for machining AISI P20 tool steel with a copper electrode. The machining parameters like discharge current (Ip), pulse-on time (T_{on}), work time (T_w), lift time (T_{up}) and inter electrode gap (IEG) were experimented with side impulse flushing. It is an intermittent flushing through side jet , which is done through a solenoid valve that is synchronized with the lifting of tool. The dielectric is directed between the IEG to accomplish removal of the debris. According to Lee and Li [2001], the increase of the flushing pressure increases the tool wear during machining so the basic advantage of flushing during tool lift up will reduce the tool wear.

For five machining parameters, each at three levels, twenty-seven experiments were conducted and the machining parameters with their levels are presented in Table 4.1. The fixed parameters were duty cycle (T_{au}), voltage (V), flushing pressure (Fp) and polarity. The duty cycle is the ratio of the pulse-on time and total cycle time (T_{on} +

T_{off}). The quill is actuated with the help of D.C. Servo motor, and this speed of quill can be controlled by servo sensitivity.

Table 4.1: Machining parameters and their levels

Control Parameters					
Parameter	Symbol	Level			Unit
		1	2	3	
Discharge current	Ip	2	5	8	A
Pulse on Time	T_{on}	100	300	500	μs
Lift Time	T_{up}	0.0	0.7	1.4	s
Work time	T_w	0.2	0.6	1.0	s
Inter Electrode Gap	IEG	90	170	250	μm
Fixed Parameters					
Duty Cycle	τ		90		%
Voltage	V		45		V
Impulse Flushing Pressure	Fp		0.3		Kgf/cm^2

In this experiment, a semi-circular shaped workpiece material (100 mm diameter and 10 mm thickness) was used after hardening. The cylindrical copper tool with 30 mm diameter and the work piece are shown in Fig. 4.1. Commercial grade EDM oil (specific gravity = 0.763) was used as dielectric fluid. For each experimental run, machining was carried out for 60 min and, MRR and TWR were calculated by measuring the weight loss method. MRR and TWR along with the machining parameters are tabulated in Table 4.2.

Fig. 4.1: Tool and Workpiece

Table 4.2: Observation table

Run no.	Ip (A)	Ton (μs)	Tup (s)	Tw (s)	IEG (μm)	MRR (mm^3/min)	TWR (mm^3/min)
1	2	100	0	0.2	90	1.8910	0.0085
2	2	100	0	0.2	170	1.9639	0.0149
3	2	100	0	0.2	250	1.8832	0.0161
4	2	300	0.7	0.6	90	0.5987	0.0064
5	2	300	0.7	0.6	170	0.6645	0.0106
6	2	300	0.7	0.6	250	0.6412	0.0149
7	2	500	1.4	1	90	0.3227	0.0127
8	2	500	1.4	1	170	0.2845	0.0021
9	2	500	1.4	1	250	0.3355	0.0127
10	5	100	0.7	1	90	1.0000	0.0161
11	5	100	0.7	1	170	1.8110	0.0234
12	5	100	0.7	1	250	1.5180	0.0297
13	5	300	1.4	0.2	90	0.6355	0.0106
14	5	300	1.4	0.2	170	0.5265	0.0096
15	5	300	1.4	0.2	250	0.3185	0.0136
16	5	500	0	0.6	90	2.9490	0.0085
17	5	500	0	0.6	170	3.1465	0.0139
18	5	500	0	0.6	250	2.5987	0.0042
19	8	100	1.4	0.6	90	4.4900	0.0359
20	8	100	1.4	0.6	170	3.7134	0.0446
21	8	100	1.4	0.6	250	3.7665	0.0476
22	8	300	0	1	90	9.7643	0.0361
23	8	300	0	1	170	9.6072	0.0297
24	8	300	0	1	250	9.9724	0.0330
25	8	500	0.7	0.2	90	6.4968	0.0181
26	8	500	0.7	0.2	170	5.5520	0.0064
27	8	500	0.7	0.2	250	4.8089	0.0106

4.1.2 Influence of EDM parameters on MRR

The effects of various machining parameters like Ip, T_{on}, T_w, T_{up} and IEG on MRR are shown in Fig. 4.2. This figure indicates that discharge current (Ip) is directly proportional to MRR. This is expected because an increase in pulse current produces stronger spark, which produces the higher temperature, causing more material to melt and erode from the workpiece. Besides, it is evident that the other factors did not influence MRR much when compared to Ip [Ghoreishi and Tabari, 2007]. MRR increased with T_{on} from 100 μs to 300 μs, and after that it started to decrease. As the pulse-on time increases, the total energy supply to the workpiece is more, so more material is eroded from workpiece. But, with higher T_{on}, the plasma formed between the IEG actually hinders the energy transfer and thus reduces MRR [Saha and Choudhury, 2009; Kung et al., 2009].

MRR usually decreases with T_{up}, it is because with increase in T_{up}, the tool temperature decreases considerably. T_w is slightly increasing MRR because longer T_w results in more machining and less of idle time as the quill is lifted less often. Similar findings have been reported by Marafona and Araujo [2009], where they obtained T_w (Ram cycle) as the most significant factor in their experiment. IEG has no significant effect on MRR, as substantiated by ANOVA (Table 4.3) . In the table, the columns represent sources of variation, Degrees of Freedom (DF), Sequential Sum of Squares (Seq SS), Mean of Squares (MS), statistic F and P. The last column represents % contribution of the factors or sources of variation.

Table 4.3: Analysis of variance for MRR

Source	DF	Seq SS	MS	F	P	% contribution
Ip	2	162.989	81.4946	379.61	0.000	70.24
T_{on}	2	6.409	3.2046	14.39	0.014	2.76
T_{up}	2	50.626	25.3129	117.91	0.000	21.81
T_w	2	9.573	4.7867	22.30	0.007	4.12
IEG	2	0.301	0.1504	0.70	0.549*	0.130
T_{on}xIEG	4	0.419	0.1048	0.49	0.784*	0.18
T_{up}xIEG	4	0.191	0.0477	0.22	0.913*	0.08
T_wxIEG	4	0.656	0.1641	0.76	0.600*	0.28
Residual Error	4	0.859	0.2147			0.37
Total	26	232.023				100
*Insignificant factor						

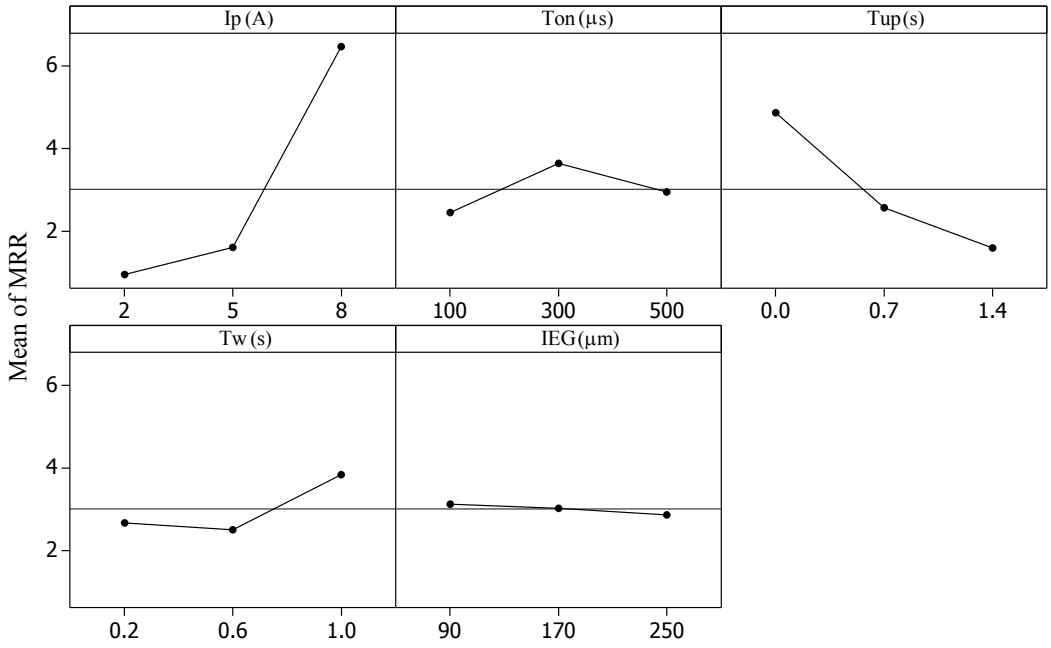

Fig. 4.2: Main effect plots for MRR

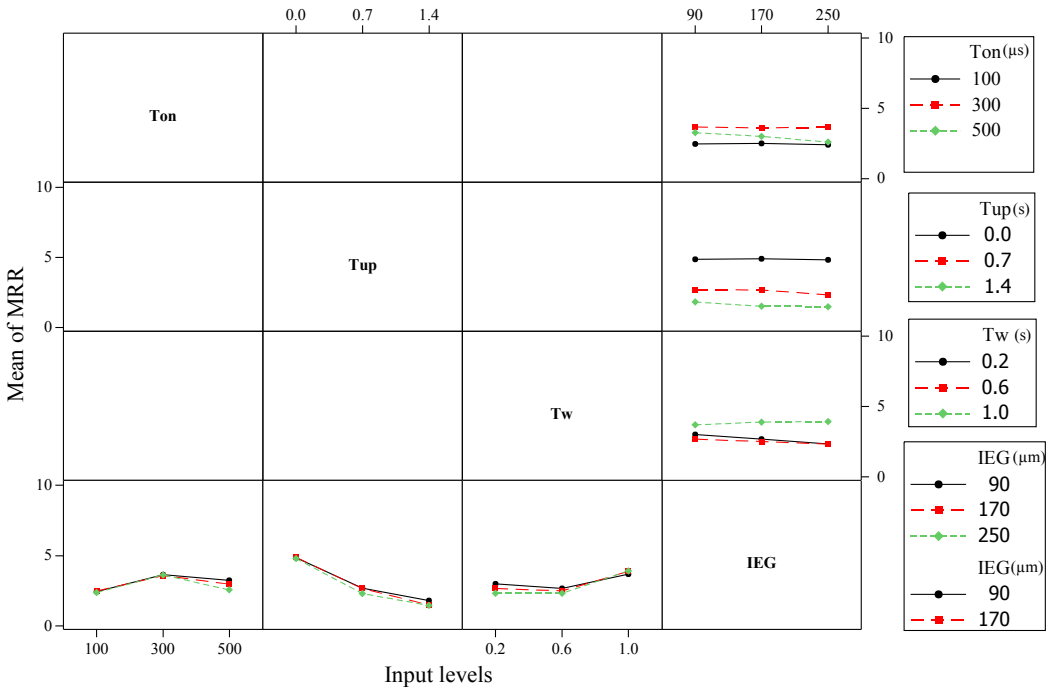

Fig. 4.3: Interaction plots for MRR

Table 4.3 clearly indicates that IEG, the interaction T_{on} x IEG, T_{up} x IEG and T_w x IEG are not important in influencing MRR, which is also shown in Fig. 4.3, where as Ip , T_{on}, T_{up} and T_w are the significant factors at 95% confidence level for MRR. In this table, it is observed that Ip is the most important factor because its percentage contribution is 70.24%, followed by T_{up}, T_w and T_{on} with percentage contributions 21.81%, 4.12% and 2.76%, respectively.

4.1.3 Influence of EDM parameters on TWR

Influence of EDM parameters on TWR is shown in Fig. 4.4, which indicates that Ip is directly proportional to TWR. As Ip increases the pulse energy increases and thus more heat energy is produced in the workpiece- tool interface that leads to increased melting and evaporation of the electrode. One can interpret that Ip has a significant direct impact on TWR [Dhar et al., 2007]. Pulse-on time is inversely proportional to the tool wear rate. At higher T_{on}, more energy is released between IEG resulting in dissociation of dielectric fluid, thus carbon particles are released. These particles get deposited on the copper tool surface forming a protective layer, which is basically a thick carbon layer that reduces TWR [Habib, 2009]. Whereas, TWR tends to increase rapidly with T_w to an optimum level and then remains almost constant. It is because more T_w results in increases of the temperature of tool, so high tool wear is expected. T_{up} and IEG has no significant effect on TWR. It is confirmed by ANOVA (Table 4.4). This table clearly indicates that T_{up}, IEG, the interaction T_{on} x IEG, T_{up} x IEG and T_w x IEG is not important for influencing TWR, and also conformed by Fig. 4.5 . Ip is the most important factor because its the percentage contribution is 41.65%, then followed by T_{on} and T_w with the percentage contribution, 30.21% and 12.71%, respectively.

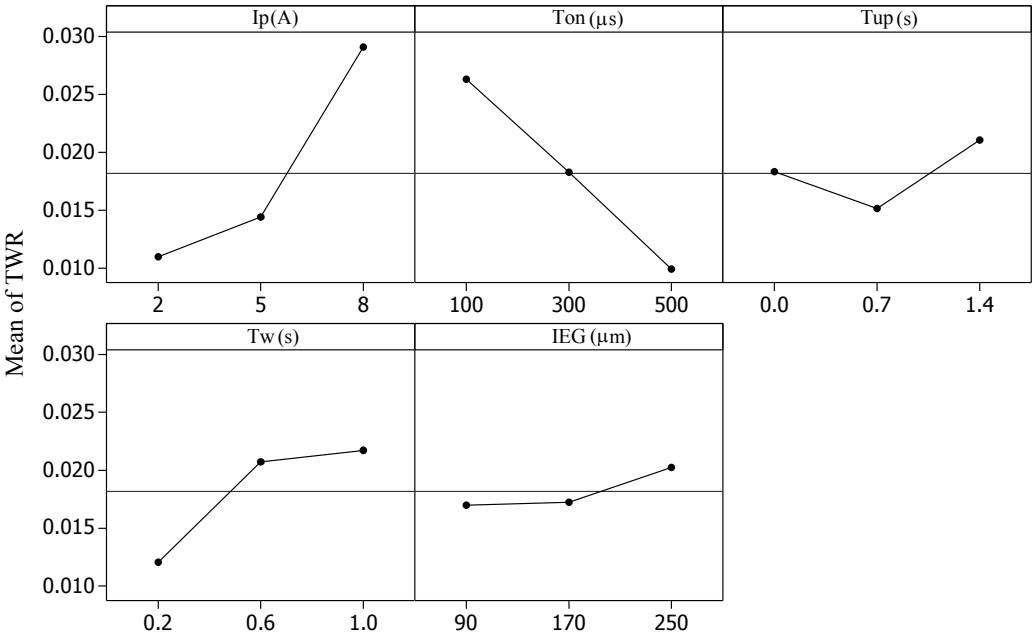

Fig. 4.4: Main effect plots for TWR

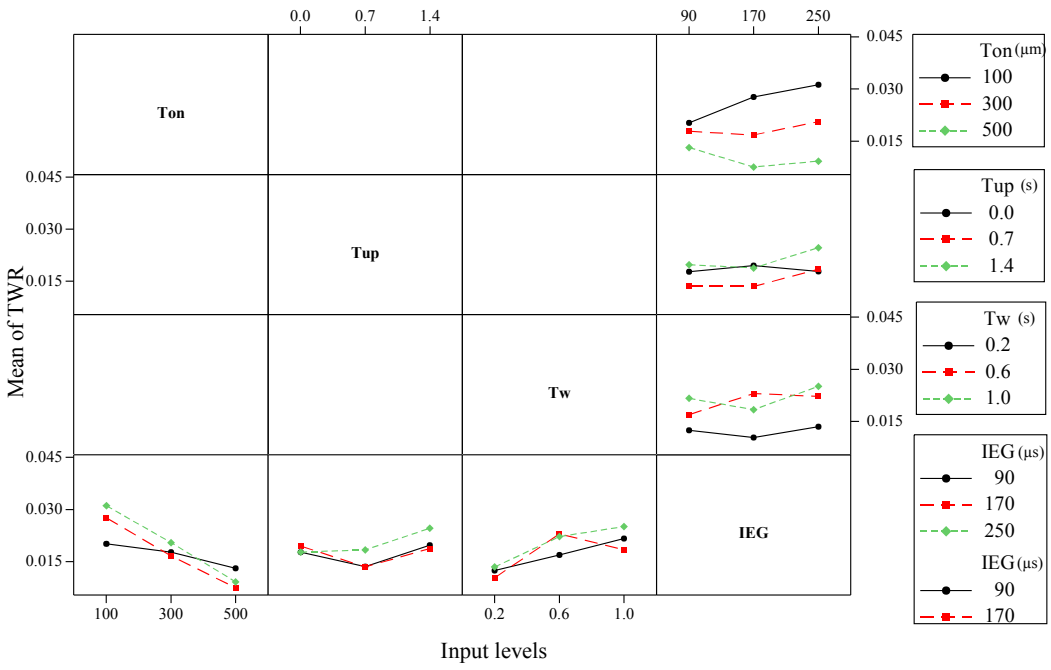

Fig. 4.5: Interation plots for TWR

Table 4.4: Analysis of variance for TWR

Source	DF	Seq SS	MS	F	P	% contribution
Ip	2	0.001668	0.000834	63.88	0.001	41.65
T_{on}	2	0.001210	0.000605	46.55	0.002	30.21
T_{up}	2	0.000158	0.000079	6.05	0.062*	3.94
T_w	2	0.000509	0.000255	19.51	0.009	12.71
IEG	2	0.000060	0.000030	2.29	0.218*	1.49
T_{on}xIEG	4	0.000202	0.000059	3.88	0.109*	5.04
T_{up}xIEG	4	0.000054	0.000013	1.03	0.488*	1.34
T_wxIEG	4	0.000089	0.000022	1.71	0.308*	2.22
Residual Error	4	0.000052	0.000013			1.29
Total	26	0.004004				100
*Insignificant factor						

4.1.4 Multi-objective optimisation using grey relation analysis

In GRA, multiple performances can be unified to a single response, *i.e.* GRG for ease in optimisation [Lin et al., 2000]. Five EDM process parameters are considered for optimising MRR and TWR, simultaneously. The steps for calculation of GRG are mentioned in chapter 2 in 3.6.1. The experimental findings in table 4.2 are used to calculate the normalised MRR and TWR, which are presented in Table 4.5. These normalised values are used to calculate GRC for both the responses using Equation 3.6 and 3.7. Subsequently, GRG is evaluated from GRG's for each experimental run. According to GRG rules, all the experimental run are related to "higher is better policy" [Tosun and Pihtili, 2010]. The experimental run versus GRG plot is shown in Fig. 4.6. It is the Pareto graph of GRGs and the run numbers 24, 23 and 26 are having the three highest GRG values.

In Table 4.6, the mean of the GRG for each level of the EDM parameters, and the total mean of GRG are summarised for each factor levels. The higher value of GRG means comparability sequence has a stronger correlation to the reference sequence. The main effect plot for GRG is shown in Fig. 4.7. It can be concluded from the graph that the optimal EDM parameter setting is Ip=8A, T_{on} =500μs, T_{up}=0.0 s, T_w=1.0 s, and IEG=170μm. Fig. 4.7 and Table 4.6 indicates the effect of EDM parameters on the multi-performance characteristics for maximum MRR and minimum TWR. The significance of the factors on overall quality characteristics of the EDM process has also been evaluated quantitatively with ANOVA for GRG (Table 4.7). Result of

Table 4.5: Grey relational analysis response table

Run	Normalised		GRC $\zeta_i(k)$		GRG (γ)	Rank
	MRR	TWR	MRR	TWR		
1	0.166	0.859	0.375	0.780	0.578	11
2	0.173	0.719	0.377	0.640	0.508	16
3	0.165	0.692	0.375	0.619	0.497	20
4	0.032	0.905	0.341	0.841	0.591	9
5	0.039	0.813	0.342	0.728	0.535	14
6	0.037	0.719	0.342	0.640	0.491	21
7	0.004	0.767	0.334	0.682	0.508	18
8	0.000	1.000	0.333	1.000	0.667	5
9	0.005	0.767	0.335	0.682	0.508	17
10	0.074	0.692	0.351	0.619	0.485	22
11	0.158	0.532	0.372	0.516	0.444	23
12	0.127	0.393	0.364	0.452	0.408	25
13	0.036	0.813	0.342	0.728	0.535	15
14	0.025	0.834	0.339	0.751	0.545	12
15	0.004	0.747	0.334	0.664	0.499	19
16	0.275	0.859	0.408	0.780	0.594	8
17	0.295	0.741	0.415	0.658	0.537	13
18	0.239	0.954	0.396	0.915	0.656	6
19	0.434	0.257	0.469	0.402	0.436	24
20	0.354	0.066	0.436	0.349	0.392	27
21	0.359	0.000	0.438	0.333	0.386	26
22	0.979	0.253	0.959	0.401	0.680	4
23	0.962	0.393	0.930	0.452	0.691	2
24	1.000	0.322	1.000	0.424	0.712	1
25	0.641	0.648	0.582	0.587	0.585	10
26	0.544	0.905	0.523	0.841	0.682	3
27	0.467	0.813	0.484	0.728	0.606	7

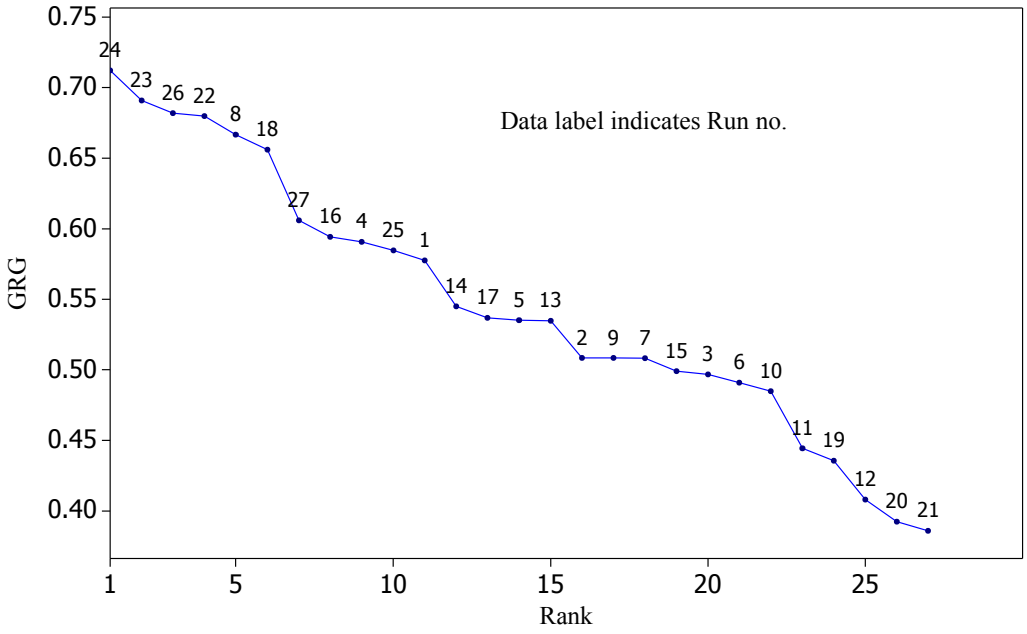

Fig. 4.6: Grey relation grades for the multi-performance

Table 4.6: Response table for GRG

EDM Parameters	Average GRG(γ_i) by factor level			Max-Min
	Level 1	Level 2	Level 3	
Ip	0.5425	0.5226	0.5744	0.0518
T_{on}	0.4594	0.5865	0.5937	0.1343
T_{up}	0.6059	0.5363	0.4973	0.1085
T_w	0.5594	0.5131	0.5670	0.0539
IEG	0.5545	0.5558	0.5292	0.0265
Mean of GRGs for all experimental runs (γ_m) = 0.5465				

ANOVA indicates that T_{on} and T_{up} are significant factors and the other factors are non-significant. Ip is the most significant factor for both MRR and TWR individually, but it influences these responses in conflicting manner; as a result, the combined effect of Ip on GRG is insignificant.

4.1.5 Confirmatory experiment

The estimated or predicted GRG ($\hat{\gamma}$) at the optimum level of the machining parameter can be calculated by Equation 4.1 .

$$\hat{\gamma} = \gamma_m + \sum_{i=1}^{q} (\bar{\gamma}_i - \gamma_m) \tag{4.1}$$

Table 4.7: ANOVA for GRG

Source	DF	Seq SS	MS	F	P	% contribution
Ip	2	0.012292	0.006146	3.51	0.132*	5.37
T_{on}	2	0.102752	0.051376	29.37	0.004	44.91
T_{up}	2	0.054391	0.027195	15.55	0.013	23.77
T_w	2	0.015315	0.007658	4.38	0.098*	6.69
IEG	2	0.004042	0.002021	1.16	0.402*	1.76
T_{on}xIEG	4	0.012120	0.003030	1.73	0.304*	5.29
T_{up}xIEG	4	0.012233	0.003058	1.75	0.301*	5.34
T_wxIEG	4	0.008643	0.002161	1.24	0.421*	3.71
Residual Error	4	0.006998	0.001749			3.05
Total	26	0.228786				100
*Insignificant factor						

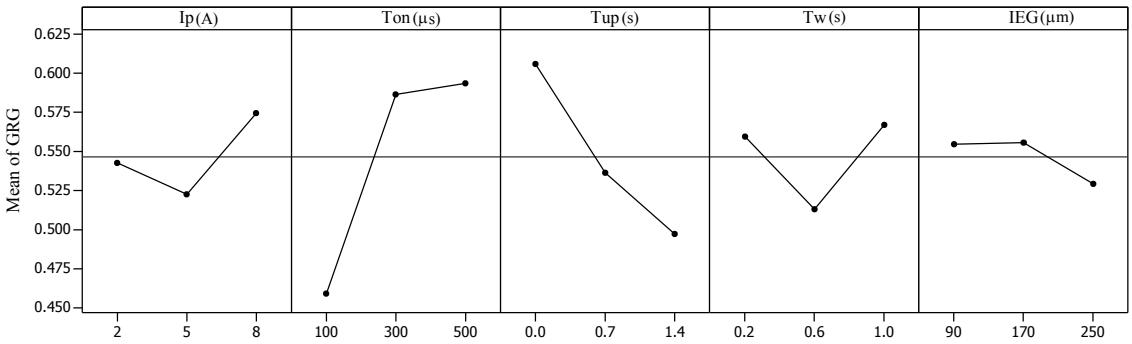

Fig. 4.7: Effect of EDM parameter level on the GRG

Table 4.8: Results of confirmatory experiment

	Initial machining parameter	Optimum machining parameter	
Level	Ip=3A, T_{on} =400μs, T_{up}=1.0s, T_w=0.8s, IEG=130μm	Ip=8A, T_{on} =500μs, T_{up}=0.0s, T_w=1.0s, IEG=170μm	
		Prediction value	Experimental value
MRR(mm^3/min)	0.8938	9.1950	10.4700
TWR(mm^3/min)	0.0093	0.0218	0.01091
GRG	0.5533	0.6531	0.86042
Improvement in GRG= 0.0998 (18.03%)			

Where γ_m is mean of GRGs all experimental runs, $\bar{\gamma_i}$ mean of GRG at the optimum level of i^{th} parameter, and q is the number of machining parameters that significantly affect GRG.

To demonstrate the method of quantifying the quality improvement, the initial machining parameters are assumed to be Ip=3A, T_{on} =400μs, T_{up}=1.0s, T_w=0.8s and IEG=130μm. With this setting, the experimental values of MRR and TWR were 0.8938 mm^3/min and 0.0093 mm^3/min, respectively. Table 4.8 shows the optimum parameters and the predicted MRR, TWR and GRG. Machining with these optimal process setting would improve MRR from 0.8938 mm^3/min to 9.195 mm^3/min, whereas TWR would increase from 0.0093 mm^3/min to 0.0218 mm^3/min. The large increase in MRR offsets the disadvantage of a little increase in TWR, so there is an increase of GRG from 0.5533 to 0.6531, which is an improvement of 18.03%. The optimal results were verified through confirmatory experiments and the results are in good agreement with the predicted values. Thus, it can be concluded that the quality characteristics can be greatly improved through this study.

4.1.6 Conclusions

L_{27} OA based Taguchi design was used to study MRR and TWR of EDM on AISI P20 tool steel with side impulse flushing. MRR is affected by T_{up} and T_w. It decreases with T_{up} and slightly increases with T_w . IEG has no effect on MRR. TWR increases with T_w to an optimal level and then it remains almost constant. T_{up} and IEG has

no significant effect on TWR. grey relation analysis was adopted to optimise the EDM process with multiple performance characteristics, *i. e.*, MRR and TWR. The optimal EDM parameter settings were found to be Ip =8A, T_{on} = 500μs, T_{up}= 0.0s, T_w=1s, and IEG=170μm for maximum MRR and minimum TWR, simultaneously. A confirmatory test was done to support the findings and an improvement of 18.03% in GRG was observed.

4.2 Multi-objective optimisation of EDM process using fuzzy-logic technique

In this section, the optimisation of multiple responses *i.e.*, MRR , TWR and OC of EDM has been accomplished using Fuzzy logic. A prior knowledge of the studied process is thus necessary to achieve a realistic model. The influences of machining parameters *i.e.* discharge current (Ip), pulse-on time (T_{on}), electrode work time (T_w), and lift time (T_{up}) has been analysed on AISI P20 tool steel as a workpiece. Fuzzy logic technique have been implemented to convert the multiple responses into a single one and optimised. Finally, a conformation test was conducted by considering the optimal process parameters obtained from fuzzy logic optimisation technique.

4.2.1 Experiment, material and method

RSM is a collection of mathematical and statistical techniques. Generally useful for modelling and analysis of problems in which output or response is influenced by several variables with a goal to find the correlation between the response and the variables [Montgomery, 2001]. A Central Composite Design (CCD) predicts the performance characteristic at high degree of accuracy during experimentation. Therefore, RSM using CCD with four variables yield a total of 30 runs in three blocks, where the cardinal points used are; sixteen cube points, eight axial points and six centre points [Minitab16, 2011]. Discharge current, pulse-on time, tool work time and tool lift time were the four experimental factors capable of influencing the process responses, namely, MRR, TWR and OC. Hence, these factors were considered for exploration.

In this experiment, the workpiece and tool were set as anode and cathode, respectively. An electrolytic pure copper with a diameter of 12 mm was used as tool electrode. The workpiece material used for this experiment was AISI P20 tool steel (semi-circular shape 100mm diameter and 5mm thick) as shown in Fig. 4.8 along with the electrode. Commercial grade EDM oil (specific gravity = 0.763 freezing point = 94° C) was used as dielectric fluid.

Experiments were conducted considering the effects of various machining parameters on EDM process. These studies were undertaken to investigate the effects of

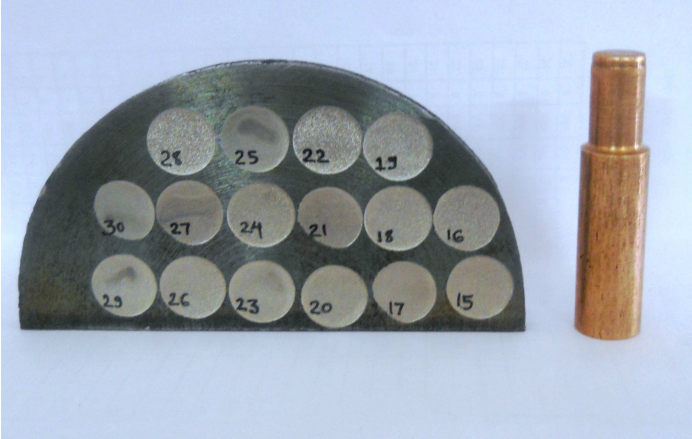

Fig. 4.8: Copper tool and AISI P20 tool steel workpiece

Ip, T_{on}, T_{up} and T_w on MRR, TWR and OC. The selected control parameters and their values at different levels are listed in Table 4.9. The other parameters such as duty cycle (τ), voltage (V), flushing pressure (Fp), Servo Sensitivity (SEN), Inter Electrode Gap (IEG) and polarity were held fixed. Lateral flushing with a pressure of 0.3 kgf/cm^2 was used.

Table 4.9: Different variable and their levels in RSM design

Control Parameter				
Parameter	Level			Unit
	1	2	3	
Discharge current (Ip)	1	3	5	A
Pulse-on Time (T_{on})	10	80	150	μs
Work time (T_w)	0.2	0.6	1.0	s
Lift Time (T_{up})	0.0	0.75	1.5	s
Fixed Parameter				
Duty Cycle (τ)		90		%
Voltage (V)		45		V
Flushing Pressure (F_p)		0.3		Kgf/cm^2
Sensitivity (SEN)		6		
Inter electrode gap (IEG)		90		μm

To attain more accurate results, the workpiece was machined for 60 min for each combination run of the experiment. Then MRR and TWR was calculated by weight loss method using precision electronic balance with an accuracy of 1 mg. The tool maker microscope with a least count of 1 μm was used for measurement of OC. The planning matrix of the experimental observed data are shown in Table 4.10.

Table 4.10: Planning matrix of the experiment and their observed data

Run no.	PtType	Blocks	Ip (A)	T_{on} (μs)	T_w s	T_{up} s	MRR (mm^3/min)	TWR (mm^3/min)	OC (mm)
1	0	2	3	80	0.6	0.8	1.6701	0.0210	0.178
2	1	2	5	150	1.0	1.5	3.8217	0.0107	0.195
3	1	2	1	10	1.0	1.5	0.1682	0.0157	0.007
4	1	2	1	150	1.0	0.0	0.5758	0.0112	0.210
5	1	2	5	10	1.0	0.0	4.3618	0.3997	0.093
6	0	2	3	80	0.6	0.8	1.3792	0.0214	0.168
7	1	2	5	150	0.2	0.0	10.6642	0.0479	0.193
8	1	2	1	150	0.2	1.5	0.1048	0.0025	0.018
9	1	2	5	10	0.2	1.5	0.8917	0.3421	0.267
10	1	2	1	10	0.2	0.0	0.4106	0.0351	0.101
11	-1	3	3	80	0.6	0.0	4.1529	0.0571	0.165
12	-1	3	3	80	0.2	0.8	1.7622	0.0298	0.145
13	-1	3	3	10	0.6	0.8	1.3248	0.1768	0.188
14	-1	3	5	80	0.6	0.8	5.2389	0.1920	0.165
15	0	3	3	80	0.6	0.8	1.9219	0.0326	0.174
16	-1	3	3	150	0.6	0.8	2.1892	0.0051	0.196
17	-1	3	1	80	0.6	0.8	0.3039	0.0069	0.026
18	0	3	3	80	0.6	0.8	2.5873	0.0330	0.141
19	-1	3	3	80	0.6	1.5	1.3649	0.0192	0.185
20	-1	3	3	80	1.0	0.8	2.2726	0.0393	0.122
21	1	1	1	150	1.0	1.5	0.2623	0.0274	0.126
22	1	1	5	150	1.0	0.0	11.0658	0.0559	0.194
23	1	1	5	10	1.0	1.5	1.5987	0.3356	0.155
24	0	1	3	80	0.6	0.8	2.0170	0.0266	0.162
25	1	1	1	10	1.0	0.0	0.4812	0.0431	0.114
26	0	1	3	80	0.6	0.8	1.9490	0.0327	0.161
27	1	1	1	150	0.2	0.0	0.4909	0.0045	0.125
28	1	1	5	150	0.2	1.5	3.2838	0.0091	0.195
29	1	1	5	10	0.2	0.0	4.3631	0.4145	0.173
30	1	1	1	10	0.2	1.5	0.1274	0.0087	0.042

4.2.2 Effect of EDM parameters on MRR

In the EDM process, the influence of various machining parameters like Ip, T_{on}, T_w and T_{up} on MRR are shown in the main effect plot in Fig. 4.9. From the graph, it is concluded that discharge current is directly proportional to MRR. Moreover, it is evident that the other factors does not have much significant effect on MRR as compared to Ip. Similar conclusions were shown by Ghoreishi and Tabari [2007]. MRR increases with T_{on}, this is due to the fact that higher T_{on} results in more energy transfer to the work piece. So, more material is eroded and removed.

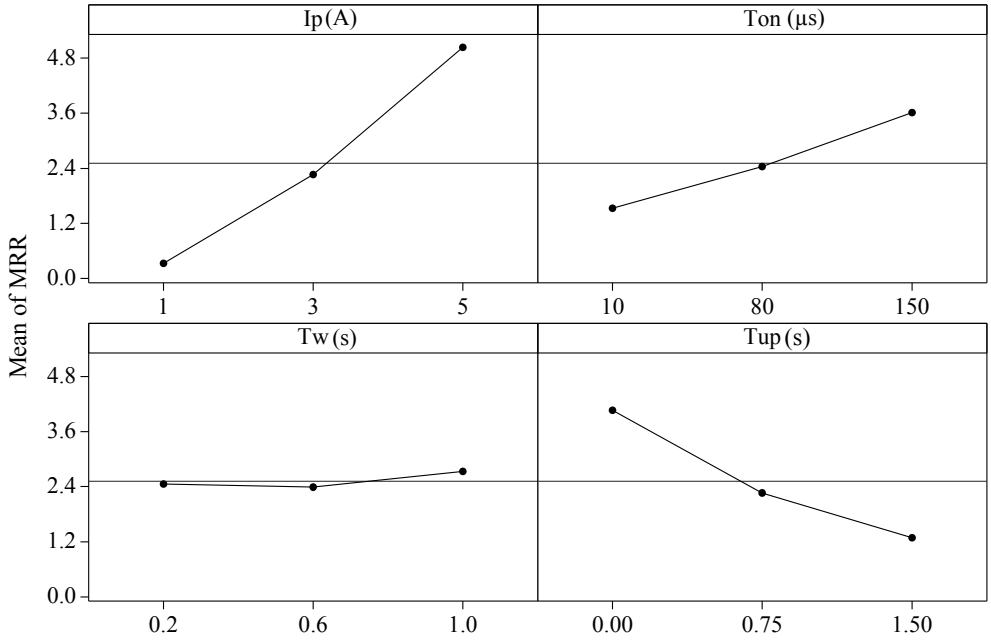

Fig. 4.9: Variation of MRR with Ip, T_{on}, T_w, and T_{up}

MRR usually decreases with T_{up} and it is due to considerable decrement of work-piece temperature with the increment in T_{up}. Hence, the most of the discharge energy is consumed to re-heat the tool and work piece, resulting in decrease in material removal efficiency. It is evident from the same figure that T_w has a very little influence on MRR in this experiment. The interaction factor like $Ip \times T_{on}$, $Ip \times T_{up}$ and $T_{on} \times T_{up}$ have significant effect on MRR with percent contribution of 8.81 %, 11.17 % and 2.11 %, respectively. $Ip \times T_{on}$ are found to be directly proportional to MRR as shown in Fig. 4.10. Higher values of these two parameter releases high energy resulting more material removal from the workpiece. The remaining factors have inverse rela-

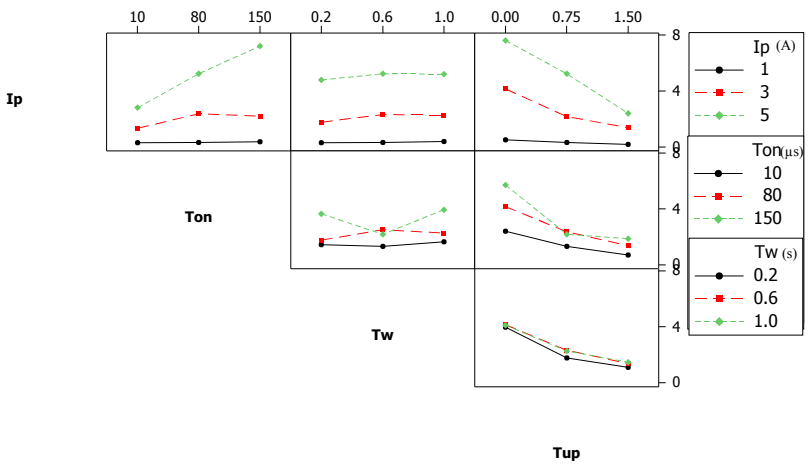

Fig. 4.10: Interaction plot for MRR in RSM design

tion with MRR. So, higher values of lift time with higher current and pulse duration produces less temperature in IEG resulting in less material removal.

The ANOVA for MRR is shown in Table 4.11, where the columns represent sources of variation, DF, Seq SS, MS, statistic F and P. The last column represents % contribution of the factors or sources of variation. It reveals that there is no blocking effect on the observations. Moreover, the factor T_w, along with its interaction terms like, $Ip \times T_w$, $T_{on} \times T_w$ and $T_w \times T_{up}$ are found to be insignificant for 95% of confidence interval, *i*.e. factors having P-value more than 0.05. Besides, none of the square terms have any significant effect on the response. These non-significant terms are eliminated by the backward elimination process. The F-value, P-value and the % contribution of the significant terms after elimination are presented in the ANOVA Table 4.12 after elimination. In this table, the insignificant factors are marked as * in P column and the lack-of-fit is found to be insignificant, which represents that model is sufficient. Equation 4.2 represents MRR model depicting significant linear and interaction terms. Fig. 4.11 shows the normal probability plot for MRR. This plot implies that the data are fairly normal and there is no deviation from the normality with 95% confidence. This shows the efficiency of the developed model.

$$\begin{aligned} MRR &= -1.39961 + 1.16764Ip - 8.1939 \times 10^{-4}T_{on} + \\ &\quad 1.40666T_{up} + 0.00775618Ip \times T_{on} - 0.815129 \\ &\quad Ip \times T_{up} - 0.0101112T_{on} \times T_{up} \end{aligned} \tag{4.2}$$

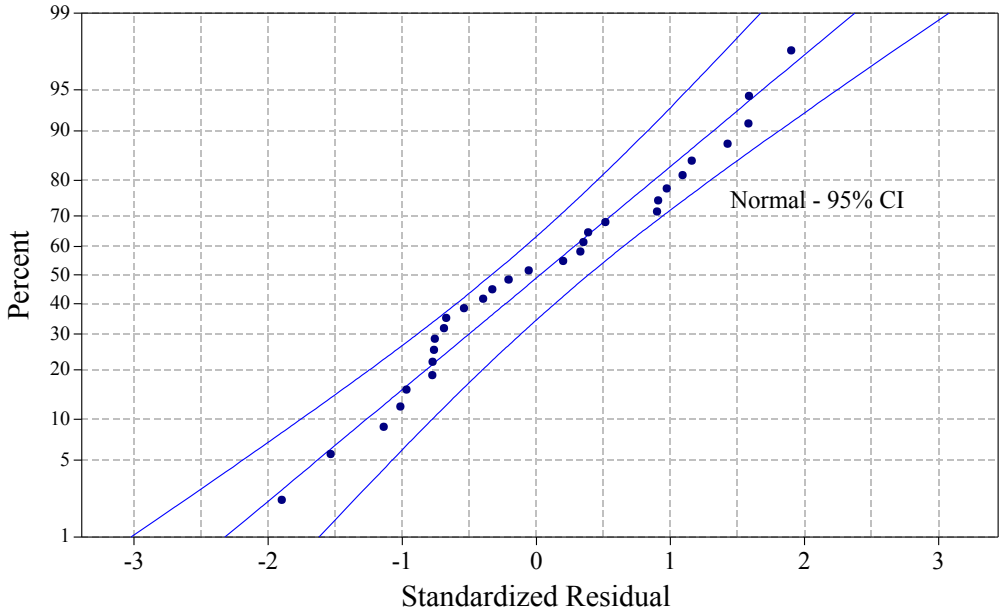

Fig. 4.11: Normal probability plot for MRR

Table 4.11: ANOVA table for MRR (before elimination)

Source	DF	Seq SS	Adj MS	F	P	% contribution
Blocks	2	0.178	0.6043	0.88	0.439*	0.08
Regression	14	204.969	14.6407	21.25	0.000	95.73
Linear	4	154.113	38.5283	55.92	0.000	71.98
Ip	1	99.708	99.7083	144.7	0.000	46.57
T_{on}	1	19.491	19.4914	28.29	0.000	9.10
T_w	1	0.35	0.3498	0.51	0.489*	0.16
T_{up}	1	34.564	34.5639	50.16	0.000	16.14
Square	4	3.4	0.85	1.23	0.344*	1.59
Ip*Ip	1	2.298	1.0055	1.46	0.249*	1.07
T_{on}* T_{on}	1	0.131	0.3763	0.55	0.473*	0.06
T_w* T_w	1	0.005	0.0394	0.06	0.815*	0.00
T_{up}* T_{up}	1	0.966	0.966	1.4	0.258*	0.45
Interaction	6	47.456	7.9093	11.48	0.000	22.16
Ip* T_{on}	1	18.866	18.8657	27.38	0.000	8.81
Ip* T_w	1	0.104	0.1042	0.15	0.704*	0.05
Ip* T_{up}	1	23.92	23.9197	34.71	0.000	11.17
T_{on}* T_w	1	0.008	0.0083	0.01	0.914*	0.00
T_{on}* T_{up}	1	4.509	4.5086	6.54	0.024	2.11
T_w* T_{up}	1	0.049	0.0492	0.07	0.793*	0.02
Residual Error	13	8.958	0.689			4.18
Lack-of-Fit	10	8.643	0.8643	8.25	0.055*	4.04
Pure Error	3	0.314	0.1048			0.15
Total	29	214.104				
S = 0.830089 R-Sq = 95.82% R-Sq(adj) = 90.67%						

4.2.3 Effect of EDM parameters on TWR

Main effect plot for TWR is shown in Fig. 4.12 for significant factor, which indicates that Ip is directly proportional to TWR. Pulse-on time is inversely proportional to the tool wear rate. Whereas, TWR tends to decrease with increase in T_{up} to an optimum level and then increases slightly. It is because more T_{up} results in deceasing of the temperature of tool, so less tool wear is expected. T_w has no significant effect on TWR.

With reference to Table 4.13, all square terms and some interaction terms such as $Ip \times T_{on}$, $Ip \times T_{up}$ and $T_{on} \times T_{up}$ are found to be significant for TWR this is also described in interaction plot for TWR that is shown in Fig. 4.13. And their % contribution is found to be 23.93 %, 0.46 % and 0.20 %, respectively, they are conformed by ANOVA for TWR (after elimination) in Table 4.14. In this table, the

Table 4.12: ANOVA table for MRR (after elimination)

Source	DF	Seq SS	Adj MS	F	P	%contribution
Regression	6	201.058	33.5096	59.07	0.000	93.91
Linear	3	153.764	51.2545	90.36	0.000	71.82
Ip	1	99.708	99.7083	175.77	0.000	46.57
T_{on}	1	19.491	19.4914	34.36	0.000	9.1
T_{up}	1	34.564	34.5639	60.93	0.000	16.14
Interaction	3	47.294	15.7647	27.79	0.000	22.09
Ip* T_{on}	1	18.866	18.8657	33.26	0.000	8.81
Ip* T_{up}	1	23.92	23.9197	42.17	0.000	11.17
T_{on}* T_{up}	1	4.509	4.5086	7.95	0.010	2.11
Residual Error	23	13.047	0.5673			6.09
Lack-of-Fit	8	7.404	0.9255	2.46	0.063*	3.46
Pure Error	15	5.643	0.3762			2.64
Total	29	214.104				
S = 0.753164 R-Sq = 93.91% R-Sq(adj) = 92.32%						

lack-of- fit is found to be insignificant, so the design model is significant.

With the increase of $Ip \times T_{on}$ the tool wear rate decreases, because the higher combination of current with pulse duration possibly forces the metal particles to stick on the tool surface, which develops a shield against wear, with an possibility of less tool wear. $Ip \times T_{up}$ and $T_{on} \times T_{up}$ are found to be less significant than the earlier terms in respect to TWR. And Fig. 4.14 shows the normal probability plot for TWR that indicates outliers don exist in the data, because standardized residues are between -2 and 2. The non- significant terms are eliminated in the subsequent model by backward elimination method. Equation 4.3 represents the model TWR that is shown below:

$$\begin{aligned} TWR &= -0.00543631 + 0.0242142Ip - 9.54717 \times 10^{-4} \\ &\quad T_{on} + 0.122170T_w - 0.0109522T_{up} + 0.012362 \\ &\quad Ip^2 + 8.34779 \times 10^{-6}T_{on}^2 - 0.0966540T_w^2 \\ &\quad -5.85361 \times 10^{-4}Ip \times T_{on} - 0.00754418 \\ &\quad Ip \times T_{up} + 1.43702 \times 10^{-4}T_{on} \times T_{up} \end{aligned} \tag{4.3}$$

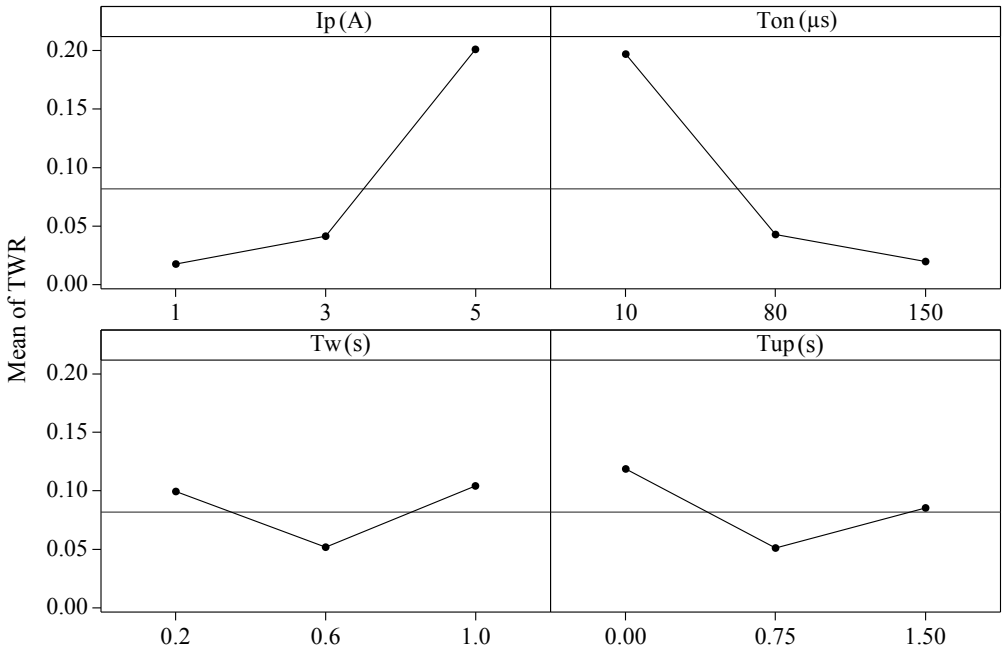

Fig. 4.12: Variation of TWR with Ip, T_{on}, T_w, and T_{up}

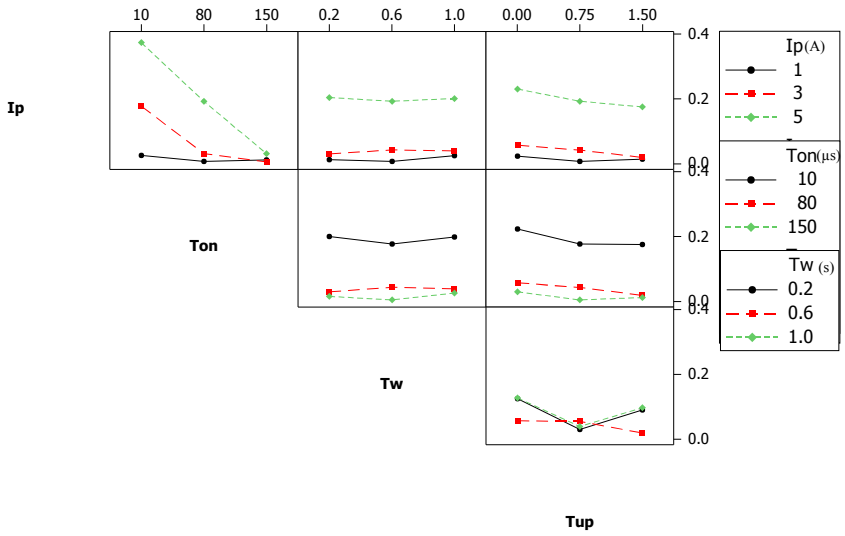

Fig. 4.13: Interaction plot for TWR

Table 4.13: ANOVA table for TWR (before elimination)

Source	DF	Seq SS	Adj MS	F	P	% contribution
Blocks	2	0.009131	0.000511	3.76	0.052	2.03
Regression	14	0.440779	0.031484	1215.95	0.000	98.17
Linear	4	0.298436	0.074609	2881.47	0.000	66.47
Ip	1	0.151716	0.151716	5859.39	0.000	33.79
T_{on}	1	0.14167	0.14167	5471.43	0.000	31.55
T_w	1	0.00011	0.00011	4.26	0.060*	0.02
T_{up}	1	0.00494	0.00494	190.79	0.000	1.1
Square	4	0.031553	0.007888	304.65	0.000	7.03
Ip*Ip	1	0.025809	0.007751	299.35	0.000	5.75
T_{on}* T_{on}	1	0.005301	0.005539	213.91	0.000	1.18
T_w* T_w	1	0.000349	0.000237	9.14	0.010	0.08
T_{up}* T_{up}	1	0.000094	0.000094	3.62	0.079*	0.02
Interaction	6	0.11079	0.018465	713.13	0.000	24.68
Ip* T_{on}	1	0.107454	0.107454	4149.97	0.000	23.93
Ip* T_w	1	0.000213	0.000213	8.22	0.013	0.05
Ip* T_{up}	1	0.002049	0.002049	79.13	0.000	0.46
T_{on}* T_w	1	0.000141	0.000141	5.43	0.036	0.03
T_{on}* T_{up}	1	0.000911	0.000911	35.17	0.000	0.2
T_w* T_{up}	1	0.000023	0.000023	0.87	0.367*	0.01
Residual Error	13	0.000337	0.000026			0.08
Lack-of-Fit	10	0.000318	0.000032	5.13	0.103*	0.07
Pure Error	3	0.000019	0.000006			0
Total	29	0.448993				
S = 0.00508849 R-Sq = 99.93% R-Sq(adj) = 99.83%						

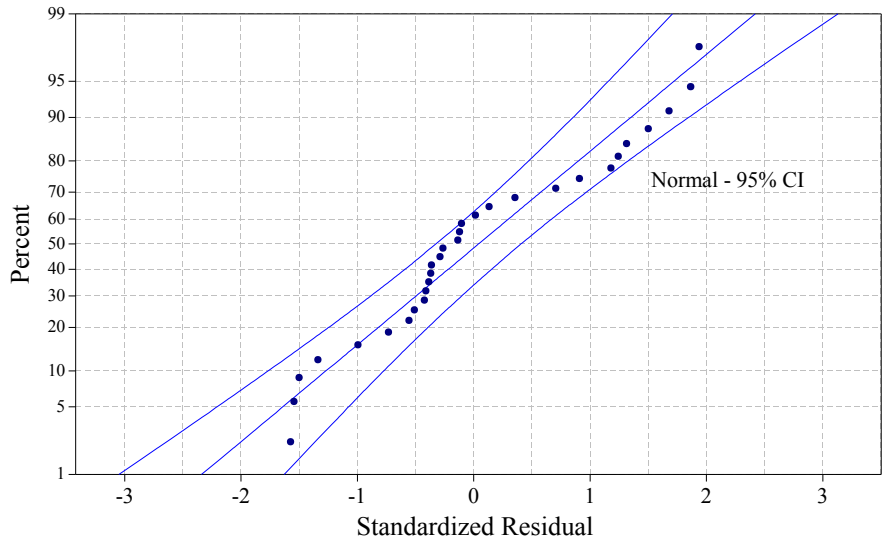

Fig. 4.14: Normal probability plot for TWR

Table 4.14: ANOVA table for TWR (after elimination)

Source	DF	Seq SS	Adj MS	F	P	% contribution
Regression	10	0.44673	0.044673	375.08	0.000	99.50
Linear	4	0.298436	0.074609	626.43	0.000	66.47
Ip	1	0.151716	0.151716	1273.83	0.000	33.79
T_{on}	1	0.14167	0.14167	1189.49	0.000	31.55
T_w	1	0.00011	0.00011	0.93	0.348*	0.02
T_{up}	1	0.00494	0.00494	41.48	0.000	1.10
Square	3	0.03788	0.012627	106.02	0.000	8.44
Ip*Ip	1	0.033121	0.006942	58.28	0.000	7.38
T_{on}* T_{on}	1	0.004081	0.00475	39.88	0.000	0.91
T_w* T_w	1	0.000679	0.000679	5.7	0.028	0.15
Interaction	3	0.110414	0.036805	309.02	0.000	24.59
Ip* T_{on}		0.107454	0.107454	902.21	0.000	23.93
Ip* T_{up}		0.002049	0.002049	17.2	0.001	0.46
T_{on}* T_{up}		0.000911	0.000911	7.65	0.012	0.20
Residual Error	19	0.002263	0.000119			0.50
Lack-of-Fit	14	0.0021	0.00015	4.6	0.051*	0.47
Pure Error	5	0.000163	0.000033			0.04
Total	29	0.448993				
S = 0.0109134 R-Sq = 99.50% R-Sq(adj) = 99.23%						

4.2.4 Effect of EDM parameters on Over-cut

The OC is measured by half the difference between the sizes of the cavity and the diameter of the electrode in EDM process. Minimum OC is always desired for better result. The effects of various machining parameters such as Ip, T_{on}, T_w and T_{up} on OC are presented in the main effect plot shown in Fig. 4.15. This graph indicates that the discharge current is directly proportional to OC. General explanation for higher OC is that the high current with straight polarity results in large erosion. As spark energy is more at higher current, the crater formed on the work material is large in width and hence results in increment of OC [Singh et al., 2004b]. OC increases gradually with the increase in pulse-on time, as it is responsible for maintaining continuation of spark at tool and workpiece interface [Jeswani, 1981]. The T_w and T_{up} have no significant effect on OC according to the ANOVA that are shown in Table 4.15.

The square terms likes Ip^2, T_{on}^2, and interaction terms such as $Ip \times T_w$, $Ip \times T_{up}$ and $T_{on} \times T_w$ have significant effects on OC. $Ip \times T_w$ has an influence in a reverse manner for OC. With a combination of high current and high working time, flushing

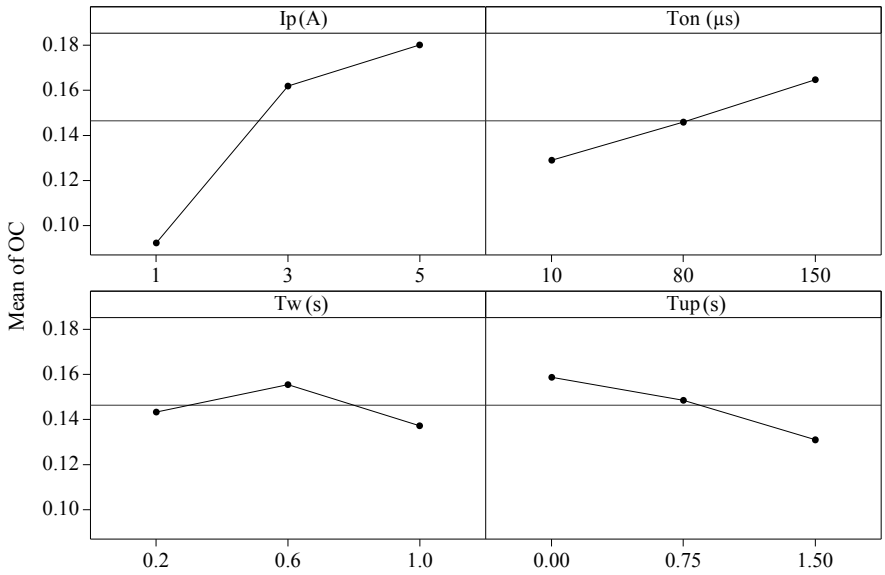

Fig. 4.15: Variation of OC with Ip, T_{on}, T_w, and T_{up}

effect flops, so less OC is expected. The interaction of $Ip \times T_{up}$ is directly proportional to OC. High current and more lift time facilitates more material removal and better flushing, resulting in higher OC. $T_{on} \times T_w$ has direct influence on OC, which is due to higher pulse-on time and higher work time, more material is removed from the surface so higher OC is expected. The effect of all interaction factor on OC are shown in Fig. 4.16. The insignificant terms were eliminated by the backward elimination process that is presented in Table 4.16 . In this table the lack-of-fit is not significant, which indicates that the model is sufficient.

The developed model is fairly efficient as there is no deviation of the OC data points in the normal probability plot shown in Fig. 4.17. The model obtained from regression equation for OC shows the influence of linear, square and interaction terms as shown in Equation 4.4.

$$\begin{aligned} OC &= 0.0384288 + 0.113163Ip - 0.00151786T_{on} + \\ &\quad 0.00577445T_w - 0.0775635T_{up} - 0.0147248Ip^2 \\ &\quad +7.60730 \times 10^{-6}T_{on}^2 - 0.0283032Ip \times T_w + \\ &\quad 0.021447Ip \times T_{up} + 9.12681 \times 10^{-4}T_{on} \times T_w \end{aligned} \tag{4.4}$$

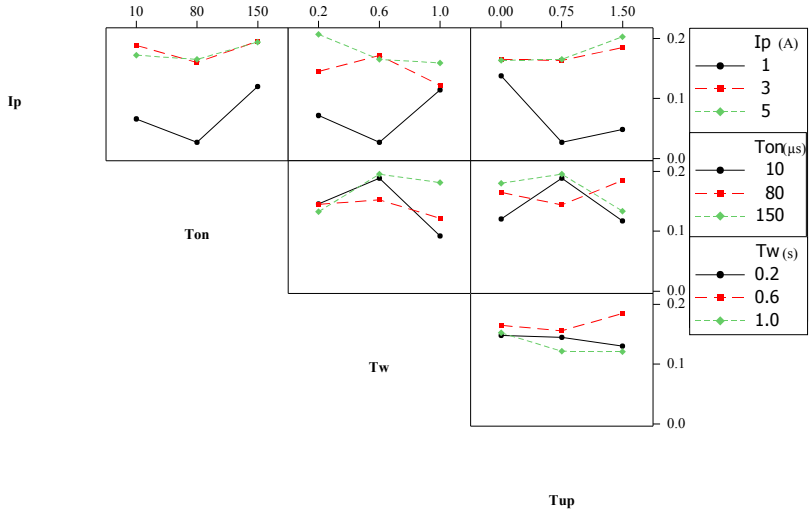

Fig. 4.16: Interaction plot for OC

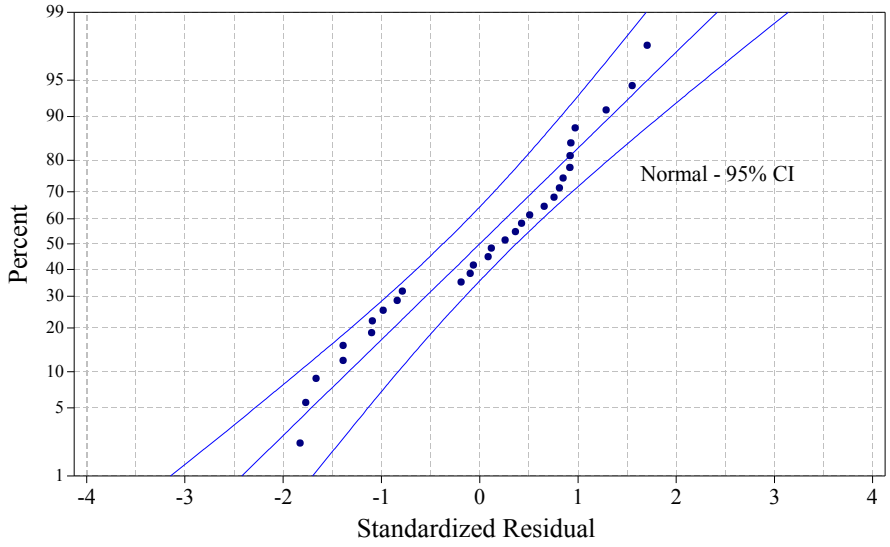

Fig. 4.17: Normal probability plot for OC

Table 4.15: ANOVA table for OC (before elimination)

Source	DF	Seq SS	Adj MS	F	P	% contribution
Blocks	2	0.000323	0.000226	0.58	0.572*	0.30
Regression	14	0.100788	0.007199	18.56	0.000	94.95
Linear	4	0.048443	0.012111	31.22	0.000	45.63
Ip	1	0.041187	0.041187	106.16	0.000	38.80
T_{on}	1	0.005378	0.005378	13.86	0.003	5.07
T_w	1	0.000108	0.000108	0.28	0.607*	0.10
T_{up}	1	0.001771	0.001771	4.56	0.052*	1.67
Square	4	0.014016	0.003504	9.03	0.001	13.20
Ip*Ip	1	0.008575	0.009297	23.96	0.000	8.08
T_{on}* T_{on}	1	0.003671	0.003227	8.32	0.013	3.46
T_w* T_w	1	0.000886	0.001345	3.47	0.085*	0.83
T_{up}* T_{up}	1	0.000883	0.000883	2.28	0.155*	0.83
Interaction	6	0.038329	0.006388	16.47	0.000	36.11
Ip* T_{on}	1	0.00102	0.00102	2.63	0.129*	0.96
Ip* T_w	1	0.008203	0.008203	21.14	0.000	7.73
Ip* T_{up}	1	0.016558	0.016558	42.68	0.000	15.60
T_{on}* T_w	1	0.010449	0.010449	26.93	0.000	9.84
T_{on}* T_{up}	1	0.001908	0.001908	4.92	0.045	1.80
T_w* T_{up}	1	0.000191	0.000191	0.49	0.495*	0.18
Residual Error	13	0.005044	0.000388			4.75
Lack-of-Fit	10	0.004473	0.000447	2.35	0.261*	4.21
Pure Error	3	0.00057	0.00019			0.54
Total	29	0.106154				
S = 0.0196969 R-Sq = 95.25% R-Sq(adj) = 89.40%						

Table 4.16: ANOVA table for OC (after elimination)

Source	DF	Seq SS	Adj MS	F	P	% contribution
Regression	9	0.095802	0.010645	20.57	0.000	90.24
Linear	4	0.048443	0.012111	23.4	0.000	45.63
Ip	1	0.041187	0.041187	79.57	0.000	38.79
T_{on}	1	0.005378	0.005378	10.39	0.004	5.06
T_w	1	0.000108	0.000108	0.21	0.653*	0.10
T_{up}	1	0.001771	0.001771	3.42	0.079	1.66
Square	2	0.012149	0.006074	11.74	0.000	11.44
Ip*Ip	1	0.007363	0.011949	23.09	0.000	6.93
T_{on}* T_{on}	1	0.004786	0.004786	9.25	0.006	4.50
Interaction	3	0.03521	0.011737	22.68	0.000	33.16
Ip* T_w	1	0.008203	0.008203	15.85	0.001	7.72
Ip* T_{up}	1	0.016558	0.016558	31.99	0.000	15.59
T_{on}* T_w	1	0.010449	0.010449	20.19	0.000	9.75
Residual Error	20	0.010352	0.000518			9.75
Lack-of-Fit	15	0.009513	0.000634	3.78	0.075*	8.96
Pure Error	5	0.000839	0.000168			0.79
Total	29	0.106154				
S = 0.0227509 R-Sq = 90.25% R-Sq(adj) = 85.86%						

4.2.5 Multi-objective optimisation using fuzzy logic technique

In this study, MRR, TWR and OC are three quality characteristics, which are to be optimised using fuzzy logic method. S/N ratios are calculated for the experimental results that can be used to measure the deviation of those characteristics from the desired values. Usually, there are three categories of performance characteristics in the analysis of the S/N ratio: the lower-the-better, the higher- the-better, and the nominal-the-best [Puri and Deshpande, 2004]. For MRR is higher-the-better performance characteristic is considered. The S/N ratio for the j^{th} experimental run x_{ij}, which is calculated by Equation 4.5. TWR and OC lower-the-better performance characteristic is considered. The S/N ratios can be expressed by Equation 4.6.

$$x_{ij} = -10\log(\frac{1}{n}\sum_{k=1}^{n}\frac{1}{y_{ijk}^2}) \text{ for i} = 1 \tag{4.5}$$

$$x_{ij} = -10\log(\frac{1}{n}\sum_{k=1}^{n}y_{ijk}^2) \text{ for i} = 2,3 \tag{4.6}$$

Where y_{ijk} is the experimental value of the i^{th} performance characteristic in the

j^{th} run at the k^{th} test and n is the number of replicate (n=1). The observed MRR, TWR and OC values are converted to S/N ratios and shown in Table 4.17.

The fuzzifier uses membership functions to fuzzify S/N ratios of each performance characteristic. Then, the inference engine (Mamdani fuzzy inference system) performs fuzzy reasoning on fuzzy rules to generate a fuzzy value. Finally, the defuzzifier converts fuzzy predicted value into MPCI . This process was repeated for all the runs of experiment and respective MPCI value was found out (Table 4.17).

Fuzzy values are defined by the membership functions and Fig. 4.18a, 4.18b and 4.18c are showing the graphical representation of five fuzzy subsets (Very Small, Small, Medium, Large, and Very Large) assigned to inputs, *i*.e., for the S/N ratios of MRR (x_{1j}), TWR (x_{2j}) and OC (x_{3j}) for the j^{th} run. Fig. 4.18d is showing the output membership functions in which the seven fuzzy subsets (Tiny, Very Small, Small, Medium, Large, Very Large, and Huge) are assigned to an output, *i.* e., MPCI (Y_j). The suffix j for each symbol can be dropped for simplicity without losing ambiguity. Various degrees of membership of the fuzzy sets are calculated based on the values of x_1, x_2, x_3 and Y for each run. The relationship between three inputs and the output is represented in the form of if-then control rules, that are:

Rule 1: if x_1 is Large and x_2 is Large and x_3 is Very Small then Y is Medium else

Rule 2: if x_1 is Small and x_2 is Large and x_3 is Very Small then Y is Large else

$\vdots$

Rule N: if x_1 is Medium and x_2 Medium and x_3 is Medium then Y is Huge.

For each rule, the three inputs are assigned in the fuzzy subsets corresponding membership functions, $\mu(x_1)$ and $\mu(x_2)$, $\mu(x_3)$. The output is assigned to any of the five fuzzy subset membership functions is $\mu(Y)$. Fuzzy module of MATLAB Software was used to generate the rules for the present study, which yielded 30 rules as shown in Fig. 4.19. Fuzzy rules are directly derived based on the fact that larger-the-better characteristic for MPCI. By max-min compositional operation, the fuzzy reasoning of these rules yield fuzzy outputs. Finally, the centre of gravity defuzzification method is adopted to transform the fuzzy inference output into a non-fuzzy value Y [Lin and Lin, 2005], which is known as the crisp output.

Table 4.17: S/N ratio for responses and MPCI

	S/N- Ratio			
Run no	MRR	TWR	OC	MPCI
1	4.4548	33.5763	15.0160	0.4763
2	11.6450	39.3892	14.1993	0.6800
3	-15.4835	36.1042	43.5436	0.6799
4	-4.7946	39.0268	13.5556	0.3601
5	12.7933	7.9643	20.5838	0.5200
6	2.7925	33.3884	15.4757	0.4422
7	20.5586	26.3863	14.2731	0.6799
8	-19.5941	52.0710	34.8945	0.6800
9	-0.9955	9.3180	11.4812	0.2000
10	-7.7295	29.1039	19.8579	0.3600
11	12.3670	24.8651	15.6503	0.5432
12	4.9211	30.5074	16.7726	0.4571
13	2.4430	15.0503	14.4938	0.3016
14	14.3848	14.3330	15.6503	0.4398
15	11.8699	29.7393	15.2215	0.4606
16	6.8057	45.9091	14.1771	0.7691
17	-10.3454	43.1745	31.4861	0.6799
18	10.0685	29.6360	17.0249	0.5900
19	2.7020	34.3451	14.6566	0.4400
20	7.1305	28.1121	18.2978	0.5160
21	-11.6240	31.2365	17.9479	0.3600
22	20.8797	25.0474	14.2731	0.6799
23	4.0753	9.4843	16.1934	0.3355
24	6.0941	31.4884	15.8285	0.4649
25	-6.3537	27.3014	18.9116	0.3600
26	5.7962	29.7054	15.8655	0.4565
27	-6.1801	46.9856	18.0918	0.5051
28	10.3275	40.8127	14.1993	0.6800
29	12.7959	7.6493	15.2215	0.3930
30	-17.8974	41.2217	27.6077	0.5200

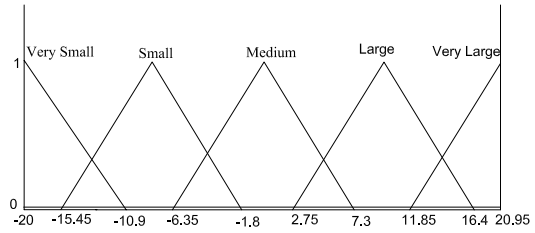

(a) MRR

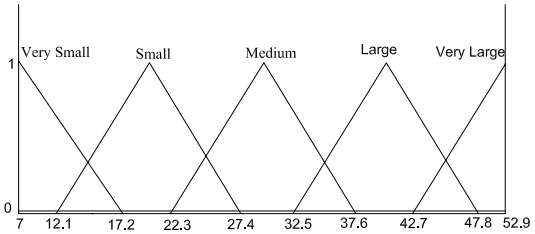

(b) TWR

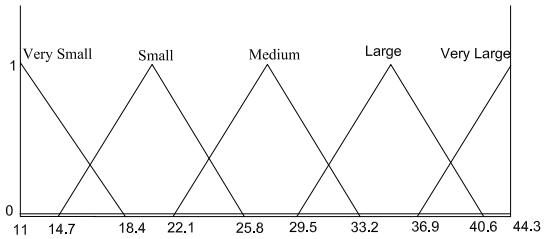

(c) OC

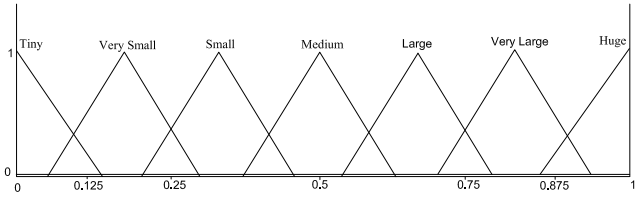

(d) MPCI

Fig. 4.18: Membership function for MRR, TWR, OC and MPCI

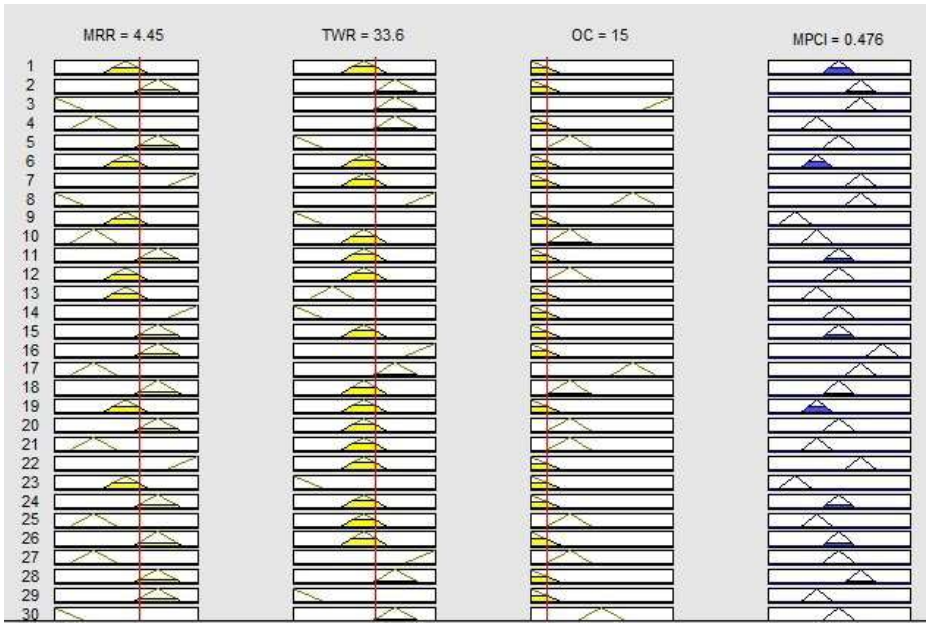

Fig. 4.19: Fuzzy logic reasoning procedure for run no 1

Table 4.18: Response table for MPCI

EDM Parameter	Average MPCI by factor level		
	Level 1	Level 2	Level 3
Ip	0.5006	0.5012	0.5120
T_{on}	0.4078	0.5082	0.5993
T_w	0.4972	0.5222	0.4990
T_{up}	0.4890	0.5207	0.5084
Mean of MPCI = 0.5010			

The crisp value Y is called as MPCI. Based on the above discussion, larger the MPCI smaller is the variance of the performance characteristics around the desired value. Table 4.17 shows the MPCI for each run. The mean of MPCI for each level of the machining parameters is summarized in Table 4.18. However, the relative importance amongst the machining parameters for the multiple performance characteristics still needs to be known so that the optimal combinations of the machining parameter levels can be determined more accurately. For that main effect plot MPCI was plotted (Fig. 4.20). From the ANOVA (Table 4.19), it can be concluded that T_{on} has most significant effect on MPCI. The following factor settings, according to the MPCI graph, have been identified as to yield the best combination of process variables: Ip= 5A, $T_{on} = 150\mu s$, T_w= 0.6s, and T_{up}= 0.75s.

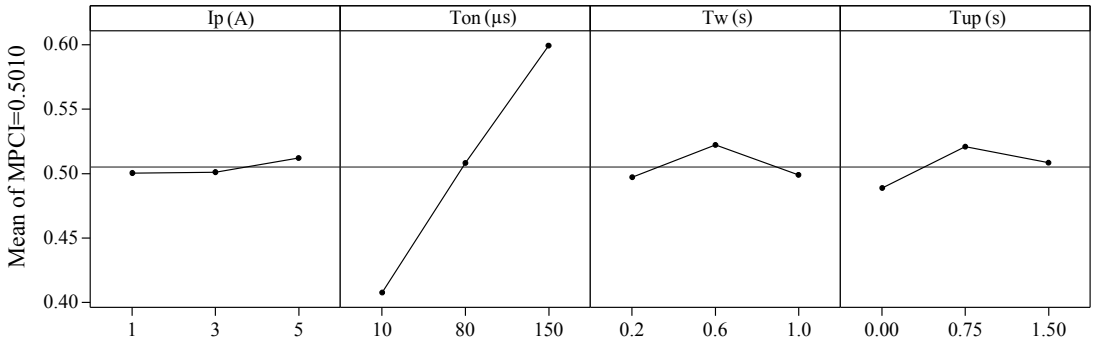

Fig. 4.20: MPCI graph

Table 4.19: Analysis of Variance for MPCI

Source	DF	Seq SS	Adj MS	F	P
Regression	6	0.337357	0.056226	5.47	0.001
Linear	4	0.167431	0.041858	4.07	0.012
Ip	1	0.000591	0.000591	0.06	0.813*
T_{on}	1	0.165140	0.165140	16.05	0.001
T_w	1	0.000015	0.000015	0.00	0.970*
T_{up}	1	0.001686	0.001686	0.16	0.689*
Interaction	2	0.169926	0.084963	8.26	0.002
Ip*T_{on}	1	0.103362	0.103362	10.05	0.004
Ip*T_{up}	1	0.066564	0.066564	6.47	0.018
Residual Error	23	0.236618	0.010288		
Lack-of-Fit	18	0.221937	0.012330	4.20	0.060*
Pure Error	5	0.014681	0.002936		
Total	29	0.573975			

* = Insignificant factor

4.2.6 Analysis of result and conformation test

The optimum results were verified through confirmatory experiments. The estimated or predicted MPCI ($\widehat{Y}$) at the optimum level of the machining parameter can be calculated by Equation 4.7:

$$\widehat{Y} = Y_m + \sum_{i=1}^{q} (\overline{Y_i} - Y_m) \tag{4.7}$$

Where Y_m is mean of MPCI's of all experimental runs, $\overline{Y_i}$ is the mean of MPCI at the optimum level of i^{th} parameter, and q is the number of machining parameters that significantly effect MPCI. Table 4.20 shows the result of confirmatory test and

Table 4.20: Result of confirmatory experiment for fuzzy logic

	Initial machining parameter	Optimum machining parameter	
Level	Ip=3A, T_{on} = 80μs, T_w=0.6s and T_{up}=0.75s	Ip=5A, T_{on} = 150μs, T_w=0.6s and T_{up}=0.75s	
		Prediction value	Experimental value
MRR	1.6701		7.6838
TWR	0.02095		0.0661
OC	0.1775		0.2013
MPCI	0.5690	0.5993	0.6801
Improvement of MPCI = 0.1111			

the optimum levels of process parameter, MRR, TWR and OC were found to be 7.6838 mm^3/min, 0. 0661 mm^3/min and 0.2013 mm, respectively. The MPCI for first run of experiment is 0.5690 and it increases to 0.6801 for optimal design, with an improvement of 0.1111.

4.2.7 Conclusions

It can be concluded that MRR decreases with the electrode lift time whereas working time has no effect on it. TWR initially decreases with electrode lift time to optimum level and then slightly increases, whereas work time has no significant effect on it. OC is neither affected by lift time nor by work time.

The optimal factor settings of maximum MRR, minimum TWR and OC obtained from fuzzy logic technique is: Ip= 5A, T_{on} = 150μs, T_w= 0.6s and T_{up}= 0.75s. The experimental value of performance characteristics for this setting of process variables for the confirmatory test was found to be 7.6838 mm^3/min , 0.0661 mm^3/min and 0.2013 mm for MRR, TWR and OC, respectively. It is asserted from this study that quality characteristics can be greatly improved using fuzzy logic technique.

4.3 Multi-response optimisation of EDM using Fuzzy-TOPSIS and its sensitivity analysis

In this research work, the optimisation of EDMwith multiple attributes such as White Layer Thickness (WLT), SCD, SR and OC has been work out by theTOPSIS method in fuzzy environment. The optimal solution for a numerical example was obtained for five decision makers' preferences on the four responses. A sensitivity analysis is carried out to study the sensitivity of the five decision makers' preferences on optimal machining parameters. AISI P20 tool steel has been selected as a workpiece with copper tool electrode.

4.3.1 Experimental planning

Experiments were conducted to study the effects of various machining parameters on EDM process. This study have been undertaken to investigate the effects of pulse current (Ip), pulse-on time (T_{on}) and tool work time (T_w) and tool lift time (T_{up}) on WLT, SCD, SR and OC. The above mentioned machining parameters are effecting the process responses, hence, these factors were considered for exploration. The workpiece, tool and experimental condition are discussed in section 4.2.

The measurement of WLT was carried out with an optical microscope with 400X optical zoom. After garbing the image, recast area was measured by using PDF x-change viewer software and then the area was divided by total micrography length (166.46 μm) , to get the average hight of recast layer. The surface crack density was measured with the help of SEM at 1000X magnification from top-view of the workpiece. Randomly three sample area were selected on each specimen and the length of cracks were measured by using software. The average crack length was obtained it dividing the crack length by the micro-graphic area (10649.072 μm^2) to get the SCD. The measurement of SR (Ra value) was made with portable style type profilometer. The planning matrix of the experimental observed data are shown in Table 4.21

Table 4.21: Observation table for input parameters and output responses

Run no.	Pt Type	Blocks	Ip (A)	T_{on} (μs)	T_w (s)	T_{up} (s)	Area of WL (μm^2)	WLT (μm)	Crack length (μm)			SCD (μm/μm^2)	SR (μm)
									1	2	3		
1	0	2	3	80	0.6	0.75	2072.76	12.45	181.81	315.18	173.92	0.0210	4.867
2	1	2	5	150	1.0	1.50	4723.97	28.38	90.97	96.53	63.01	0.0078	7.133
3	1	2	1	10	1.0	1.50	625.06	3.76	782.89	638.90	693.99	0.0662	1.733
4	1	2	1	150	1.0	0.00	1244.95	7.48	696.51	648.50	901.07	0.0703	1.733
5	1	2	5	10	1.0	0.00	2602.27	15.63	185.69	257.23	228.18	0.0210	3.400
6	0	2	3	80	0.6	0.75	2531.69	15.21	77.54	28.42	105.55	0.0066	5.200
7	1	2	5	150	0.2	0.00	4474.78	26.88	69.78	131.47	8.31	0.0066	5.867
8	1	2	1	150	0.2	1.50	1709.71	10.27	475.61	525.49	932.97	0.0605	2.000
9	1	2	5	10	0.2	1.50	2907.89	17.47	0.00	0.00	13.09	0.0004	3.667
10	1	2	1	10	0.2	0.00	1157.56	6.95	76.46	477.50	90.26	0.0202	2.067
11	-1	3	3	80	0.6	0.00	3036.73	18.24	68.21	105.45	123.21	0.0093	4.667
12	-1	3	3	80	0.2	0.75	2283.33	13.72	140.19	124.58	85.96	0.0110	5.267
13	-1	3	3	10	0.6	0.75	1214.99	7.30	0.00	0.00	33.59	0.0011	3.200
14	-1	3	5	80	0.6	0.75	3856.21	23.17	0.00	0.00	30.09	0.0009	6.067
15	0	3	3	80	0.6	0.75	2440.24	14.66	147.43	111.41	46.75	0.0096	5.067

Continued on next page

Table 4.21: *Observation table for input parameters and output responses*

Run	Pt	Blocks	Ip	T_{on}	T_w	T_{up}	Area of WL	WLT	Crack length (μm)			SCD	SR
no.	Type		(A)	(μs)	(s)	(s)	(μm^2)	(μm)	1	2	3	(μm/μm^2)	(μm)
16	-1	3	3	150	0.6	0.75	2880.09	17.30	226.26	250.63	116.46	0.0186	5.067
17	-1	3	1	80	0.6	0.75	827.64	4.97	589.13	651.28	793.24	0.0637	2.900
18	0	3	3	80	0.6	0.75	2995.11	17.99	128.22	145.43	154.51	0.0134	5.400
19	-1	3	3	80	0.6	1.50	2714.13	16.30	23.94	26.49	49.16	0.0031	4.667
20	-1	3	3	80	1.0	0.75	2164.15	13.00	120.00	249.41	129.23	0.0156	4.800
21	1	1	1	150	1.0	1.50	1597.18	9.59	668.59	749.23	787.98	0.0690	1.733
22	1	1	5	150	1.0	0.00	4967.50	29.84	58.56	66.93	169.96	0.0092	5.533
23	1	1	5	10	1.0	1.50	2755.41	16.55	588.62	257.26	336.40	0.0370	3.267
24	0	1	3	80	0.6	0.75	2735.77	16.43	13.97	42.25	29.49	0.0027	4.800
25	1	1	1	10	1.0	0.00	523.68	3.15	851.36	778.44	703.73	0.0730	1.667
26	0	1	3	80	0.6	0.75	3042.06	18.27	39.73	76.15	112.13	0.0071	4.967
27	1	1	1	150	0.2	0.00	1542.58	9.27	698.87	615.97	761.85	0.0650	1.867
28	1	1	5	150	0.2	1.50	4097.41	24.61	126.60	41.24	53.14	0.0069	6.600
29	1	1	5	10	0.2	0.00	3261.62	19.59	0.00	0.00	30.91	0.0010	3.000
30	1	1	1	10	0.2	1.50	1112.62	6.68	248.22	289.32	198.23	0.0230	1.833

4.3.2 Influence of EDM parameters on WLT

The influence of the various machining parameter Ip, T_{on} , T_w and T_{up} on WLT are shown in main effect plot Fig. 4.21. This plot indicates that pulse current is directly proportional to WLT. High pulse-on current produces more discharge energy at spark point resulting in formation of recast layer on the workpiece surface [Hascalik and Caydas, 2007]. The optical image of white layer are shown in Fig. 4.22. The pulse-on time is also directly proportional to WLT because the higher pulse-on duration, high energy is produced so the thickness of molten metal is more, which can't be removed by flushing [Bhattacharyya et al., 2007]. The work time and tool lift time has no significant effect on WLT, and it is confirmed by ANOVA Table 4.22. The non-significant terms are eliminated by the backward elimination process. The F-value and P-value of the significant terms are presented in the ANOVA Table 4.23 after elimination. In this table, the insignificant factors are marked as * in P column and the lack-of-fit is found to be insignificant, which represents that model is sufficient. Analysis of variance table indicates the one square terms (T_{up}^2) and two interaction terms $Ip \times T_{on}$ and $T_{on} \times T_w$ are found to be significant. This is also shown in Fig. 4.23.

The residual plot of WLT is shown in Fig. 4.24, This arrangement is useful to determine whether the model meets the assumptions of the analysis. Normal probability plot show the data are normally distributed and the variables are influencing the response. There is no deviation from the normality with 95 % confidence in Fig. 4.24a. Residuals versus fitted values presented here shows the variance is constant and a non-linear relationship exists as well as no outliers exist in the data (Fig. 4.24b). Histogram proves the data are not skewed and no outliers exist as shown in Fig 4.24c. Residuals versus order of the data specify that there are no significant effect due to time or data collection order(Fig. 4.24d).

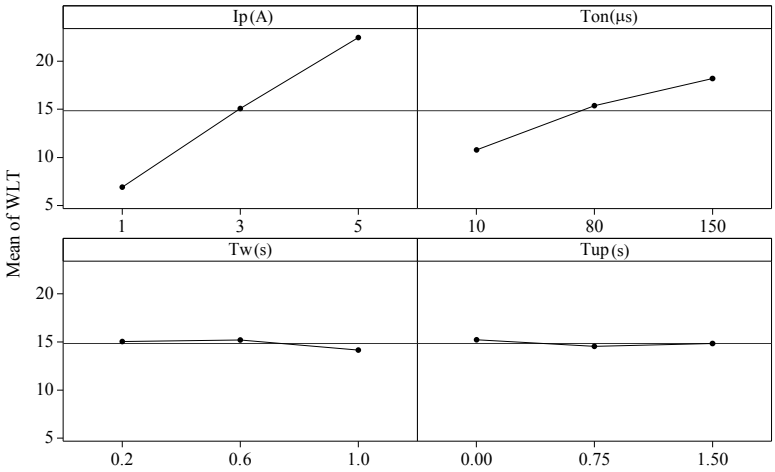

Fig. 4.21: Main effect plots for WLT

Table 4.22: Analysis of Variance for WLT (Before elimination)

Source	DF	Seq SS	Adj SS	Adj MS	F	P
Blocks	2	4.98	7.63	3.82	1.26	0.317*
Regression	14	1437.70	1437.70	102.69	33.85	0.000
Linear	4	1339.32	1339.32	334.83	110.37	0.000
Ip	1	1089.04	1089.04	1089.04	359.00	0.000
T_{on}	1	246.01	246.01	246.01	81.10	0.000
T_w	1	3.62	3.62	3.62	1.19	0.295*
T_{up}	1	0.65	0.65	0.65	0.21	0.652*
Square	4	31.26	31.26	7.82	2.58	0.087*
Ip*Ip	1	3.11	0.51	0.51	0.17	0.689*
T_{on}* T_{on}	1	8.37	12.46	12.46	4.11	0.064*
T_w* T_w	1	0.47	3.40	3.40	1.12	0.309*
T_{up}* T_{up}	1	19.31	19.31	19.31	6.36	0.025
Interaction	6	67.11	67.11	11.19	3.69	0.023
Ip* T_{on}	1	37.20	37.20	37.20	12.26	0.004
Ip* T_w	1	7.63	7.63	7.63	2.51	0.137*
Ip* T_{up}	1	4.40	4.40	4.40	1.45	0.250*
T_{on}* T_w	1	15.75	15.75	15.75	5.19	0.040
T_{on}* T_{up}	1	0.00	0.00	0.00	0.00	0.971*
T_w* T_{up}	1	2.13	2.13	2.13	0.70	0.417*
Residual Error	13	39.44	39.44	3.03		
Lack-of-Fit	10	28.39	28.39	2.84	0.77	0.671*
Pure Error	3	11.05	11.05	3.68		
Total	29	1482.12				
S = 1.74172 R-Sq = 97.34% R-Sq(adj) = 94.06%						

*=insignificant factor

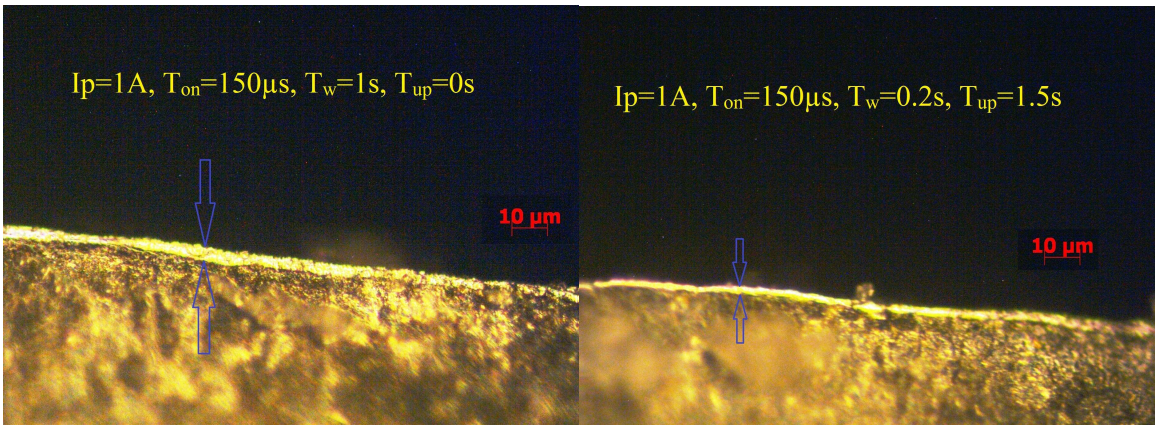

(a) Run no.=4 *(b)* Run no.=8

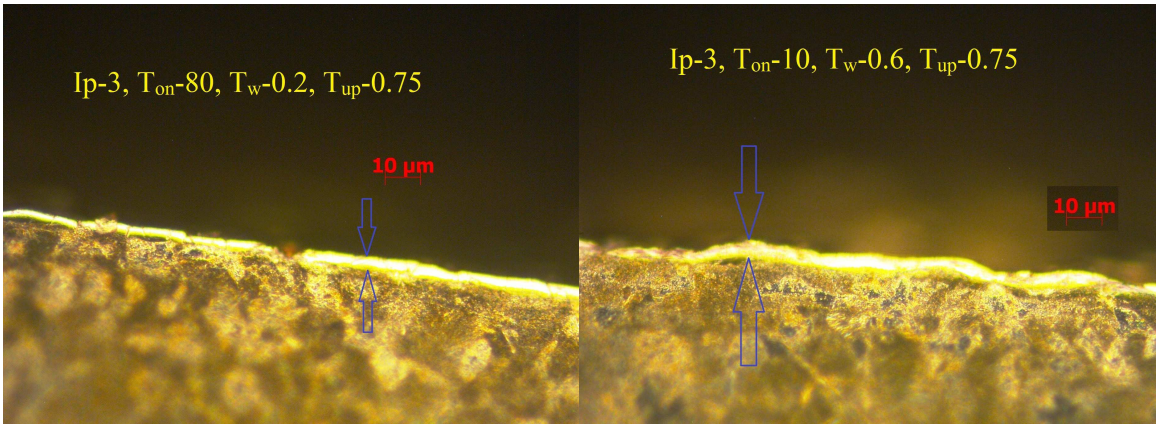

(c) Run no.=12 *(d)* Run no.=13

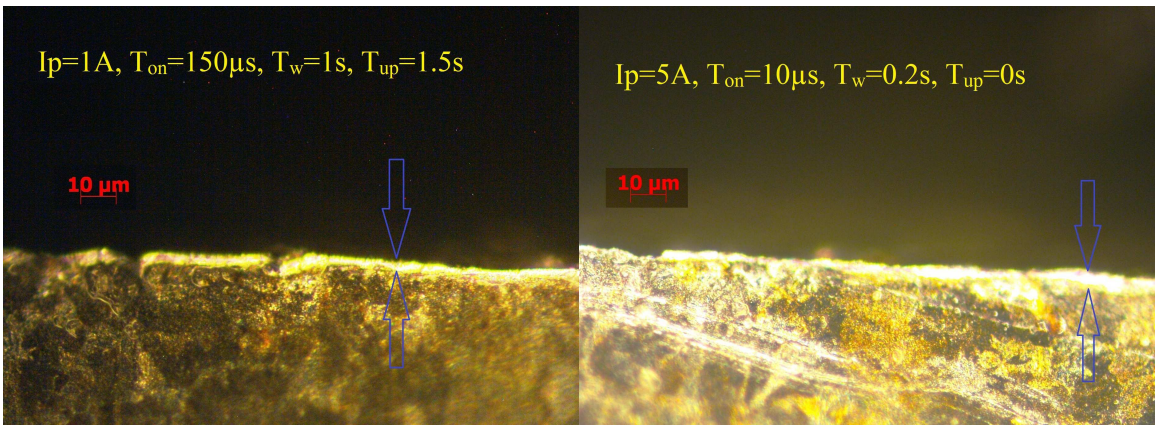

(e) Run no.=21 *(f)* Run no.=29

Fig. 4.22: Representative optical microscopic images of WLT with magnification 400X.

Table 4.23: Analysis of Variance for WLT (After elimination)

Source	DF	Seq SS	Adj SS	Adj MS	F	P
Regression	7	1394.05	1394.05	199.15	49.75	0.000
Linear	4	1339.32	1339.32	334.83	83.64	0.000
Ip	1	1089.04	1089.04	1089.04	272.04	0.000
T_{on}	1	246.01	246.01	246.01	61.45	0.000
T_w	1	3.62	3.62	3.62	0.9	0.352*
T_{up}	1	0.65	0.65	0.65	0.16	0.691*
Square	1	1.78	1.78	1.78	0.44	0.512*
T_{up}* T_{up}	1	1.78	1.78	1.78	0.44	0.512*
Interaction	2	52.95	52.95	26.47	6.61	0.006
Ip* T_{on}	1	37.2	37.2	37.2	9.29	0.006
T_{on}* T_w	1	15.75	15.75	15.75	3.93	0.060*
Residual Error	22	88.07	88.07	4		
Lack-of-Fit	17	63.88	63.88	3.76	0.78	0.685*
Pure Error	5	24.19	24.19	4.84		
Total	29	1482.12				
S = 2.00080 R-Sq = 94.06% R-Sq(adj) = 92.17%						

*=insignificant factor

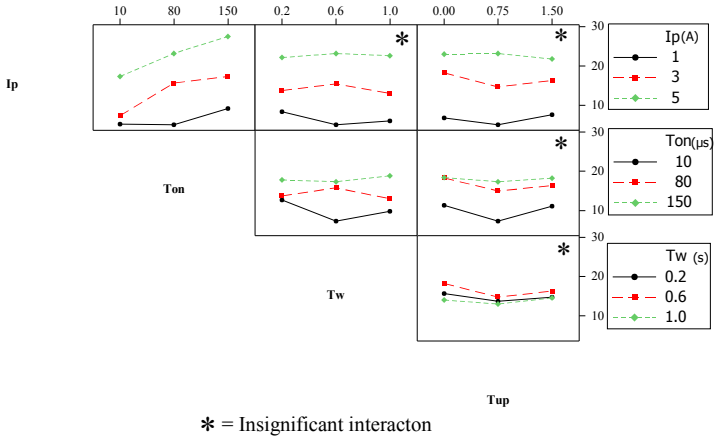

Fig. 4.23: Interaction plots for WLT

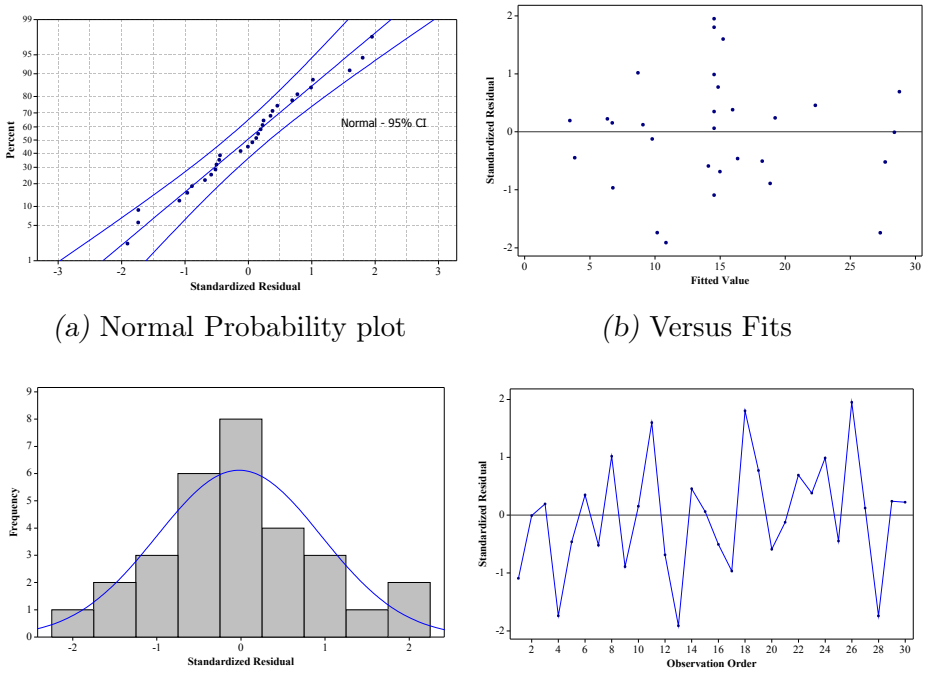

(a) Normal Probability plot *(b)* Versus Fits

(c) Histogram *(d)* Versus Order

Fig. 4.24: Residual plot for WLT

4.3.3 Influence of EDM parameters on SCD

Fig. 4.25 depicts the SEM images of surface cracks formed on the surfaces machined with different parametric combinations. The figure clearly shows that increase in Ip leads to reduction SCD. However, very high T_{on} (*i.e.* 150 μs) combined with lower value of Ip (*i.e.*1 A) (Figure 4.25e) results in severe formation of cracks. The Influence of various machining parameters like Ip, T_{on}, T_w and T_{up} on SCD is presented in Fig. 4.26 in the form of main effect plots. It is evident that the pulse current is inversely proportional to SCD. The decrease in SCD can be attributed to the fact that increase in Ip results in layer thickness of the molten material, which has a tendency to fill the voids thereby decreasing the chance of crack propagation. It is also evident that SCD first decreases with pulse-on time up to an optimum level and then starts increasing. Similar observation was also noted for T_w and T_{up}. At higher pulse-on time (150 μs), WLT is more and the induced stress gets more severe [Lee and Li, 2003] resulting in increase in SCD. ANOVA results (Table 4.24 and 4.25) indicate that the tool lift time is not significant parameter for SCD. But, the Ip^2 and $Ip \times T_{on}$ and $T_{on} \times T_w$ are give the significantly effect on SCD, this is also shown in Fig 4.27.

The normal probability, histogram, fitted value and observation order Vs Standardized residual are shown in the residual plot of SCD (Fig. 4.28). This graph indicates that the developed model is efficient as there is no deviation for normality of the SCD in Fig 4.28a. And no outliers exist in the data in the graph of residual verses fitted value in Fig 4.28b. The Fig 4.28c shows that the data are not skewed and no outliers exist. Residuals versus order of the data specify that there is no significant effect due to time or data collection order as per Fig. 4.28d.

Table 4.24: Analysis of Variance for SCD (Before elimination)

Source	DF	Seq SS	Adj SS	Adj MS	F	P
Blocks	2	0.0013	0.0000	0.0000	0.09	0.918*
Regression	14	0.0166	0.0166	0.0012	22.14	0.000
Linear	4	0.0118	0.0118	0.0029	54.93	0.000
Ip	1	0.0098	0.0098	0.0098	182.92	0.000
T_{on}	1	0.0003	0.0003	0.0003	5.22	0.040
T_w	1	0.0017	0.0017	0.0017	31.57	0.000
T_{up}	1	0.0000	0.0000	0.0000	0.00	0.959*
Square	4	0.0027	0.0027	0.0007	12.61	0.000
Ip*Ip	1	0.0027	0.0013	0.0013	24.78	0.000
T_{on}* T_{on}	1	0.0000	0.0000	0.0000	0.01	0.927*
T_w* T_w	1	0.0000	0.0000	0.0000	0.71	0.414*
T_{up}* T_{up}	1	0.0000	0.0000	0.0000	0.49	0.495*
Interaction	6	0.0021	0.0021	0.0004	6.63	0.002
Ip* T_{on}	1	0.0008	0.0008	0.0008	14.46	0.002
Ip* T_w	1	0.0002	0.0002	0.0002	2.88	0.114*
Ip* T_{up}	1	0.0000	0.0000	0.0000	0.68	0.424*
T_{on}* T_w	1	0.0011	0.0011	0.0011	21.32	0.000
T_{on}* T_{up}	1	0.0000	0.0000	0.0000	0.39	0.544*
T_w* T_{up}	1	0.0000	0.0000	0.0000	0.08	0.778*
Residual Error	13	0.0007	0.0007	0.0001		
Lack-of-Fit	10	0.0006	0.0006	0.0001	1.43	0.425*
Pure Error	3	0.0001	0.0001	0.0000		
Total	29	0.018648				
S = 0.00732191 R-Sq = 96.26% R-Sq(adj) = 91.66%						

*=insignificant factor

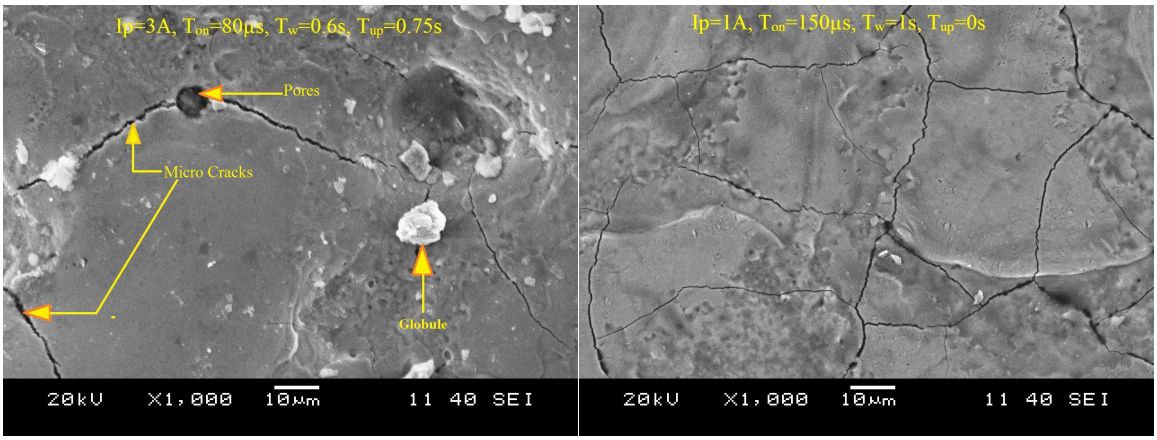

(a) Run no.=1 *(b)* Run no.=4

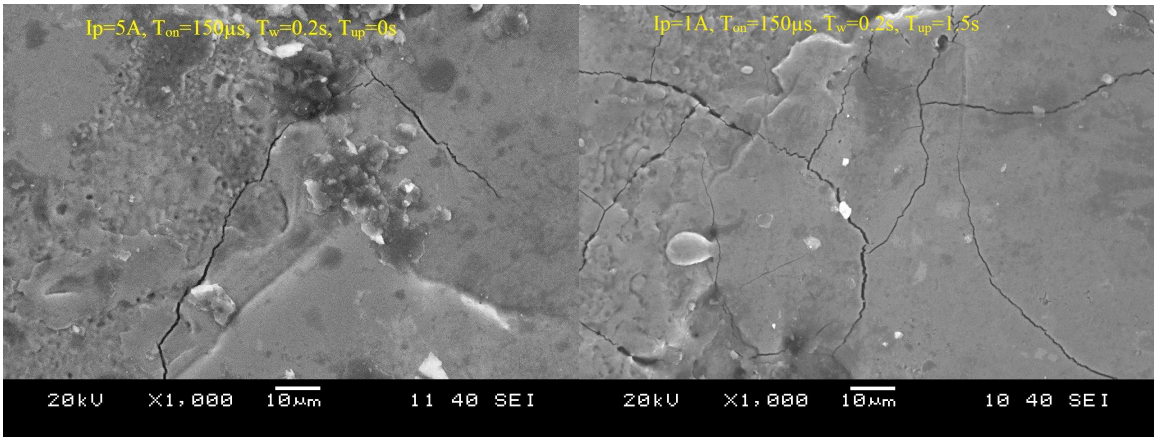

(c) Run no.=7 *(d)* Run no.=8

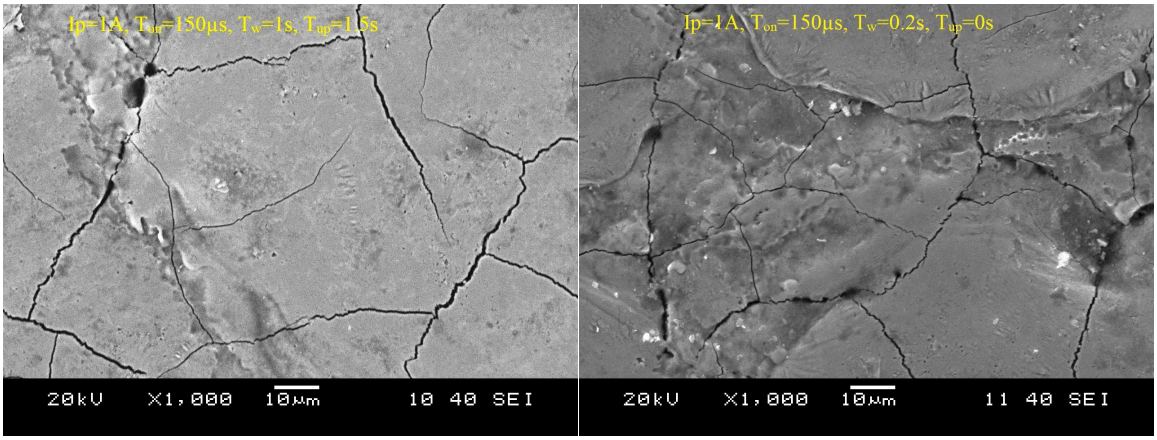

(e) Run no.=21 *(f)* Run no.=27

Fig. 4.25: Representative SCM images of SCD with magnification 1000X.

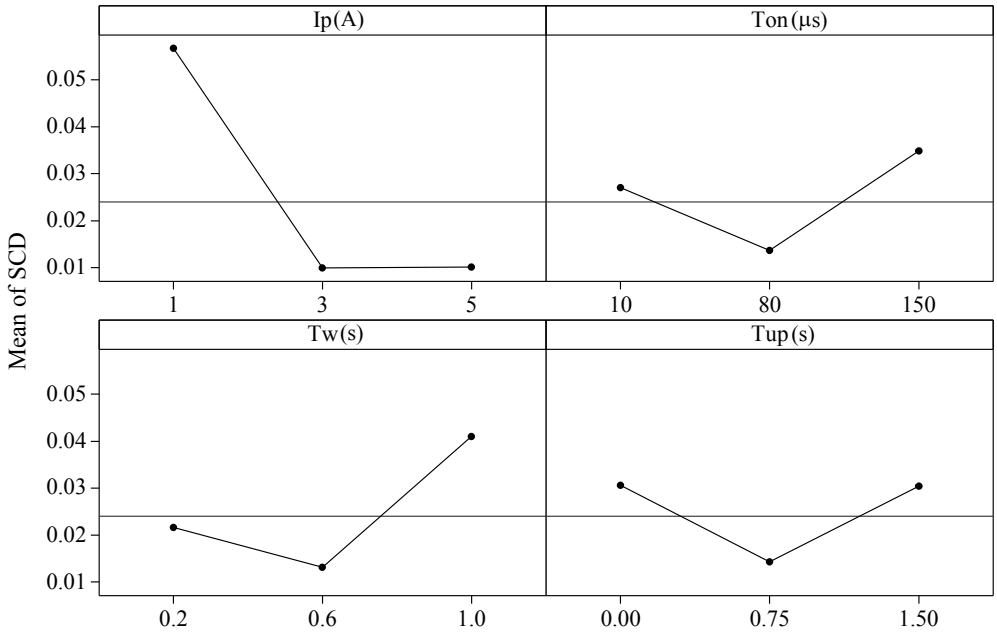

Fig. 4.26: Main effect plots for SCD

Table 4.25: Analysis of Variance for SCD (After elimination)

Source	DF	Seq SS	Adj SS	Adj MS	F	P
Regression	6	0.017673	0.017673	0.002946	69.52	0.000
Linear	3	0.011779	0.011779	0.003926	92.67	0.000
Ip	1	0.009807	0.009807	0.009807	231.46	0.000
T_{on}	1	0.00028	0.00028	0.00028	6.60	0.017*
T_w	1	0.001692	0.001692	0.001692	39.95	0.000
Square	1	0.003976	0.003976	0.003976	93.86	0.000
Ip* Ip	1	0.003976	0.003976	0.003976	93.86	0.000
Interaction	2	0.001918	0.001918	0.000959	22.64	0.000
Ip* T_{on}	1	0.000775	0.000775	0.000775	18.29	0.000
T_{on}* T_w	1	0.001143	0.001143	0.001143	26.98	0.000
Residual Error	23	0.000974	0.000974	0.000042		
Lack-of-Fit	8	0.00056	0.00056	0.00007	2.53	0.058*
Pure Error	15	0.000415	0.000415	0.000028		
Total	29	0.018648				

S = 0.00650902 R-Sq = 94.77% R-Sq(adj) = 93.41%

*=insignificant factor

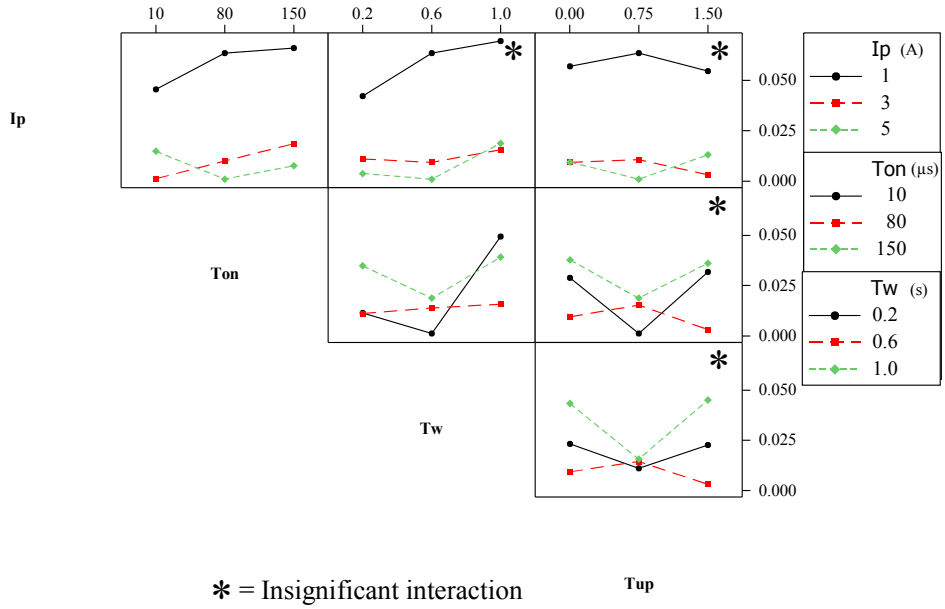

Fig. 4.27: Interaction plots for SCD

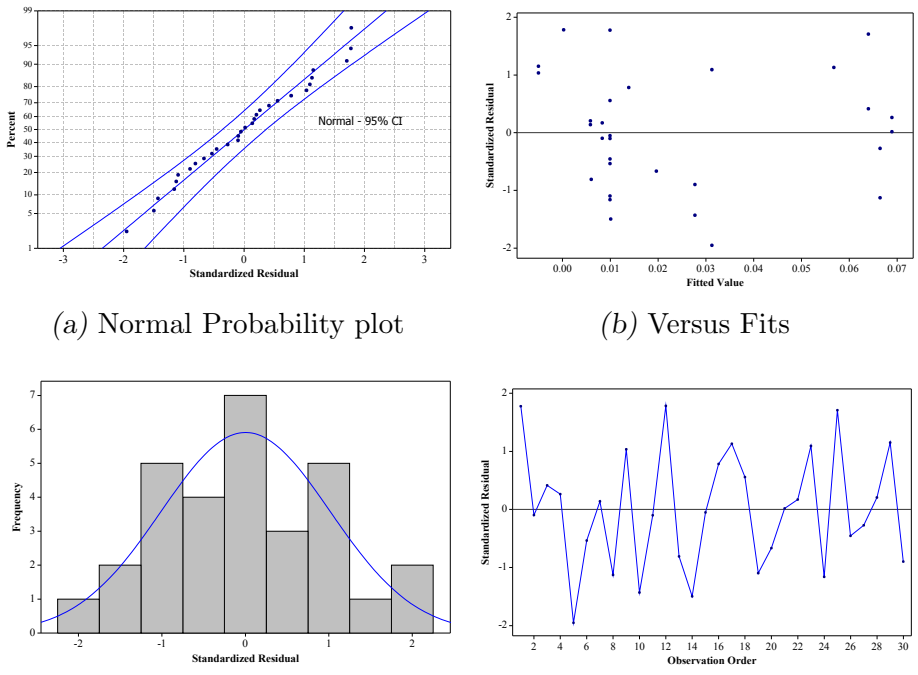

(a) Normal Probability plot *(b)* Versus Fits

(c) Histogram *(d)* Versus Order

Fig. 4.28: Residual plot for SCD

4.3.4 Influence of EDM parameters on SR

The main effect plots of SR are shown in Fig. 4.29. This figure indicates that pulse current has the most significant influence as compared to other factors, because higher pulse current causes more energy to be released for melting leading to formation of cracks and hence resulting a poor surface finish [Guu et al., 2003]. When pulse-on time is increasing SR increases up to a maximum level then it starts to decrease slightly. As the pulse-on time increases, the total energy supplied to the workpiece is more, so more material is eroded from the surface of workpiece resulting in increase of SR. But with higher pulse-on time, the plasma formed between the inter electrode gap hinders energy transfer thus small craters are formed, so SR reduces. Initially with increase in T_{up}, SR increases to a maximum level and later it decrease. High T_{up}, results better flushing, which yield good surface finish. T_w has no significant effect on the surface roughness, as substantiated by ANOVA (Table 4.26).

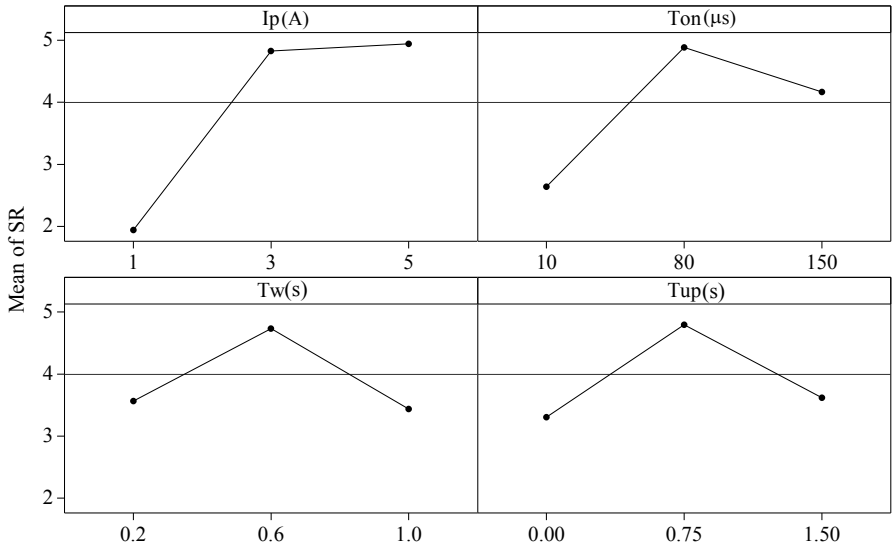

Fig. 4.29: Main effect plots for SR

The insignificant terms were eliminated in the backward elimination process that are shown in Table 4.27. This table indicates that Ip^2 , T_{on}^2 and T_{up}^2 terms are significant and some interaction terms such as $Ip \times T_{on}$, $Ip \times T_{up}$ and $T_{on} \times T_{up}$ also have significant effect on SR as shown in Fig 4.30.

The residual plots of SR are shown in Fig. 4.31. Fig. 4.31a shows the normal probability plot which gives the information that the data are normally distributed

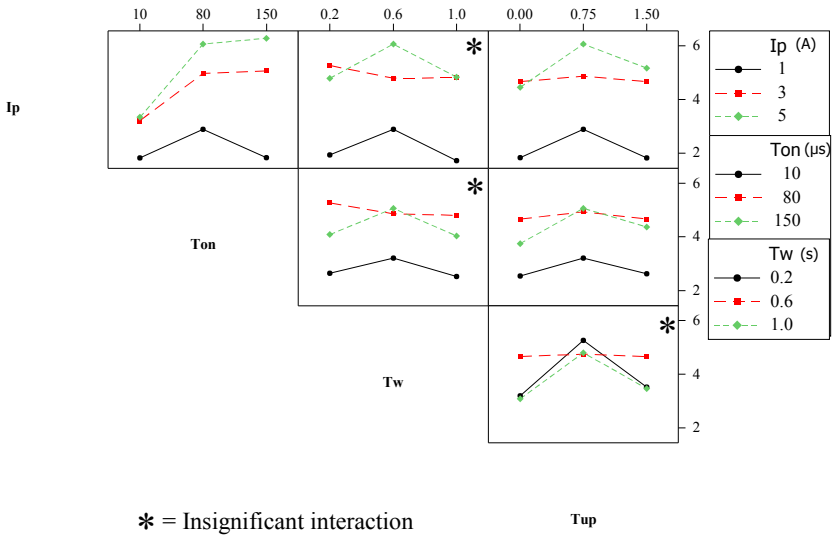

Fig. 4.30: Interaction plots for SR

(confidence level is 95%) .

Residuals versus fitted curve signify that the variance is constant, a non-linear relationship exists in the data as shown in Fig 4.31b. Fig. 4.31c indicates that the histogram of the residual data has no outliers and skewed to right. Residual versus order of the data signifies that there are no systematic error in the data due to time or data collection order as shown in Fig. 4.31d.

Table 4.26: Analysis of Variance for SR (Before elimination)

Source	DF	Seq SS	Adj SS	Adj MS	F	P
Blocks	2	7.8164	0.3044	0.1522	2.97	0.086*
Regression	14	71.0911	71.0911	5.0779	99.19	0.000
Linear	4	51.5209	51.5209	12.8802	251.59	0.000
Ip	1	40.56	40.56	40.56	792.27	0.000
T_{on}	1	10.4424	10.4424	10.4424	203.98	0.000
T_w	1	0.0735	0.0735	0.0735	1.44	0.252*
T_{up}	1	0.4449	0.4449	0.4449	8.69	0.011
Square	4	10.0529	10.0529	2.5132	49.09	0.000
Ip*Ip	1	6.7925	0.6768	0.6768	13.22	0.003
T_{on}* T_{on}	1	2.9747	1.8834	1.8834	36.79	0.000
T_w* T_w	1	0.007	0.0038	0.0038	0.07	0.790*
T_{up}* T_{up}	1	0.2787	0.2787	0.2787	5.44	0.036
Interaction	6	9.5173	9.5173	1.5862	30.98	0.000
Ip* T_{on}	1	8.6289	8.6289	8.6289	168.55	0.000
Ip* T_w	1	0.0743	0.0743	0.0743	1.45	0.250*
Ip* T_{up}	1	0.522	0.522	0.522	10.20	0.007
T_{on}* T_w	1	0.0053	0.0053	0.0053	0.10	0.754*
T_{on}* T_{up}	1	0.2836	0.2836	0.2836	5.54	0.035
T_w* T_{up}	1	0.0033	0.0033	0.0033	0.06	0.803*
Residual Error	13	0.6655	0.6655	0.0512		
Lack-of-Fit	10	0.5371	0.5371	0.0537	1.25	0.477*
Pure Error	3	0.1284	0.1284	0.0428		
Total	29	79.5731				
S = 0.226262 R-Sq = 99.16% R-Sq(adj) = 98.13%						

*=insignificant factor

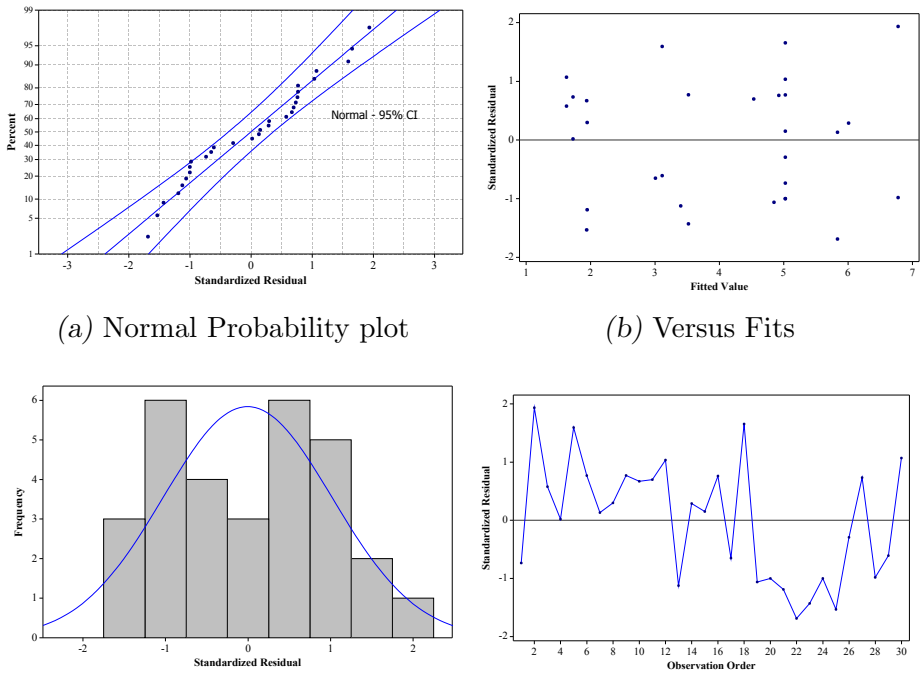

(a) Normal Probability plot *(b)* Versus Fits

(c) Histogram *(d)* Versus Order

Fig. 4.31: Residual plot for SR

Table 4.27: Analysis of Variance for SR (After elimination)

Source	DF	Seq SS	Adj SS	Adj MS	F	P
Regression	9	78.4448	78.4448	8.7161	154.5	0.000
Linear	3	51.4474	51.4474	17.1491	303.99	0.000
Ip	1	40.56	40.56	40.56	718.98	0.000
T_{on}	1	10.4425	10.4425	10.4425	185.11	0.000
T_{up}	1	0.4449	0.4449	0.4449	7.89	0.011
Square	3	17.5629	17.5629	5.8543	103.78	0.000
Ip*Ip	1	13.778	0.7636	0.7636	13.54	0.001
T_{on}* T_{on}	1	3.4689	2.1173	2.1173	37.53	0.000
T_{up}* T_{up}	1	0.316	0.316	0.316	5.6	0.028
Interaction	3	9.4345	9.4345	3.1448	55.75	0.000
Ip* T_{on}	1	8.6289	8.6289	8.6289	152.96	0.000
Ip* T_{up}	1	0.522	0.522	0.522	9.25	0.006
T_{on}* T_{up}	1	0.2836	0.2836	0.2836	5.03	0.036
Residual Error	20	1.1283	1.1283	0.0564		
Lack-of-Fit	5	0.2865	0.2865	0.0573	1.02	0.440*
Pure Error	15	0.8418	0.8418	0.0561		
Total	29	79.5731				
S = 0.237515 R-Sq = 98.58% R-Sq(adj) = 97.94%						

*=insignificant factor

4.3.5 Multi-response optimisation using Fuzzy-TOPSIS method

In this section, TOPSIS method is used to optimize the input parameters on responses WLT, SCD, SR and OC. This method is used in fuzzy environments [Uysal and Tosun, 2012], which fits human thinking under actual environment. The fuzzy linguistic variable were designated using trapezoidal fuzzy number that are shown in Fig. 4.32. These linguistic values are denoted by fuzzy numbers that are shown in Table 4.28. The five decision makers give their decisions of responses for each attribute weight in linguistic term, that are shown in Table 4.29. The average fuzzy weight of the decision makers for each response parameter are shown in the same table.

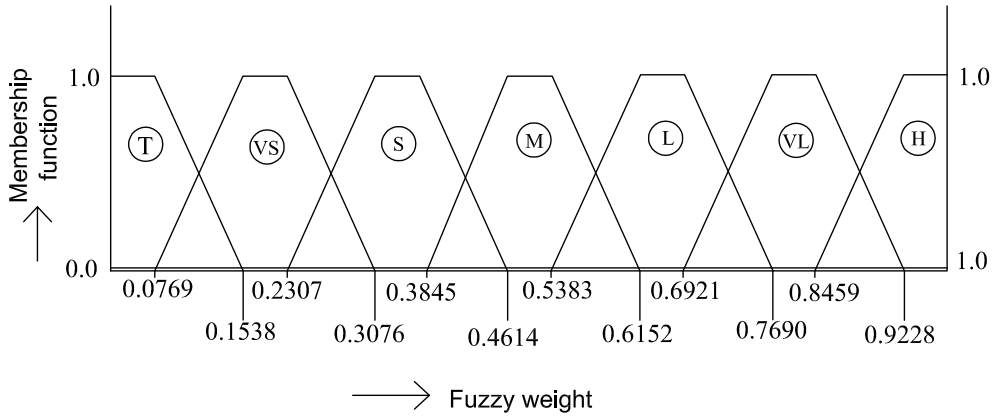

Fig. 4.32: Membership function of responses

Table 4.28: Linguistic variable for the important weight of each output

Fuzzy subset	fuzzy Weight
Tiny (T)	(0.000, 0.000, 0.0769, 0.1538)
Very Small (VS)	(0.0769, 0.1538, 0.2307, 0.3076)
Small (S)	(0.2307, 0.3076, 0.3845, 0.4612)
Medium (M)	(0.3845, 0.4614, 0.5383, 0.6152)
Large (L)	(0.5383, 0.6152, 0.6921, 0.7690)
Very Large (VL)	(0.6921, 0.7690, 0.8459, 0.9228)
Huge (H)	(0.8459, 0.9228, 1.000, 1.000)

In the next step, the normalised matrix (R_{ij}'s), is calculated with the help of Equation 4.8.

Table 4.29: Decision maker for responses with aggregated fuzzy weight

Responses	Decision Maker (DM)					Average fuzzy weight
	DM-1	DM-2	DM-3	DM-4	DM-5	
WLT	VS	S	S	T	S	(0.1538, 0.2153, 0.2922, 0.3691)
SCD	S	VS	VS	S	T	(0.1230, 0.1846, 0.2615, 0.3348)
SR	S	M	S	M	M	(0.3230, 0.3999, 0.4768, 0.5537)
OC	M	S	S	VS	S	(0.2307, 0.3076, 0.3845, 0.4612)

$$R_{ij} = \frac{x_{ij}}{\sqrt{\sum_{j=1}^{30} x_{ij}^2}} \tag{4.8}$$

where x_{ij} is the experimental value of the i^{th} attribute of the j^{th} experimental run. $R'_{ij}s$ are tabulated in Table 4.30.

Then, R_{ij}'s are multiplied by fuzzy weights of each attribute given in table 4.29. The resultant matrix is called the weighted performances matrix (S_{ij}). Tables 4.31 represent the fuzzy weighted performance S_{ij} for WLT and SCD. Where S_{ij} is the weighted performance of i^{th} attributes for j^{th} experimental run. Table 4.32 shows the same for SR and OC. After that, the chosen substitute should have the shortest distance from the Positive Ideal Solution (S^+), *i.e.*, the solution that maximizes the benefit criteria. The minimizes the cost criteria; and the farthest from the Negative Ideal Solution (S^-), *i.e.*, the solution that maximizes the cost criteria and minimizes the benefit criteria. The S^+ and S^- are calculated by following Equation 4.9 & 4.10, and presented in Table 4.33.

$$\begin{aligned} S^+ = [max(S_{ij})]j \in Jor[min(S_{ij})j \in J'], \quad \text{j} = 1, 2, ...30 \\ = (S_1^+, S_2^+, S_3^+, S_4^+) \end{aligned} \tag{4.9}$$

$$\begin{aligned} S^- = [min(S_{ij})]j \in Jor[max(S_{ij})j \in J'], \quad \text{j} = 1, 2, ...30 \\ = (S_1^-, S_2^-, S_3^-, S_4^-) \end{aligned} \tag{4.10}$$

Where J is related to the higher-the-better performance characteristics and J' is related to the lower-the-better performance characteristics. In the present case, all the responses are of lower-the-better type, hence J' is considered. The attributes of

Table 4.30: Normalised response value with CCI

Run	R_{ij}				Closness cofficent		
no.	WLT	SCD	SR	OC	d_j^-	d_j^+	CCI
1	0.138	0.111	0.206	0.205	0.382	0.355	0.518
2	0.316	0.041	0.302	0.226	0.227	0.511	0.308
3	0.042	0.349	0.073	0.008	0.568	0.169	0.771
4	0.083	0.371	0.073	0.243	0.376	0.362	0.509
5	0.174	0.111	0.144	0.108	0.483	0.255	0.654
6	0.169	0.035	0.220	0.195	0.397	0.341	0.538
7	0.299	0.035	0.248	0.224	0.285	0.452	0.387
8	0.114	0.319	0.085	0.021	0.526	0.212	0.713
9	0.194	0.002	0.155	0.309	0.377	0.361	0.510
10	0.077	0.107	0.087	0.118	0.577	0.161	0.782
11	0.203	0.049	0.197	0.191	0.395	0.343	0.535
12	0.153	0.058	0.223	0.168	0.411	0.327	0.557
13	0.081	0.006	0.135	0.218	0.512	0.225	0.695
14	0.258	0.005	0.256	0.191	0.336	0.401	0.456
15	0.163	0.051	0.214	0.201	0.394	0.344	0.534
16	0.192	0.098	0.214	0.226	0.338	0.399	0.459
17	0.055	0.336	0.122	0.031	0.510	0.227	0.692
18	0.200	0.071	0.228	0.163	0.378	0.359	0.513
19	0.181	0.016	0.197	0.214	0.405	0.332	0.550
20	0.145	0.082	0.203	0.141	0.439	0.299	0.595
21	0.107	0.364	0.073	0.147	0.432	0.305	0.586
22	0.332	0.049	0.234	0.224	0.274	0.464	0.371
23	0.184	0.195	0.138	0.179	0.394	0.344	0.534
24	0.183	0.014	0.203	0.187	0.419	0.319	0.568
25	0.035	0.385	0.070	0.131	0.473	0.264	0.642
26	0.203	0.037	0.210	0.186	0.392	0.345	0.532
27	0.103	0.343	0.079	0.144	0.441	0.296	0.598
28	0.274	0.036	0.279	0.226	0.270	0.468	0.366
29	0.218	0.005	0.127	0.201	0.460	0.277	0.624
30	0.074	0.121	0.077	0.048	0.628	0.110	0.851

Table 4.31: Weighted normalized matrix of WLT and SCD

Run no.	S_{ij}	
	WLT	SCD
1	(0.0213, 0.0298, 0.0405, 0.0511)	(0.0136, 0.0204, 0.0290, 0.0375)
2	(0.0485, 0.0679, 0.0922, 0.1165)	(0.0051, 0.0076, 0.0108, 0.0139)
3	(0.0064, 0.0090, 0.0122, 0.0154)	(0.0429, 0.0644, 0.0913, 0.1181)
4	(0.0128, 0.0179, 0.0243, 0.0307)	(0.0456, 0.0684, 0.0969, 0.1254)
5	(0.0267, 0.0374, 0.0508, 0.0642)	(0.0136, 0.0204, 0.0290, 0.0375)
6	(0.0260, 0.0364, 0.0494, 0.0624)	(0.0043, 0.0064, 0.0091, 0.0118)
7	(0.0460, 0.0644, 0.0873, 0.1103)	(0.0043, 0.0064, 0.0091, 0.0118)
8	(0.0176, 0.0246, 0.0334, 0.0422)	(0.0392, 0.0589, 0.0834, 0.1080)
9	(0.0299, 0.0418, 0.0568, 0.0717)	(0.0003, 0.0004, 0.0006, 0.0007)
10	(0.0119, 0.0166, 0.0226, 0.0285)	(0.0131, 0.0197, 0.0279, 0.0360)
11	(0.0312, 0.0437, 0.0593, 0.0749)	(0.0060, 0.0091, 0.0128, 0.0166)
12	(0.0235, 0.0328, 0.0446, 0.0563)	(0.0071, 0.0107, 0.0152, 0.0196)
13	(0.0125, 0.0175, 0.0237, 0.0300)	(0.0007, 0.0011, 0.0015, 0.0020)
14	(0.0396, 0.0555, 0.0753, 0.0951)	(0.0006, 0.0009, 0.0012, 0.0016)
15	(0.0251, 0.0351, 0.0476, 0.0602)	(0.0062, 0.0093, 0.0132, 0.0171)
16	(0.0296, 0.0414, 0.0562, 0.0710)	(0.0121, 0.0181, 0.0256, 0.0332)
17	(0.0085, 0.0119, 0.0162, 0.0204)	(0.0413, 0.0620, 0.0878, 0.1137)
18	(0.0308, 0.0431, 0.0585, 0.0738)	(0.0087, 0.0130, 0.0185, 0.0239)
19	(0.0279, 0.0390, 0.0530, 0.0669)	(0.0020, 0.0030, 0.0043, 0.0055)
20	(0.0222, 0.0311, 0.0422, 0.0534)	(0.0101, 0.0152, 0.0215, 0.0278)
21	(0.0164, 0.0230, 0.0312, 0.0394)	(0.0448, 0.0672, 0.0951, 0.1231)
22	(0.0510, 0.0714, 0.0970, 0.1225)	(0.0060, 0.0090, 0.0127, 0.0164)
23	(0.0283, 0.0396, 0.0538, 0.0679)	(0.0240, 0.0360, 0.0510, 0.0660)
24	(0.0281, 0.0393, 0.0534, 0.0675)	(0.0018, 0.0026, 0.0037, 0.0048)
25	(0.0054, 0.0075, 0.0102, 0.0129)	(0.0473, 0.0711, 0.1007, 0.1303)
26	(0.0313, 0.0438, 0.0594, 0.0750)	(0.0046, 0.0069, 0.0098, 0.0127)
27	(0.0158, 0.0222, 0.0301, 0.0380)	(0.0422, 0.0633, 0.0896, 0.1160)
28	(0.0421, 0.0589, 0.0800, 0.1010)	(0.0045, 0.0067, 0.0095, 0.0123)
29	(0.0335, 0.0469, 0.0637, 0.0804)	(0.0006, 0.0010, 0.0014, 0.0018)
30	(0.0114, 0.0160, 0.0217, 0.0274)	(0.0149, 0.0224, 0.0317, 0.0410)

Table 4.32: Weighted normalized matrix of SR and OC

Run no.	S_{ij}	
	SR	OC
1	(0.0664, 0.0822, 0.0980, 0.1138)	(0.0474, 0.0632, 0.0790, 0.0948)
2	(0.0974, 0.1206, 0.1438, 0.1670)	(0.0521, 0.0694, 0.0868, 0.1041)
3	(0.0236, 0.0293, 0.0349, 0.0405)	(0.0018, 0.0024, 0.0030, 0.0035)
4	(0.0236, 0.0293, 0.0349, 0.0405)	(0.0561, 0.0748, 0.0935, 0.1121)
5	(0.0465, 0.0575, 0.0686, 0.0796)	(0.0250, 0.0333, 0.0416, 0.0499)
6	(0.0711, 0.0880, 0.1049, 0.1218)	(0.0450, 0.0599, 0.0749, 0.0899)
7	(0.0801, 0.0991, 0.1182, 0.1373)	(0.0516, 0.0688, 0.0860, 0.1032)
8	(0.0273, 0.0338, 0.0403, 0.0468)	(0.0048, 0.0064, 0.0080, 0.0096)
9	(0.0500, 0.0619, 0.0738, 0.0857)	(0.0712, 0.0949, 0.1187, 0.1423)
10	(0.0281, 0.0348, 0.0416, 0.0483)	(0.0271, 0.0362, 0.0452, 0.0543)
11	(0.0637, 0.0788, 0.0940, 0.1092)	(0.0441, 0.0587, 0.0734, 0.0881)
12	(0.0719, 0.0890, 0.1061, 0.1232)	(0.0387, 0.0516, 0.0645, 0.0774)
13	(0.0437, 0.0541, 0.0645, 0.0750)	(0.0503, 0.0671, 0.0839, 0.1006)
14	(0.0828, 0.1025, 0.1222, 0.1419)	(0.0441, 0.0587, 0.0734, 0.0881)
15	(0.0691, 0.0856, 0.1021, 0.1185)	(0.0463, 0.0617, 0.0771, 0.0925)
16	(0.0691, 0.0856, 0.1021, 0.1185)	(0.0522, 0.0696, 0.0870, 0.1044)
17	(0.0395, 0.0489, 0.0583, 0.0677)	(0.0071, 0.0095, 0.0119, 0.0142)
18	(0.0738, 0.0914, 0.1089, 0.1265)	(0.0376, 0.0501, 0.0627, 0.0752)
19	(0.0637, 0.0788, 0.0940, 0.1092)	(0.0494, 0.0659, 0.0823, 0.0988)
20	(0.0656, 0.0812, 0.0968, 0.1124)	(0.0325, 0.0433, 0.0541, 0.0649)
21	(0.0236, 0.0293, 0.0349, 0.0405)	(0.0338, 0.0451, 0.0564, 0.0676)
22	(0.0756, 0.0936, 0.1115, 0.1295)	(0.0516, 0.0688, 0.0860, 0.1032)
23	(0.0445, 0.0552, 0.0658, 0.0764)	(0.0414, 0.0552, 0.0690, 0.0827)
24	(0.0656, 0.0812, 0.0968, 0.1124)	(0.0432, 0.0576, 0.0719, 0.0863)
25	(0.0227, 0.0281, 0.0335, 0.0389)	(0.0303, 0.0404, 0.0504, 0.0605)
26	(0.0678, 0.0839, 0.1000, 0.1162)	(0.0430, 0.0573, 0.0716, 0.0859)
27	(0.0254, 0.0315, 0.0375, 0.0436)	(0.0333, 0.0444, 0.0554, 0.0665)
28	(0.0902, 0.1117, 0.1331, 0.1546)	(0.0521, 0.0694, 0.0868, 0.1041)
29	(0.0410, 0.0508, 0.0605, 0.0703)	(0.0463, 0.0617, 0.0771, 0.0925)
30	(0.0249, 0.0308, 0.0367, 0.0426)	(0.0111, 0.0148, 0.0185, 0.0222)

Table 4.33: Positive and negative ideal value

		S_i^+ and S_i^-
WLT	S_1^-	(0.0510, 0.0714, 0.0970, 0.1225)
	S_1^+	(0.0054, 0.0075, 0.0102, 0.0129)
SCD	S_2^-	(0.0473, 0.0711, 0.1007, 0.1303)
	S_2^+	(0.0003, 0.0004, 0.0006, 0.0007)
SR	S_3^-	(0.0974, 0.1206, 0.1438, 0.1670)
	S_3^+	(0.0227, 0.0281, 0.0335, 0.0389)
OC	S_4^-	(0.0712, 0.0949, 0.1187, 0.1423)
	S_4^+	(0.0018, 0.0024, 0.0030, 0.0035)

S_{ij} is a normalised positive trapezoidal fuzzy number with the range of zero to one.

After calculating the S_{ij} matrix, the next step is to finding the distance of positive ideal solutions (d_j^+) and negative ideal solutions (d_j^-) by using Equation 4.11 and 4.12.

$$d_j^+ = \sum_{i=1}^{4} d(S_{ij}, S_j^+), \quad \text{j} = 1, 2, ...30 \tag{4.11}$$

$$d_j^- = \sum_{i=1}^{4} d(S_{ij}, S_j^-), \quad \text{j} = 1, 2, ...30 \tag{4.12}$$

$$d(x, y) = \sqrt{\frac{1}{4}[(x_1 - y_1)^2 + ... + (x_4 - y_4)^2]} \tag{4.13}$$

Where d(x,y) is the distance between two fuzzy numbers. This distance of two trapezoidal fuzzy number is calculated using the Equation 4.13. The value of d_j^+ and d_j^- are shown in previous table 4.30. The Closeness Coefficient (CCI), which is calculated by Equation 4.14. This CCI value indicates the closeness of each experimental value to the ideal solution, which are shown in same table 4.30.

$$CCI = \frac{d_j^-}{d_j^+ + d_j^-} \tag{4.14}$$

4.3.6 Optimum parameters setting for EDM process using fuzzy-TOPSIS

Higher the closeness coefficient value indicates better performances, hence, the machining parameters with the greatest closeness coefficient will indicate optimal combination. According to the main effect plot for CCI (shown in Fig. 4.33), the following factor settings have been identified as the best combination of process parameter: I_p= 1A (level '1'), T_{on} = 10μs (level '1'), T_w = 0.2s (level '1'), and T_{up} = 1.5s (level '3'). The mean value of CCI for each level of the machining parameters is tabulated in Table 4.34.

Five decision makers (DM) give their preferences on the responses (WLT, SCD, SR and OC), then the optimal results were computed. A sensitivity analysis is performed in the next section to find if DMs change their preferences, how it might effect the optimal results.

Table 4.34: Response table for mean of CCI

Level	Ip	T_{on}	T_w	T_{up}
1	0.6826	0.6736	0.5987	0.5669
2	0.5605	0.5597	0.5599	0.5696
3	0.4678	0.4775	0.5521	0.5765

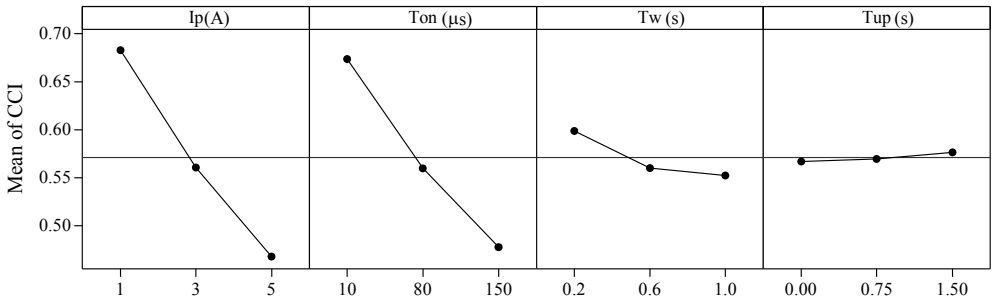

Fig. 4.33: Mean graph of CCI

4.3.7 Sensitivity analysis

The exploration of sensitivity of DMs preferences on the optimal parameters will be of paramount interest. In order to reduce the complexity of the test, it is assumed that all the five DMs give the same preferences for each of the response from among the fuzzy linguistic values that are given in table 4.29. A full factorial experiment design is considered that yield a total of 54 combinations of DM judgements that are possible, which is summarized in Table 4.35. The Fuzzy-TOPSIS technique is applied on all of these 54 combination of DM judgements and the optimal levels of Ip ($Opt\ Ip$), T_{on} ($Opt\ T_{on}$), T_w ($Opt\ T_w$) and T_{up} ($Opt\ T_{up}$) are obtained, which are shown in the same table.

Table 4.35: Sensitivity analysis result

Sl.	All Decision Maker preferences				Optimal level			
No.	Pre-WLT	Pre-SCD	Pre-SR	Pre-OC	$Opt\ Ip$	$Opt\ T_{on}$	$Opt\ T_w$	$Opt\ T_{up}$
1	T	T	S	VS	1	1	1	3
2	T	T	S	S	1	1	1	3
3	T	T	S	M	1	1	1	3
4	T	T	M	VS	1	1	1	1

Continued on next page

Table 4.35: *Sensitivity analysis result*

Sl.	All Decision Maker preferences				Optimal level			
No.	Pre-WLT	Pre-SCD	Pre-SR	Pre-OC	*Opt Ip*	*Opt* T_{on}	*Opt* T_w	*Opt* T_{up}
5	T	T	M	S	1	1	1	3
6	T	T	M	M	1	1	1	3
7	T	VS	S	VS	1	1	1	3
8	T	VS	S	S	1	1	1	3
9	T	VS	S	M	1	1	1	3
10	T	VS	M	VS	1	1	1	3
11	T	VS	M	S	1	1	1	3
12	T	VS	M	M	1	1	1	3
13	T	S	S	VS	2	1	1	2
14	T	S	S	S	2	1	1	2
15	T	S	S	M	1	1	1	2
16	T	S	M	VS	1	1	1	1
17	T	S	M	S	1	1	1	3
18	T	S	M	M	1	1	1	3
19	VS	T	S	VS	1	1	1	3
20	VS	T	S	S	1	1	1	3
21	VS	T	S	M	1	1	1	3
22	VS	T	M	VS	1	1	1	1
23	VS	T	M	S	1	1	1	3
24	VS	T	M	M	1	1	1	3
25	VS	VS	S	VS	1	1	1	3
26	VS	VS	S	S	1	1	1	3
27	VS	VS	S	M	1	1	1	3
28	VS	VS	M	VS	1	1	1	3
29	VS	VS	M	S	1	1	1	3
30	VS	VS	M	M	1	1	1	3
31	VS	S	S	VS	2	1	1	2

Continued on next page

Table 4.35: *Sensitivity analysis result*

Sl.	All Decision Maker preferences				Optimal level			
No.	Pre-WLT	Pre-SCD	Pre-SR	Pre-OC	*Opt Ip*	*Opt* T_{on}	*Opt* T_w	*Opt* T_{up}
32	VS	S	S	S	1	1	1	2
33	VS	S	S	M	1	1	1	2
34	VS	S	M	VS	1	1	1	2
35	VS	S	M	S	1	1	1	3
36	VS	S	M	M	1	1	1	3
37	S	T	S	VS	1	1	1	3
38	S	T	S	S	1	1	1	3
39	S	T	S	M	1	1	1	3
40	S	T	M	VS	1	1	1	1
41	S	T	M	S	1	1	1	3
42	S	T	M	M	1	1	3	3
43	S	VS	S	VS	1	1	1	3
44	S	VS	S	S	1	1	1	3
45	S	VS	S	M	1	1	1	3
46	S	VS	M	VS	1	1	1	3
47	S	VS	M	S	1	1	1	3
48	S	VS	M	M	1	1	1	3
49	S	S	S	VS	1	1	1	2
50	S	S	S	S	1	1	1	2
51	S	S	S	M	1	1	1	2
52	S	S	M	VS	1	1	1	2
53	S	S	M	S	1	1	1	3
54	S	S	M	M	1	1	1	3

In table 4.21, the '0' value in column 'pt type' indicates the central points. The responses WLT, SCD, SR and OC of these experimental runs are used to calculate CCI values for all 54 combination of DM judgements. The ANOVA of CCI values is

tabulated in Table 4.36, which confirmed that 77.49% contribution of CCI values is due to the DMs preferences on SCD (Pre-SCD). The contribution of DMs preferences on other responses are 4.61%, 2.04% and 0.23% for OC, SR and WLT, respectively. The Pre-SCD has utmost change on CCI as compare to other DMs preferences that are displayed in same ANOVA table, so the DMs should choose the preferences of SCD very carefully.

Table 4.36: ANOVA for CCI value of centre point

Source	DF	Seq SS	Adj MS	F	P	% Contribution
Pre-WLT	2	0.00155	0.00078	1.91	0.150*	0.23
Pre-SCD	2	0.52736	0.26368	649.05	0.000	77.49
Pre-SR	1	0.01386	0.01386	34.12	0.000	2.04
Pre-OC	2	0.03137	0.01569	38.61	0.000	4.61
Error	262	0.10644	0.00041			
Total	269	0.68058				

*= insignificant factor

ANOVA on the optimal levels of *Opt Ip*, *Opt* T_w and *Opt* T_{up} are calculated and presented in Table 4.37. There is no change of *Opt* T_{on} with DMs preferences, so no ANOVA can be calculated. Hence, the *Opt* T_{on} column in Table 4.37 is omitted. Pre-WLT is not affecting the optimal levels of any parameter, *i.e.* the *Opt Ip*, *Opt* T_w and *Opt* T_{up}. Pre-SCD have significant effect on *Opt Ip* and *Opt* T_{up}, but not effecting the *Opt* T_w. Pre-SR have significant effect the *Opt Ip* only, but not effecting any other optimal parameters. Pre-OC have no significant effect on any other parameter except the *Opt* T_{up}. The interaction of Pre-SCD×Pre- SR is found to be significant for the *Opt Ip* and *Opt* T_{up}, whereas, the interaction of Pre-SCD×Pre-OC is found to be significant for the *Opt* T_{up}. The interaction of Pre-SR×Pre-OC is found to be significant for the *Opt* T_{up} and no other two factor interactions are found to be significant. It can be suggested that the DMs should choose the SCD first and foremost with utter caution as its % contribution to CCI is the highest. The Pre-SCD is effecting *Opt Ip* and *Opt* T_{up} and its preference combination with Pre-SR and Pre-OC are also important.

The *Opt Ip* verses DMs preferences are plotted in Fig. 4.34a and it can be concluded that *Opt Ip* is level '1' for most of the DMs judgements. The optimal results obtained for the example shown in Section 4.3.6 has 100%, 100% and 83.33% match-

Table 4.37: Abridge ANOVA for optimum level of Ip, T_w and T_{up}

		Opt Ip		Opt T_w		Opt T_{up}	
Source	DF	F	P	F	P	F	P
Pre-WLT	2	1.56	0.229*	1.00	0.381*	0.21	0.815*
Pre-SCD	2	4.67	0.018	1.00	0.381*	26.15	0.000
Pre-SR	1	4.67	0.039	1.00	0.326*	0.21	0.654*
Pre-OC	2	1.56	0.229*	1.00	0.381*	20.59	0.000
Pre-WLT×Pre-SCD	4	1.56	0.214*	1.00	0.424*	0.21	0.933*
Pre-WLT×Pre-SR	2	1.56	0.229*	1.00	0.381*	0.21	0.815*
Pre-WLT×Pre-OC	4	0.78	0.549*	1.00	0.424*	0.21	0.933*
Pre- SCD×Pre-SR	2	4.67	0.018	1.00	0.381*	18.74	0.000
Pre- SCD×Pre-OC	4	1.56	0.214*	1.00	0.424*	5.76	0.000
Pre- SR× Pre-OC	2	1.56	0.229*	1.00	0.381*	20.59	0.000
Error	28						
Total	53						

*= insignificant factor

ing results with Pre-SCD 'Tiny', 'Very Small' and 'Small', respectively, which is also marked in the same figure. Whereas, the *Opt* T_{on} is level '1' for any DMs preferences as shown in Fig. 4.34b, and this is 100% matching with results of the example. Fig. 4.34c shows that whatever the decision makers prefer, the optimal T_w is level '1', except for one DM judgement combination. But, *Opt* T_{up} varies with the DMs judgements widely and show an erratic pattern which is described Fig. 4.34d. The optimal results of the example has 83.33%, 100% and 66.66% matching with Pre-SCD 'Tiny', 'Very Small' and 'Small', respectively.

There is 70.37% overall matching of the optimal results of the example shown in Section 4.3.6 [Awasthi et al., 2010] with fifty four various combinations of DM judgements.

4.3.8 Conclusions

In the present work, surface integrity and dimensional accuracy of AISI P20 grade tool steel after EDM have been investigated followed by multi-response optimisation using fuzzy- TOPSIS method. The following conclusions may be drawn from the current study:

1. Both Ip and T_{on} are directly proportional to WLT. The T_w and T_{up} have no significant influence on WLT.

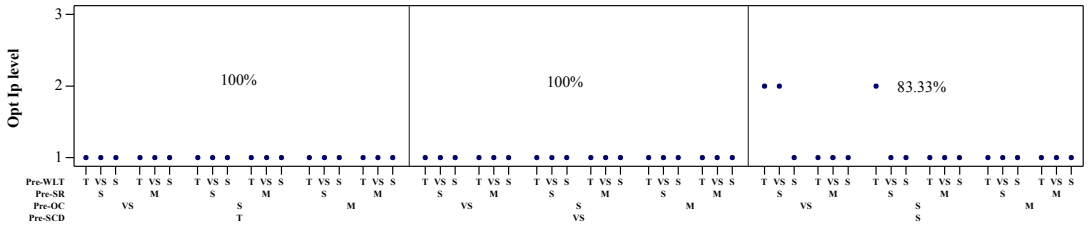

(a) Opt Ip

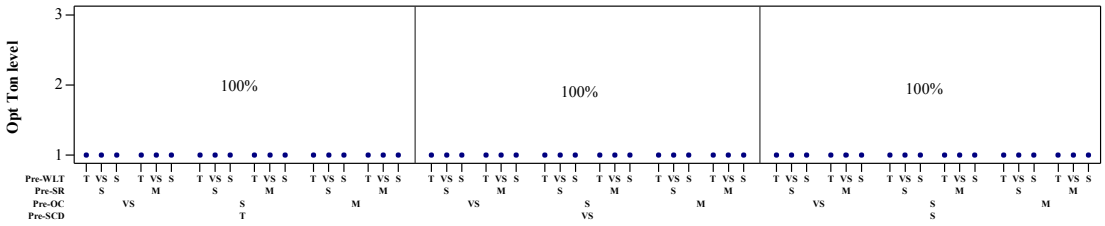

(b) Opt T_{on}

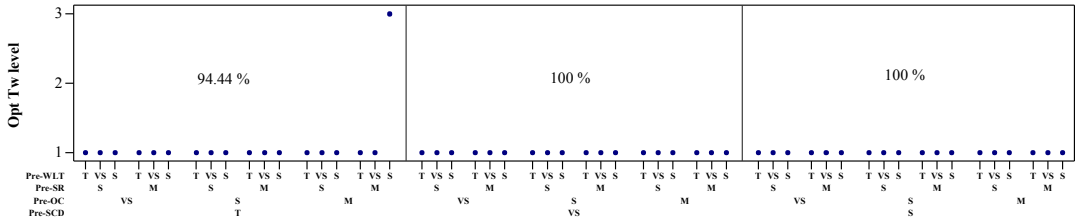

(c) Opt T_w

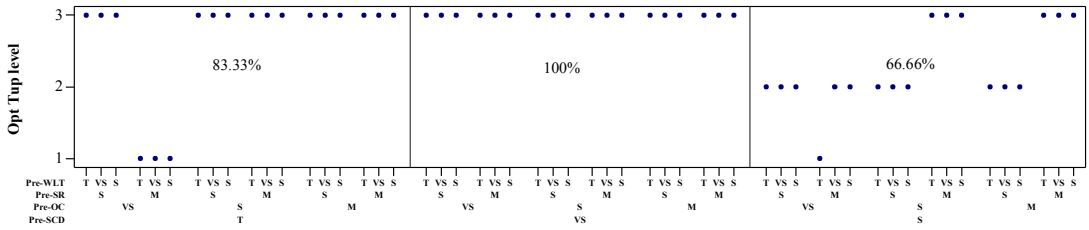

(d) Opt T_{up}

Fig. 4.34: Individual plots of (a) Opt Ip (b) Opt T_{on} (c) Opt T_w (d) Opt T_{up}

2. The pulse current is inversely proportional to SCD. With increase in T_w, the SCD decreases up to an optimum level and then starts increasing. Ton should also be selected so as to achieve minimum SCD. However, T_{up} has no significant effect on SCD.

3. SR initially increases with T_{up} up to a particular level then starts decreasing with further T_{up}, whereas T_w has been found to be an insignificant parameter under the given operating condition.

4. Higher pulse current and pulse duration have detrimental influence on the dimensional accuracy (OC).

5. The optimum setting of process parameters of Ip= 1A, T_{on}=10μs, T_w=0.2s and T_{up}=1.5s based on the decision makers' preferences on the four responses has been achieved.

6. The sensitivity test shows that the decision makers' preferences of SCD and SR are significant for optimal pulse current, whereas the preferences of the responses SCD and OC are significant for optimal tool lift time.

7. The optimal levels of tool work time and pulse-on time are not affected by any decision makers' preferences on any of the responses.

8. The decision makers' preferences of SCD is most important and should be chosen first and very carefully followed by the preferences of OC and SR, whereas preference of WLT has no consequence on the optimal values of the parameters.

9. Therefore, the Fuzzy-based TOPSIS has been found to be an effective technique for simultaneous optimization of multiple responses among contradicting inter relationship between input and output parameters and to finally recommend an optimal parametric combination for best performance in terms of surface integrity and dimensional accuracy during EDM of AISI P20 grade tool steel.

4.4 Influence of different tool electrode materials on EDMed surface integrity and dimensional accuracy of AISI P20 tool steel

The present work aims at investigating the effect of different different tool electrode materials *i.e.* (brass, copper and graphite) as well as EDM process variables (Ip , T_{on}, Tau and P) on different characteristics of surface integrity such as SR, WLT and SCD and dimensional accuracy.

4.4.1 Experimental set-up and planing

In this study, a mixed level L_{18} OA based on Taguchi design has been used to investigate the influence of four EDM process variables (Ip , T_{on}, Tau and P) on SR, SCD, WLT and OC. Since the DOE involves four factors, three of which having three levels each with remaining one having two levels, the total number of eighteen experiments for each tool material has been planed. Both control and fixed variables along with their corresponding levels and values are provided in Table 4.38.

Table 4.38: Machining variables and their levels

Control variables				
Parameter	Levels			Unit
	1	2	3	
Discharge current (Ip)	2	5	8	A
Pulse on Time (T_{on})	50	75	100	μs
Duty Cycle (Tau)	75	85	95	%
Polarity	+	-		
Fixed variables				
Voltage (V)		45		V
Sensitivity		6		
Inter Electrode Gap		90		μ
Tool work time		0.6		s
Tool lift time		0.3		s
Flushing presser (Fp)		0.3		Kgf/cm^2

AISI P20 tool steel was machined used with EDM after heat treatment, which has been described in section 3.1. The cylindrical shaped tool electrodes (copper, brass, graphite), having 12 mm diameter were selected, as shown in Fig. 4.35. For each experiment run, machining was done for 30 min. and various responses were measured.

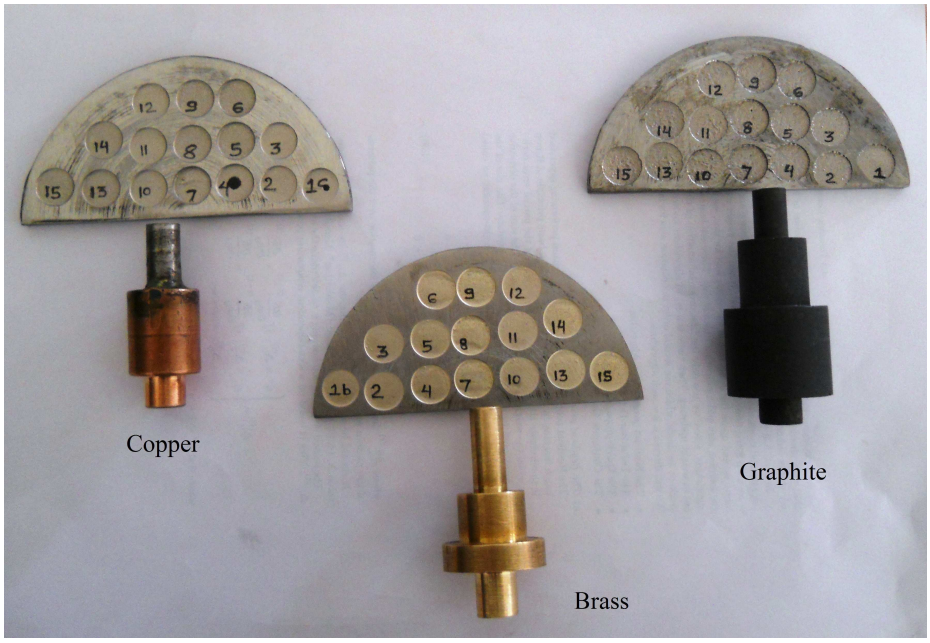

Fig. 4.35: Workpiece and three different tool materials

Methodology for measurement of various performance measures (SR, SCD, WLT and OC) has been described in section 3. The various data pertaining to different tool materials obtained for calculation of SCD and WLT are provided in Table 4.39. The detailed experimental results are tabulated in Table 4.40 and 4.41 along with the machining parameters.

Table 4.39: Relevant data for different tool materials for calculation of WLT and SCD

Run no.	Crack length (μm)									Area of WL (μm^2)		
	Brass			Copper			Graphite			Brass	Copper	Graphite
	1st	2nd	3rd	1st	2nd	3rd	1st	2nd	3rd			
1	250.69	195.50	381.36	453.95	362.70	482.65	468.46	565.00	386.35	2639.39	4864.56	996.36
2	191.61	101.36	236.28	308.81	356.63	329.26	400.00	356.00	305.00	2772.23	5430.11	1154.85
3	283.05	115.14	191.13	339.90	368.46	416.70	704.16	567.95	316.99	3652.26	5524.69	979.02
4	0.00	18.65	56.62	356.24	215.72	70.60	22.00	25.00	29.00	5369.31	5859.55	4114.61
5	24.10	0.00	15.32	214.72	203.69	116.66	112.59	174.69	217.27	4663.78	6503.83	4570.42
6	0.00	0.00	71.68	63.00	105.30	396.36	417.87	275.49	227.64	6101.98	6518.22	5374.75
7	35.61	70.81	0.00	236.62	256.06	197.76	377.00	335.00	378.00	5456.27	6978.96	7067.13
8	20.00	40.00	10.30	0.00	86.30	139.23	150.00	130.00	175.00	5790.61	7249.35	8162.14
9	20.00	25.00	82.00	0.00	180.36	250.69	408.23	510.89	612.83	6441.78	7556.36	9988.14
10	312.25	263.39	223.58	311.10	294.53	274.99	438.00	301.00	330.00	2155.32	4731.96	1151.96
11	185.23	146.16	206.15	220.40	207.03	306.02	503.11	299.43	91.71	2550.16	4842.48	2116.71
12	328.61	239.70	207.61	312.96	334.99	325.56	342.25	486.79	370.50	3063.39	5203.19	2240.55
13	0.00	87.12	92.06	93.76	104.72	62.15	285.00	330.00	335.00	3215.23	4813.16	3121.61
14	50.00	35.00	34.00	114.40	0.00	0.00	336.67	30.86	73.30	3366.85	5224.87	4178.95
15	29.00	33.00	40.00	0.00	46.30	99.75	116.20	328.87	288.11	4239.87	5595.82	5177.27
16	41.42	38.49	22.03	98.36	0.00	156.76	225.00	333.00	300.00	3754.49	5989.81	7558.94
17	19.00	25.00	23.00	0.00	145.36	95.36	478.62	595.00	502.00	3859.18	6807.23	7916.67
18	35.00	39.00	44.00	145.36	123.36	169.36	601.00	590.00	615.00	4605.02	6894.20	8594.76

Table 4.40: Experimental results of SCD and WLT corresponding to different input parameters

Run no.	P	Ip (A)	T_{on} (μm)	Tau (%)	SCD ($\mu m/\mu m^2$)			WLT(μm)		
					Brass	Copper	Graphite	Brass	Copper	Graphite
1	-	2	50	75	0.0231	0.0352	0.0385	13.663	25.181	5.158
2	-	2	75	85	0.0148	0.027	0.0288	14.351	28.109	5.978
3	-	2	100	95	0.0164	0.0305	0.0431	18.906	28.599	5.068
4	-	5	50	85	0.0021	0.0174	0.0021	27.794	30.332	21.299
5	-	5	75	95	0.0011	0.0145	0.0137	24.142	33.667	23.659
6	-	5	100	75	0.002	0.0153	0.025	31.587	33.742	27.822
7	-	8	50	75	0.003	0.0187	0.0296	28.244	36.127	36.583
8	-	8	75	85	0.002	0.0061	0.0124	29.975	37.526	42.251
9	-	8	100	95	0.0035	0.0117	0.0415	33.346	39.116	51.704
10	+	2	50	95	0.0223	0.0239	0.029	11.157	24.495	5.963
11	+	2	75	75	0.015	0.0199	0.0242	13.201	25.067	10.957
12	+	2	100	85	0.0217	0.0264	0.0325	15.858	26.934	11.598
13	+	5	50	95	0.005	0.0071	0.0257	16.644	24.915	16.159
14	+	5	75	75	0.0033	0.0031	0.012	17.429	27.047	21.632
15	+	5	100	85	0.0028	0.004	0.0199	21.948	28.967	26.800
16	+	8	50	85	0.0029	0.0069	0.0232	19.435	31.006	39.129
17	+	8	75	95	0.0019	0.0065	0.0427	19.977	35.238	40.981
18	+	8	100	75	0.0033	0.0119	0.049	23.838	35.688	44.491

Table 4.41: Experimental results of SR and OC corresponding to different input parameters

Run no.	P	Ip (A)	T_{on} (μm)	Tau (%)	SR (μm)			OC (mm)		
					Brass	Copper	Graphite	Brass	Copper	Graphite
1	-	2	50	75	2.170	3.800	5.333	0.183	0.046	0.013
2	-	2	75	85	2.460	4.933	8.000	0.262	0.091	0.112
3	-	2	100	95	2.790	4.266	7.467	0.356	0.159	0.145
4	-	5	50	85	3.020	4.800	7.467	0.410	0.609	0.254
5	-	5	75	95	3.370	5.530	10.333	0.426	0.658	0.326
6	-	5	100	75	3.460	4.920	9.100	0.690	0.700	0.298
7	-	8	50	75	3.600	4.766	9.200	0.710	0.669	0.362
8	-	8	75	85	3.900	6.260	11.767	0.980	0.699	0.413
9	-	8	100	95	4.000	6.160	11.533	1.283	0.752	0.399
10	+	2	50	95	2.810	4.000	9.467	0.156	0.240	0.047
11	+	2	75	75	2.680	4.200	9.600	0.236	0.299	0.068
12	+	2	100	85	2.810	4.193	9.333	0.493	0.338	0.114
13	+	5	50	95	3.200	5.466	9.000	0.465	0.580	0.130
14	+	5	75	75	2.840	6.600	10.467	0.696	0.652	0.207
15	+	5	100	85	3.130	6.400	9.560	0.865	0.740	0.234
16	+	8	50	85	3.720	7.600	12.133	1.412	0.714	0.378
17	+	8	75	95	3.850	8.400	13.567	1.695	0.744	0.390
18	+	8	100	75	4.200	8.000	12.633	1.855	0.760	0.437

4.4.2 Effect of EDM parameters on SR for different tool materials

The main effect plots for SR as the function of different EDM parameters (Ip , T_{on}, Tau and P) corresponding to different tool material are shown in Fig. 4.36. The figure clearly indicates that negative polarity is suitable for copper and graphite electrodes, while the brass electrode is not affected the polarity

Fig. 4.36 also clearly indicates that the discharge current is the most influencing parameter as compared to other factors for all there electrode materials. The same figure also shows that the higher SR was obtained with graphite tool as compared to brass and copper electrodes. Due to the lower thermal conductivity of graphite, temperature is high at the sparking point of the workpiece. Hence, more material is eroded from the surface resulting in poor surface finish.

When pulse-on time increases, initially there is slightly increase in SR and then it decreases slightly for all three electrode materials. It is also evident that SR is not affected by pulse-on time for copper and brass electrode. However, pulse-on time has significant influence on SR while machining with graphite tool. This is also

confirmed by the results of abridged ANOVA Table 4.42. In ANOVA table, only the source of variation, DF, P statics and % contribution columns are presented for subtle comparison of significant factors for the three tool materials. Table 4.42 also signifies SR is not affected by duty cycle for any of the three electrode materials.

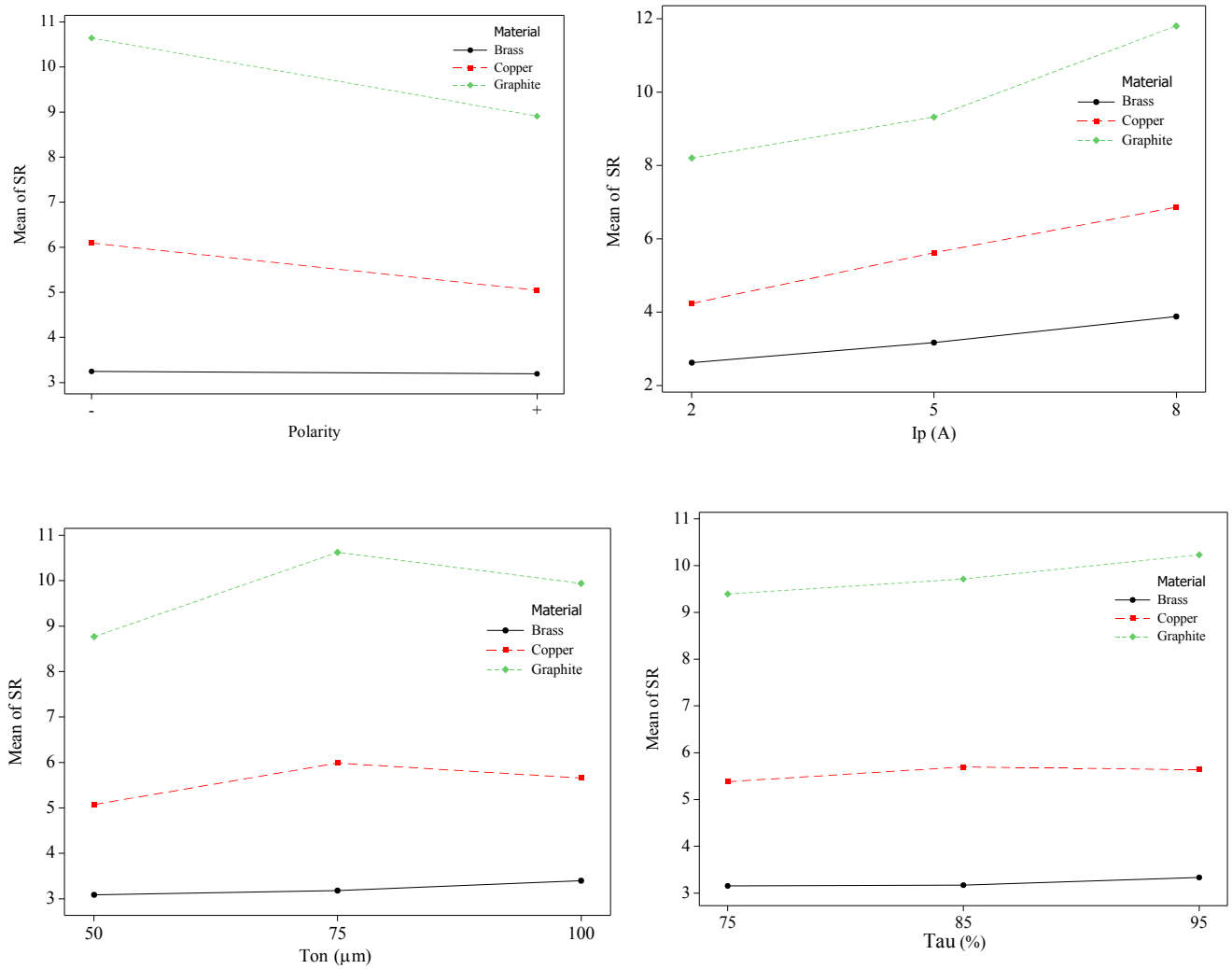

Fig. 4.36: Main effect plots for SR with different electrode materials

Table 4.42: Abridged ANOVA for SR with the three electrode material

Source		Brass		Copper		Graphite	
of variation	DF	P	% cont.	P	% cont.	P	% cont.
P	1	0.581*	0.22	0.011	14.61	0.000	18.88
Ip	2	0.000	85.45	0.000	61.63	0.000	57.35
T_{on}	2	0.052*	5.47	0.129*	7.63	0.002	14.83
T_{au}	2	0.258*	2.10	0.725*	1.00	0.128*	3.02
Residual Error	10		6.76		15.11		5.92
Total	17						

* = Insignificant at 95%

4.4.3 Effect of EDM parameters on OC for different tool materials

The OC is calculated by half the difference between the sizes of the cavity and the diameter of the tool in EDM process with the help of Equation 3.3.

Minimum over cut is always desirable for good dimensional accuracy in EDM. The effect of various machining parameters on OC are presented in the main effect plots shown in Fig. 4.37. This figure presents that the polarity has significant influence on OC with copper and brass tool, but not with graphite. Brass exhibited poor dimensional accuracy by resulting in higher OC as compared to graphite and copper. The OC is low due to the fact that at low current brass with reverse polarity and its high spark dispersing effects [Lee and Li, 2001]. Discharge current is directly proportional to OC in brass and graphite tool material. But, with copper as tool material, when discharge current increases, OC first increases up to a maximum level then almost remains constant. The spark energy is more at higher current, so the crater formed on the work material is large and hence results in increment of OC [Singh et al., 2004b].

OC increases gradually with the increase in pulse-on time, as it is responsible for maintaining continuation of spark at tool and workpiece interface [Jeswani, 1981]. The duty cycle is not significantly affecting OC for all three electrode materials that are presented in Table 4.43.

Table 4.43: Abridged ANOVA for OC with the three electrode material

Source		Brass		Copper		Graphite	
of variation	DF	P	% cont.	P	% cont.	P	% cont.
P	1	0.012	7.99	0.022	2.41	0.085*	1.67
Ip	2	0.000	74.50	0.000	91.60	0.000	88.12
T_{on}	2	0.029	8.86	0.049	2.69	0.021	5.30
T_{au}	2	0.997*	0.01	0.942*	0.04	0.683*	0.36
Residual Error	10		8.65		3.26		4.56
Total	17						

* = Insignificant at 95%

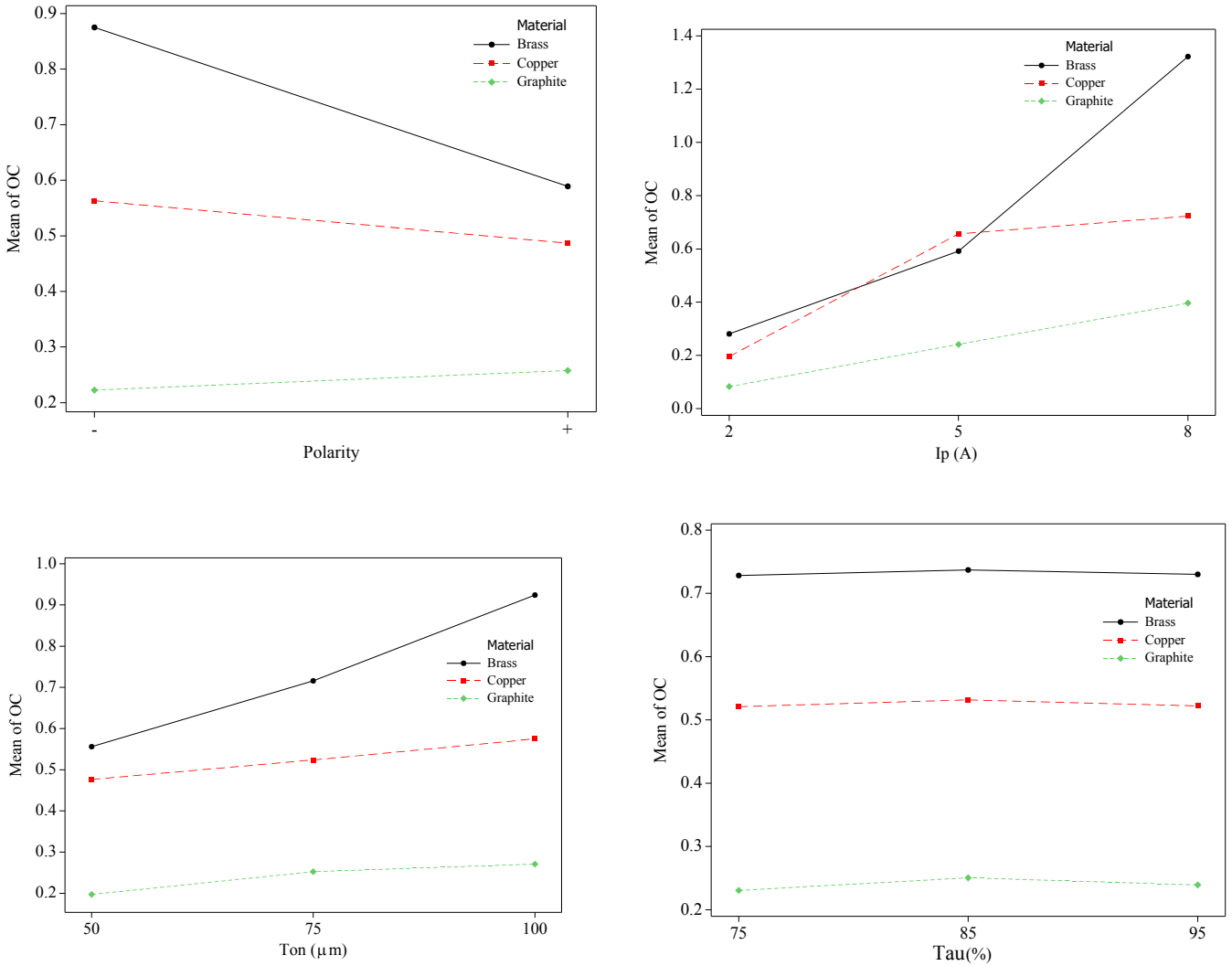

Fig. 4.37: Main effect plots for OC with the three different electrode materials

4.4.4 Effect of EDM parameters on WLT for different tool materials

Typical representative optical micro-graphs of the white layer are depicted in Fig. 4.38, 4.39 and 4.40, with brass, copper and graphite as electrode materials respectively. The main effect plots for WLT are shown in Fig. 4.41, and this plot indicates that polarity of copper and brass tool material affects WLT, but with graphite tool material, it does not affect significantly. This can be explained by the higher melting point of graphite than that of brass and copper. However, brass and copper tool materials result in lower value of WLT in straight polarity. Since reverse polarity leads to higher wear rate of copper tool, there by increasing the amount of molten materials on the workplace surface during EDM this causes increasing WLT.

Pulse current is causes increase in WLT for all tool electrode materials.This can be explained by the fact that more pulse current generate more discharge energy at the sparking point resulting in increasing recast layer thickness [Hascalik and Caydas, 2007].

During EDM with higher current highest WLT is obtained with graphite tool. Since low thermal conductivity of graphite ensures generation of higher temperature at the spark point resulting in molten pool of material and thicker re-solidified layer on the workpiece surface due to similar reason WLT has also been found to be directly proportional to pulse-on time for all three tool materials [Bhattacharyya et al., 2007]. The duty cycle is insignificant parameter for WLT for all the three tool material which is confirmed by abridged ANOVA shown in Table 4.44.

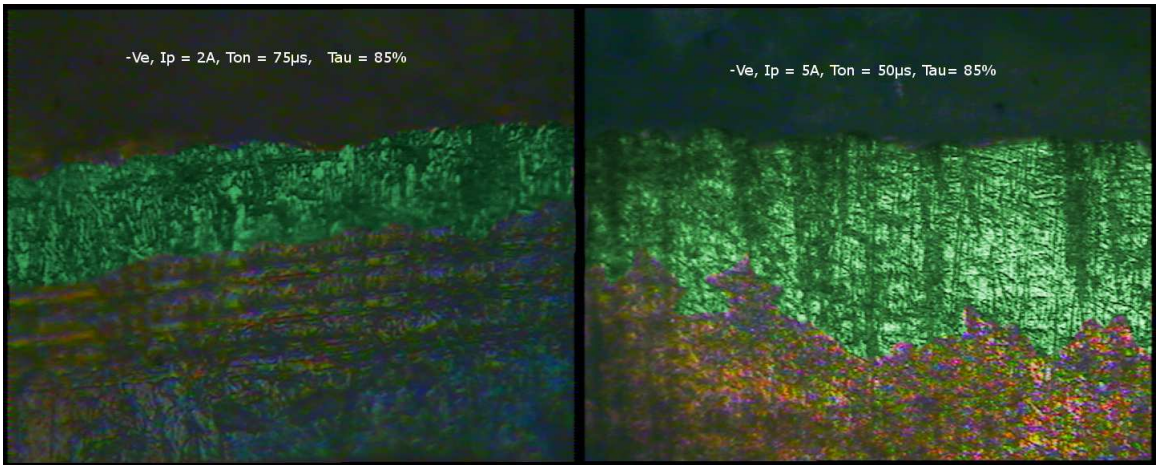

(a) Run no. 2 *(b)* Run no. 4

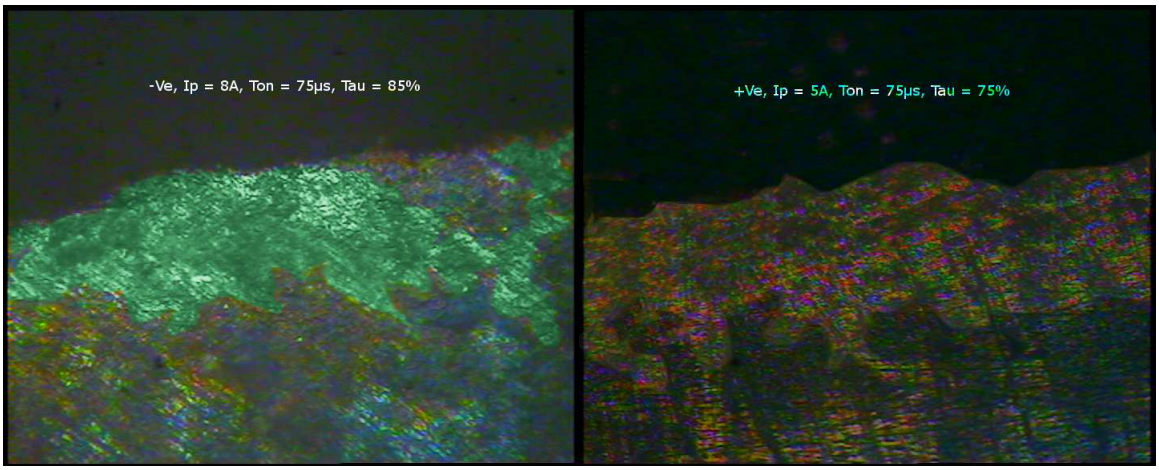

(c) Run no. 8 *(d)* Run no. 14

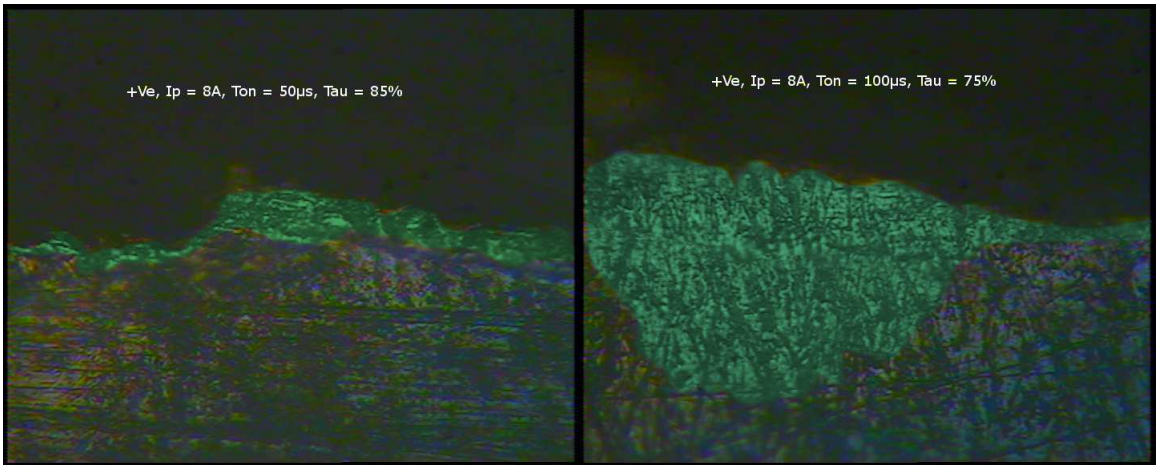

(e) Run no. 16 *(f)* Run no. 18

Fig. 4.38: Representative optical microscopic images of WLT with brass electrode

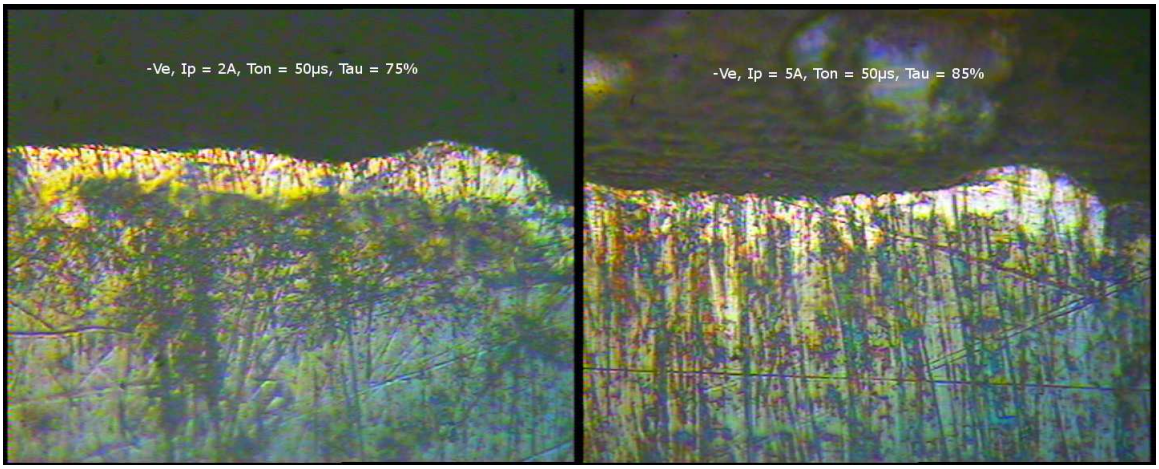

(a) Run no. 1 *(b)* Run no. 4

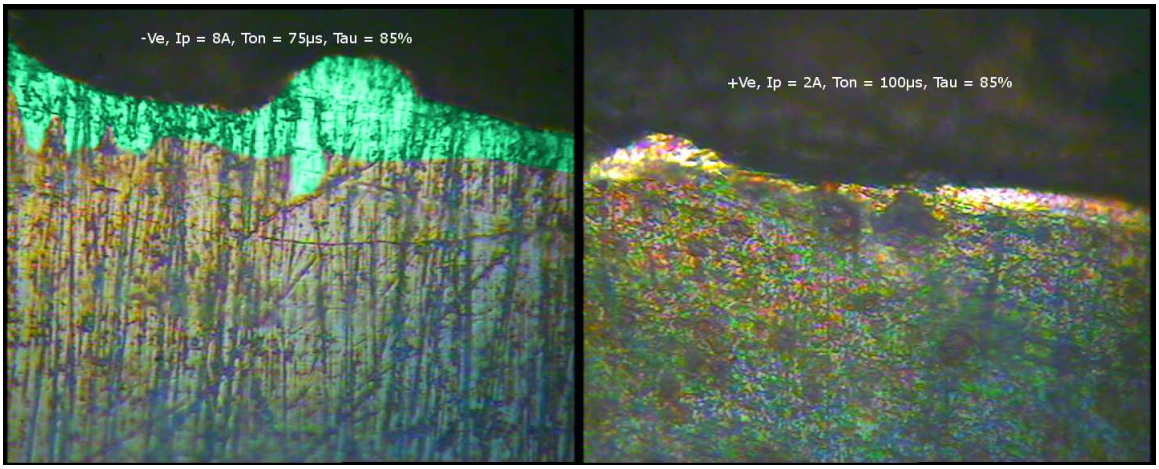

(c) Run no. 8 *(d)* Run no. 12

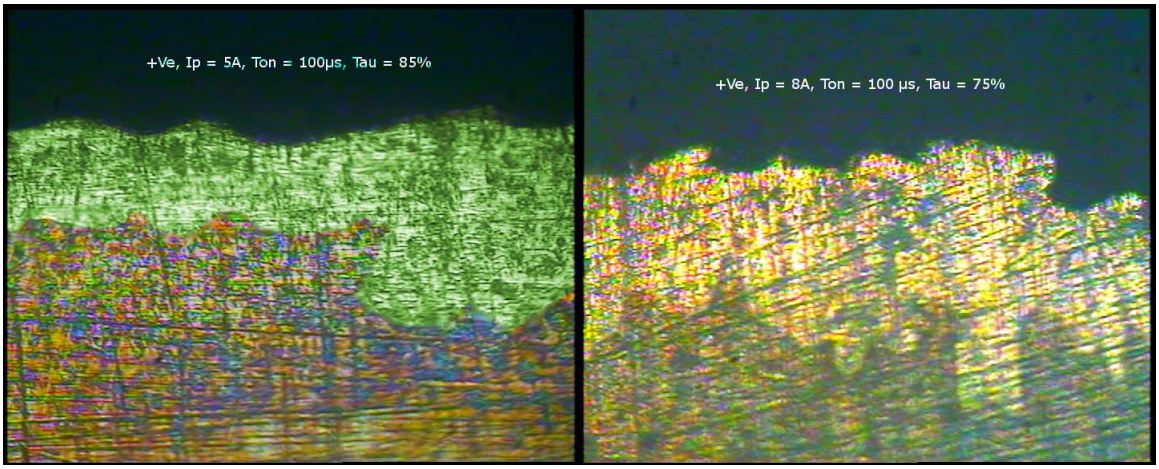

(e) Run no. 15 *(f)* Run no. 18

Fig. 4.39: Representative optical microscopic images of WLT with copper electrode

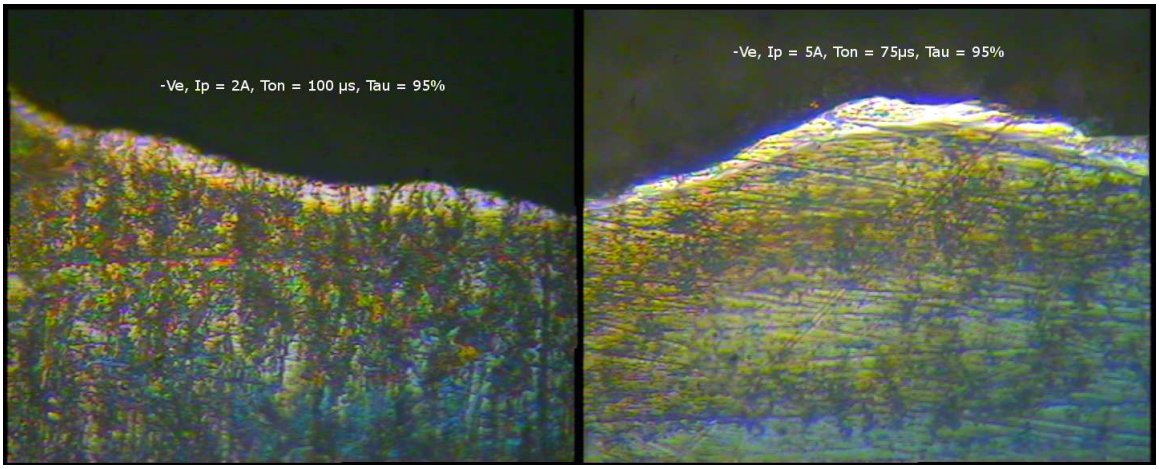

(a) Run no. 3 *(b)* Run no. 5

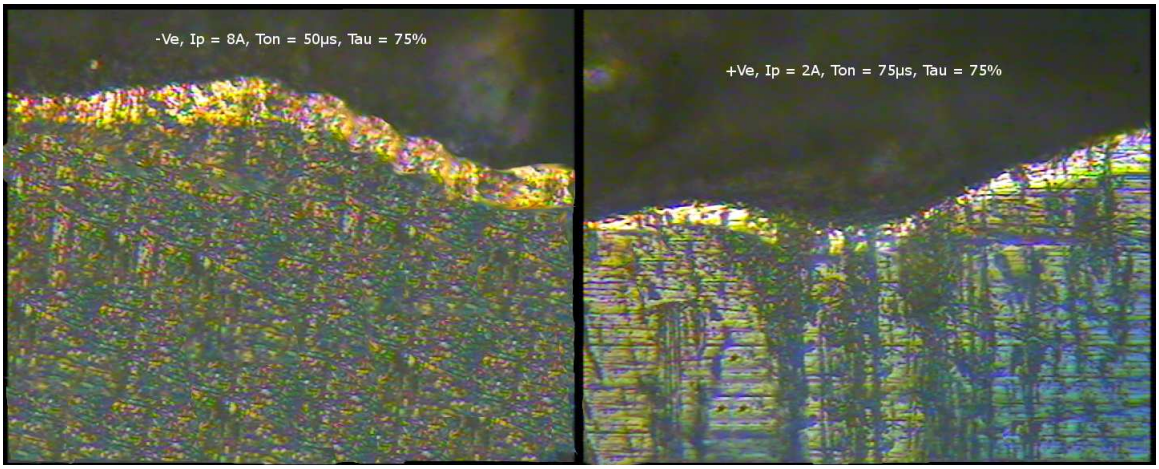

(c) Run no. 7 *(d)* Run no. 12

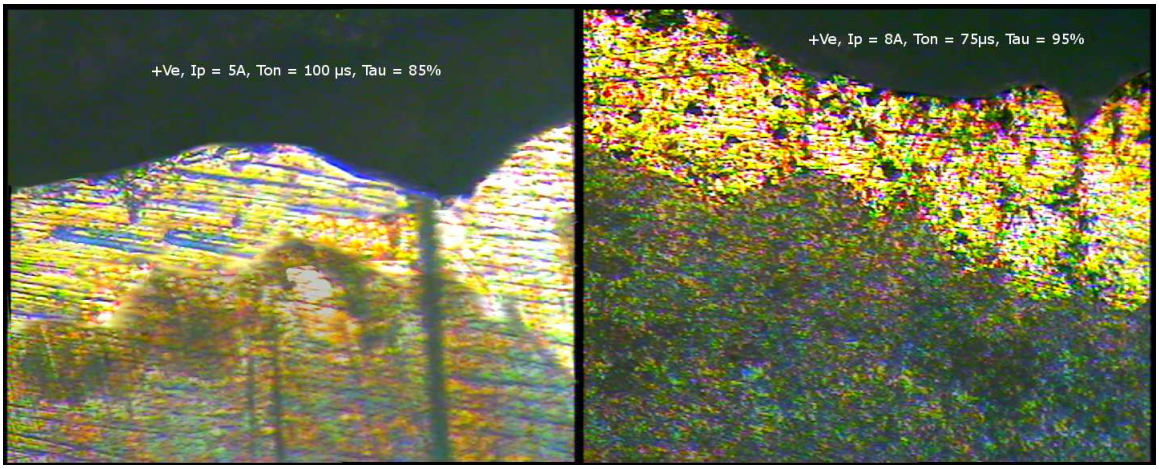

(e) Run no. 15 *(f)* Run no. 17

Fig. 4.40: Representative optical microscopic images of WLT with graphite electrode

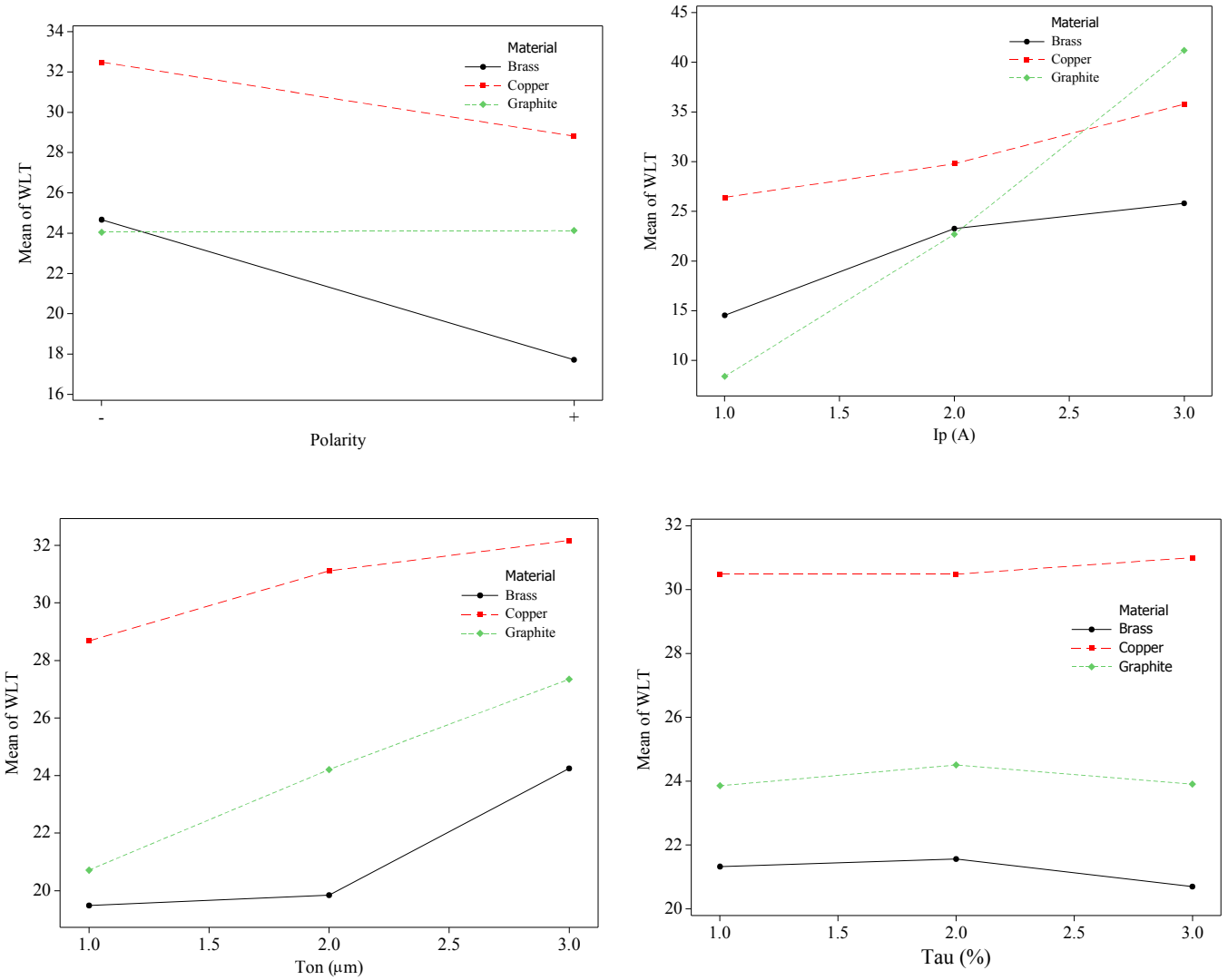

Fig. 4.41: Main effect plots for WLT with different electrode material

Table 4.44: Abridged ANOVA for WLT with the three electrode material

Source		Brass		Copper		Graphite	
of variation	DF	P	% cont.	P	% cont.	P	% cont.
P	1	0.000	27.71	0.000	15.70	0.934*	0.00
Ip	2	0.000	53.59	0.000	70.18	0.000	94.69
T_{on}	2	0.012	10.75	0.002	9.99	0.001	3.85
T_{au}	2	0.821*	0.31	0.697*	0.29	0.851*	0.05
Residual Error	10		7.63		3.85		1.41
Total	17						

* = Insignificant at 95%

4.4.5 Effect of EDM parameters on SCD for different tool materials

Surface crack density is one of the important characteristics in machine surface integrity SCD should always be minimised in order to prevent the product form fatigue failure. Typical representative SEM images depicting the formation of surface cracks are shown in Fig. 4.42, 4.43 and 4.44. This SCD is influenced by various machining parameters like Ip, T_{on} and Tau . In Fig. 4.45, the main effects for SCD are plotted. From this plot, it is confirmed that the discharge current is inversely proportional to SCD for brass and copper electrode. It is because WLT is more from the high current, so more molten metal is produced to fill the crack surface that results in reducing cracks. But, for graphite tool material, when the discharge current increases, SCD decreases up to an optimum level and then starts to increase. The effect of the pulse-on time on SCD is to reduce it up to an optimum level and then to increase for all the three tool materials. Because this is because initially, molten metal removed from the sparking point of workpiece, that leads to formation of cracks on the workpiece formation of surface cracks. When T_{on} increases more molten metal is produced and part of is flushed away. The remaining molten material gets deposited on cracks, that reduces the crack length. On further increase of pulse-on time, the duration of pulse-off time reduces, that lead to higher temperature and more WLT.

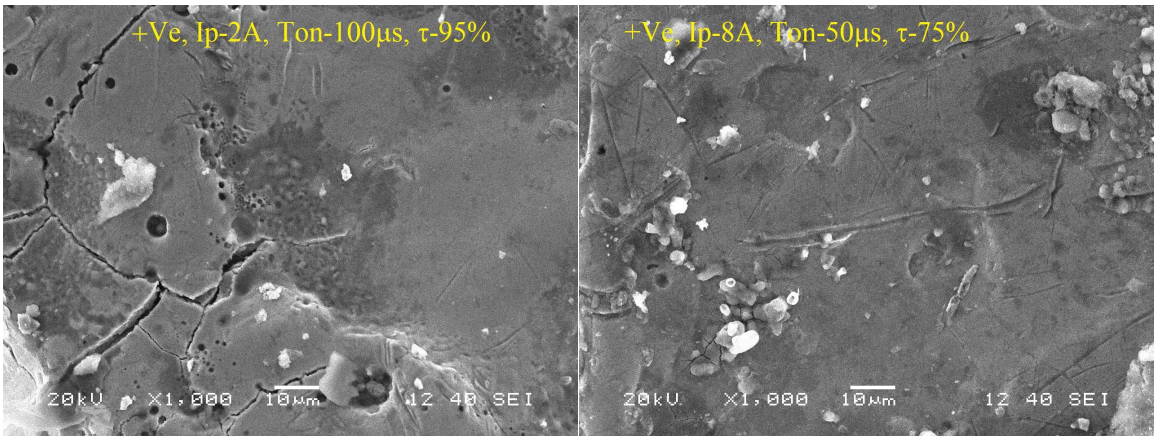

(a) Run no. 3 *(b)* Run no. 7

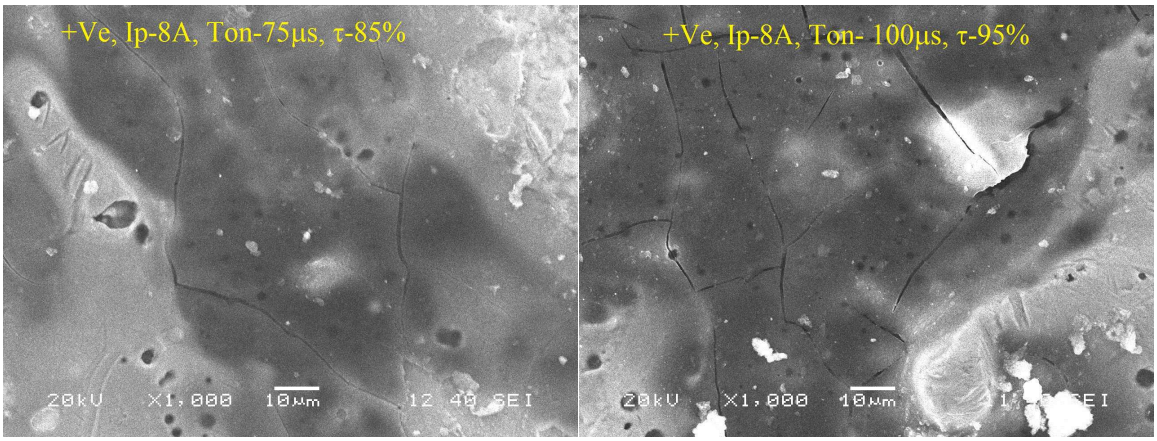

(c) Run no. 8 *(d)* Run no. 9

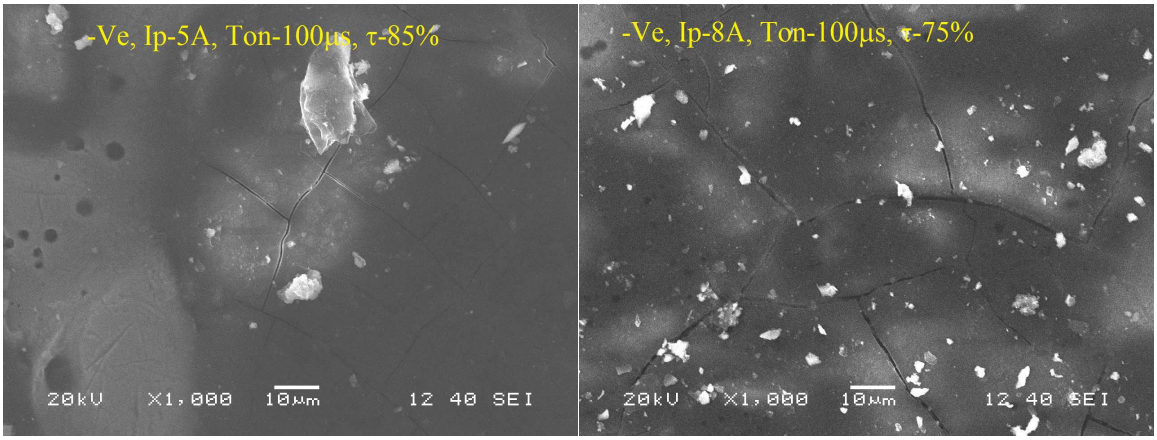

(e) Run no. 15 *(f)* Run no. 18

Fig. 4.42: Representative SEM images of SCD with brass electrode

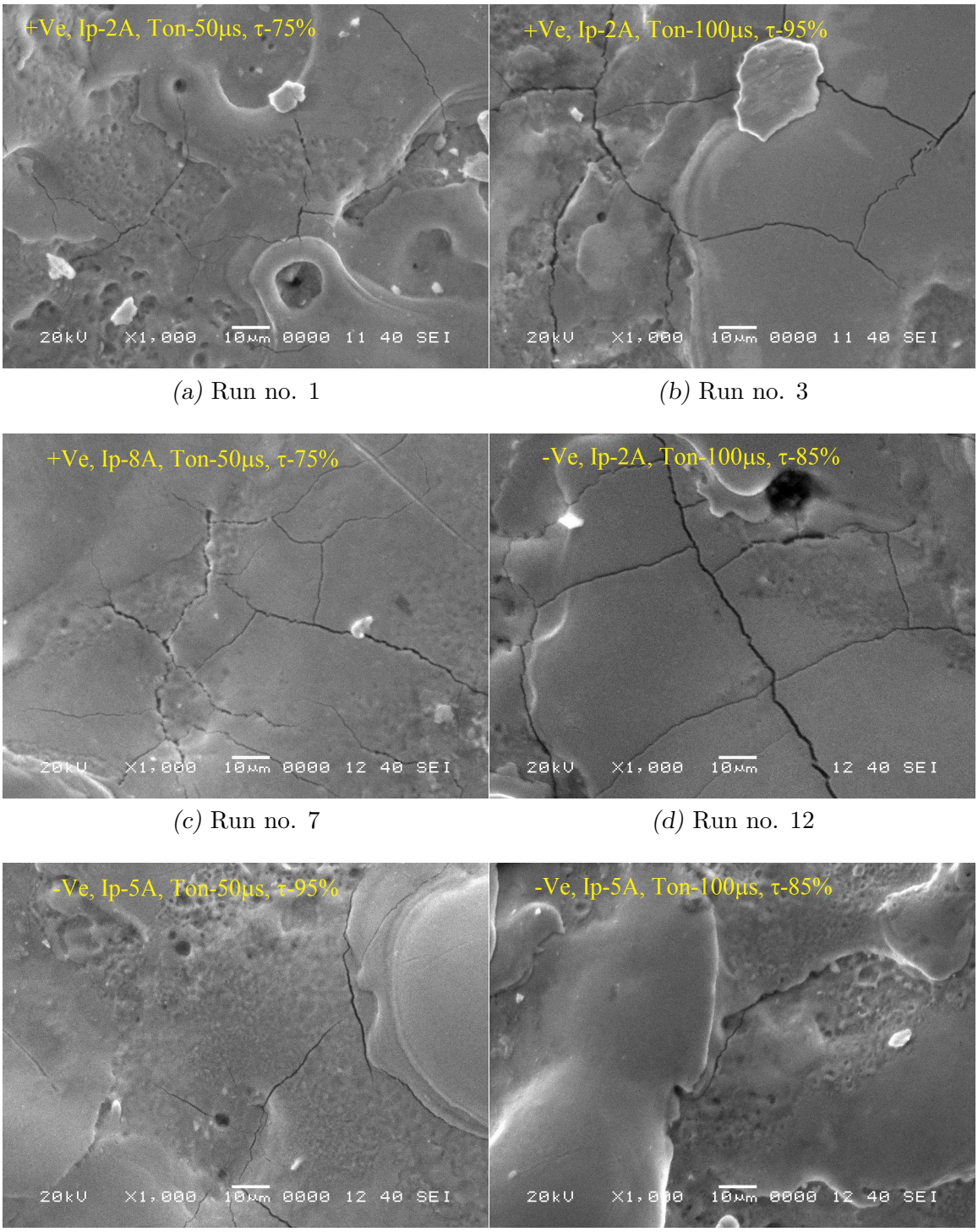

(a) Run no. 1 *(b)* Run no. 3

(c) Run no. 7 *(d)* Run no. 12

(e) Run no. 13 *(f)* Run no. 15

Fig. 4.43: Representative SEM images of SCD with copper electrode

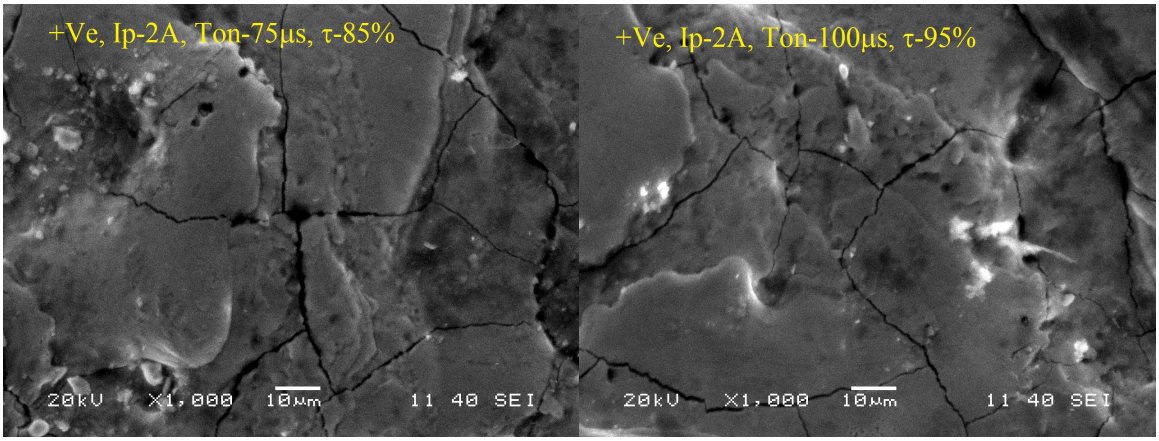

(a) Run no. 2 *(b)* Run no. 3

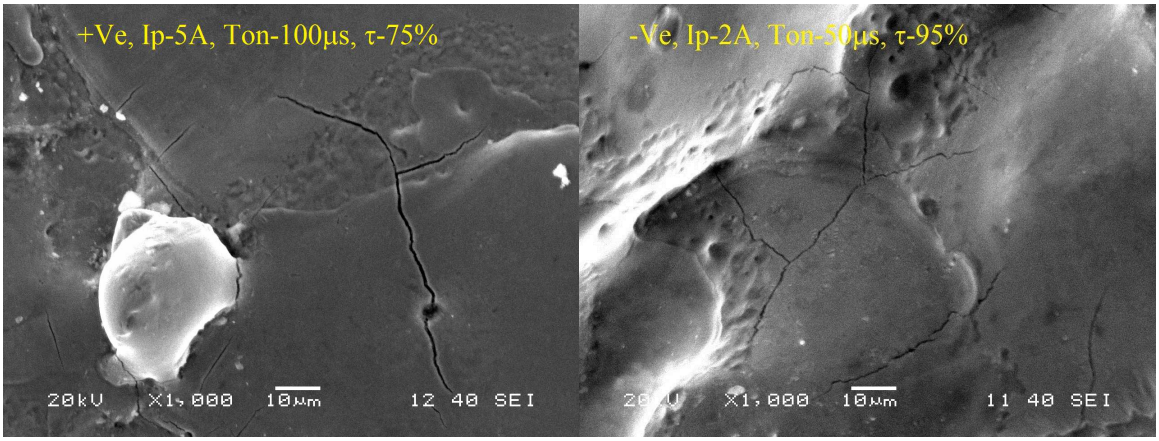

(c) Run no. 6 *(d)* Run no. 10

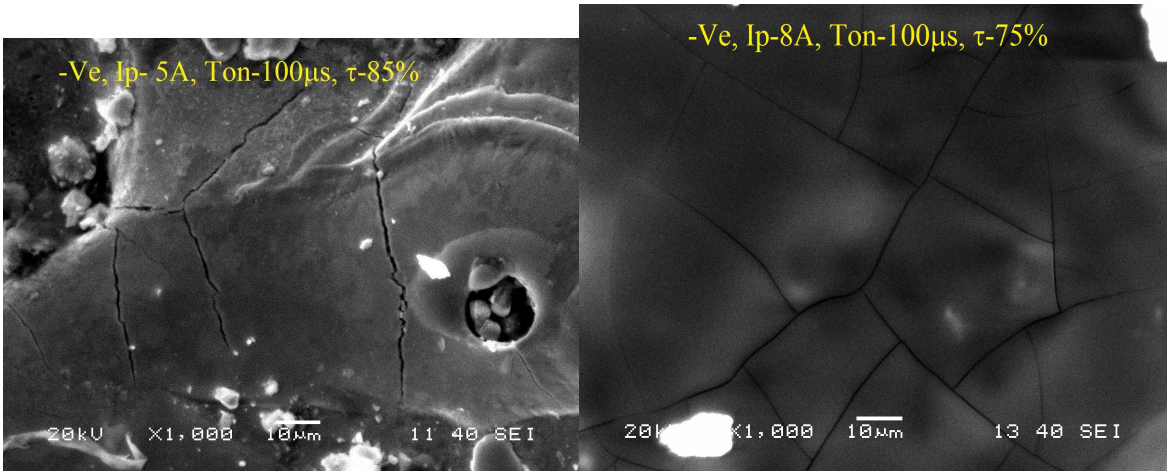

(e) Run no. 15 *(f)* Run no. 18

Fig. 4.44: Representative SEM images of SCD with graphite electrode

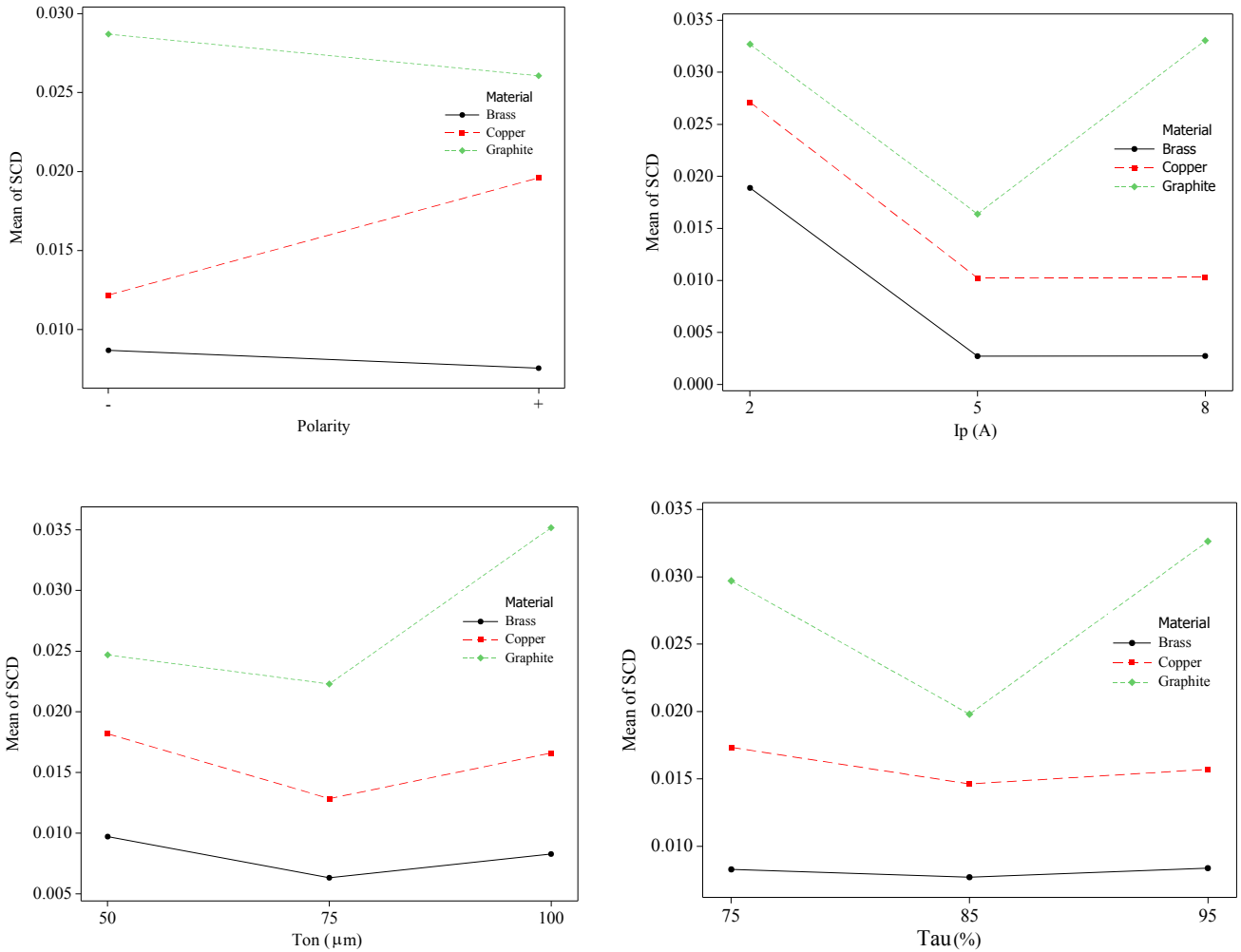

Fig. 4.45: Main effect plots for SCD with different electrode material

Table 4.45: Abridged ANOVA for SCD with the three electrode material

Source		Brass		Copper		Graphite	
of variation	DF	P	% cont.	P	% cont.	P	% cont.
P	1	0.284*	0.53	0.000	15.56	0.432*	1.15
Ip	2	0.000	92.29	0.000	71.52	0.002	40.45
T_{on}	2	0.057*	3.10	0.034	5.65	0.019	20.88
T_{au}	2	0.837*	0.18	0.340*	1.38	0.021	20.13
Residual Error	10		3.99		5.83		17.38
Total	17						

* = Insignificant at 95%

The duty cycle is not significant for SCD with copper and brass tool material that are described in Table 4.45. But, in the case of graphite duty cycle has significant effect on SCD.

4.4.6 Conclusions

From the preceding result and discussion, following conclusion can be down.

- In the analysis of SR, the use of negative polarity is most suitable with copper and graphite electrodes, but not with brass electrode. Higher SR is obtained with graphite tool as compared to brass and copper electrodes. The pulse-on time is does not significantly affect SR with copper and brass as electrode materials. Whereas only the graphite tool affects SR significantly. The duty cycle dose not significantly affecting SR for any of the three electrode materials.

- The polarity has significant effect on OC with copper and brass tools, but not with graphite. Discharge current is directly proportional to OC in brass and graphite tool materials. But, with copper as tool material, when discharge current increases, OC first increases up to a maximum level then almost remain constant. The duty cycle is not significant parameter for OC and for all the three electrode materials.

- In the analysis of WLT, the polarity of copper and graphite tool materials affect significantly, but not for graphite electrode. Copper and brass electrodes give less WLT in straight polarity. Discharge current is directly proportional to WLT for all tool electrode materials, and with graphite tool results in thicker WLT with higher current. The duty cycle not significantly effecting WLT for all three electrode materials.

- SCD is inversely proportional to discharge current for brass and copper electrodes. But, for graphite tool material, when the discharge current increases, SCD is decreasing up to an optimum level, after that it starts to increase. The effect of the pulse-on time on SCD is to reduce it up to an optimum level and then to increase, for all the three tool materials. The duty cycle is not significant for SCD with copper and brass tool material. But, in the case of graphite duty cycle has significant effect on SCD, and the optimal value is obtained at $Tau = 85\%$.

4.5 Study of discharge characteristics during EDM process through wavelet transform of V-I waveforms

During EDM, electrical discharges at the gap between the tool and workpiece are used to remove material from the surface of the workpiece. While machining, various voltage-current (V-I) waveforms are captured and these waveforms affect the quality and productivity of EDM process. In this section, various EDM waveforms are discussed followed by the analysis of the same using wavelet transform. The result obtained from these transform can be used to identify the various discharge characteristics of EDM. The influence of different EDM parameters (Ip, T_{on} and T_{au}) on the formation of different EDM pulses has also been investigated.

4.5.1 Experimental procedure and design

In the current study, AISI P20 tool steel was machined using EDM with copper electrode as tool and a commercial grade of EDM oil as dielectric. L_8 OA-based Taguchi design of experiment has been adopted to analyse the influence of EDM parameters on discharge characteristics. The three factors, with two factors at two levels and one factor at four levels, a total number of eight experiments were conducted. Control and fixed machining parameters along with their levels and values are presented in Table 4.46.

Table 4.46: Parameter and their levels

Control Parameters						
Parameter	Symbol	Levels				Unit
		1	2	3	4	
Pulse-on Time	T_{on}	50	300	650	900	μs
Discharge current	Ip	1	8			A
Duty Cycle	Tau	70	90			%
Fixed Parameters						
Voltage	V	45				V
Flashing Pressure	Fp	0.3				Kgf/cm^2
Sensitivity	SEN	6				
Inter electrode gap	IEG	90				μm
Work time	T_w	0.6				s
Lift Time	T_{up}	0				s

During machining, various discharge (V-I) waveforms are generated and these

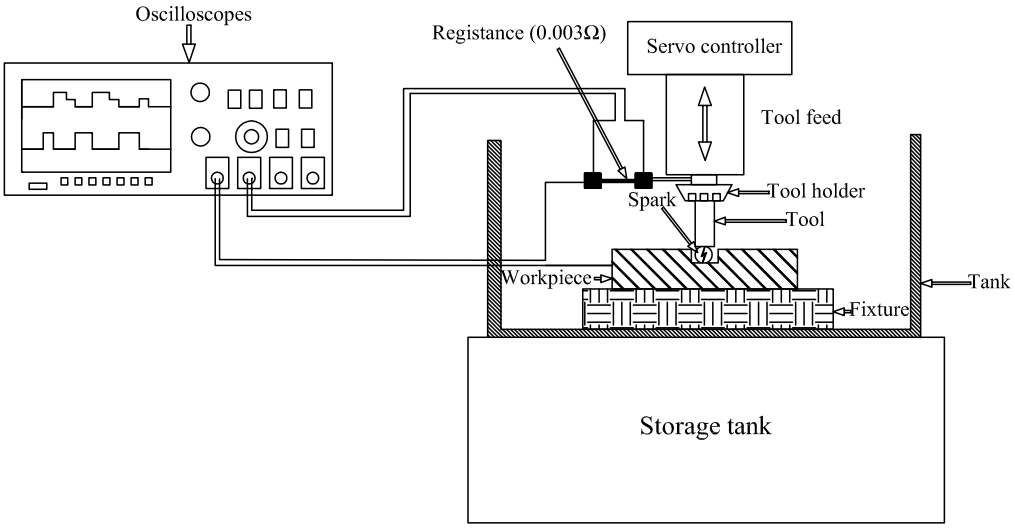

Fig. 4.46: Electric circuit of EDM set-up

waveforms can be analysed to detect different discharge (pulse) characteristics such as open, spark, transient arc, arc and short pulses, detail of which has already been discussed in chapter 1 (section 1.4).

Every experimental run was repeated for five times and the signal was captured for a duration of 1ms with the help an oscilloscope (make: Tektronix 4000) which was integrated with the EDM circuit (as shown in Fig. 4.46 and 4.47) to capture the exact voltage and current waveform during EDM. Oscilloscope is commonly calibrated so that voltage vs time can be plotted. This allows the measurement of peak-to- peak voltage of relative to time corresponding to several related signals. The current was remeasured by the voltage drop across the resistance (0.003 Ω) with the scale of 1A= 0.003V, which was also attached to the EDM circuit. These two signals were transferred simultaneously to a dual channel oscilloscope and the data was saved using USB device.

Analysis of V-I waveforms can provide useful information on different discharge characteristics in EDM. Therefore, the current study aims at investigating the influence of different EDM parameters like Ip, T_{on} and T_{au} on the pulse characteristics using wavelet transform as a pulse discrimination methodology.

Wavelet transform is a technique specifically designed for handling transient non

Fig. 4.47: Photographic view of EDM set-up

stable electrical signals. For certain classes of signals and images, wavelet analysis gives the information about signal analysis techniques and signal data [Matlab, 2011]. Although other techniques like Fourier transforms are also used in processing signals, they are usually not recommended in processes like EDM since signals are transferred from time to frequency domains. Wavelet transform on the other hand, is much simpler than Fourier transform and can provide both time and frequency related information [Yu et al., 2001]. After such decomposition, the information can be used for filtering and recognition of signal characteristics. The methodology of wavelet transform is presented in C. For the current purpose, wavelet transform techniques has been carried out using 'wavelet transform' toolbox in Matlab 2013 using Daubechies three- order wavelet (Db3) and decomposition level was kept at 3 (CA3). Similar methodology has also been adopted by previous researchers [Jiang et al., 2012].

4.5.2 Analysis of EDM waveforms using wavelet transform

The actual V-I characteristics for different experimental run in EDM have been demonstrated in Fig. 4.48. The obtained signals were analysed using wavelet transform to obtain both frequency of occurrence of various types of EDM pulses along with time of occurrence. The wavelet transform results for different experimental runs are shown in Fig. 4.49. After obtaining wavelet transform results corresponding to different experimental runs, EDM pulses have been identified according to the information provided in Table 4.47 [Jiang et al., 2012].The frequency of occurrence (n) of various discharge characteristics thus obtained are provided for different machining conditions in Table 4.48. It may be noted that no short pulse could be detected form the analysis.

Table 4.47: Correlation between discharge characteristics and computed values (Db3) in wavelet transform [Jiang et al., 2012]

Spark characteristics	Wavelet transform
	Threshold
open	≥ 150
spark	$80 \sim 150$
transient arc	$70 \sim 80$
arc	$20 \sim 70$
short	< 20

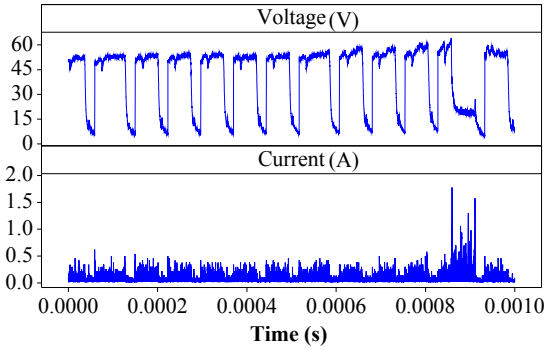

(a) T_{on}= 50 μs, Ip =1A, T_{au} = 70%

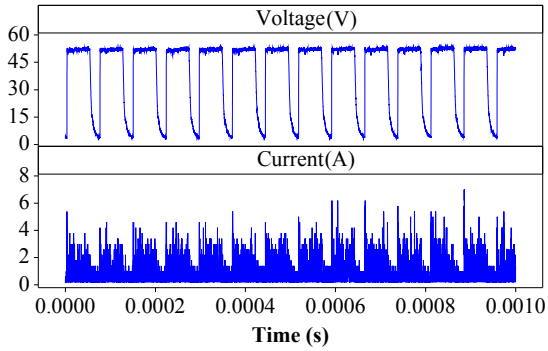

(b) T_{on}= 50 μs, Ip =8A, T_{au} = 90%

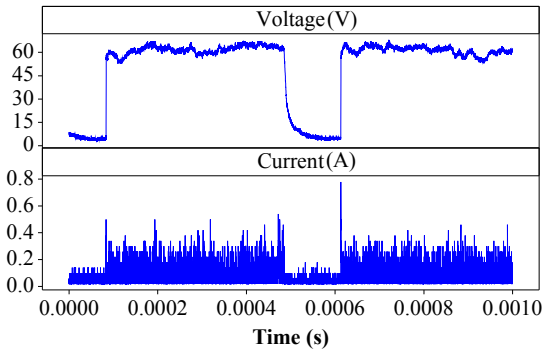

(c) T_{on}= 300 μs, Ip =1A, T_{au} = 70%

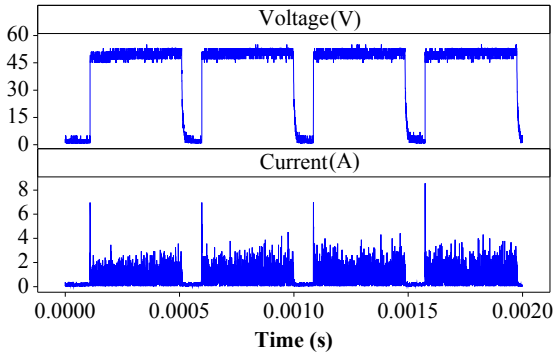

(d) T_{on}= 300 μs, Ip =8A, T_{au} = 90%

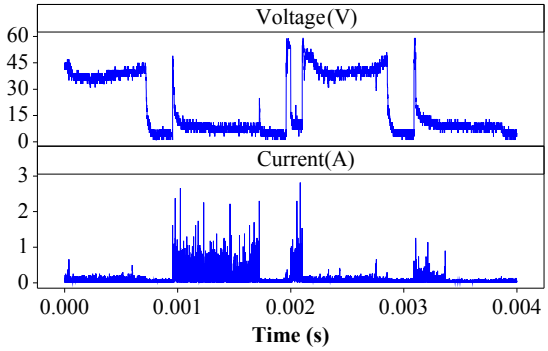

(e) T_{on}= 650 μs, Ip =1A, T_{au} = 70%

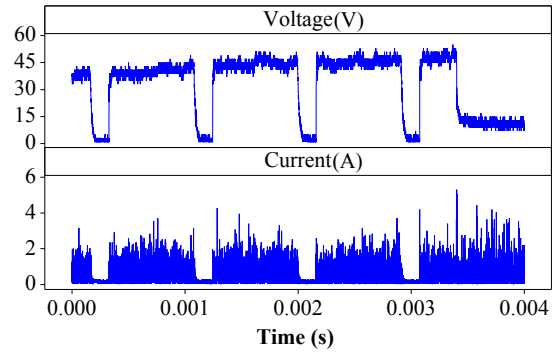

(f) T_{on}= 650 μs, Ip =8A, T_{au} = 90%

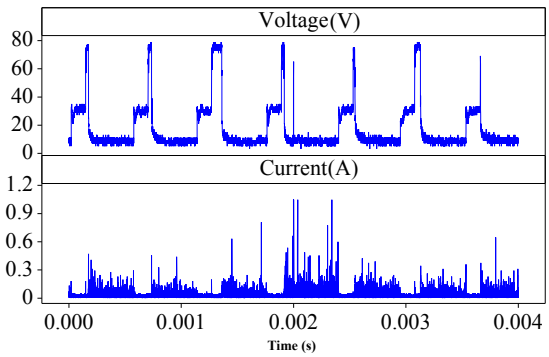

(g) T_{on}= 950 μs, Ip =1A, T_{au} = 70%

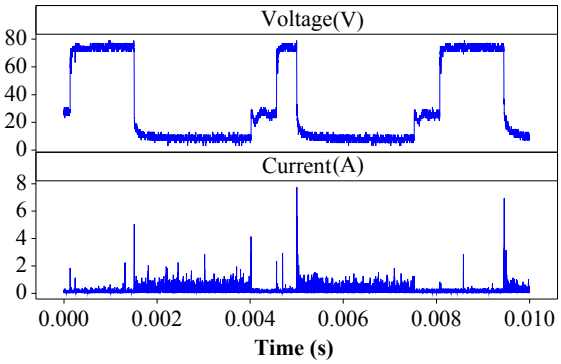

(h) T_{on}= 950 μs, Ip =8A, T_{au} = 90%

Fig. 4.48: V-I waveforms obtained during different experimental runs

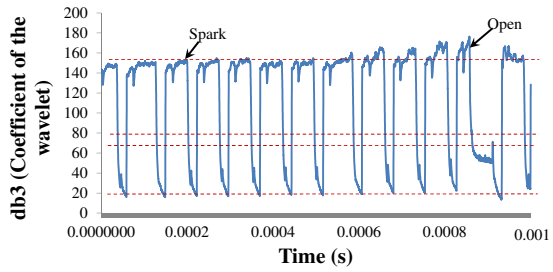

(a) T_{on}= 50 μs, Ip =1A, T_{au} = 70%

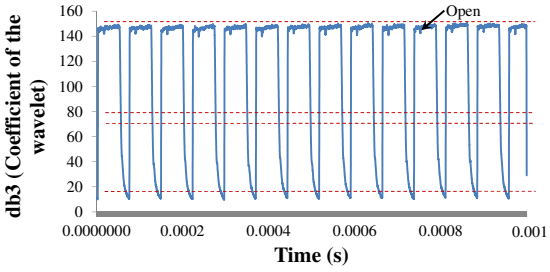

(b) T_{on}= 50 μs, Ip =8A, T_{au} = 90%

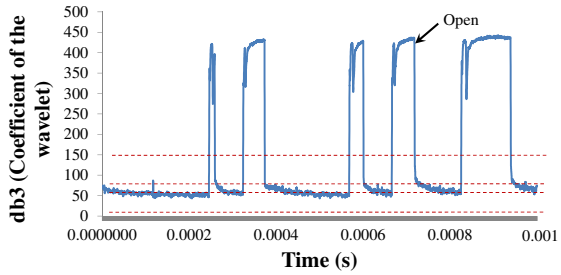

(c) T_{on}= 300 μs, Ip =1A, T_{au} = 70%

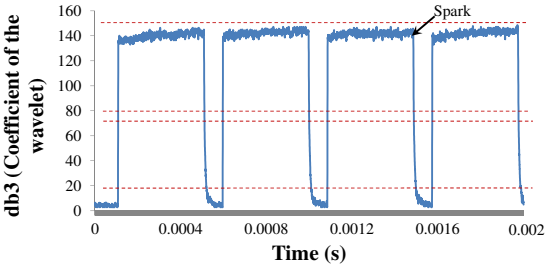

(d) T_{on}= 300 μs, Ip =8A, T_{au} = 90%

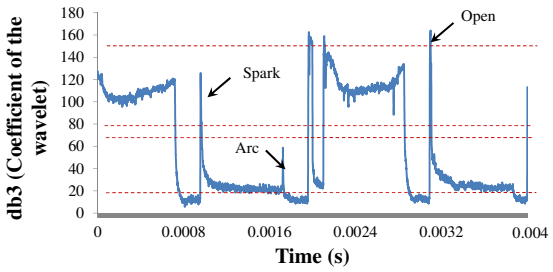

(e) T_{on}= 650 μs, Ip =1A, T_{au} = 70%

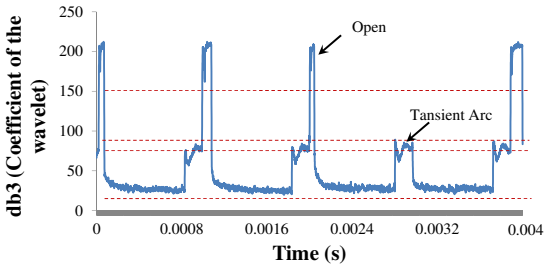

(f) T_{on}= 650 μs, Ip =8A, T_{au} = 90%

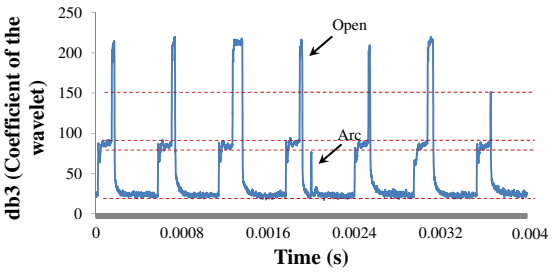

(g) T_{on}= 950 μs, Ip =1A, T_{au} = 70%

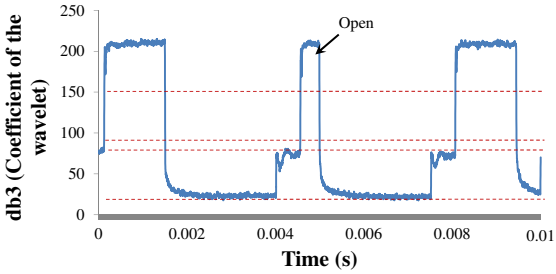

(h) T_{on}= 950 μs, Ip =8A, T_{au} = 90%

Fig. 4.49: Wavelet transform results for different experimental runs

Table 4.48: Spark characteristics observed for various experimental runs

Run no.	T_{on} (μs)	Ip (A)	Tau (%)	discharge characteristics				
				short	arc	transient arc	spark	open
1	50	1	70	0	0	1	37	26
2	50	8	90	0	0	1	39	27
3	300	1	70	0	0	0	4	10
4	300	8	90	0	0	0	16	6
5	650	1	70	0	3	6	13	13
6	650	8	90	0	3	7	12	12
7	950	1	70	0	9	8	6	30
8	950	8	90	0	10	4	3	15

Fig. 4.50 shows the main effect plots for different discharge characteristics. It is evident that number of spark pulses is directly proportional to T_{on} whereas number of arc pulses is inversely proportional to T_{on}. ANOVA results (shown in Table 4.49-4.52) indicate that other parameters like Ip, T_{au} are insignificant as far as discharge characteristics in EDM are concerned. Since no short pulse could be detected during experiment, corresponding main effect plots and ANOVA could not be provided.

ANOVA results show that only pulse-on time is a significant parameter for spark and arc pulses during EDM of AISI P20 tool steel. Good spark characteristics were obtained at low pulse-on time that is 50 μs which when increased resulted in the formation of arc. This can be explained by the fact that when T_{on} is increased, it becomes more difficult for dielectric to flush away molten debris form the sparking zone leading to the formation of arc pulses. Since low pulse-on time adversely affects MRR (*i.e.* productivity), it is recommended to utilise improved flushing technique in order to avoid the possibility of formation of arc at higher value of pulse-on time. No proper correlation between occurrence of the other pulses and the EDM parameters could be established during the current study. Therefore, it may be concluded that transient arc pulse, open pulse and short pulse are independent of variation of Ip, T_{on} and T_{au} while machining AISI P20 tool steel using EDM.

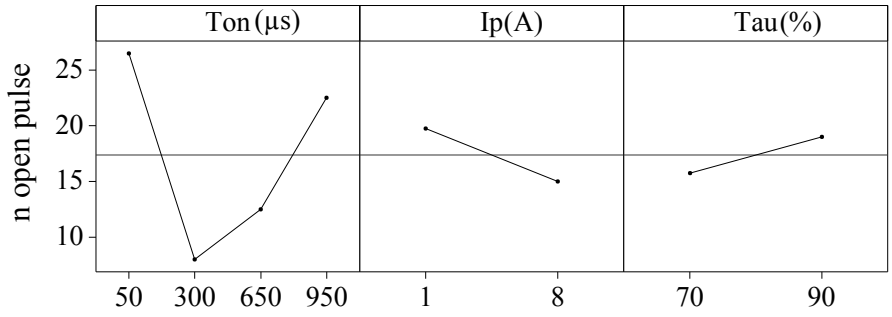

(a) Open

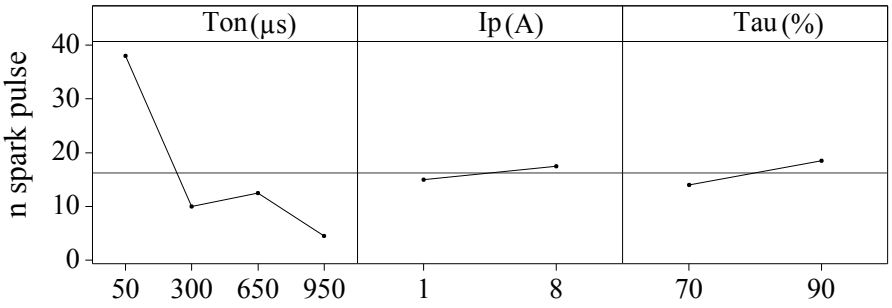

(b) Spark

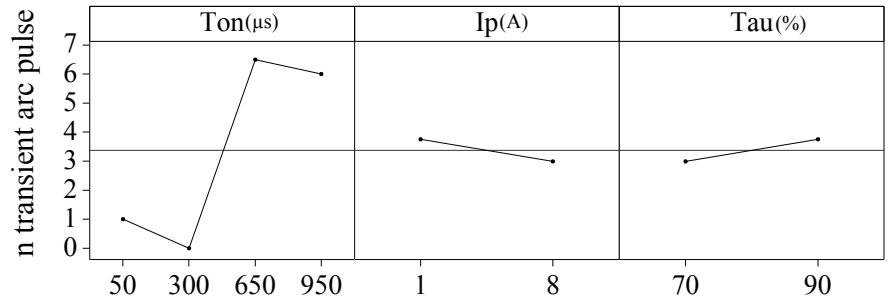

(c) Transient arc

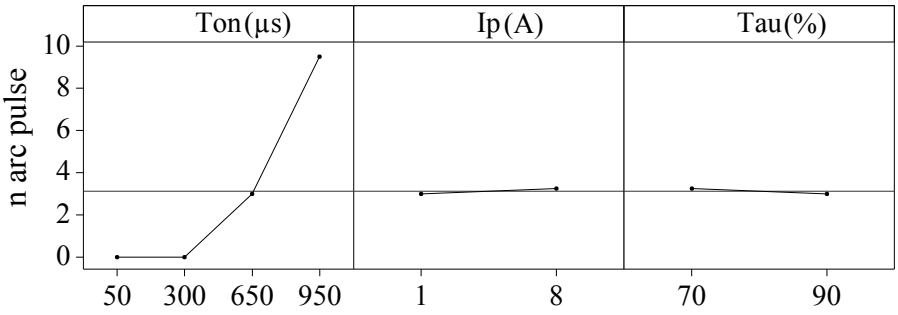

(d) Arc

Fig. 4.50: Main effect plots for different pulse characteristics

Table 4.49: ANOVA for open pulse

Source of variation	DF	Seq SS	Adj MS	F	P	% Contribution
Ton	3	442.38	147.46	5.34	0.162*	78.45
Ip	1	45.13	45.12	1.63	0.330*	8.00
Tau	1	21.13	21.13	0.76	0.474*	3.75
Residual Error	2	55.25	27.63			9.80
Total	7	563.88				
S = 5.256 R-Sq = 90.2% R-Sq(adj) = 65.7%						
* = Insignificant factor						

Table 4.50: ANOVA for spark pulse

Source of variation	DF	Seq SS	Adj MS	F	P	% Contribution
Ton	3	1328.5	442.83	34.06	0.029	94.39
Ip	1	12.5	12.5	0.96	0.430*	0.89
Tau	1	40.5	40.5	3.12	0.220*	2.88
Residual Error	2	26	13			1.85
Total	7	1407.5				
S = 3.606 R-Sq = 98.2% R-Sq(adj) = 93.5%						
* = Insignificant factor						

Table 4.51: ANOVA for transient arc pulse

Source of variation	DF	Seq SS	Adj MS	F	P	% Contribution
Ton	3	67.375	22.458	7.19	0.125*	88.80
Ip	1	1.125	1.125	0.36	0.609*	1.48
Tau	1	1.125	1.125	0.36	0.609*	1.48
Residual Error	2	6.25	3.125			8.24
Total	7	75.875				
S = 1.768 R-Sq = 91.8% R-Sq(adj) = 71.2%						
* = Insignificant factor						

Table 4.52: ANOVA for arc pulse

Source of variation	DF	Seq SS	Adj MS	F	P	% Contribution
Ton	3	120.375	40.125	321	0.003	99.59
Ip	1	0.125	0.125	1	0.423*	0.10
Tau	1	0.125	0.125	1	0.423*	0.10
Residual Error	2	0.25	0.125			0.21
Total	7	120.875				
S = 0.3536 R-Sq = 99.8% R-Sq(adj) = 99.3%						
* = Insignificant factor						

4.5.3 Conclusions

In the current study, the influence of various EDM process variables on different discharge characteristics has been investigated by analysing the obtained V-I waveform using wavelet transform. The following conclusion may be drawn:

- Different pulse characteristics during EDM of AISI P20 tool steel were obtained which include spark, open, arc and transient arc. However, no short circuit pulse could be detected.
- Only pulse-on time (T_{on}) was found to be significant parameter for spark and arc pulses. Pulse current and duty cycle did not have any systematic influence on the pulse characteristics.
- Good spark characteristics were obtained at $T_{on} = 50$ μs. However, further increase in Ton resulted in suppression of spark and formation of arc pulses.
- Other discharge characteristics like open and transient arc pulses were found to be independent of variation of EDM parameters under the chosen operating range.

Chapter V

Major Conclusions

5. MAJOR CONCLUSIONS

During the current research work, the influence of various Electric Discharge Machining (EDM) process parameters has been studied on productivity, quality characteristics, surface integrity and discharge characteristics during machining of AISI P20 tool steel and also to recommend optimal settings of the process parameters using different multi-objective optimisation techniques. Productivity in EDM is characterised by Material Removal Rate (MRR) which should as high as possible, while quality is associated with Tool Wear Rate (TWR) and Radial Overcut (OC) which should be minimised. Different aspects of surface integrity considered in the current study include Surface Roughness (SR), White Layer Thickness (WLT) and Surface Crack Density (SCD). Simultaneous optimisation of multiple responses was carried out using Grey Relational Analysis (GRA), fuzzy logic and fuzzy-based TOPSIS methodologies. A comparative study was undertaken wherein the influence of different tool electrode materials (brass, copper and graphite) on surface integrity and dimensional accuracy (OC) was investigated. Finally the effect of different EDM parameters on different pulse characteristics was studies by analysing the EDM waveform using wavelet transform. The following major conclusions obtained from the entire work has been summarised as follows:

1. MRR is directly proportional to Ip and T_{on}. MRR is also affected by T_{up} and T_w. It decreases with T_{up} and slightly increases with T_w. Inter electrode gap has no effect on MRR.

2. TWR is directly proportional to Ip, but inversely proportional to T_{on}. TWR increases with T_w to an optimal level and then it remains almost constant. T_{up} has no significant effect on TWR.

3. OC is directly proportional to Ip and T_{on}. Both T_{up} and T_w found to be insignificant parameters for over-cut phenomenon.

4. WLT is directly proportional to Ip, T_{on} and T_w, while T_{up} has no significant effect on it.

5. SCD is inversely proportional to Ip. SCD decreases with T_{on} upto a particular value and then starts increasing. Similar trend is also observed by T_w and T_{up}.

6. The sensitivity test of fuzzy-Technique for Order of Preference by Similarity to Ideal Solution (TOPSIS) methods shows that the decision makers' preferences of SCD is most important and should be chosen first and very carefully. Then, comes the preferences of OC and SR, whereas preferences of WLT has no consequence on the optimal values of the parameters.

7. Copper and brass electrodes result in low value of WLT under straight polarity, whereas the polarity has no significant effect on graphite tool electrode.

8. SCD is inversely proportional to discharge current for both brass and copper electrodes. For graphite tool material, SCD first deceases with discharge current up to an optimum level, and then starts to increase. The duty cycle is not significant for SCD for copper and brass tool materials. But, in the case of graphite duty cycle has significant effect on SCD, and the optimal value is obtained at $Tau = 85$ %.

9. Analysis of EDM waveform using wavelet transform shows that pulse on time is directly proportional to number of spark pulses and is inversely proportional to number of arc pulses. However, other pulse characteristics like open and transient arc were independent of variation of EDM parameters under the given operating condition.

5.1 Recommendation of future work

Analysis of the results developed from the current work promoters quite a few possible additions to the research. A few of them are listed below,

- An adaptive control system (servo controller) that can both capture and analyse EDM waveforms real time and make suitable adjustment to improve the process inefficiency.

- Effect of dielectric materials can also be studied on the EDM performance measures during machining AISI P20 tool steel.
- Attempt can also be made to study the effect of EDM parameters on residual stress and hardness both on the top surface and also at various depths beneath the machined surface.

APPENDIX

A. EXPERIMENTAL APPARATUS USED

Experimental apparatus

A.1 Muffle furnace

This furnace is used for heat treatment process for AISI P20 tool steel workpieces material.

Fig. A.1: Muffle furnance

A.2 Electronic balanced weight machine

Precision electronic balance weight machine was used to measure the weigh of the workpiece and tool. And the capacity of machining is 300 gm with, an accuracy of 0.001 gm.

Fig. A.2: Electronic balance weight machine

A.3 Surface Roughness Analyser

The measurement of Surface Roughness (SR) (Ra value) was made with portable style type profilometer, Talysurf (Model: Taylor Hobson, Surtronic 3+) , with parameters cut-off length, $L_n = 4$ mm, sample length, $L_c = 0.8$ mm and filter = 2CR ISO.

Fig. A.3: Talysurf Surface Roughness Analyser

A.4 Tool maker microscope

The tool maker microscope with a least count of 1 μm was used for measurement of Radial Overcut (OC).

Fig. A.4: Tool maker microscope
Make : Carl Zeiss, Germany

A.5 Optical microscope

The measurement of White Layer Thickness (WLT) was carried out with an optical microscope with 400X optical zoom.

Fig. A.5: Optical Microscope

A.6 Oscilloscope

The capturing the voltage and current waveform of an electrical signal and data in oscilloscope (make: Tektronix 4000) that are arranged with the Electric Discharge Machining (EDM) circuit.

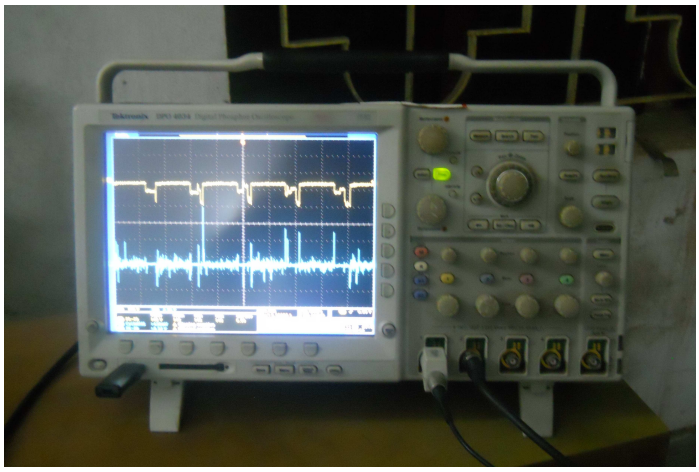

Fig. A.6: Digital Phosphor Oscilloscopes (Tektronix 4000 Series)

A.7 Emery grinder and polisher

The etching process was used as polisher and grinder while measuring the white layer thickness. In this process workpiece was polished with 120 grit silicon carbide emery paper with the help of emery grinder, after that it was polished subsequently with emery polishing paper 200, 300, 400 and 600 grit size paper, in alternate direction. After polishing, it was finished with drum grinder with silk cloth and diamond polishing.

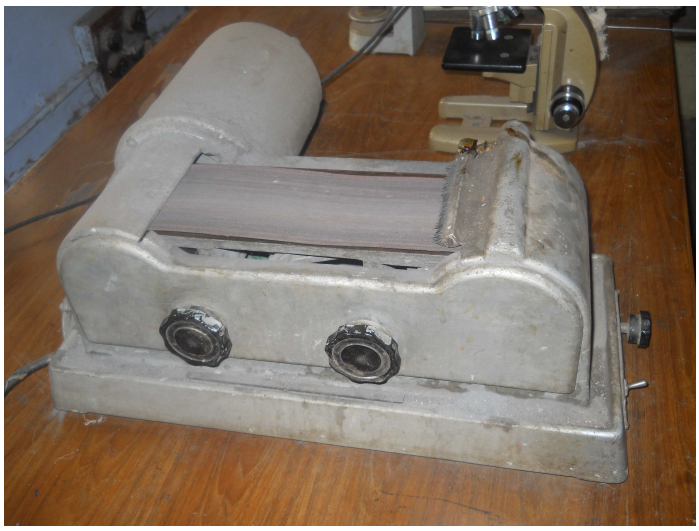

(a) Emery grinder

(b) Polisher

Fig. A.7: Emery grinder and polisher

A.8 Scanning electron microscopy (SEM)

This apparatus used to analyse and measure the white layer thickness and surface crack density.

Fig. A.8: Scanning electron microscopy
Brand:Jeol, Japan
Model:Jeol JSM-6480LV,

B. DESIGN OF EXPERIMENT

B.1 Introduction to design of experiments (DOE)

The use of experiments in an efficient way to analyse and optimize a given process is a problem statement which should be paid added attention to in the engineering community. Normally, experiments are first performed and the measured data is analysed afterwards. In contrast to this, statistical methods, like the concept of Design of Experiments (DOE), should be used to plan experimental designs and perform sets of well selected experiments to get the most informative combination out of the given factors. DOE is an essential piece of the reliability program pie. It plays an important role allowing the simultaneous investigation of the effects of various factors and thereby facilitating design optimization.

DOE is a tool to develop an experimentation approach. It is extensively used in the advance of manufacturing processes to maximize yield and reduce variability. To achieve these objectives, properly designed experiments are much more efficient than that of one- factor-at-a-time experiments, which involve changing a single factor at a time to study the effect of the factor on the response. When the effect that a factor has on the response is changed due to the presence of one or more other factors, that relationship is called an ‘ interaction’. Sometimes the interaction effects are more significant than the discrete factor effect. This is because the application environment of the response comprises the presence of many of the factors together instead of isolated occurrences of single factors at different times.

DOE helps in:

- Identifying relationships between cause and effect.
- Providing an understanding of interactions among causative factors.
- Determining the levels at which to set the controllable factors (product di-

mension, alternative material, alternative designs, etc.) in order to optimize reliability.

- Minimizing experimental error (noise).
- Improving the robustness of the design or process to variation.

Types of DOE techniques

The most prevalent experimental approaches are Factorial design, Taguchi's design, and Response Surface Methodology (RSM). The first DOE technique are used 'Factorial' or 'Classical DOE', which allows to differentiate which factors are most significant and helps in identifying important interactions among the factors. The main objective of Taguchi's design is to find a 'robust' response that is insensitive to factor variations and noise. RSM consists of an experimental approach for exploring the settings of input parameter and to develop a quadratic model suitably approximating relationship between the response and the input parameters. Subsequently, optimising the levels or values of the input variables that produce desirable response value.

B.2 Taguchi method

The Taguchi method has been used to optimise single quality characteristic and produced better quality products at a low cost [Ross, 1988]. In this method is the "robust" parameter design, the main aim is to find factor settings that minimize response deviation, while adjusting (or keeping) the process on target. After you determine which factors affect deviation, that are find to settings for controllable factors that will either reduce the deviation, make the product insensitive to changes in (noise) factors, or both [Minitab16, 2011].

B.3 Response surface methodology (RSM)

RSM is a collection of mathematical and statistical techniques that are useful for modelling and analysis of problems in which output or response is influenced by several variables and the goal is to find the correlation between the response and the variables [Montgomery, 2001].

B.3.1 Procedure of RSM

RSM is sequential in nature and at the outset, screening experiments are conducted to reduce the list of contestant variables to a comparatively few. The techniques for the analysis of the second-order model are presented by Myers and Montgomery [1995]. The steps shown below are typical of a response surface experiment. Depending on the experiment, one may carry out some of the steps in a different order, perform a given step more than once, or eliminate a step.

- Choose the response for an experimental investigation. Determine what the influencing factors are, that is, what the process conditions are those influence the values of the response variable.
- Create the response surface experiment design according to a central composite design.
- Set the factor levels and replicate the design.
- Randomize the design to change the order of the runs.
- Perform the experiment and collect the response data.
- Analyse the response surface design to fit a model to the experimental data.
- Optimize the response to obtain a numerical and graphical analysis.

A second-order model is given in the Equation B.1.

$$y = \beta_0 + \sum_{i=1}^{m} \beta_i x_i + \sum_{i=1}^{m} \beta_{ii} x_i^2 + \sum_{i,j=1,i\neq j}^{m} \beta_{ij} x_i x_j + e \tag{B.1}$$

Where y = response, x_i = m independent variables
β_i, β_{ii} = unknown coefficients are the estimates of the population regression coefficients and e = random error term.

B.4 Central composite design

The Central Composite Design (CCD) is a design extensively used for approaching second order response surfaces. It is possibly the most widely established set of second order designs. It was presented initially by Catalkaya and Sengul [2006], the CCD has been popular among the researchers. There are 2^m numbers of cube points, axial points and centre points (at least 3-5 points). If the design is blocked the centre points are divided equally among the blocks. A face centred design $\alpha = 1$ is chosen so that the axial points lie on the face of the cube as shown in Fig. B.1 for two variables. The two important properties of CCD are orthogonality and rotatable [Pradhan, 2010]. An orthogonal block design allows for model terms and block effects to be estimated independently and minimize the variation in the regression coefficients. A rotatable design provides the desirable property of constant prediction variance at all points that are equidistant from the design centre, thus improving the quality of the prediction. This study shows that the waveform of discharge status at every pulse of the Electric Discharge Machining (EDM) process in the form of wavelet transform can be clearly recognized. Therefore, the duration of each waveform can be clearly knows. If these data are used as input signals for EDM process, the quality of components produced by EDM will be considerably improved.

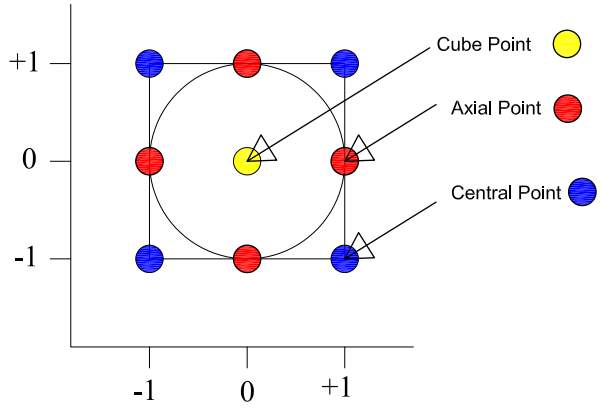

Fig. B.1: Two-Variable Face Centred Composite Design

B.5 Analysis of variance (ANOVA)

Experimental factors will influence the response and so will be due to unknown causes or measurement errors in experiments, there exists some variability. Every experimental data set is most likely to shown certain variability, but whether such change is due to inputs factors or due to random factors is to be answered by Analysis of Variance (ANOVA). The method tries to carry out the following.

- Decomposes the deviation of the experimental data in relation to possible sources; the source may be from the main effect, from the interaction, or may be from experimental error.
- Measures the magnitude of variation due to all sources.
- Recognize the main and interactions effects which have significant effects on variation of data.

B.5.1 Sum of squares (SS)

The distance between any point in a set of data and the mean of the data is the deviation. Sum of Squares is the sum of all such squared deviations. SS_{Total} is the total variation in the data. $SS_{Regression}$ is the portion of the variation explained by the model, while SS_{Error} is the portion not explained by the model and is attributed to error. The calculations are:

$$SS_{Total} = \sum_{i}^{n}\sum_{j}^{r}(y_{ij} - \bar{y}_{..})^2 \tag{B.2}$$

$$SS_{Error} = \sum_{i}^{n}\sum_{j}^{r}(y_{ij} - \hat{y}_{i})^2 \tag{B.3}$$

$$SS_{Regression} = SS_{Total} - SS_{Error} \tag{B.4}$$

where $y_{ij} = i^{th}$ observed response of j^{th} replicate, $\hat{y}_i = i^{th}$ fitted response, and $\bar{y}_{..}$ = mean of all $(n \times r)$ observations.

The sum of squares for r set of replicates are calculated and added together to create the pure error sum of squares (SS_{PE}). Sum of square error SS_{Error} is the sum of pure error sum of squares SS_{PE} and sum of squares lack of fit SS_{LOF}.

$$SS_{PE} = \sum_{i}^{n}[\sum_{j}^{r}(y_{ij} - \bar{y}_{i.})^2] \quad \text{(B.5)}$$

$$SS_{LOF} = SS_E - SS_{PE} \quad \text{(B.6)}$$

where $\bar{y}_{i.}$ = mean of r replicates of i^{th} observed response.

B.5.2 Degree of freedom

It depicts the number of independent variables needed to calculate the sum of squares the response data. The degrees of freedom for each component of the model are:

$$\begin{aligned} DF_{Regression} &= t - 1 \\ DF_{Error} &= n - t \\ DF_{Total} &= n - 1 \\ DF_A &= a - 1 \\ DF_B &= b - 1 \\ DF_{AB} &= (a-1)(b-1) \\ DF_{PE} &= n - m \end{aligned} \quad \text{(B.7)}$$

where n = number of observations, t = number of terms in the model, a, b = number of levels of factors A and B, respectively. DOF of pure error DF_{PE} is n - m, where n = number of observations and m = the number of distinct x-values.

B.5.3 Mean square

In an ANOVA, the term Mean Square refers to an estimate of the population variance based on the variability among a given set of measures. The calculation for the mean square for the model terms is:

$$MS_{Term} = \frac{AdjSS_{Term}}{DF_{Term}} \quad \text{(B.8)}$$

F-value:

F-value is the measurement of distance between individual distributions. More

the F-value, less is the P-value. F is a test to determine whether the interaction and main effects are significant. The formula for the model terms is:

$$F = \frac{MS_{Term}}{MS_{Error}} \tag{B.9}$$

Larger values of F support rejecting the null hypothesis that there is not a significant effect

P-value:

P-value is used in hypothesis tests helps to decide whether to reject or fail to reject a null hypothesis. The p-value is the probability of obtaining a test statistic that is at least as extreme as the actual calculated value, if the null hypothesis is true. A commonly used cut- off value for the p-value is 0.10.

B.5.4 Model adequacy check

The adequacy of the underlying model can be checked from ANOVA as follows: It is always necessary to examine the fitted model to ensure that it provides an adequate approximation to the true system.

R^2 (R-sq):

Coefficient of determination; indicates how much variation in the response is explained by the model. The higher the R^2, the better the model fits your data. The formula is:

$$R^2 = 1 - \frac{SS_{Error}}{SS_{Total}} \tag{B.10}$$

Another presentation of the formula is:

$$R^2 = \frac{SS_{Regression}}{SS_{total}} \tag{B.11}$$

Adjusted R^2 (R-sq adj): Adjusted R^2 accounts for the number of factors in your model. The formula is:

$$R^2 = 1 - \frac{MS_{(Error)}}{SS_{Total}/DF_{Total}} \tag{B.12}$$

Lack-of-fit test: This test checks the straight line fit of the model. To calculate the pure error lack-of-fit test:

1. Calculate the pure error mean square:

$$MS_{PE} = \frac{SS_{PE}}{DF_{PE}}$$

2. Calculate the lack-of-fit mean square:

$$MS_{LOF} = \frac{SS_{LOF}}{DF_{SSE} - DF_{PE}}$$

3. Calculate the F-statistic = MS_{LOF}/MS_{PE} and corresponding p-value.

   Large F-values and small p-values suggest that the model is inadequate.

C. WAVELET TRANSFORMATION

C.1 Introduction to the Wavelet transformation

Wavelet analysis decomposes sounds and images into component waves, called wavelet, of varying duration [James, 2008]. The wavelet transform has become a powerful tool for an identification of signal and image processing applications. It is useful for the capturing the digital image files and for transmitting images faster and more consistently [Selesnick, 2007]. Nowadays, wavelet transformation is commonly applied to the time-frequency- transformations.

The wavelet transform can be categorised into Continuous Wavelet Transforms (CWT) and Discrete Wavelet Transforms (DWT). The signal divided into continuous-time function and wavelets by using CWT. Different Fourier transform, the continuous wavelet transform keeps the capacity to construct a time-frequency representation of a signal that offers accurate time and frequency localization. This section delivers a formal scientific definition of the DWT.

C.1.1 Discrete wavelet transforms

The signals which is described by a sequence of numbers or pairs of numbers is called discrete signals [Shih and Shu, 2009]. DWT is the separately sampled for numerical analysis and functional analysis is any wavelet transform. The main advantage it has over Fourier transforms is chronological resolution: it captures both frequency and time information. These coefficients in wavelet transform can be compressed more easily because the information is statistically concentrated in just a few coefficients. This principle is called 'transform coding' and is presented in Equation C.1.

$$\begin{aligned} C(a,b) \qquad &= \int_R s(t)\tfrac{1}{\sqrt{a}}\psi\left(\tfrac{t-b}{a}\right)dt \\ &(a=2^j, b=k2^j, (j,k)\in \mathbf{Z}^2) \end{aligned} \tag{C.1}$$

where $s(t)$ is the original signal and $\psi(t)$ is a wavelet function that satisfies the admissible condition. The scaling and shifting parameters in the wavelet transform are a and b, respectively, [Jiang et al., 2012]. A small scaling parameter relates to a compressed wavelet function. As a result, the quickly changing features in the signal $s(t)$, *i.e.* high- frequency components, can be found from the wavelet transform by using a small scaling parameter.

The original signal is decomposed as well as down sampled in wavelet decomposition. The signal passes through a low-pass and high-pass filters and emerge as two signals, one signal being the high-scaled low frequency components and the other being low scaled high frequency components. The decomposition process is iterative and with successive iteration, the one signal is broken down into lower level resolutions. The number of decomposition level can be obtained by trial and error method. An efficient method has been suggested by Mallat [1989] for deionising signals with filters.

Of many types of DWT, Daubechies wavelets is quite popular. It is based on the use of recurrence relations to produce increasingly finer discrete samplings of an contained mother wavelet function. There are a intimate of orthogonal wavelets defining a discrete wavelet transform and characterized by a maximal number of vanishing moments for some given support. With each wavelet type of this class, there is a scaling function (called the father wavelet) which generates an orthogonal multi resolution analysis.

REFERENCES

Abu Zeid, O. (1996). The role of voltage pulse off-time in the electrodischarge machined AISI T1 high-speed steel. *Journal of Materials Processing Technology*, 61(3):287–291.

Ali, M. Y. and Mohammad, A. S. (2008). Experimental study of conventional wire electrical discharge machining for microfabrication. *Materials and Manufacturing Processes*, 23(7):641–645.

Amini, S., Atefi, R., and Solhjoei, N. (2010). The influence of EDM parameters in finishing stage on surface quality of hot work steel using artificial neural network. In *AIP Conference Proceedings*, volume 1315, pages 1228–1233.

Amorima, F. and Weingaertner, W. (2005). The influence of generator actuation mode and process parameterson the performance of finish EDM of a tool steel. *Journal of Materials Processing Technology*, 166:411–416.

Amorima, F. and Weingaertner, W. (2007). The behavior of graphite and copper electrodes on the finish die-sinking Electrical Discharge Machining (EDM) of AISI P20 tool steel. *Journal of the Brazilian Society of Mechanical Sciences and Engineering*, 29:367–371.

Aslan, N. (2008). Multi-objective optimization of some process parameters of a multi-gravity separator for chromite concentration. *Separation and Purification Technology*, 64(2):237–241.

Assarzadeh, S. and Ghoreishi, M. (2013). A dual response surface-desirability approach to process modeling and optimization of Al2O3 powder-mixed electrical discharge machining (pmedm) parameters. *International Journal of Advanced Manufacturing Technology*, 64(9-12):1459–1477.

Awasthi, A., Chauhan, S. S., and Goyal, S. K. (2010). A fuzzy multicriteria approach for evaluating environmental performance of suppliers. *International Journal of Production Economics*, 126(2):370–378.

Baraskar, S., Banwait, S., and Laroiya, S. (2013). Multiobjective optimization of electrical discharge machining process using a hybrid method. *Materials and Manufacturing Processes*, 28(4):348–354.

Beri, N., Kumar, A., Maheshwari, S., and Sharma, C. (2011a). Optimisation of electrical discharge machining process with cuw powder metallurgy electrode using grey relation theory. *International Journal of Machining and Machinability of Materials*, 9(1-2):103–115.

Beri, N. b., Maheshwari, S., Sharma, C., and Kumar, A. b. (2011b). Multi-objective parametric optimisation during electrical discharge machining of inconel 718 with different electrodes. *International Journal of Materials Engineering Innovation*, 2(3-4):236–248.

Bhattacharyya, B., Gangopadhyay, S., and Sarkar, B. R. (2007). Modelling and analysis of EDMed job surface integrity. *Journal of Materials Processing Technology*, 189(1-3):169–177.

Bleys, P., Kruth, J., Lauwers, B., Zryd, A., Delpretti, R., and Tricarico, C. (2002). Real-time tool wear compensation in milling EDM. *CIRP Annals - Manufacturing Technology*, 51(1):157–160.

Boothroyd, G. and Winston, A. K. (1989). *Non-Conventional Machining Processes. Fundamentals of Machining and Machine Tools.* Marcel Dekker, New York, p 491.

Catalkaya, E. and Sengul, F. (2006). Application of box-wilson experimental design method for the photo degradation of bakery's yeast industry with UV/H2O2 and UV/H2O2/Fe(II) process. *Journal of Hazardous Material*, 128:201–207.

Caydas, U. and Hascalik, A. (2007). Modeling and analysis of electrode wear and white layer thickness in die-sinking EDM process through response surface

methodology. *International Journal of Advanced Manufacturing Technology*, 38(11-12):1148–1156.

Caydas, U., Hascalik, A., and Ekici, S. (2009). An adaptive neuro-fuzzy inference system (ANFIS) model for wire-EDM. *Expert Systems with Applications*, 36(3-2):6135–6139.

Chakravorty, R., Gauri, S., and Chakraborty, S. (2013). A study on the multi-response optimisation of EDM processes. *International Journal of Machining and Machinability of Materials*, 13(1):91–109.

Chakravorty, R., Gauri, S. K., and Chakraborty, S. (2012a). Optimisation of the correlated responses of EDM process using modified principal component analysis-based utility theory. *International Journal of Manufacturing Technology and Management*, 26(1-4):21–38.

Chakravorty, R., Gauri, S. K., and Chakraborty, S. (2012b). Optimization of correlated responses of EDM process. *Materials and Manufacturing Processes*, 27:337347.

Chen, D., Jhang, J., and Guo, M. (2013). Application of taguchi design method to optimize the electrical discharge machining. *Journal of Achievements in Materials and Manufacturing Engineering*, 57:76–82.

Chen, S. and Lee, L. (2010). Fuzzy multiple attributes group decision-making based on the interval type-2 topsis method. *Expert Systems with Applications*, 37(4):2790–2798.

Chiang, K. (2008). Modeling and analysis of the effects of machining parameters on the performance characteristics in the EDM process of Al2O3+TiC mixed ceramic. *International Journal of Advanced Manufacturing Technology*, 37(5-6):523–533.

Cogun, C. and Savsar, M. (1990). Statistical modelling of properties of discharge pulses in electric discharge machining. *International Journal of Machine Tools and Manufacture*, 30:467–474.

Curodeau, A., Marceau, L. F., Richard, M., and Lessard, J. (2005). New EDM polishing and texturing process with conductive polymer electrodes. *Journal of Materials Processing Technology*, 159(1):17–26.

Curodeau, A., Richard, M., and Frohn-Villeneuve, L. (2004). Molds surface finishing with new EDM process in air with thermoplastic composite electrodes. *Journal of Materials Processing Technology*, 149(1-3):278–283.

Das, M., Kumar, K., Barman, T., and Sahoo, P. (2012). Optimization of material removal rate in EDM using taguchi method. *Advanced Materials Engineering and Technology*, 626:270–274.

Dauw, D. and Snoeys, R. (1986). On the derivation and application of a real-time tool wear sensor in EDM. *CIRP Annals - Manufacturing Technology*, 35(1):111–116.

Dauw, D. F., Snoeys, R., and Dekeyser, W. (1983). Advanced pulse discriminating system for EDM process analysis and control. *CIRP Annals - Manufacturing Technology*, 32(2):541–549.

Dave, H., Desai, K., and Raval, H. (2012). Optimisation of multiple response characteristics in orbital electro discharge machining of Inconel 718 using taguchi's loss function. *International Journal of Manufacturing Technology and Management*, 25(1-3):78–94.

Dhanabalan, S., Sivakumar, K., and Sathiya Narayanan, C. (2012). Optimization of EDM process parameters with multiple performance characteristics for titanium grades. *European Journal of Scientific Research*, 68(3):297–305.

Dhar, S., Purohit, R., Saini, N., Sharma, A., and Kumar, G. H. (2007). Mathematical modeling of Electric - Discharge Machining of cast Al-4Cu-6Si alloy-10 wt.% SiC_p composites. *Journal of Materials Processing Technology*, 194(1-3):24–29.

Droza, T. J. (1998). *Tool and Manufacturing Engineering; Handbook; Machining*. USA: Society of Manufacturing Engineering.

Dvivedi, A., Kumar, P., and Singh, I. (2008). Experimental investigation and optimisation in EDM of al 6063 SiCp metal matrix composite. *International Journal of Machining and Machinability of Materials*, 3(3-4):293 – 308.

Ekmekci, B. (2007). Residual stresses and white layer in electric - discharge machining (EDM). *Applied Surface Science*, 253:9234–9240.

Ekmekci, B. (2009). White layer composition, heat treatment, and crack formation in electric - discharge machining process. *Metallurgical and Materials Transactions B: Process Metallurgy and Materials Processing Science*, 40(1):70–81.

Ekmekci, B., Elkoca, O., Tekkaya, A. E., and Erden, A. (2005). Residual stress state and hardness depth in electric discharge machining: De-ionized water as dielectric liquid. *Machining Science and Technology*, 9(1):39–61.

Ekmekci, B., Tekkaya, A. E., and Erden, A. (2006). A semi-empirical approach for residual stresses in electric discharge machining (EDM). *International Journal of Machine Tools and Manufacture*, 46:858–868.

El-Taweel, T. (2008). Multi-response optimization of EDM with Al-Cu-Si-TiC P/M composite electrode. *International Journal of Advanced Manufacturing Technology*, pages 1–14.

Erden, A. (1983). Effect of materials on the mechanism of electric discharge machining. *Journal of Engineering Materials and Technology*, 108:247–251.

Esme, U., Sagbas, A., and Kahraman, F. (2009). Prediction of surface roughness in wire electrical discharge machining using design of experiments and neural networks. *Iranian Journal of Science and Technology, Transaction B: Engineering*, 33(3):231–240.

Gadalla, A. and Tsai, W. (1989). Machining of WC-Co composites. *Materials and Manufacturing Processes*, 4(3):411–423.

Gaitonde, V. N., Karnik, S. R., Achyutha, B. T., and Siddeswarappa, B. (2006). Multi-responce optimization in drilling using Taguchi loss function. *Indian Journal of Engineering and Materials Science*, 13(6):484–488.

Gangadhar, A., Shunmugam, M., and Philip, P. K. (1992). Pulse train studies in EDM with controlled pulse relaxation,. *International Journal of Machine Tools and Manufacture*, 32 (5):651–657.

Garg, R. K., Singh, K. K., and Sachdeva, A. (2010). Review of research work in sinking EDM and WEDM on metal matrix composite materials. *The International Journal of Advanced Manufacturing Technology*, 50:611–624.

Gauri, S. K. and Chakraborty, S. (2009a). Multi-response optimisation of WEDM process using principal component analysis. *International Journal of Advanced Manufacturing Technology*, 41(7-8):741–748.

Gauri, S. K. and Chakraborty, S. (2009b). Optimisation of multiple responses for wedm processes using weighted principal components. *International Journal of Advanced Manufacturing Technology*, 40(11-12):1102–1110.

Ghoreishi, M. and Tabari, C. (2007). Investigation into the effect of voltage excitation of pre-ignition spark pulse on the Electro-Discharge Machining (EDM) process. *Materials and Manufacturing Processes*, 22(7):833–841.

Ghosh, A. and Mallik, A. K. (1985). *Manufacturing Science*. Affiliated East-West Press Private Limited.

Golshan, A., Gohari, S., and Ayob, A. (2012). Multi-objective optimisation of electrical discharge machining of metal matrix composite Al/SiC using non-dominated sorting genetic algorithm. *International Journal of Mechatronics and Manufacturing Systems*, 5(5-6):385–398.

Gopalakannan, S. and Senthilvelan, T. (2013). Application of response surface method on machining of Al-SiC nano-composites. *Measurement: Journal of the International Measurement Confederation*, 46(8):2705–2715.

Gopalakannan, S., Senthilvelan, T., and Kalaichelvan, K. (2012). Modeling and optimization of EDM of Al 7075/10wtmatrix composites by response surface method. *Advanced Materials Research*, 488-489:856–860.

Gostimirovic, M., Rodic, D., Kovac, P., Pucovsky, V., and Sekulic, M. (2012). Modeling of material removal rate in EDM using neural fuzzy systems. *Jounal of production Engineering*, 16(1):1–4.

Guleryuz, L. F., Ozan, S., Kasman, S., and Ipek, R. (2013). The influence of process parameters of EDM on the surface roughness of aluminum matrix composites reinforced with sic particulates. *Acta Physica Polonica A*, 123(2):421–423.

Guu, Y. H. (2005). Afm surface imaging of AISI D2 tool steel machined by the EDM process. *Applied Surface Science*, 242:245–250.

Guu, Y. H. and Hocheng, H. (2001). Improvement of fatigue life of electrical discharge machined AISI D2 tool steel by TiN coating. *Materials Science and Engineering A*, 318:155–162.

Guu, Y. H., Hocheng, H., Chou, C. Y., and Deng, C. S. (2003). Effect of electrical discharge machining on surface characteristics and machining damage of AISI D2 tool steel. *Materials Science and Engineering*, 358:37–43.

Habib, S. S. (2009). Study of the parameters in electrical discharge machining through response surface methodology approach. *Applied Mathematical Modelling*, 33(12):4397–4407.

Hascalik, A. and Caydas, U. (2007). Electrical discharge machinings of titanium alloy (Ti-6Al-4V). *Applied Surface Science*, 253:9007–9016.

Ho, K. H. and Newman, S. T. (2003). State of the art electrical discharge machinings (EDM). *International Journal of Machine Tools and Manufacture*, 43:1287–1300.

Huertas Talon, J. L., Cisneros Ortega, J. C., Lopez Gomez, C., Ros Sancho, E., and Faci Olmos, E. (2010). Manufacture of a spur tooth gear in ti-6al-4v alloy by electrical discharge. *CAD Computer Aided Design*, 42(3):221–230.

Izquierdo, B., Sanchez, J., Plaza, S., Pombo, I., and Ortega, N. (2009). A numerical model of the EDM process considering the effect of multiple discharges. *International Journal of Machine Tools and Manufacture*, 49(3-4):220–229.

Jaharah, A. G., C.G.Liang, Wahid, S. Z., Rahman, M. N. A., and Hassan, C. H. C. (2008). Performance of copper electrode in electrical discharge machinings (EDM) of AISI H13 harden steel. *International Journal of Mechanical and Materials Engineering*, 3(1):25–29.

James, S. W. (2008). *A primer on WAVELETS and their scientific applications*. Chapman and Hall, Taylor & Francis Group, LIC.

Janmanee, P., Jamkamon, K., and Muttamara, A. (2012). Investigation of electrical discharge machining of tungsten carbide using EDM-C3 electrode material. *European Journal of Scientific Research*, 76(1):133–142.

Jeswani, M. (1981). Electrical discharge machinings in distilled water. *Wear*, 72(1):81–88.

Jia, Z., Zheng, X., Wang, F., Liu, W., and Zhou, M. (2011). A progressive mapping method for classifying the discharging states in micro-electrical discharge machining. *International Journal of Advanced Manufacturing Technology*, 56(1-4):197–204.

Jiang, Y., Zhao, W., Xi, X., Gu, L., and Kang, X. (2012). Detecting discharge status of small-hole EDM based on wavelet transform. *International Journal of Advanced Manufacturing Technology*, 61(1-4):171–183.

Joshi, S. and Pande, S. (2009). Development of an intelligent process model for EDM. *International Journal of Advanced Manufacturing Technology*, 45(3-4):300–317.

Joshi, S. and Pande, S. (2010). Thermo-physical modeling of die-sinking EDM process. *Journal of Manufacturing Processes*, 12(1):45–56.

Joshi, S. N. and Pande, S. S. (2011). Intelligent process modeling and optimization of die-sinking electric discharge machining. *Applied Soft Computing Journal*, 11(2):2743–2755.

Jung, J. H. and Kwon, W. T. (2010). Optimization of EDM process for multiple performance characteristics using Taguchi method and Grey relational analysis. *Journal of Mechanical Science and Technology*, 24(5):1083–1090.

Kanagarajan, D., Karthikeyan, R., Palanikumar, K., and Sivaraj, P. (2008). Influence of process parameters on electric - discharge machining of WC/30%Co composites. *Proceedings of the Institution of Mechanical Engineers, Part B: Journal of Engineering Manufacture*, 222(7):807–815.

Kanlayasiri, K. and Jattakul, P. (2013). Simultaneous optimization of dimensional accuracy and surface roughness for finishing cut of wire-EDMed K460 tool steel. *Precision Engineering*, 37(3):556–561.

Kansal, H. K., Singh, S., and Kumar, P. (2007). Effect of silicon powder mixed EDM on machining rate of AISI D2 die steel. *Journal of Manufacturing Processes*, 9(1):13–22.

Kao, C. C., Tao, J., and Shih, A. J. (2007). Near dry electrical discharge machinings. *International Journal of Machine Tools and Manufacture*, 47:2273–2281.

Karthikeyan, R., Lakshmi Narayanan, P. R., and Naagarazan, R. S. (1999). Mathematical modelling for Electric - Discharge Machining of aluminium-silicon carbide particulate composites. *Journal of Materials Processing Technology*, 87:59–63.

Keskin, Y., Halkaci, H., and Kizil, M. (2006). An experimental study for determination of the effects of machining parameters on surface roughness in Electrical Discharge Machinings (EDM). *International Journal of Advanced Manufacturing Technology*, 28(11-12):1118–1121.

Khan, A. (2008). Electrode wear and material removal rate during EDM of aluminum and mild steel using copper and brass electrodes. *International Journal of Advanced Manufacturing Technology*, 39(5-6):482–487.

Khan, A., Ali, M., and Haque, M. (2009). A study of electrode shape configuration on the performance of die sinking EDM. *International Journal of Mechanical and Materials Engineering*, 4(1):19–23.

Khanra, A. K., Patra, S., and Godkhindi, M. M. (2006). Electrical discharge machining studies on reactive sintered FeAl. *Bulletin of Materials Science*, 29(3):277–280.

Kiyak, M. and Cakir, O. (2007). Examination of machining parameters on surface roughness in EDM of tool steel. *Journal of Materials Processing Technology*, 191(1-3):141–144.

Kodlinge, P. G. and Khire, M. (2013). Some studies on machinability of tungsten carbide during EDM operations. *International Journal of Engineering Science and Technology*, 3(1):10–13.

Kruth, J., Stevens, L., Froyen, L., and Lauwers, B. (1995). Study of the white layer of a surface machined by die-sinking electro-discharge machining. *CIRP Annals - Manufacturing Technology*, 44(1):169 – 172.

Kumar, N., Kumar, L., Tewatia, H., and Yadav, R. (2012). Comparative study for MRR on die-sinking EDM using electrode of copper & graphite. *International Journal of Advanced Technology & Engineering Research*, 2(2):170–174.

Kumar, S. and Singh, T. P. (2007). A comparative study of the performance of different EDM electrode materials in two dielectric media. *IE(I) Journal-PR*, 97.

Kung, K. and Chiang, K. (2008). Modeling and analysis of machinability evaluation in the wire electrical discharge machining (WEDM) process of aluminum oxide-based ceramic. *Materials and Manufacturing Processes*, 23(3):241–250.

Kung, K. Y., Horng, J. T., and Chiang, K. T. (2009). Material removal rate and electrode wear ratio study on the powder mixed Electrical Discharge Machinings of cobalt-bonded tungsten carbide. *International Journal of Advanced Manufacturing Technology*, 40(1-2):95–104.

Kunieda, M. and Kobayashi, T. (2004). Clarifying mechanism of determining tool electrode wear ratio in EDM using spectroscopic measurement of vapor density. *Journal of Materials Processing Technology*, 149(1-3):284–288.

Kunieda, M. and Masuzawa, T. (1988). A fundamental study on a horizontal EDM. *CIRP Annals - Manufacturing Technology*, 37(1):187–190.

Kuppan, P., Rajadurai, A., and Narayanan, S. (2007). Influence of EDM process parameters in deep hole drilling of inconel 718. *International Journal of Advance Manufacturing Technology*, 38:74–84.

Kuruvila, N. and Ravindra, H. V. (2011). Parametric influence and optimization of wire EDM of hot die steel. *Machining Science and Technology*, 15:47–75.

Lajis, M. A., Mohd Radzi, H. C. D., and Nurul Amin, A. K. M. (2009). The implementation of taguchi method on EDM process of tungsten carbide. *European Journal of Scientific Research*, 26(4):609–617.

Lee, H. T., Hsu, F. C., and Tai, T.-Y. (2004). Study of surface integrity using the small area EDM process with a copper-tungsten electrode. *Materials Science and Engineering A*, 364:346–356.

Lee, H. T. and Tai, T. Y. (2003). Relationship between EDM parameters and surface crack formation. *Journal of Materials Processing Technology*, 142:676–683.

Lee, L., Lim, L., and Wong, Y. (1990.). Towards a better understanding of the surfac features of electro-discharge machined tool steels. *Journal of Materials Processing Technology*, 24:513–523.

Lee, L., Lim, L., and Wong, Y. (1992). Towards crack minimisation of EDMed surfaces. *Journal of Materials Processing Tech.*, 32(1-2):45–54.

Lee, S. H. and Li, X. (2003). Study of the surface integrity of the machined workpiece in the EDM of tungsten carbide. *Journal of Materials Processing Technology*, 139:315–321.

Lee, S. H. and Li, X. P. (2001). Study of the effect of machining parameters on the machining characteristics in Electrical Discharge Machinings of tungsten carbide. *Journal of Materials Processing Technology*, 115(3):344–358.

Lee, T. C. and Lau, W. S. (1991). Some characteristics of electrical discharge machinings of conductive ceramics,. *Materials and Manufacturing Processes*, 6 (4):635–648.

Lim, L., Lee, L., Wong, Y., and Lu, H. (1991). Solidification microstructure of electrodischarge machined surfaces of tool steels. *Materials Science and Technology*, 7(3):239–248.

Lin, J. L. and Lin, C. L. (2005). The use of the grey-fuzzy logic for the optimization of the manufacturing process. *Journal of Manufacturing Process Technology*, 160:9–14.

Lin, J. L., Wang, K., Yan, B., and Tarng, Y. S. (2000). Optimization of the Electrical Discharge Machinings process based on the taguchi method with fuzzy logics. *Journal of Materials Processing Technology*, 102(1):48–55.

Lin, K. W. and Wang, C. C. (2010). Optimizing multiple quality characteristics of Wire Electrical Discharge Machining via Taguchi method-based gray analysis for magnesium alloy. *Journal of CCIT*, 39(1):23–34.

Lin, Y., Chen, Y., Lin, C., and Tzeng, H. (2008). Electrical discharge machining (EDM) characteristics associated with electrical discharge energy on machining of cemented tungsten carbide. *Materials and Manufacturing Processes*, 23(4):391–399.

Lin, Y., Cheng, C., Su, B., and Hwang, L. (2006). Machining characteristics and optimization of machining parameters of SKH 57 high-speed steel using electrical-discharge machining based on Taguchi method. *Materials and Manufacturing Processes*, 21(8):922–929.

Mahdavinejad, R. A. and Mahdavinejad, A. (2005). ED machining of WC-Co. *Journal of Materials Processing Technology*, 162-163(SPEC. ISS.):637–643.

Mallat, S. G. (1989). Theory for multiresolution signal decomposition: the wavelet representation. *IEEE Transactions on Pattern Analysis and Machine Intelligence*, 11(7):674–693.

Mamalis, A., Vosniakos, G., Vacevanidis, N., and Junzhe, X. (1988). Residual stress distribution and structural phenomena of high-strength steel surfaces due to EDM and ball-drop forming. *CIRP Annals - Manufacturing Technology*, 37(1):531–535.

Mamalis, A. G., Vosniakos, G. C., Vaxevanidis, N. M., and Prohaszka, J. (1987). Macroscopic and microscopic phenomena of electro-discharge machined steel surfaces: An experimental investigation. *Journal of Mechanical Working Technology*, 15:335–356.

Marafona, J. and Wykes, C. (2000). A new method of optimising material removal rate using EDM with copper tungsten electrodes. *International Journal of Machine Tools and Manufacture*, 40:153–164.

Marafona, J. D. and Araujo, A. (2009). Influence of workpiece hardness on EDM performance. *International Journal of Machine Tools and Manufacture*, 49(9):744–748.

Matlab (2011). *Global Optimization Toolbox Users Guide*. The MathWorks, Inc. Natick, 2011.

Minitab16 (2011). *Minitab User Manual Release 16*. State College, PA, USA,.

Mohan, B., Rajadurai, A., and Satyanarayana, K. G. (2002). Effect of SiC and rotation of electrode on Electric Discharge Machining of Al-SiC composite. *Journal of Materials Processing Technology*, 124:297–304.

Mohd Abbas, N., Solomon, D. G., and Fuad Bahari, M. (2007). A review on current research trends in electrical discharge machining (EDM). *International Journal of Machine Tools and Manufacture*, 47:1214–1228.

Mohri, N., Suzuki, M., Furuya, M., Saito, N., and Kobayashi, A. (1995). Electrode wear process in electrical discharge machinings. *CIRP Annals - Manufacturing Technology*, 44(1):165–168.

Mohri, N., Takezawa, H., Furutani, K.and Ito, Y., and Sata, T. (2000). New process of additive and removal machining by EDM with a thin electrode. *CIRP Annals - Manufacturing Technology*, 49(1):123–126.

Montgomery, D. C. (2001). *Design and Analysis of Experiments*. Wiley, New York.

Mukherjee, R. and Chakraborty, S. (2012). Selection of EDM process parameters using biogeography-based optimization algorithm. *Materials and Manufacturing Processes*, 27:954–962.

Murugesan, S. and Balamurugan, K. (2012). Optimization by grey relational analysis of EDM parameters in machining Al-15% SiC MMC using multihole electrode. *Journal of Applied Sciences*, 12(10):963–970.

Myers, R. and Montgomery, D. (1995). *Response Surface Methodology, Process and Product Optimization Using Designed Experiments.* Wiley, New York.

Natarajan, N. and Arunachalam, R. M. (2011). Optimization of Micro-EDM with multiple performances characteristics using Taguchi method and Greyrelation analysis. *Journal of Scientific and Industrial Research*, 70(7):500–505.

Ndaliman, M., Hazza, M., Khan, A. A., and Ali, M. Y. (2012). Development of a new model for predicting EDM properties of Cu-TaC compact electrodes based on artificial neural network method. *Indian Journal of Applied Research*, 6:192–199.

Padhee, S., Nayak, N., Panda, S. K., Dhal, P. R., and Mahapatra, S. S. (2012). Multi-objective parametric optimization of powder mixed electro-discharge machining using response surface methodology and non-dominated sorting genetic algorithm. *Sadhana - Academy Proceedings in Engineering Sciences*, 37(2):223–240.

Panda, D. (2010a). Parametric study of relative erosion of cathode and anode of sae L_7 low alloy tool steel in EDM using grey relational concept in L_9 orthogonal array. *International Journal of Machining and Machinability of Materials*, 7(3-4):226–247.

Panda, D. K. (2010b). Modelling and optimization of multiple process attributes of electrodischarge machining process by using a new hybrid approach of neuro-grey modeling. *Materials and Manufacturing Processes*, 25(6):450–461.

Pandey, A. K. and Dubey, A. K. (2012). Taguchi based fuzzy logic optimization of multiple quality characteristics in laser cutting of Duralumin sheet. *Optics and Lasers in Engineering*, 50(3):328–335.

Pandey, P. C. and Jilani, S. T. (1986). Plasma channel growth and the resolidified layer in EDM. *Precision Engineering*, 8:104–110.

Pandey, P. C. and Shan, H. S. (1980). *Modern Machining Processes*. Tata McGraw-Hill, New Delhi.

Pey Tee, K. T., Hosseinnezhad, R., Brandt, M., and Mo, J. (2013). Pulse discrimination for electrical discharge machining with rotating electrode. *Machining Science and Technology*, 17(2):292–311.

Prabhu, S. and Vinayagam, B. (2013). Multi objective optimisation of swcnt-based electrical discharge machining process using grey relational and fuzzy logic analysis. *International Journal of Machining and Machinability of Materials*, 13(4):439–463.

Prabhu, S. and Vinayagam, B. K. (2009). Effect of graphite electrode material on EDM of AISI D2 tool steel with multiwall carbon nanotube using regression analysis. *International Journal of Engineering Studies*, 1:93104.

Pradhan, D. and Jayswal, S. C. (2011). Behaviour of copper and aluminium electrodes on EDM of EN-8 alloy steel. *International Journal of Engineering Science and Technology*, 3(7):5492–5499.

Pradhan, M. and Biswas, C. (2010). Neuro-fuzzy and neural network-based prediction of various responses in electrical discharge machinings of AISI D2 steel - NF and NN based prediction of responses in EDM of D2 steel. *International Journal of Advanced Manufacturing Technology*, pages 1–20.

Pradhan, M. K. (2010). Experimental investigation and modelling of surface integrity, accuracy and productivity aspects in EDM of AISI D2 steel. *Ph. D. Thesis, NIT Rourkela*. ID Code : 2977.

Pradhan, M. K. (2012). Determination of optimal parameters with multi response characteristics of EDM by response surface methodology, grey relational analysis and principal component analysis. *International Journal of Manufacturing Technology and Management*, 26(1-4):56–80.

Pradhan, M. K. (2013). Estimating the effect of process parameters on MRR, TWR and radial overcut of EDMed AISI D2 tool steel by RSM and GRA coupled with PCA. *International Journal of Advanced Manufacturing Technology*, 68:591–605.

Prajapati, S. B., Patel, N. S., and Asal, V. D. (2013). Prediction of process parameters of wire EDM for AISI A2 using ANN. *Indian Journal of Applied Research*, 3:217–218.

Puertas, I. and Luis, C. J. (2004). A study of optimization of machining parameters for Electrical Discharge Machining of boron carbide. *Materials and Manufacturing Processes*, 19(6):1041–1070.

Puertas, I., Luis, C. J., and Alvarez, L. (2004). Analysis of the influence of EDM parameters on surface quality, MRR and EW of WC-Co. *Journal of Materials Processing Technology*, 153-154(1-3):1026–1032.

Puri, Y. M. and Deshpande, N. V. (2004). Simultaneous optimization of multiple quality characteristics of WEDM based on fuzzy logic and taguchi technique. *Fifth Asia Pacific Industrial Engineering and Management Systems Conference*, 14:18.1–18.12.

Rahman, M. M., Khan, M. A. R., Kadirgama, K., Noor, M. M., and Bakar, R. A. (2010). Mathematical modeling of material removal rate for Ti-5Al-2.5Sn through EDM process: A surface response method. In *European Conference of Chemical Engineering, ECCE'10, European Conference of Civil Engineering, ECCIE'10, European Conference of Mechanical Engineering, ECME'10, European Conference of Control, ECC'10*, pages 34–37.

Rajendran, S., Marimuthu, K., and Sakthivel, M. (2013). Study of crack formation and resolidified layer in EDM process on T90Mn2W50Cr45 tool steel. *Materials and Manufacturing Processes*, 28(6):664–669.

Rajurkar, K. and Pandit, S. (1988). Recent progress in electrical discharge machine technology and research. *Proceedings of Manufacturing International 88, Atlanta, GA,*, pages 219–226.

Ramasawmy, H., Blunt, L., and Rajurkar, K. (2005). Investigation of the relationship between the white layer thickness and 3d surface texture parameters in the die sinking EDM process. *Precision Engineering*, 29(4):479–490.

Rao, G. K. M., Satyanarayana, S., and Praveen, M. (2008). Influence of machining parameters on Electric Discharge Machining of maraging steels an experimental investigation. *Proceedings of the World Congress on Engineering*, 2:2–4.

Rebelo, J. C., Morao Dias, A., Kremer, D., and Lebrun, J. L. (1998). Influence of EDM pulse energy on the surface integrity of martensitic steels. *Journal of Materials Processing Technology*, 84:90–96.

Reddy, V., Reddy, H., and Kumar, V. (2010). Selection of cutting velocity in wire-EDM process using taguchi-fuzzy approach. *Journal of Manufacturing Technology Research*, 2(1-2):109–121.

Reza, M. S., Azmir, M. A., Tomadi, S. H., Hassan, M. A., and Daud, R. (2010). Effects of polarity parameter on machining of tool steel workpiece using electrical discharge machining. *National Conference in Mechanical Engineering Research and Postgraduate Students*, pages 621–626.

Roethel, F., Garbajs, V., and Kosec, L. (1976). Contribution to the micro-analysis of the spark eroded surfaces. *Ann CIRP*, 25(1):135–140.

Ross, P. J. (1988). Taguchi techniques for quality engineering. *McGraw-Hill,New york*.

Saha, S. K. and Choudhury, S. K. (2009). Experimental investigation and empirical modeling of the dry Electric Discharge Machining process. *International Journal of Machine Tools and Manufacture*, 49(3-4):297–308.

Salah, N. and Ghanem, F.and Atig, K. (2006). Numerical study of thermal aspects of Electric - Discharge Machining process. *International Journal of Machine Tools and Manufacture*, 46(7-8):908–911.

Salah, N. B., Ghanem, F., and Atig, K. B. (2008). Thermal and mechanical numerical modelling of electric discharge machining process. *Communications in Numerical Methods in Engineering*, 24(12):2021–2034.

Salonitis, K., Stournaras, A., Stavropoulos, and P., Chryssolouris, G. (2009). Thermal modeling of the material removal rate and surface roughness for die-sinking EDM. *International Journal of Advanced Manufacturing Technology*, 40(3-4):316–323.

Schumacher, B. (2004). After 60 years of EDM the discharge process remains still disputed. *Journal of Materials Processing Technology*, 149(1-3):376–381.

Selesnick, I. W. (2007). Wavelet transforms - a quick study. *Physics Today magazine*.

Shih, H. R. and Shu, K. M. (2008). A study of electrical discharge grinding using a rotary disk electrode. *International Journal of Advanced Manufacturing Technology*, 38(1-2):59–67.

Shih, H. R. and Shu, K. M. (2009). Application of wavelet transform and its advantages compared to fourier transform. *Journal of Physical Sciences*, 13:121–134.

Simao, J., Lee, H. G., Aspinwall, D. K., Dewes, R. C., and Aspinwall, E. M. (2003). Workpiece surface modification using Electrical Discharge Machinings. *International Journal of Machine Tools and Manufacture*, 43:121–128.

Singh, A. and Ghosh, A. (1999). A thermo-electric model of material removal during electric discharge machining. *International Journal of Machine Tools and Manufacture*, 39:669–682.

Singh, P. N., Raghukandan, K., and Pai, B. C. (2004a). Optimization by Grey relational analysis of EDM parameters on machining $Al - 10\%SiC_p$ composites. *Journal of Materials Processing Technology*, 155(1-3):1658–1661.

Singh, S., Maheshwari, S., and Pandey, P. (2004b). Some investigations into the Electric Discharge Machining of hardened tool steel using different electrode materials. *Journal of Materials Processing Technology*, 149(1-3):272–277.

Singh, S., Maheshwari, S., and Pandey, P. C. (2004c). Some investigations into the electric - discharge machining of hardened tool steel using different electrode materials. *Journal of Materials Processing Technology*, 149:272–277.

Sivapirakasam, S. P., Mathew, J., and Surianarayanan, M. (2011). Multi-attribute decision making for green electrical discharge machining. *Expert Systems with Applications*, 38(7):8370 – 8374.

Sivasankar, S., Jeyapaul, R., and Bhanu Prasad, V. (2012). Performance study of various tool materials for electrical discharge machining of hot pressed ZrB2. *Multidiscipline Modeling in Materials and Structures*, 8(4):505–523.

Snoeys, R., Staelens, F., and Dekeyser, W. (1986). Current trends in non-conventional material removal processes. *CIRP Annals - Manufacturing Technology*, 35(2):467–480.

Soni, J. S. and Chakraverti, G. (1996). Experimental investigation on migration of material during EDM of die steel (T215 Cr12). *Journal of Materials Processing Technology*, 56(1-4):439–451.

Soveja, A., Cicala, E., Grevey, D., and Jouvard, J. M. (2008). Optimisation of ta6v alloy surface laser texturing using an experimental design approach. *Optics and Lasers in Engineering*, 46(9):671–678.

Staelens, F. and Kruth, J. (1989). A computer integrated machining strategy for planetary EDM. *CIRP Annals - Manufacturing Technology*, 38(1):187–190.

Suganthi, X. H., Natarajan, U., Sathiyamurthy, S., and Chidambaram, K. (2013). Prediction of quality responses in micro-EDM process using an adaptive neuro-fuzzy inference system (ANFIS) model. *International Journal of Advanced Manufacturing Technology*, pages 1–9. Article in Press.

Thillaivanan, A.and Asokan, P., Srinivasan, K., and Saravanan, R. (2010). Optimization of operating parameters for EDM process based on the Taguchi method and artificial neural network. *International Journal of Engineering Science and Technology*, 2(12):6880–6888.

Thomson, P. (1989). Surface damage in electro discharge machining. *Materials Science and Technology*, 5(11):1153–1157.

Tosun, N. and Pihtili, H. (2010). Gray relational analysis of performance characteristics in mql milling of 7075 Al alloy. *International Journal of Advanced Manufacturing Technology*, 46(5-8):509–515.

Tsai, H., Yan, B., and Huang, F. (2003a). EDM performance of Cr/Cu-based composite electrodes. *International Journal of Machine Tools and Manufacture*, 43(3):245–252.

Tsai, H. C., Yan, B. H., and Huang, F. Y. (2003b). EDM performance of Cr/Cu-based composite electrodes. *International Journal of Machine Tools and Manufacture*, 43:245–252.

Tsai, K.-M. and Wang, P.-J. (2001a). Comparisons of neural network models on material removal rate in electrical discharge machinings. *Journal of Materials Processing Technology*, 117:111–124.

Tsai, K.-M. and Wang, P.-J. (2001b). Semi-empirical model of surface finish on electrical discharge machining. *International Journal of Machine Tools & Manufacture*, 41:1455–1477.

Tzeng, Y. and Chen, F. (2007). Multi-objective optimisation of high-speed Electrical Discharge Machining process using a Taguchi fuzzy-based approach. *Materials and Design*, 28(4):1159–1168.

Uysal, F. and Tosun, O. (2012). Fuzzy TOPSIS-based computerized maintenance management system selection. *Journal of Manufacturing Technology Management*, 23(2):212–228.

Wang, C. C. and Yan, B. H. (2000). Blind-hole drilling of Al2O3/6061Al composite using rotary electro-discharge machining. *Journal of Materials Processing Technology*, 102:90–102.

Wang, C. C.and Chow, H., Yang, L. D., and Lu, C. (2009). Recast layer removal after electrical discharge machinings via taguchi analysis: A feasibility study. *Journal of Materials Processing Technology*, 209(8):4134–4140.

Wang, P.-J. and Tsai, K.-M. (2001). Semi-empirical model on work removal and tool wear in electrical discharge machining. *Journal of Materials Processing Technology*, 114(1):1–17.

Wang, C. C.and Lin, Y. (2009). Feasibility study of Electrical Discharge Machinings for W/Cu composite. *International Journal of Refractory Metals and Hard Materials*, 27(5):872–882.

Wu, K. L., Yan, B. H., Huang, F. Y., and Chen, S. C. (2005). Improvement of surface finish on SKD steel using electro-discharge machining with aluminum and surfactant added dielectric. *International Journal of Machine Tools and Manufacture*, 45:1195–1201.

Yu, S. F., Lee, B. Y., and Lin, W. S. (2001). Waveform monitoring of electric discharge machining by wavelet transform. *International Journal of Advanced Manufacturing Technology*, 17(5):339–343.

Yu, Z., Masuzawa, T., and Fujino, M. (1998). Micro-EDM for three-dimensional cavities - development of uniform wear method. *CIRP Annals - Manufacturing Technology*, 47(1):169–x34.

Zeid, O. (1997). On the effect of electrodischarge machining parameters on the fatigue life of AISI D6 tool steel. *Journal of Materials Processing Technology*, 68(1):27–32.

Zhang, L., Jia, Z., Liu, W., and Li, A. (2012). A two-stage servo feed controller of micro-EDM based on interval type-2 fuzzy logic. *International Journal of Advanced Manufacturing Technology*, 59(5-8):633–645.

BIODATA

SHAILESH KUMAR DEWANGAN
E-mail- shaileshdewangan123@gmail.com
Mob: - + 91 9777523948

Personal Information:

Date of Birth: 04-02-1986

Nationality Indian

Address S/O- Sri Suresh Dewangan

57-Ashok Vihar Colony-II

Science College Road, Chantidhi, Bilaspur

Chattisgarh State, PIN-495001

EDUCATION

2013 Ph. D. Dissertation Submitted

2010 M.Tech, N.I.T. Rourkela.

PROFESSIONAL AFFILIATIONS

Member of the International Association of Engineers (IAENG). Member number 110578.

Member of the International Association of Computer Science and Information Technology (IACSIT). Member number 80340139.

Published papers in referred journals

1. S. Dewangan, C. K. Biswas and S. Gangopadhyay "Influence of different tool materials on EDM surface integrity of AISI P20 tool steel", *International Journal of Materials and Manufacturing Process*, DOI: 10.1080/10426914.2014.930892 (Accepted).

2. S. Dewangan and C. K. Biswas "Optimisation of Machining Parameters using Gray Relation Analysis for EDM with Impulse Flushing", *International Journal of Mechatronics and Manufacturing System*, Vol. 6, No. 2, 2013, pp. 144-157.

3. H. Dalai, S. Dewangan, S. Datta, S. K. Patel and S. S. Mahapatra "A Case Study on Quality and Productivity Optimization in Electric Discharge Machining (EDM)" *Advanced Materials Research, Trans Tech Publications, Switzerland*, DOI: 10.4028. Vol. 445, 2012, pp. 27-32.

4. S. Dewangan, C. K. Biswas, R. Ganjir, R. K. Sahu, A. K. Mondal, and K. K. Kanaujia "An Investigation on Electro Discharge Erosion of Mild Steel using Fuzzy Logic", *International journal of manufacturing technology and industrial engineering (IJMTIE)*, Vol. 2, No. 2, January-June 2011, pp. 67-72.

5. R. Sethy, C. K. Biswas and S. Dewangan "Multi Response Optimisation for Correlated Responses in EDM using Principal Component Analysis", *Advanced Materials Manufacturing & Characterization*, Vol. 3, No. 2, January-June 2013, pp. 520-523.

Communicated paper list

1. S. Dewangan, C. K. Biswas and S. Gangopadhyay "Multi-Response Optimization of Surface Integrity Characteristics of EDM Process using Grey-Fuzzy Logic-based Hybrid Approach", *International Journal of Advance Manufacturing Technology*, (Under Review).

2. S. Dewangan, C. K. Biswas and S. Gangopadhyay " Study of Surface Integrity and Dimensional accuracy in EDM using Fuzzy TOPSIS and Sensitivity Analysis", *Journal of the International Measurement Confederation*, (Under Review).

Articles presented in International/National Conferences

1. S. Dewangan, C. K. Biswas and S. Gangopadhyay, "Optimization of the quality and productivity characteristics of AISI P20 tool steel in EDM process using PCA-based grey relation analysis", in *5th International and 26th All India Manufacturing Technology, Design and Research Conference AIMTDR 2014*, Department of Mechanical Engineering, IIT Guwahati, Guwahati, India, Dec. 12-14, 2014 (Accepted for oral presentation).

2. S. Dewangan, C. K. Biswas and S. Gangopadhyay, "Modeling of surface roughness in EDM of AISI P20 tool steel", in *1st International Conference on Mechanical Engineering: Emerging Trends for Sustainability (IC MEETS 2014)*, M A N I T Bhopal, India. Jan. 29-31, 2014.

3. S. Dewangan, C. K. Biswas and S. Gangopadhyay, "Optimization of the Surface Integrity Characteristics of EDM Process using PCA based Grey Relation Investigation", in *3rd International Conference on Materials Processing and Characterisation (ICMPC 2014)*, GRIET, Hyderabad, March 8-9, 2014.

4. S. Dewangan, C. K. Biswas and R. Sethy, "Multiple Response Optimisation of EDM Process Using Grey-Fuzzy Logic Technique", in *3rd International Conference on Production and Industrial Engineering (CPIE-2013)*, NIT Jalandhar, India, Mar 29-31, 2013, pp. 756-759.

5. S. Dewangan and C. K. Biswas "ANN Model to Predict Surface Roughness of AISI P20 Tool Steel in EDM Process with Impulse Flushing", in *International Conference on Material Science (ICMS-2013)*, Tripura University Feb 21-23, 2013.

6. C. K. Biswas and S. Dewangan "Optimisation of EDM Process with Fuzzy Logic Technique", in *International conference on Metallurgical, Manufacturing and Mechanical Engineering (ICMMME-2012)*, Dubai (UAE), Dec. 26-27, 2012.

7. R. Sethy, S. Dewangan and C. K. Biswas "Multi Response Optimization for Correlated Responses in EDM using Principal Component Analysis" *2nd Annual International Conferences on Material Processing and Characterization (ICMPC 2013)*, Gokaraju Rangaraju Institute of Engineering and Technology Bachupally, Hyderabad, India16-17 March 2013, pp-207-209.

8. S. Dewangan and C. K. Biswas "Experimental Investigation of Machining Parameters for EDM Using U-Shaped Electrode of AISI P20 Tool Steel" *International Conference on Emerging Trends in Mechanical Engineering (ICETME-2011)*, Thapar University, Patiala (India), Feb 24-26, 2011, pp-348-352.

9. S. Dewangan, C. K. Biswas, R. Ganjir, R. K. Sahu, A. K. Mondal, and K. K. Kanaujia "An Investigation on Electro Discharge Erosion of Mild Steel using Fuzzy Logic", *5th International Conference on Advances in Mechanical Engineering (ICAME-2011)*, S.V. N.I.T., Surat, Gujarat, India, June 06-08, 2011, pp- 706-710.

10. R. Ganjir, C. K. Biswas and S. Dewangan "Estimation of MRR on Electrochemical machining by using Taguchi Method" *International conference on innovative science & Engineering Technology- 2011*, V.V.P. Engineering college, Rajkot, Gujarat (India), April 08-09, 2011 ISBN 978-81-906377-9-4 pp- 362-365.

11. H. Dalai, S. Dewangan, S. Datta , S.K. Patel, S.S. Mahapatra and C.K. Biswas "A case study on quality and productivity optimization in Electric Discharge Machining (EDM)", *14th International Conference in Advanced Materials and Processing Technologies AMPT-2011*, Istanbul Turkey, 13-16 July.

12. S. Dewangan, C. K. Biswas and S. N. Sahu "Selection of machining parameter in EDM process with impulse flushing system using three different electrode materials" *AICTE Sponsored National Conference on Emerging Trend & its*

Application in Engineering (NCETAE 2011), IGIT Sarang (Odisha), Dec.26-58, 2011, PP- 120-124.

Compliance Report as per comments by PhD thesis examiners

Made by
Shailesh Kumar Dewangan
Department of Mechanical Engineering
National Institute of Technology,
Rourkela, India

[August , 2014]

Suggestions by Indian Examiner

Comments:

The **thesis contains a good amount of scholastic work worth appreciating**. However, while reading the thesis one can't help making some comments with the sole aim of motivating the young researcher to take up as a challenge in improving the presentation.

Response

The candidate humbly appreciates the observation made by the respected examiner. The candidate has put utmost effort to address the points raised by the examiner in order to improve overall quality of the thesis.

1). The Literature Review presented can't possibly be qualified as a review. It's indeed more of a catalogue then a review which should have brought out the understanding of the researcher, and similarities and conflicts between different findings, gaps, etc.

Response

The format of Literature Review has been carefully modified as per the recommendation of the examiner. The detailed correction has been marked in the old thesis.

2). The **entire thesis**, particularly Chapters 1&2, should have been edited with care. There are simple spelling mistakes – to mention a few:

i). "When sufficient voltage is generated ……. Starts emitting sum electrons" p4

ii). "Gadalla …… dislodging of WC gains, which …… conductivity" p7

iii). "Arc takes place …… is evident for Fig. 1.3" p8

iv). "Usually, spark ….. stability then arc pulses." P8

v). "Easy manufacturability and chip cost." P12

vi). "In this experiment …… after harding." P64

Response

The candidate sincerely regrets the inadvertent mistakes. Due care has been taken to thoroughly check typographical mistakes through out the thesis. All corrections have been marked in the old thesis.

3). Many sentences in the entire thesis have been very poorly or wrongly constructed without any verb or with two verbs- at times the meaning is confusing. A few examples:

i). "These waveforms are discusses followed by …….. transform." pvii

ii). "Despite the fact …… electrical energy it into thermal energy through …." p5

iii). "The flow of discharge current continuous and there will be …." p6

iv). "The appreciable amount of material is transformed between workpiece and electrode undergo ….. phase reaction." p6

v). "In order to avoid …… must be remove." p8

vi). "This time allows…. To be wash out of the arc gap" p9

vii). "EDM are used in different application, they are listed in point below" p12

ix). "….besides MRR can be …. With reduced TWR using….. roughness" p16

x). "The model was able to predict the shape of the crater formed during the material removal was also validated experimentally" p17

Response

The candidate expresses his sincere apology for language issues in the thesis. In addition to all the sentences pointed out by the examiner, the entire thesis has been revised with particular emphasis on Chapter 1 and 2 as suggested by the examiner. Detailed corrections have been highlighted in the previous version of the thesis and also in 'List of corrections made'.

4). Three journal publication have been listed – one published from Great Britain, another from Delhi (it charges Rs 7500 per article) and the third one from Hyderabad (Gokaraju Rangaraju Institute of Engg & Technology). Young researchers should publish papers in refereed (SCOPUS INDEXED) journals.

Response

The candidate humbly accepts the valuable suggestions of the examiner. However, the candidate would like to clarify the following

1. **The paper titled 'Optimisation of Machining Parameters using Gray Relation Analysis for EDM with Impulse Flushing' was published in International Journal of Mechatronics and Manufacturing System of Inderscience Publisher. This is a refereed and Scopus indexed journal.**
2. **Another paper titled 'A Case Study on Quality and Productivity Optimization in Electric Discharge Machining (EDM)' was published in Advanced Materials Research, Trans Tech Publications, Switzerland. This is also a refereed and Scopus indexed journal. It may be noted that this paper was published from an international conference AMPT-2011 held at Istanbul, Turkey after further peer review.**
3. **Two other papers titled 'An Investigation on Electro Discharge Erosion of Mild Steel using Fuzzy Logic' and 'Multi Response Optimisation for Correlated Responses in EDM using Principal Component Analysis' were published in 'International Journal of Manufacturing Technology and Industrial Engineering' and 'Advanced Materials Manufacturing & Characterization' respectively which, however, are not a scopus indexed journals. However, these papers were published from international conferences titled, ICAME-2011 held at S.V. NIT, Surat and 3rd international conference on materials processing and characterization, held at GRIET, Hyderabad, respectively. In fact, organizing committee of these conferences recommended publication of these papers in respective journals. The authors did not submit these papers for publication in any international journal.**
4. **A fourth paper has been recently accepted for publication with detail as follows**
   Influence of Different Tool Electrode Materials on EDMed Surface Integrity of AISI P20 Tool Steel, Materials and Manufacturing Processes (Taylor and Francis), *Available Online, DOI:10.1080/10426914.2014.930892.*
   Therefore, the candidate at present has three papers published in reviewed and Scopus indexed international journals.

<u>It may kindly be noted that the candidate has never paid any fee for publication of any article in any international journal.</u>

5). Ph D Thesis is a pride document both for owner as well as the Institute which may like to keep a copy in its library. To qualify this, the present thesis should be thoroughly edited.

Response

The candidate is grateful for the invaluable suggestions. The language of the thesis has been thoroughly edited as per the recommendation of the respected examiner.

<u>Suggestions by Foreign Examiner</u>

TITLE

The title of the thesis does relate to its contents but the word "multi objectives optimization" seems to misleading. This is because it is not been discussed clearly in the thesis. This can be rectified if the candidate does have a clear and comprehensive definition the meaning of multi-objectives optimization in the thesis.

Response

It may kindly be noted that multi-objective optimization has been comprehensively defined in section 2 (Literature Review), page number 30 (which has been marked) of the revised version of the thesis. In addition, this definition has also been added in section 3.6 (Experimental details and analytical techniques) of the revised thesis.

ABSTRACT

The purpose of abstract is to give a concise and precise statement of the intention and findings of the research, and it strongly influences whether the research is well carried out or otherwise. In addition the abstract should assist the reader by giving a brief understanding and focus of the research that is not really the case for the abstract of this thesis. The candidate does provide sufficient information in the abstract. The structure (flow of paragraph) is properly written.

Response

The abstract has been made more precise and written including all the information as per the recommendation of the examiner.

INTRODUCTION

The introduction does summary and reflect a strong justification for the current research. The candidate assesses some previous work by explicitly highlighting the limitations of the existing work. Since EDM SMEs have been widely research in the past, the motivation for the current research is clear.

In addition it is quite effortless to related to the various description used in the thesis to identify the relationship of the previous work and the work that was carried out by the candidate.

Response

The research gap has been clearly identified from the detailed literature review. The limitation of the previous work has been correlated to the plan of work that has been undertaken.

ANALYSIS AND INTREPETATION OF RESULTS

One improvement that can be considered is to give more elaboration on the results and discussion of each finding. As it is the discussion gives a broad statements rather than describing in detail the analysis of the outcome from the experiment carried out. In other words proviso more information and elaboration of the results from the experiments in particular it will more sufficient evidence of the outcome measures of the findings, By having a thorough discussion of the findings it will provide sufficient evidence of the outcomes that show the significant of the research.

Response

Detailed justification of each of the findings, as per the advice of the examiner, from the current research work has been clearly highlighted in the previous version of the thesis.

REFERENCES/BIBLIOGRAPHY

The references used in this work mostly coming from literature of refereed journals. Numerous references are cited and used that give some credence with respect to research. In addition it is focused on the work and this is sound enough to support the research that being carried out. *One minor drawback, it seems that the referencing style is not following a standard format, and various format can be found through the thesis.*

Response

Minor correction has been on referencing style making it uniform throughout, as per the suggestion of the examiner.

PRESENTATION/STRUCTURE

The presentation of this thesis is well organized and structure in a systematic manner.

One minor drawback in the structure is in the Chapter 4 (Results and Discussion), throughout the chapter the tables and figures are not properly referred and been place in inappropriate sequence, since too many figure and tables used in this chapter, it is hard to keep refer to it due to unstructured placement of both the figure and tables. Beside, from time to time the candidate just leaves the tables and figures to be interpreted by the reader without giving any brief explanation on the results and information that can be gained from the tables and figures tabulated and plotted.

Response

The candidate regrets the inconvenience regarding the sequence of figures and tables. The relative position of some of the figures and tables has been changed for better proximity to the text where they have been referred. It may also kindly be noted that all the figures and tables have been duly referred in the text and they have been highlighted in the old copy of the thesis.

The language used need to be rechecked and improved. Some sentence used is quite ambiguous, it does not give a clear understanding of the work been carried out. The spelling of the words needs to be checked.

Response

The candidate expresses his sincere apology for language issues in the thesis. The language of the entire thesis has been thoroughly edited as per the recommendation of the respected examiner. Detailed corrections have been highlighted in the previous version of the thesis and also in 'List of corrections made'.

ACCOMPLISHMENT

Form the Ph D research perspective, the candidate has shown the understanding of the research carried out by the proposing the some significant findings in relating to the EDM work. This is supported by carrying out various experiments that has given the credibility of the research carried out.

The candidate humbly appreciates the observation made by the respected examiner.

RECOMMENDATION

Minor modification of thesis require

List of corrections made in the thesis

Shailesh Kumar Dewangan
Department of Mechanical Engineering
National Institute of Technology,
Rourkela-769008, Odissa, India

List of corrections made in the thesis

(Heading no, page no, para no, line refers to the thesis before correction)

Topic	Heading	Page no.	Para graph	Line	Before correction	After correction
Abstract		v	1	1	Electric Discharge Machining (EDM) is one of the machining *process*, which is used to produce critical shape on *any type of* hard or brittle conductive material and it can also be *well* applied for materials that are *impossible* to machine with traditional machining processes.	Electric Discharge Machining (EDM) is one of the non traditional machining processes used to produce critical shape on hard or brittle conductive materials and it can also be successfully applied on materials that are extremely difficult-to-machine using traditional machining processes.
		v	1	8	Quality is associated with minimization of Tool Wear Rate (TWR) and Radial Overcut (OC), and the productivity is associated with maximisation of Material Removal Rate (MRR). Surface integrity includes analysis of White Layer Thickness (WLT), Surface Crack Density (SCD) and Surface Roughness (SR) of the workpiece.	Remove
		vii	1	1	*While machining* in EDM, *the* various discharge waveforms	In EDM various discharge waveforms
		vii	1	3	These waveforms are discuses followed by	Remove
		vii	1	5	and wavelet transform *is* used to *analysis* the discharge waveforms.	and wavelet transform was used to analyse the discharge waveforms
		vii	1	7	*and* no other machining parameters significantly *effect* any other three types of waveform pulses.	while no other machining parameter significantly affected any of the three types of waveform pulses
		vii	1	8	It is found to be directly proportional to number of "spark" pulses and is inversely proportional to number of "arc" pulses. Thus, giving an useful information about the EDM machining state with different machining settings.	The study indicated that pulse-on time was inversely proportional to number of "spark" pulses and directly proportional to number of "arc" pulses, thus giving an useful information about state of EDM under different machining condition.
Introduction	1	2	1	1	mechanical *component*	mechanical components
	1	2	1	5	medical appliance, *and*	medical appliance and
	1	2	1	10	*size*, and	size and
	1.1	2	2	1	EDM technique was first developed by an English scientist, Joseph Priestly in 1970s.	English scientist Joseph Priestly first observed erosive influence of electric discharge way back in 1770s.
	1.1	2	2	2	Electrical discharge machining was not fully taken advantage of	full advantage of this technique was not utilized
	1.1	2	2	3	how the erosive effects of the technique could *be* controlled and used for machining.	to control the erosive effects of the technique, to be used for machining.
	1.1	2	2	6	These *processes were* not very precise	This process was not very precise

Introduction	1.1	2	2	7	*may be* defined as	is defined as
	1.1	2	3	1	extraordinary *progresses* in improving	extraordinary progress in improving
	1.1	2	3	3	unattended machining from	unattended machining, from
	1.1	2	3	4	cavity or *cavities was*	cavity or cavities, was
	1.1	3	1	1	*R&D* areas.	research and development segment.
	1.2.1	3	4	4	between the *two* electrode	between electrode and workpiece
	1.2.1	3	4	5	and a small spark jumps.	with occurrence of small spark.
	1.2.1	3	4	6	the spark gap subsequently *increased, the* electrode is lowered	the spark gap subsequently increase. The electrode is then lowered
	1.2.1	3	4	7	.. the process can continue uninterrupted.	.. the process continue uninterrupted.
	1.2.2	4	1	2	.. *wire used as* electrode to cut through metal by using electrical sparks.	.. wire is used as an electrode to cut metal by using electrical sparks.
	1.2.2	4	1	5	This process is typically used to cut plates up to thick *as* 300mm and to make punches, tools, and dies from hard *metals* that are *difficult to machine* with other methods.	This process is typically used to cut plates up to thickness of 300mm and to make punches, tools, and dies from hard materials that are difficult-to-machine using other methods.
	1.2.3	4	2	1	EDM except that *using rotary* disk electrode.	EDM except that it uses a rotary disk as an electrode.
	1.3	4	3	1	The process of the material removal by a	The process of the material removal in EDM takes place by a
	1.3	4	3	2	commonly known as electric discharge machining	remove
	1.3	4	3	3	This spark is *generated between* the tool and work piece, the heat is generated near the zone melt and *vaporizes the materials in the sparking zone.*	The spark produced between the tool and work piece, generates the large amount of heat in the sparking zone, melting and vaporizing the work piece material.
	1.3	4	4	1	The tool is cathode and work piece *is* anode.	The tool is considered as cathode and work piece as anode.
	1.3	4	4	3	tool starts emitting *sum* electrons.	tool starts emitting some electrons.
	1.3	4	4	4	positively *charge* workpiece	positively charged workpiece
	1.3	5	1	1	some parts of workpiece and tool *materials.*	some parts of workpiece and tool material as well.
	1.4	5	2	3	*debatable,* the most	debatable. The most
	1.4	5	2	4	energy *it* into thermal	energy into thermal
	1.4	5	2	7	even vaporization *of material.*	even vaporization.
	1.4	6	2	1	The flow of discharge current continuous	The flow of discharge current is continuous
	1.4	6	2	3	The temperature *rise* between	The temperature rises between
	1.4	6	2	4	*results* in formation of a small molten	resulting in formation of small molten
	1.4	6	2	6	Some of the molten metal directly *vaporized*	Some of the molten metal directly vaporizes
	1.4	6	4	3	the process of migration of material from the *work-piece* and *electrode*	the process of migration of material from the workpiece and tool
	1.4	6	4	4	The appreciable amount of material is transformed between workpiece and electrode undergo alloying with the contacting surface by means of a solid,	Appreciable amount of materials is transferred between the active surfaces (form which discharges occur) and the tool resulting in allowing by means

					liquid or gaseous phase reaction.	of solid, liquid or gaseous phase reactions.
	1.4	6	4	7	Phases of sparking *of* MRM (breakdown, discharge and erosion) *is* highly influenced by the types of eroded electrode	Phases of sparking during MRM (breakdown, discharge and erosion) are highly influenced by the types of eroded tool electrode
	1.4	7	1	7	*elucidated* the material removal	related material removal
	1.4	7	1	10	by the *dislodging* of WC gains,	by dislodgement of WC grains
	1.4	7	1	10	On the other hand, Lee and Lau [1991] argued that thermal spalling as well contributes to the mechanism of material removal during the sparking of composite ceramics due to the physical and mechanical properties promotes abrupt temperature gradients from normal melting and evaporation.	removed
	1.4	7	2	2	EDM is a thermal process of eroding electrically conductive materials with a series of successive electric sparks *and the* complex phenomenon	EDM which is a thermal process of eroding electrically conductive materials with a series of successive electric sparks, is a complex phenomenon
Introduction	1.4	7	2	4	tool and the workpiece, thermodynamics	tool and the workpiece are thermodynamics
	1.4	8	1	1	spark causing melting and evaporating the electrodes, microstructural changes and metallurgical transformations of material, *are still* not clearly understood.	sparks causing melting and evaporation of the electrodes, microstructural changes and metallurgical transformations of material which are still not clearly understood.
	1.4	8	1	1	melting and *evaporating* the electrodes	melting and evaporation of the electrodes.
	1.4	8	1	2	material, are still not	material, which are still not
	1.4	8	1	4	melting and evaporation of *workpiece*	melting and evaporation of the same.
	1.5	8	2	4	Open pulse takes *places*	Open pulse takes place
	1.5	8	2	9	evident for Fig.1.3.	evident from Fig. 1.3.
	1.5	8	2	10	machining stability *then* arc pulses	machining stability than arc pulses
	1.5	8	2	13	pulses must be *remove*	pulses must be prevented
	1.6	9	4	1	between *the sparks*	between the two consecutive sparks
	1.6	9	4	2	This time allows the molten material to solidify and to be wash out of the arc gap.	During this time, the molten metal solidifies and is washed out of the spark gap
	1.6	9	4	3	This parameter *is to affect* the	This parameter affects the
	1.6	10	2	1	The dielectric fluid *carry out* three *most* important purposes in *the* EDM.	Dielectric fluid serves three important purposes in EDM.
	1.6	10	2	3	*voltages conducting* the flow of current.	voltage to allow the flow of current.
	1.6	11	1	1	dielectric in to the *inter electrode gap*.	dielectric into the IEG
	1.6	11	1	3	which can *destroy the workpiece.*	which can adversely affect the quality of machined workpiece.
	1.7	11	2	1	Tool material should be such that it *would* not	Tool material should be such that it should not
	1.7	11	2	7	High electrical conductivity *of electrons are cold emitted* more easily and there is less bulk	High electrical conductivity, that enables to emit more cold electrons easily and there is less

					electrical heating.	bulk electrical heating.
	1.7	12	1	1	the same heat load, *the local*	the same heat load: The local
	1.7	12	2	1	and same tool wear by weight *there*	and same tool wear by weight: There
	1.7	12	4	1	Easy manufacturability and *chip* cost.	Easy manufacturability and low cost.
	1.7	12	5	1	The different electrode materials which are *used commonly such* as brass,	The different electrode materials which are commonly used are brass
	1.8	12	6	1	EDM *are* used in different application, they are *listed in point below.*	EDM is used in different applications which are discussed below:
	1.8	12	10	2	*item it* is used	item .It is used
	1.8	12	11	1	It is used for forging, extrusion, wire *drawing, thread* cutting.	It is used for forging, extrusion, wire drawing and thread cutting dies.
	1.8	12	12	1	Higher *Tolerance* limits can be obtained in EDM. Hence *areas* that require higher surface accuracy use *the* EDM process.	Higher tolerance limits can be obtained in EDM. Hence applications that require higher surface accuracy use EDM process.
	1.8	13	1	2	automotive R&D *areas*.	Automotive R&D segments.
	1.8	13	2	1	machined by *the* EDM	machined by EDM
Literature review	2.1	15	1	4	between 1993 *to* 2003 has been reported	between 1993 and 2003 has been reported
	2.1	15	1	10	They presented *its* summary	They presented the summary of research work
	2.1	15	1	13	evaluation for *instance* MRR, TWR and	evaluation for MRR, TWR and
	2.1.1	15	2	1	parameters on various performance *measure*	parameters on various performance measures
	2.1.1	15	3	1	Kuppan et al. [2007] derived mathematical model for MRR of deep hole drilling of Inconel 718 using Response Surface Methodology (RSM) and revealed that MRR is more influenced by Ip, Tau and electrode rotation. For higher MRR, a large pulse current is encouraged to increase electrode wear implanting electrode material onto the workpiece	Removed
	2.1.1	17	2	1	added	In addition to erosion of workpiece, EDM also results in removal of material from the tool electrode. The former corresponds to material removal rate (MRR) whereas the latter contributes to what is known as tool wear rate (TWR). Many researchers[Karthikeyan et al., 1999; Dhar et al., 2007; Kung et al., 2009; Lin et al., 2008; Tsai et al., 2003b] have found out that TWR increased with MRR. Heat and impulsive force which are generated across IEG during electrical discharge erode both workpiece and tool electrode. Their is a general agreement among researcher that

						increasing peak current (Ip) causes TWR to increase. However, influence of pulse-on time on TWR has been debated. Kung et al. [2009] observed quick increase of TWR with increase in Ton. Due to increase in discharge energy associated with higher Ton. On the other hand, the inverse relationship has also been reported [Karthikeyan et al., 1999; Lin et al., 2008]. Dhar et al. [2007] intial increase followed by decrease in TWR when pulse-on duration was increased form 200 to 400 μs.
	2.1.1	18	2	2	added	Since overcut phenomenon is directly related to discharge energy, higher MRR would result in more overcut in EDM [Singh et al., 2004c; Dhar et al., 2007]. Therefore, pulse current is directly proportional to overcut [Singh et al., 2004c; Dhar et al., 2007].
	2.1.1	18	2	5	When low diameteral OC is the requirement En-31 may be preferred over copper and aluminium electrodes.	Copper and aluminum electrodes might be preferred option over copper-tungsten and brass electrodes for machining En-31 tool steel since the latter resulted in increase in diameteral overcut.
	2.1.1	18	4	3	Heat *Affective* Zone (HAZ), micro-cracks, *and* residual *Stresses*,	Heat Affected Zone (HAZ), micro-cracks, residual stresses,
	2.1.1	18	4	8	EDM has many advantages *but,* the	EDM has many advantages the
	2.1.1	18	5	2	machined surface *relate* to	machined surface related to
	2.1.1	18	5	3	roughness *are* commonly	roughness is commonly
	2.1.1	19	1	6	*craters and* is often covered	craters. It is often covered
	2.1.1	19	1	7	The molten metal *were* expelled	The molten metal was expelled
	2.1.1	19	2	6	work, *and* dielectric liquid	work, dielectric liquid
	2.1.1	19	2	11	by discharge *and consequently*, the	by discharge. Consequently, the
	2.1.1	19	2	12	electrode *and* AISI H3 tool steel workpiece *and* the	electrode AISI H3 tool steel workpiece with the
	2.1.1	19	2	14	and T_{off} *and it* was	and T_{off} . It was
	2.1.1	20	1	3	Jaharah et al. [2008] investigated SR on AISI H13 tool steel. However, the optimum condition for Ra was obtained at low Ip, low T_{on}, and T_{off}. Ip was the major factor affecting the response.	removed
	2.1.1	20	1	13	study developed a model for SR and *started* that with the increasing in process parameters,	study developed a model for SR and stated that with the increase in process parameters,
	2.1.1	20	2	9	It is claimed *to fit and* predict SR	It is claimed that model predicts SR
	2.1.1	21	1	5	*that* attainable by normal	the value attainable by normal
	2.1.1	21	3	1	Lee et al. [2004] *revealed* experimentally	Lee et al. [2004] studied experimentally

	2.1.1	21	3	10	the formation crack.	the formation of crack.
	2.1.1	21	3	10	added	Similar study of EDM parameters on thickness of white layer has also been reported by Ramasawmy et al. [2005].
	2.1.1	22	1	1	qualitatively *that the* formation	qualitatively, the formation
	2.1.1	22	1	6	Ramasawmy et al. [2005] experimentally investigated the effect of the EDM process parameters Ip and Ton on the thickness of the white layer.	Removed
	2.1.1	22	1	15	EDM of steel *and a* correlation among surface morphology	EDM of steel. A correlation between surface morphology
	2.1.1	22	1	19	equations; it is clearly shown that their dimensional dependence on pulse energy.	equations. Their dependence on pulse energy is clearly shown.
	2.1.1	23	3	1	Cracks *are* initiating from	Cracks initiate from
	2.1.1	23	3	5	under such *circumvents.*	under such circumstance.
	2.1.1	23	3	10	Crack Critical Line (CCL) *is introduced* to	Crack Critical Line (CCL) to
	2.1.2	25	1	4	Ip , Ton, Tau *and V* , flushing pressure, dielectric fluid, polarity	Ip , Ton, Tau, V, flushing pressure, dielectric fluid and polarity
	2.1.2	26	3	1	Lin et al. [2008] *had* examined the *effects* of attached magnetic force on EDM *machining affect* such as MRR, TWR, SR using electrolytic copper as tool and work-piece was SKD 61 steel. They used L18 OA based on Taguchi design *and parameters* namely polarity, discharge current, pulse on time, high-voltage auxiliary *Current (IH),* no-load voltage and servo reference voltage (Sv).	Lin et al. [2008] examined the effect of magnetic force on EDM characteristics. Responses such as MRR, TWR and SR were analysed using electrolytic copper as tool and SKD 61 steel as workpiece. They used L18 OA based on Taguchi design. Parameters namely polarity, discharge current, pulse-on time, high-voltage auxiliary current (IH), no-load voltage and servo reference voltage (Sv) were chosen.
	2.1.2	26	3	5	They described that with EDM with magnetic force, the surface integrity can attain a high efficiency and better machining stability.	It was concluded that magnetic force-assisted EDM resulted in process with higher efficiency and stability and improved surface integrity in terms of lower SR and reduced surface cracks.
	2.1.2	27	3	1	had *investigation* on MRR	had investigated on MRR
	2.1.2	27	3	4	ANOVA indicating	ANOVA and indicated
	2.1.2	28	2	5	ANN errors *with* indicated	ANN errors which indicated
	2.1.2	29	2	10	Micro Electric Discharge Machining (MEDM) *foundation* the waveforms	Micro Electric Discharge Machining (MEDM) resulted in highly distorted waveforms
	2.1.2	30	2	7	was adopted and *finding* the relations between	was adopted and found the relations between
	2.1.2	30	2	11	For *the experimentation*, *they* proved that an improvement of MRR, TWR and OC 12.88, 14.57 and 6.1%, respectively, *was observed*.	An improvement of 12.88, 14.57 and 6.1% were observed for MRR, TWR and OC respectively.
	2.1.2	31	2	6	discharge *current on the* response of MRR, SR	discharge current. The responses measured were of MRR, SR
	2.1.2	32	1	6	and finding have been conduct and recognize the responses.	removed

	2.1.2	34	2	10	and the reposes are	removed
	2.1.2	35	1	5	S/N *ratio gives* better performance compare GRA and	S/N ratio. It gave the better performance compared to GRA and
	2.1.2	35	2	8	past researchers *are* analysed	past researchers was analysed
	2.1.2	35	2	18	The control parameters selected *as*	The control parameters selected were
	2.1.3	37	1	7	*better then* copper electrode in measurement of MRR.	better than copper electrode in the measurement of MRR.
	2.1.4	37	3	3	Ip=8A, Ton= 50 µs *give the*	Ip=8A, Ton= 50 µs gave the
	2.1.4	38	1	5	process is used *performance the* finishing and	process using finishing and
	2.1.4	38	2	3	by *ANN and GA the* EDM quality characteristic.	EDM quality characteristics using ANN and GA.
	Table 2.1	39			Integrated *FEMANNGA* for	Integrated FEM, ANN, GA for
	Table 2.1	39			The +ve polarity was *found* optimum	The +ve polarity was used to find optimum
	2.1.4	43	1	15	RSM has been used to plan by Kung et al. [2009], it using cobalt-bonded tungsten carbide (WC-Co) workpiece material within the process of PMEDM. Evaluated the effect of MRR and TWR, MRR increases with an increase of aluminium powder concentration and TWR value tends to decrease with the aluminium powder concentration down to a minimum value after which it tends to increase.	Kung et al. [2009] have used RSM design to machine cobalt-bonded tungsten carbide (WC-Co) using power mixed dielectric. They evaluated MRR and TWR. MRR increases with an increase of aluminum powder concentration and TWR value tends to decrease with the aluminum powder concentration down to a minimum value after which it tends to increase.
	2.1.4	43	2	4	Simao et al. [2003] has investigation the electrode wear, workpiece surface hardness of AISI H13 hot work tool steel. With the help of micro-hardness, Percentage Contribution Ratios (PCR) for peak current, electrode polarity and pulse on time. Using partially sintered WC/Co electrodes.	Simao et al. [2003] have investigated the electrode wear, workpiece surface hardness of AISI H13 hot work tool steel using partially sintered WC/Co electrodes.
	2.1.4	44	2	1	Curodeau et al. [2005] discuss hybrid EDM process is used performance the finishing and polishing operation in dielectric deionized water and two processes describe replica and successive imprints of surface roughness.	Curodeau et al. [2005] discussed hybrid EDM process for finishing and polishing operations in deionized water. And two processes described replica and successive imprints of surface roughness.
	2.1.4	45	2	1	Puertas and Luis [2004] discuss mathematical models devised using design of experiments techniques and optimized of machining parameter for EDM of Boron carbide of conductive ceramic materials.	Puertas and Luis [2004] discussed the mathematical models devised using design of experimental techniques and optimized machining parameters for EDM of Boron carbide, a conductive ceramic material.
	2.1.4	45	2	10	However, the highest *TWR were* found for the diamond shaped electrodes.	However, the highest TWR was found for the diamond shaped electrodes.
	2.1.5	46	4	1	Dauw et al. [1983] developed a EDM pulse discriminator (EDM-PD) for EDM process analysis	Dauw et al. [1983] developed an EDM pulse discriminator (EDM-PD) for EDM process

					and on-line control.	analysis and an on-line control.
	2.2	48	1	3	systematically *to* optimised the process variables with a view to obtain favourable surface integrity.	systematically optimised the process variables with a view to obtain favourable surface integrity
Experimental details and analytical techniques	**3.1**	51	1	3	The enlarge view of experimental set-up with tool and workpiece are shown *in 3.1*	The enlarge view of experimental set-up with tool and workpiece are shown in Fig. 3.1
	3.1	51	1	3	The Die sinking Electric Discharge Machining (EDM) *are* shown in Fig. 3.2.	Full view of machine setup for die shinking Electric Discharge Machining (EDM) is shown in Fig. 3.2.
	3.1	51	1	5	AISI P20 tool steel semi-circular *shaped* (100 mm diameter and 10 mm thickness) *was used*.	AISI P20 tool steel having semi-circular shape (100 mm diameter and 10 mm thickness).
	3.1	51	2	1	The cylindrical copper, brass and graphite tools are used as experiments.	removed
	Fig. 3.2	52	Fig. 3.2		Die sinker EDM, brand : Electronica Elektra Plus : Model : PS 50 ZNC	Experimental setup for die sinking EDM
	3.1	52	1	1	EDM oil (specific gravity = 0.763, *freezing* point = 94◦C) was used as dielectric fluid. The impulse flushing and side flushing *are used as different setting of experiments*.	EDM oil (specific gravity = 0.763, flash point = 94◦C) was used as dielectric fluid under The impulse flushing and side flushing modes.
	Table 3.3	53	Table 3.3		*Poisson?* Ratio	Poisson's Ratio
	3.2.1	54	Heading		Description of tool *electrode*	Description of tool electrodes
	3.2.1	54	2	1	In this experiments using copper, brass and graphite tool electrode materials with the 30mm and 12mm diameters was used.	Current study used cylindrical copper tool electrode with diameter of 30mm and 12mm while brass and graphite tool electrodes of 12mm diameter were used.
	3.2.1	54	2	2	The detail description of selection of tool electrode with proper dimension has been provided in the chapter 4 in results and dissolution.	The detailed description of selection of tool electrodes along with dimension has been provided in the chapter 4.
	3.3	54	1	1	• *Tool* work time (T_w) • *Tool* lift time (T_{up})	• Work time (T_w) • Lift time (T_{up})
	3.4.2	55	4	3	The density of AISI P20 tool steel material is ρ_w = 7.85x10^{-3}g/mm^3, and density of copper electrode is ρ_t = 8.92x10^{-3}, g/mm^3.	The density of AISI P20 tool steel material is ρ_w = 7.85x10^{-3}g/mm^3 and density of copper electrode is ρ_t = 8.92x10^{-3} g/mm^3.
	3.4.4	56	4	2	*Diameter* of tool.	diameter of tool
	3.6	59	Heading		Optimisation techniques	Multi-objective optimisation techniques
	3.6	59	1	1	With an aim to *optimisation* EDM parameters for *obtain* favourable output responses,	Multi-objective optimisation is an area of multiple performance characteristics index that is concerned with mathematical optimisation problems including more than one objective function to be optimised simultaneously. EDM is characterized by multiple performance measures such as MRR, TWR, OC, SR, WLT,

						SCD etc. Therefore, with an aim to optimise EDM parameters for obtaining favourable output responses, number of multi-objective optimisation techniques were applied in the present research work. These methodologies have been briefly discussed as follow:
	3.6.2	60	1	4	Fuzzy logic system (Mamdani type) mainly *consist* of fuzzifier	Fuzzy logic system (Mamdani type) mainly consists of fuzzifier
	3.6.2	61	1	5	in *the* section 4.3.5	in section 4.3.5
Results and discussion	**4.1.1**	63	2	5	The sparking cycle diagram is shown in Fig. 4.4, which consists of T_w and T_{up}. During the working time T_w multiple sparks occur with a pulse duration Ton and pulse off time T_{off} . The impulse flushing is performed when quill is lifted up for T_{up} duration.	Remove
	4.1.4	70	1	4	The experimental findings in *Table 4.2* are used to calculate the normalised MRR and TWR, which are presented in Table 1.5.	The experimental findings in table 4.2 are used to calculate the normalised MRR and TWR, which are presented in Table 1.5.
	4.2	76	1	4	The influence of machining parameters *i. e*. discharge current (Ip), …… tool steel as a workpiece.	The influences of machining parameters i.e. discharge current (Ip), ……. tool steel as a workpiece.
	4.2.1	77	1	5	During the working time Tw multiple sparks occur with ------- was set at 90μm.	Remove (Repeated)
	4.2.2	77	3	3	and surface plot in Fig. 4.10.	Remove
	4.2.3	83	1	1	and surface plot in Fig. 4.14.	Remove
	4.2.4	85	1	5	and surface plot in Fig. 4.18.	Remove
	4.3.1	101	3	1	RSM using central composite design with four variables….. and six centre points [Minitab16, 2011].	Remove (Repeated)
	4.3.1	103	Name of Table		Design matrix	Observation table for input parameters and output responses
	4.3.5	118	2	1	Then, Rij's are multiplied by fuzzy weights of each attribute given *in Table* 4.29.	Then, Rij 's are multiplied by fuzzy weights of each attribute given in table 4.29.
	4.3.5	122	2	3	The value of d^+_j and d^-_j are shown in *Table 1.30.*	The value of d^+_j and d^-_j are shown in previous table 1.30.
	4.3.5	122	2	5	which are shown in same table	which are shown in same table 1.30
	4.3.7	123	1	3	the fuzzy linguistic values that are given *in Table 1.29.*	the fuzzy linguistic values that are given in table 1.29.
	4.3.7	123	1	4	In other words, all DMs preferences on WLT (Pre-WLT) can be 'T' or 'VS' or 'S', because DM-1 to DM-5 have weighted WLT attribute as one of the linguistic values as shown in Table 1.29. Similarly, the DMs preferences of SCD (Pre-SCD), SR (Pre-SR) and OC (Pre-OC) are chosen among the values present in corresponding	Remove

					row in the same table.	
	4.3.7	123	1	8	A full factorial experiment design was considered *which* yield a total of 54 *combination* of DM judgements that are possible, which is summarised in Table 4.35.	A full factorial experiment design is considered that yield a total of 54 combinations of DM judgements that are possible, which is summarized in Table 4.35.
	4.3.7	126	1	1	In Table 4.21,	In table 4.21,
Reference		183	6	3	*Journal of the Braz. Soc. of Mech. Sci. & Eng.,*	*Journal of the Brazilian Society of Mechanical Sciences and Engineering,*
		185	2	2	An adaptive neuro-fuzzy inference system (anfis) model for wire-edm.	An adaptive neuro-fuzzy inference system (ANFIS) model for wire-EDM.
		188	3	2	*Int. J. Mach. Tools Manuf.,* 32 (5):651–657.	*International Journal of Machine Tools and Manufacture*, 32 (5):651–657.
		188	4	2	*Int J Adv Manuf Technol*, 50:611–624.	*International Journal of Advanced Manufacturing Technology*,
		193	6	2	*Mater. Process. Technol.*, 24:513–523.	*Journal of Materials Processing Technology*, 24:513–523.
		193	9	2	*Mater. Manuf. Processes*, 6 (4):635–648.	*Materials Science and Technology*, 7(3):239–248.
		195	3	3	Tools & Manufacture,	Tools and Manufacture,
		198	4	2	MRR and ew of WC-Co.	MRR and EW of WC-Co.